Dissection génétique de la résistance végétale contre les virus

Par

Xiaofang Ma

thèse en cotutelle

présentée au Département de biologie en vue
de l'obtention du grade de docteur ès sciences (Ph.D.)
FACULTÉ DES SCIENCES,
UNIVERSITÉ DE SHERBROOKE

au College of Plant Science and Technology, en vue de
l'obtention du grade de docteur ès sciences (Ph.D.)
HUAZHONG AGRICULTURAL UNIVERSITY

Sherbrooke, Québec, Canada, Septembre, 2015

Genetic dissection of plant-virus interactions

By

Xiaofang Ma

co-supervised thesis

submitted to the Department of Biology in fulfillment of
requirements for the degree of Doctor Philosophiae (Ph.D.)
FACULTÉ DES SCIENCES, UNIVERSITÉ DE SHERBROOKE

and to the College of Plant Science and Technology in fulfillment of
requirements for the degree of Doctor Philosophiae (Ph.D.)
HUAZHONG AGRICULTURAL UNIVERSITY

Sherbrooke, Québec, Canada, September, 2015

Le 25 âout 2015

le jury a accepté la thèse de Madame Xiaofang Ma
dans sa version finale.

Membres du jury

Professeur Peter Moffett
Directrice de recherche
Département de biologie, Université de Sherbrooke

Professeur Guoping Wang
Codirecteur de recherche
College of Plant Science and Technology, Huazhong Agricultural University

Professeur Zhongqi Qin
Évaluateur externe
Institute of Fruit and Tea, Hubei Academy of Agricultural Sciences

Associated Professeur Wenxing Xu
Évaluateur interne
College of Plant Science and Technology, Huazhong Agricultural University

Professeur Kamal Bouarab
Président-rapporteur
Département de biologie, Université de Sherbrooke

Acknowledgements

I would like to express my sincerest gratitude to the following people and institutions:

- Dr. Peter Moffett, I can not express in words how much I appreciate your help during my time (20120918-20140909) in Sherbrooke, especially at my arrival in this new and interesting country. You helped me where you could, on a more scientific side, thank you for your invaluable scientific input, your patience and your help with presentation and thesis correcting.
- Dr. Guoping Wang, I am so appreciated your and Dr Ni Hong's help during my time in you lab. You helped me so much, also thank you for your invaluable scientific input, your patience and your help with presentation and thesis correcting.
- Dr. Kamal Bouarab and Dr. Daniel Lafontaine, thank you for your scientific suggestions during my study time in University of Sherbrooke.
- Members in Peter Moffett's Lab, who includes: Chantal Brosseau, Therese Wallon, Shawkat Ali, Louis Valentin Meteignier, Mohamed EI Oirdi, Louis Philippe Hamel, Goretty Caamal. Thank you your guys help me a lot when I was in Canada.
- Daniel Garneau, thank you for help me the p-bodies data analysis.
- Also thank you all the members in Guoping Wang's Lab. Your guys help me a lot when I was there, I would not forget your kindness.
- The Chinese Scholarship Council, thank you for giving me the financial support to study in Canada for two years.
- And most importantly, thank you my husband (Chao Liu), for your love, support and understanding, especially during my time in Canada.

Summary

To live in host cells or to escape from host immunity, plant viruses involved a series of defense strategies. Here we investigated *Apple stem pitting virus* (ASPV) population structures and molecular diversity of ASPV pear isolates based on its function important gene CP and TGB in China, so as to infer the evolution mechanisms of ASPV. Our study showed that mutations (including insertions or deletions), purifying selection, and recombination were important factors driving ASPV evolutions in China or maybe even in the world. And also ASPV defends against it hosts by encoding a VSR. We also showed that ASPV molecular diversity not only induced different biological properties on its herbaceous host *N. occidentails* but also resulted in antigenic variation of different ASPV CP isolates, which leaded to differences in serological reactivity among rCPs of different ASPV isolates.

Plants have developed a series of mechanisms to defend themselves against viruses. Here we how *Arabidopsis* defend against. We show that virus susceptibility, recovery, and virus induced gene silencing (VIGS) appear to be separable phenomena, with AGO2 and AGO4 playing important roles in the initial susceptibility to TRV, AGO1 playing an important role in VIGS, and as yet unidentifid players mediating recovery. These results suggest the existence of distinct RNA-induced silencing complexes that target different RNA populations within the cell and over time. Furthermore, we showed that translational repression of viral RNA is likely to play an important role in virus recovery and that decapping function plays an important role in clearing viral RNA from the cell. We also showed that a decapping mutant (*DCP2*) displayed an increased VIGS and virus RNA accumulation, an important role for PBs in eliminating viral RNA.

Keywords *Apple stem pitting virus*, CP, pear, VSR, Argonaute, VIGS, RNA silencing, *Arabidopsis*, *Tobacco rattle virus*.

Sommaire

Pour se propager dans les cellules de son hôte et évader les réponses immunitaires, les virus végétaux ont développé plusieurs stratégies de défense. Ici, nous avons investigué les structures génétiques du *Apple stem pitting virus* (ASPV). Nous avons aussi étudié la diversité moléculaire des isolats d'ASPV provenant des poires en regardant les séquences des gènes CP et TGB afin de mieux comprendre les mécanismes évolutionnaires utilisés par ASPV. Nos études ont démontré que les mutations, incluant les insertions et les délétions, la sélection purificatrice et la recombinaison furent des facteurs importants dans l'évolution du l'ASPV en Chine et possiblement mondialement. Comme tous les virus végétaux, l'ASPV se défend contre le RNA silencing de l'hôte grâce à un suppresseur de RNA silencing (VSR) et nous avons montré que le VSR de l'ASPV est la protéine de capside (CP) du virus. Nous avons aussi établi que la diversité moléculaire cause non seulement une variété de symptômes chez son hôte, *Nicotiana occidentalis*. Cependant elle cause aussi de la variabilité antigénique chez différents isolats, ce qui mène à des écarts de réactivité sérologique entre isolats.

Les plantes ont développé plusieurs stratégies pour se défendre contre les virus. Ici, nous avons étudié comment la plante *Arabidopsis* se défend contre le *Tobacco rattle virus* (TRV) *via* le RNA silencing. Nous avons constaté que les phénomènes de susceptibilité, récupération et virus induced gene silencing (VIGS) sont des mécanismes séparables. Nous avons démontré que les protéines AGO2 et AGO4 sont nécessaires à la susceptibilité initiale au TRV, tandis qu'AGO1 est importante pour les VIGS, tandis que la récupération est médiée par d'autres acteurs qui n'ont pas encore été identifiés. Nos résultats suggèrent l'existence de complexes distincts ciblant différentes populations d'ARN viral et cellulaire. De plus, nous avons montré que la répression de la traduction est un mécanisme important durant la récupération de la plante suite à une infection virale, et que les complexes de décoiffage et de RNA processing jouent des rôles importants dans la dégradation des ARNs viraux. Finalement, nous avons montré que les plantes ayant une mutation dans le gène *DCP2* présentent un niveaux de VIGS accrue, ainsi qu'une augmentation des niveaux d'ARN viral. Puisque DCP2 fait partie des complexes de décoiffage qui se trouvent dans des granules spécialisés nommés processing bodies (PBs), cela suggère que les PBs jouent un rôle important dans l'élimination les virus.

Keywords *Apple stem pitting virus*, CP, pear, VSR, Argonaute, VIGS, RNA silencing, *Arabidopsis*, *Tobacco rattle virus*.

Table of Contents

List of Abbreviations

Abbreviations	Full name
+ssRNA	positive-sense single-strand RNA
ACLSV	*Apple chlorotic leaf spot virus*
AGO	ARGONAUTE(S)
AlMV	*Altroemeria mosaic virus*
ALSV	*Apple latent spherical virus*
ApLV	*Apricot latent virus*
ApMV	*Apple mosaic virus*
APV-1	*Asian prunus virus 1*
ASGV	*Apple stem grooving virus*
ASPV	*Apple stem pittingvirus*
At	*Arabidopsis thaliana*
BMMV	*Banana mild mosaic virus*
bp	base pair
CaLCuV	*Cabbage leaf curl virus*
CaMV	*Cauliflower mosaic virus*
cDNA	complementary DNA
CGRMV	*Cherry green ring mottle virus*
CMV	*Cucumber mosaic virus*
CNRMV	*Cherry necrotic rusty mottle virus*
CP	Coat protein
CRP	Cysteine-rich protein
CTAB	Cetyl-Triethylammonium Bromide
CymRSV	*Cymbidium ring spot tombusvirus*
DCL	Dicer-like
DEPC	Diethypyrocarbonate
DNA	Deoxyribonucleic acid
dpi	day post-inoculation
DRB	double stranded RNA binding protein
dsRNA	double-stranded RNA
EMS	Ethyl Methanesulfonate
ETI	Effector triggered immunity
GFP	Green fluorescent protein
GLRaV	*Grapevine leafroll associated virus*
gRNAs	genomic RNAs
GRSPaV	*Grapevine rupestris stem pitting-associated virus*
GVA	*Grapevine virus A*
GVB	*Grapevine virus B*
GVCC	Grapevine vein-clearing complex
HEN1	Hua Enhancer
HR	Hypersensitive Response
LB and RB	left and right borders
MAMPs	Microbe-associated molecular patterns
Mcs	Multiple cloning site
MID	Middle
miRNA	microRNA
MP	Movement protein

Abbreviations	Full name
NAT-siRNAs	Natural antisense transcript siRNAs
Nb	Nicotiana benthamiana
NOSt	Nopaline synthase terminator
Nt	Nucloetide
PAGE	Polyacrylamide Gel Electrophoresis
PAMPs	Pathogen associated molecular patterns
PAZ	Piwi Argaonaut and Zwille
P-bodies	Processing bodies
PDS	Phytoene desaturase
PEBV	Pea early-browning virus
PRR	Pattern recognition receptor
PTGS	Post-transciptional gene silencing
PTI	PAMP triggered immunity
PVT	*Potato virus T*
PVX	*Potato virus X*
PVYV	*Pear vine yellow virus*
R proteins	Resistant proteins
RDR	RNA Dependent RNA polymerase (in plant)
RDR1	RNA-depedent RNA polymerase1
RDR2	RNA-depedent RNA polymerase 2
RDR6	RNA-depedent RNA polymerase 6
RdRP	RNA Dependent RNA polymerase (in virus)
RISC	RNA-induced silencing complex
RNA	Ribonucleic Acid
RNAi	RNA interference
RuCV-1	*Rubus canadensis virus 1*
SAR	Systemic acquired resistance
SDE1	Silencing Defective1
SDS	Sodium Dodecyl Sulfate
sgRNAs	subgenomic RNAs
SGS2	Suppressor of Gene Silencing 3
SGS3	Suppressor of Gene Silencing 3
siRNA	small interferent RNA
sRNA	small RNA
SSMaV	*Sugarcane striate mosaic-associated virus*
ta-siRNA	trans-acting RNA
TBSV	*Tomato bushy stunt virus*
TCV	*Turnip crinkle virus*
T-DNA	Transferred DNA
TGB	Triple Gene Block
TGMV	*Tomato golden mosaic virus*
TGS	Transcriptional gene silencing
TILLING	Targeting induced local lesions in genome
TMV	*Tobacco mosaic virus*
ToRSV	*Tomato ringspot virus*
TRV	*Tobacco rattle virus*
TSV	*Tobacco streak virus*
TuMV	*Turnip mosaic virus*

Abbreviations	Full name
TVCV	*Turnip vein clearing virus*
UTR	Untranslated Region
VIGS	Virus induced gene silencing
vRNA	viral RNA
vsiRNA	viral small interferent RNA
VSR	Viral Suppressor of RNA silencing
WT	Wild type

List of Figures

List of Tables

Chapter 1 - Plant immune responses against viruses

There are two layers of plant immune responses against pathogens such as viruses, bacteria, fungi and oomycetes. First, certain conserved pathogen- or microbe-associated molecular patterns (P/MAMPs) recognized plant pattern recognition receptors (PRRs), which is called PAMP or MAMP-triggered immune (PTI). In many cases, PTI likely contributes to the so-called non-host resistance of plants. Second, to avoid plant PTI defenses, adapted microbes develop specific effector proteins to suppress PTI. To further defend the action of the microbial effectors, plants evolved specific surveillance systems involving resistance (R) proteins that directly or indirectly recognize the microbial effectors or monitor their activities in the cell to trigger the so-called effector-triggered immune (ETI) (Pieterse et al 2009) (Fig. 1-1).

Plants have developed several mechanisms to defend against viruses, such as Resistance (R) gene-mediated response, RNA silencing (Soosaar et al 2005), Lectin protein-mediated responses, and other host proteins such as Translational initiation factors, Endoplasmic Reticulum (ER) (Mandadi and Scholthof 2013). However, RNA silencing was thought to be the primary plant defense against viruses (Ding and Voinnet 2007). Recently, significant progress has been made in understanding RNA silencing and how viruses counter this ubiquitous antiviral defense.

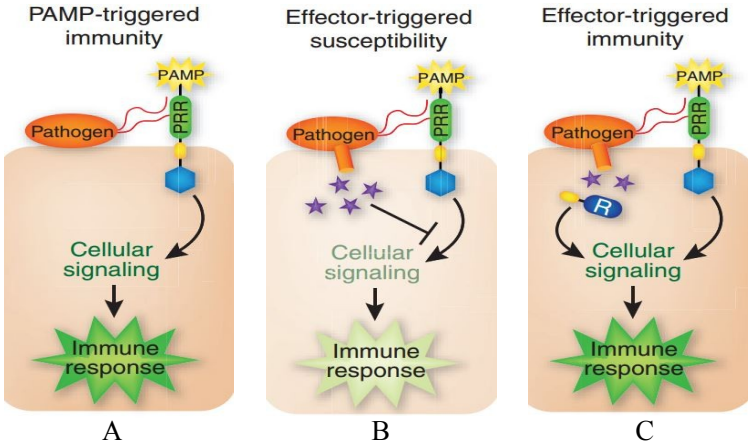

Fig. 1-1 Simplified schematic representation of the plant immune system
A, upon pathogen attack, Pathogen-or Microbial-associated molecular patterns (PAMPs or MAMPs) activate pattern-recognition receptors (PRRs) in the host, resulting in a downstream signaling cascade that leads to PAMP-triggered immunity (PTI); B, Virulent pathogens have acquired effectors (purple stars) that suppress PTI, resulting in effector-triggered susceptibility (ETS); C, In turn, plants have evolved resistance (R) proteins that recognize these attacker-specific effectors, resulting in a secondary immune response called effector-triggered immunity (ETI) (Pieterse et al 2009)

1.1 RNA Silencing in plant

1.1.1 Definition of RNA Silencing

RNA silencing is a sequence-specific RNA degradation mechanism that occurs in a broad range of eukaryotic organisms including fungi (quelling), animals (RNA interference, RNAi), and plants (post-transcriptional gene silencing, PTGS). In plants, RNA silencing is a fundamental regulator of the expression of endogenous genes and exogenous molecular parasites such as viruses, transgenes, and transposable elements (Dunoyer et al 2013). And so how does RNA silencing function?

In the past ten years, by using genetic and molecular analysis, several RNA silencing pathways in plants have been revealed (Baulcombe 2004; Brodersen and Voinnet 2006). However, those pathways share some common biochemical features: 1) formation of double-stranded RNA (dsRNA); regardless of its origin, the appearance of dsRNA in the cytoplasm of plant cells triggers RNA silencing, 2) longer precursor molecules of either perfectly or imperfectly dsRNA is cut by an enzyme, Dicer, that has RNase III domains, into small 20–25 nt dsRNAs with 2 nucleotide overhangs at the 3' ends, 3) these small dsRNA molecules are unwound and a selected sRNA strand binds to 'slicing' complexes called RISC (RNA-induced silencing complexes), which contain Argonaute (AGO) proteins to act on partially or fully complementary RNA or DNA (Fig. 1-2) (Brodersen and Voinnet 2006). Despite common features of RNA silencing in plants, there are differences between different RNA silencing pathways as reviewed by Brodersen and Voinnet in 2006 (Brodersen and Voinnet 2006). In next several paragraphs I will briefly talk about the different small RNAs produced by different RNA silencing pathways mechanism.

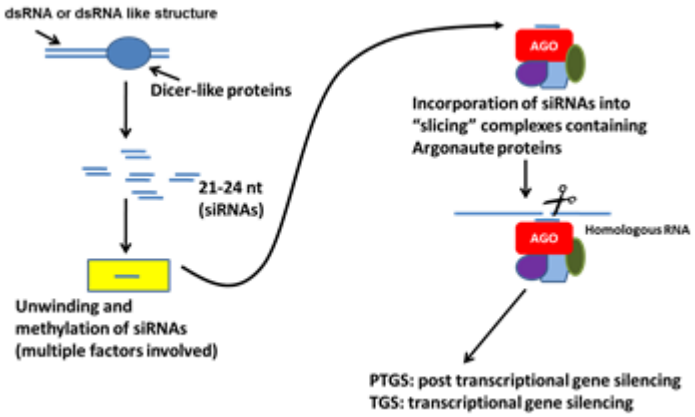

Fig. 1-2 Simplified model of plant RNA silencing pathway

1.1.2 The non-cell-autonomous nature of RNA Silencing

Plant virus infections begin with virus entry into plant cells through a wound created either by mechanical ways or a vector organism, followed by viral replicase gene expression and replication in infected cells. Then the virus begins cell-to-cell movement through plasmodesmata and long distance movement through the vascular system. It was then found that the RNA silencing shares the same movement pathway with the virus (Voinnet 2005a).

Systemic RNA silencing was firstly discovered in transgenic tobacco exhibiting spontaneous co-suppression of nitrate reductase (*Nia*) of both the transgene and the host gene (Palauqui et al 1996). Subsequently, graft experiments demonstrated the *Nia* co-suppressed state was transmitted with 100% efficiency from silenced rootstocks to non-silenced scions expressing the corresponding transgene (Palauqui et al 1997). Soon after this discovery, leaf agro-infiltration *Agrobacterium tumefaciens* carrying a GFP reporter gene into GFP transgenic *Nicotiana benthamiana* was found to trigger a systemic, sequence-specific loss of GFP expression (Voinnet and Baulcombe 1997). Since then, the 'non-cell-autonomous' character of RNA silencing has been documented, which was one of the most important properties of RNA silencing found in plants and animals. Non-cell-autonomous, in other words, is its ability to move from the cell where it has been initiated to the neighboring cells (Mlotshwa et al 2002; Yoo et al 2004; Voinnet, 2005a; Kehr and Buhtz 2008). The degree of movement of silencing signals depends on the physiological conditions and surrounding environment of the tissue.

The next question was what triggered RNA silencing moving systemically? Although virtually any RNA that shares the required sequence homology with target RNAs can trigger systemic silencing in transgenic plants, the mobile and spreading of RNA silencing signals finally was demonstrated to be mediated by small noncoding RNA (sRNA, 21-25 nucleotides in length) (Klahre et al 2002; Hewezi et al 2005; Dunoyer et al 2010; Molnar et al 2010). The functions of small RNA movement include developmental patterning, viral resistance, epigenetic changes, etc (Dunoyer et al 2013).

1.1.3 Different types of small RNAs in plants

Plant endogenous small RNAs (sRNAs) involved in regulating gene expression at transcriptional or post transcriptional level, so as to regulate plants growth and devolepment. sRNAs sizes range from 20 to 24 nt, and include microRNAs (miRNAs), small interfering RNAs (siRNAs) and so on (Table 1-1) (Axtell 2013). These sRNAs can

be distinguished based on their origin, biogenesis pathways, molecular features and their fuctions in regulationg gene expression (Brodersen and Voinnet 2006). SiRNAs can function in plants in a non-cell-autonomous manner in that they are able to move from the cell where it has been initiated to neighboring cells (Voinnet, 2005a; Melnyk et al 2011). In contrast, most plant miRNAs are relatively immobile and cell autonomous (Parizotto et al 2004; Alvarez et al 2006), although some miRNAs have been recently reported to function in non-cell-autonomous way, for instance, miR165/166 is produced in specific root cells and moves to adjacent cells, movement of miRNAs over a set number of cells could generate gradients of gene expression in meristems and primordial (Himber et al 2003).

Table1-1 Hierarchical classification system for endogenous plant small RNAs

Primary classifications	Secondary classifications	Tertiary classifications
hpRNAs small RNAs whose precursor is single-stranded hpRNA	**MiRNAs** precisely processed precursor hairpins yielding just one or a few functional small RNAs	**Lineage-specific miRNAs** miRNAs that are found in only one species or a few closely related species
		Long miRNAs 23–24-nt miRNAs that function similarly to heterochromatic siRNAs to deposit repressive chromatin marks
	Other hpRNAs Imprecisely processed precursor hairpins that do not qualify as miRNAs	
siRNAs small RNAs whose precursor is dsRNA	**Heterochromatic siRNAs** siRNAs produced chiefl from intergenic and/or repetitive regions; typically 23–24 nt in length and associated with de novo deposition of repressive chromatin marks	
	Secondary siRNAs siRNAs whose precursor dsRNA synthesis depends on an upstream small RNA trigger and subsequent RDR activity	**Phased siRNAs** secondary siRNA loci whose dsRNA precursor has a uniformly defied terminus, resulting in the production of a phased set of siRNAs
		***trans*-Acting siRNAs** secondary siRNAs that have one or more targets distinct from their locus of origin
	Natural antisense transcript siRNAs (NAT-siRNAs) siRNAs whose precursor dsRNA is formed by the hybridization of complementary and independently transcribed RNAs	***cis*-NAT-siRNAs** NAT-siRNAs whose precursors were transcribed from overlapping genes in opposite polarities
		***trans*-NAT-siRNAs** NAT-siRNAs whose precursors were transcribed from nonoverlapping genes whose mRNAs have complementarity

Note, this table was modified from the review by Axtell (Axtell 2013)

1.2 RNA silencing-associated proteins in *Arabidopsis thaliana*

Dicer-like enzymes (DCLs), Argonaute (AGO) proteins, RNA-dependent RNA polymerase (RDR) proteins, and dsRNA binding proteins (DRBs) are core components of RNA silencing pathways involved in siRNA biogenesis. In in the following sections I will discuss in detail some of these proteins.

I.2.1 Dicer-like enzymes

The Dicer or Dicer-like (DCL) (a kind of ribonuclease III enzymes) proteins found in animals, fungal and plants are large proteins (~200 kDa), which consist of seven functional domains that interact with RNA in different ways (Fig. 1-3A). These seven domains are: DExD-helicase domain, helicase-C domain, Duf283 domain (unknown function but is strongly conserved among Dicers), PAZ domain, two RNaseIII domains and double stranded RNA-binding (dsRB) domain. Dicer proteins are encoded by most eukaryotes, but plants contain all the seven characteristic domains selectively (Margis et al 2006; Chapman and Carrington 2007).

Dicer-like or DCL proteins play an important role in the miRNA and siRNA biogenesis by processing double-stranded RNAs into sRNAs, which make them essential for eukaryote organism development and viral defense. The number of Dicer or DCL proteins encoded by different organisms is different, for instance, humans, mice and nematodes each possess only one Dicer gene, insects and fungi each possess two Dicer genes, in plants, both rice and *Arabidopsis thaliana* have been reported to have four Dicer-like genes (Tijsterman and Plasterk 2004; Margis et al 2006; Liu et al 2009). The four Dicer-like (DCL) RNaseIII proteins in *Arabidopsis* are named DCL1, DCL2, DCL3, DCL4, respectively. DCL1 locates in the chromosome 1 of *Arabidopsis thaliana* genome, DCL2 and DCL3 locate in the chromosome 3, whereas DCL4 located in chromosome 5 (Fig. 1-3B).

In *Arabidopsis*, DCLs are ubiquitously, but not evenly expressed in different tissues. Different expression patterns of DCL genes were also found at different developmental stages, DCL1, 2, 3, and 4 have relatively higher expression level in flowers, but lower in rosette leaf and stem (Liu et al 2009) (Fig. 1-3C). The four Dicer-like proteins are found to have roles in generating different siRNAs. DCL1 mainly processes miRNAs (Vazquez et al 2004) that guide cleavage of homologous cellular transcripts involved in development and probably many other functions, 21 nt secondary nat-siRNAs (Vazquez et al 2004) and also has a role in the production of small RNAs from endogenous inverted

repeats. DCL2 synthesizes 24 nt primer nat-siRNAs, viral siRNAs and in *dcl4* mutant plants, it alternately processed 22 nt long siRNAs from ta-siRNA precursors (Bouche et al 2006; Deleris et al 2006). DCL3 produces 24 nt long, DNA repeat–associated siRNAs as guides for chromatin modification, RDR2-dependent siRNAs. DCL3 also produces RDR6-dependent trans-acting siRNAs. DCL4 processes dsRNA into 21nt-long siRNAs that mediate trans-acting RNA silencing (Vazquez et al 2004; Dunoyer et al 2005; Gasciolli et al 2005; Xie et al 2005; Adenot et al 2006), transgene RNA interference and some miRNAs biosynthesis.

There is functional redundancy of the four DCL in *Arabidopsis thaliana.* For instance, the functions of DCL1 and DCL3 overlap to promote *Arabidopsis* flowering. In *dcl3* mutants DCL2 and DCL4 have access to DCL3 substrates and produce 22-nucleotide and 21-nucleotide siRNAs from RDR2-dependent precursors (Gasciolli et al 2005; Moissiard et al 2007; Yang et al 2007). Some results show that in *Arabidopsis thaliana* DCL proteins interact with the HYL1/DRB family of dsRNA-binding proteins, such as that DRB4 interacts specifically with DCL4, and HYL1 most strongly interacts with DCL1. These results indicate that each HYL1/DRB family protein interacts with one specific partner among the four Dicer-like proteins (Hiraguri et al 2005).

DCL4 is the primary antiviral Dicer against (+) ssRNA viruses and produces 21 nt long viRNAs (Deleris et al 2006). viRNA synthesis by DCL2 is hardly detectable when DCL4 is functional, but DCL2 can produces 22 nt long viRNAs if DCL4 is genetically inactivated or suppressed. For instance, the coat protein of *Turnip crinkle virus* (TCV) functions as a suppressor by indirectly inhibiting DCL4 expression, which leads to hyper-accumulation of DCL2 dependent 22 nt long siRNAs (Thomas et al 2003; Deleris et al 2006). DCL3 seems play a more important role in DNA virus defense, however, loss of the Cauliflower mosaic virus-derived 24 nt siRNA in *dcl3* mutants is accompanied by an increased accumulation of virus-derived 21 nt long siRNAs (Moissiard and Voinnet 2006). The contribution of the DCL1 to immunity against some viruses is negligible because *dcl2/dcl3/dcl4* and *dcl1/dcl2/dcl3/dcl4* mutants showed similar susceptibility to *Cucumber mosaic virus* (CMV) or TCV, and DCL1-dependent viRNAs were hardly detectable even in the dcl2/dcl3/dcl4 mutant (Deleris et al 2006). These findings indicate that DCL proteins collectively contribute to the plant's defense against different viruses, and that loss or suppression of activity of one DCL can be compensated for by the activities of other DCL proteins.

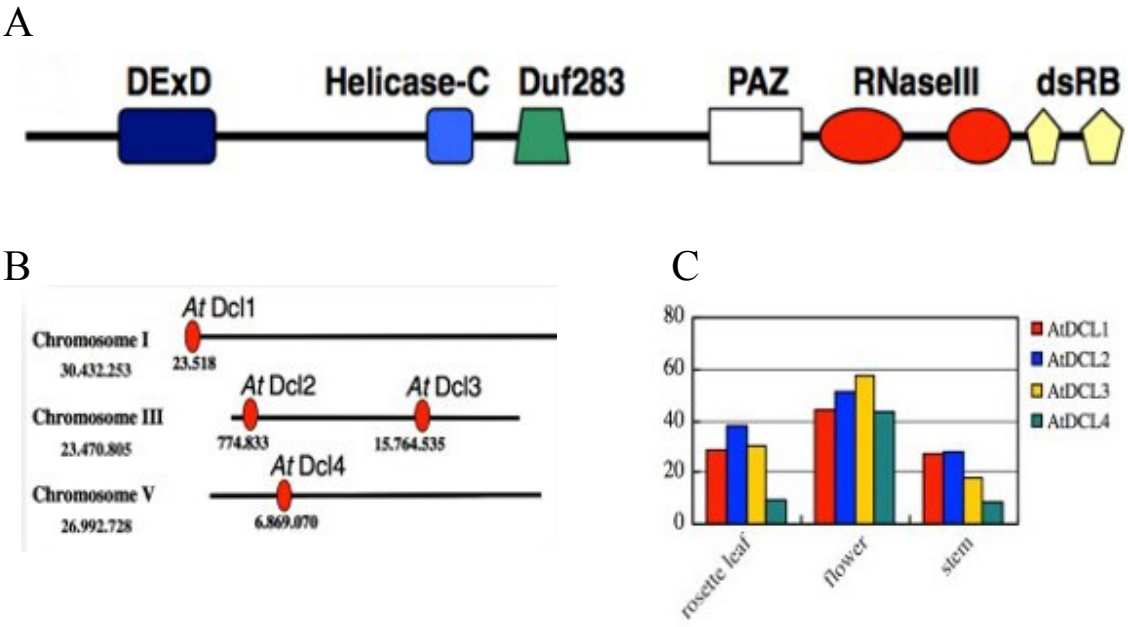

Fig. 1-3 Information on Dicer-like Enzymes
A, The linear arrangement of domains typically found in DCL (Margis et al 2006); B, The chromosome locations of DCL genes in Arabidopsis. Each chromosome is depicted approximately to scale, the number under each gene is the position on the pseudomolecule of the start of the gene (Margis et al 2006); C, Gene expression patterns of Arabidopsis DCLs in different tissues (Liu et al 2009)

1.2.2 Argonaute (AGO) proteins

The Argonaute (AGO) proteins are executor components of RISCs, bringing about degradation or translational inhibition of targeted RNAs specified by incorporated sRNAs. The word 'Argonaute' was firstly used by Karen Bohmert in 1998 to describe *Arabidopsis thaliana ago1* mutant, in which morphology of the leaves closely resembled the tentacles of a small squid of *Argonauta* genus (Bohmert et al 1998; Hutvagner and Simard 2008). The first three founding members of AGO proteins family were: element-induced wimpy testis (PIWI) of *Drosophila* P (Lin and Spradling 1997), ARGONAUTE1 (AGO1) of *Arabidopsis* (Bohmert et al 1998) and ZWILLE (ZLL) of *Arabidopsis* (Moussian et al 1998). AGOs are large proteins (90-100 kDa) consisting of a variable N-terminal domain and conserved C-terminal PAZ, MID and PIWI domains (Fig. 1-4B, C), in which the PIWI domain makes AGO proteins different from DICER proteins that also have a PAZ domain. Argonaute proteins are highly specialized small RNA-binding modules and are considered to be the key components of RNA silencing pathways. The N-terminal domain is thought to facilitate the separation of the sRNA/target transcript duplex after cleavage. The MID domain binds to the 5' phosphate of sRNAs, whereas the PAZ domain recognizes the 3' end of sRNAs. The PIWI domain resembles that of bacterial RNaseH

enzymes and exhibits endonuclease activity (Vaucheret 2008).

All AGO proteins are divided into three groups on the basis of both their phylogenetic relationships and their capacity to binding sRNAs. Group 1 members bind miRNAs and siRNAs are referred to as AGO-like proteins. Group 2 members bind PIWI-interacting RNAs (piRNAs) are referred to as PIWI-like proteins. Group 3 members have been described only in *Caenorhabditis elegans*, where they bind secondary siRNAs (Yigit et al 2006). The number of AGO proteins encoded by different organisms varies greatly, *Saccharomyces cerevisiae* does not encode any AGO proteins and does not seem to encode other small RNA pathway factors, *Schizosaccharomyces pombe* expresses one AGO-like protein, *Caenorhabditis elegans* expresses 27 AGO proteins that fall into both AGO-like and PIWI-like subfamilies, *Homo sapiens* express 8 AGO proteins that fall into both AGO-like and PIWI-like subfamilies subfamilies, plant AGO proteins are all in the AGO-like subfamily, *Oryza sativa* eoncodes 18 AGO proteins while *Arabidopsis thaliana* encodes 10 AGO proteins. (Vaucheret 2008; Ender and Meister 2010; Mallory and Vaucheret 2010; Kim et al 2011). A phylogenetic analysis of the 10 *Arabidopsis* AGO proteins placed them in three major clades: the AGO1, AGO5, and AGO10 clade; the AGO2, AGO3, and AGO7 clade; and the AGO4, AGO6, AGO8, and AGO9 clade (Fig. 1-4A). It is important to note that the distribution of the 10 *Arabidopsis* AGO proteins into three distinct clades is based on amino acid sequence similarity, and does not necessarily directly infer similarities in activity or redundancies in function.

Several studies reveal that AGO1 is ubiquitously expressed at high levels throughout developmental stages and different tissues, but its expression appears to be highest in meristem and provascular cells. However, AGO10 is initially expressed throughout the embryo but becomes limited to provascular strands and the adaxial sides of the cotyledons at about the globular stage. Thus, AGO1 and AGO10 expression patterns overlap partially, with the AGO1 expression pattern being broader than that of AGO10. Moreover, fusion of the AGO10 coding sequence to the AGO1 promoter revealed that AGO10 could partially compensate for AGO1 activity, but *ago10* mutants were not impaired in S-PTGS and show no reduction in the accumulation miRNAs, tasiRNAs or any other siRNA. By contrast, the expression profile for AGO5 is highly limited to reproductive tissues, accumulating in the sperm cell cytoplasm in mature pollen and growing pollen tubes (Schmid et al 2005; Vaucheret et al 2006; Vaucheret 2008; Mallory et al 2009; Mallory and Vaucheret 2010) (Fig. 1-4D).

Array data reveals that all three family members in the AGO2/3/7 clade have overlapping expression domains. AGO2 and 3 have high level of sequence similarity, proximal genomic positioning and same expression patterns (both AGO2 and 3 are most highly expressed in developing seeds and siliques, and at lower levels in senescing leaves and flowers). All of this strongly suggests that they have the same or similar RNA silencing roles in *Arabidopsis*, however, to date, no function has been reported for AGO3 nor has redundancy has been reported for these two proteins, suggesting that AGO3 may be a pseudogene. AGO7 is involved in tasi-RNA production, which regulates the expression of many developmentally important genes. AGO7 expression is very importance for normal leaf development, which is predominantly expressed in the vasculature of seedlings and in the cells and tissues immediately surrounding the SAM (Schmid et al 2005; Mallory and Vaucheret 2010) (Fig. 1-4D).

Results from fusing the AGO4, 6, 9 proteins to GUS reporter gene revealed that, AGO4 has widespread expression in embryos, leaves, and flowers. AGO4 is not only required for sRNA-directed DNA methylation, but also for the maintenance of heterochromatin (Irvine et al 2006). By contrast, AGO6 expression is restricted to shoot and root growth points and the vascular tissue connecting these domains, and AGO9 expression is restricted to the embryonic shoot apex region and developing ovules (Havecker 2010) (Fig. 1-5D). The amino-acid sequences of these AGO8 and AGO9 are very similar and the two genes are almost adjacent to one another on chromosome 5 of the Arabidopsis genome. The tissue-specific expression patterns of AGO8 and AGO9 mRNAs are also highly similar (Schmid et al 2005). However, the AGO8 transcript is expressed at a much lower level than AGO9 and it has been proposed that AGO8 is a pseudogene (Takahashi et al 2008).

AGO proteins are often named ‘slicer proteins’ because they cleave target ssRNAs at the duplex formed with the guide-strand small RNA. AGO proteins directly bind sRNAs, and different AGOs bind different sRNAs of specific length and preferred 5' nucleotide. For example, AGO1 binds sRNAs that are predominantly of the 21 nt size class with a 5' terminal uracil, whereas AGO2 preferentially binds 21 nt size class with a 5' terminal adenine. Usually AGO5 preferentially binds sRNAs of the 24 nt size class with a cytosine at their 5' terminal, however, AGO5 is also able to bind miR169, which is a 21 nt long miRNA with a uracil as the 5' terminal nucleotide (Irvine et al 2006; Mi et al 2008). AGOs 4, 6 and 9 also preferentially bind sRNAs of the 24 nt size class with 5' adenine

residues. The 5' terminal nucleotide preference for AGOs 3, 7, 8 and 10 remain to be determined (Mi et al 2008) (Table1-2). Because of the sRNA binding ability, most of the Arabidopsis AGO proteins have been observed to bind miRNA involved in plant development, for instance, AGO5/miR169 (Takeda et al 2008), AGO10/miR165 and miR166 (Liu et al 2009; Zhu et al 2011), AGO7/ miR390 (Montgomery et al 2008).

Among the ten Arabidopsis AGO proteins, AGO1 is the best studied. By using ago1 mutant alleles in genetic screens for reactivation of post transcriptionally silenced sense transgenes (S-PTGS), AGO1 was implicated in miRNA biogenesis. Indeed, in ago1 mutant alleles, miRNA accumulation is reduced and, at the same time miRNA target mRNA accumulation is increased, further indicating that AGO1 is necessary in the miRNA pathway (Vaucheret et al 2006). The majority of miRNAs have a 5' terminal uracil residue and are preferentially loaded by AGO1, and AGO1 has been shown to direct sRNA-mediated gene expression regulation for all currently characterized Arabidopsis miRNAs. Because AGO1 has important role of in the regulation of other genes in plants through RNA silencing, there are a lot of studies associated with how AGO1 is regulated in planta. In 2006, Hervé Vaucheret and colleagues reported that AGO1 homeostasis is maintained through the repressive action of miR168 on AGO1 mRNA and the stabilizing effect of AGO1 protein on miR168 (Vaucheret et al 2004; Vaucheret et al 2006). In 2009, the same group found that AGO1 homeostasis not only regulated by the action of the microRNA but also siRNA pathways, in this report they showed that AGO1-derived siRNAs trigger AGO1 silencing in an RDR6-, SDE5- and SGS3-dependent manner, and that production of AGO1-derived siRNAs requires the action of DCL2 and DCL4, similar to viruses and inverted repeat transgenes (Mallory and Vaucheret 2009). Recent studies have described the increased expression of miR168 and AGO1 mRNA in virus-infected plants, miR168-driven control of AGO1 can persist for a long time in virus-infected plants and can be an important component of symptom development (Varallyay et al 2010; Varallyay and Havelda 2013).

Several studies have demonstrated a role for AGO1 in RNA silencing based antiviral defense, including the following observations: (1) *ago1* hypomorphic mutants are more susceptible to CMV and TCV (Morel et al 2002; Qu et al 2008; Wang et al 2011); (2) several VSRs are able to interact directly with AGO1 (Zhang et al 2006; Baumberger et al 2007; Chiu et al 2010; Csorba et al 2010; Feng et al 2013; Varallyay and Havelda 2013); (3) AGO1 binds virus-specific siRNAs (Zhang et al 2006). In addition to AGO1, other

AGO proteins such as AGO2 (Rand et al 2005; Harvey et al 2011; Jaubert et al 2011; Scholthof et al 2011; Wang et al 2011) and AGO7 was observed in the antiviral defense (Qu et al 2008), while *ago4* plants are observed hyper-susceptibile to the bacterial pathogen *Pseudomonas syringae* (Agorio and Vera 2007). AGO2 has also been shown to act downstream of the viral secondary siRNA biogenesis together with AGO1 in a non-redundant manner, essential for defense against CMV infection (Wang et al 2011). Knock-down of *Ago2* in *N. benthamiana* by VIGS allows high accumulation of a version of *Tomato bushy stunt virus* (TBSV) lacking a VSR. At the same time, of all ten AGOs, only mutations in AGO2 allow high level accumulation of PVX in Arabidopsis, a host that it does not normally infect. These results suggest that different AGO family members are engaged by basal and induced anti-viral responses, respectively.

Table 1-2 The 5' terminal nucleotide and size preferences of *Arabidopsis* AGOs
(Kim et al 2011, Vaucheret 2008)

Gene name	Gene code	Mutant allele	Ecotype	Type of mutation	protein size (aa)	5' teminal nucleotide preference	sRNA length preference (nt)
AGO1	At1g48410	*ago1–27*	Col-0	EMS	1048	U	21
AGO2	At1g31280	*ago2–1*	Col-0	T-DNA	1014	A	21
AGO3	At1g31290	*ago3-2*	Col-0	T-DNA	1194	Unkown	Unkown
AGO4	At2g27040	*ago4-2*	Col-0	EMS	924	A	24
AGO5	At2g27880	*ago5-1*	Col-0	T-DNA	997	C	24/21
AGO6	At2g32940	*ago6-3*	Col-0	T-DNA	878	A	24
AGO7	At1g69440	*ago7-1*	Col-0	T-DNA	990	Unkown	Unkown
AGO8	At5g21030	*ago8-1*	Col-0	T-DNA	850	Unkown	Unkown
AGO9	At5g21150	*ago9-1*	Col-0	T-DNA	896	A	24
AGO10	At5g43810	*ago10-2*	Col-0	T-DNA	988	Unkown	Unkown

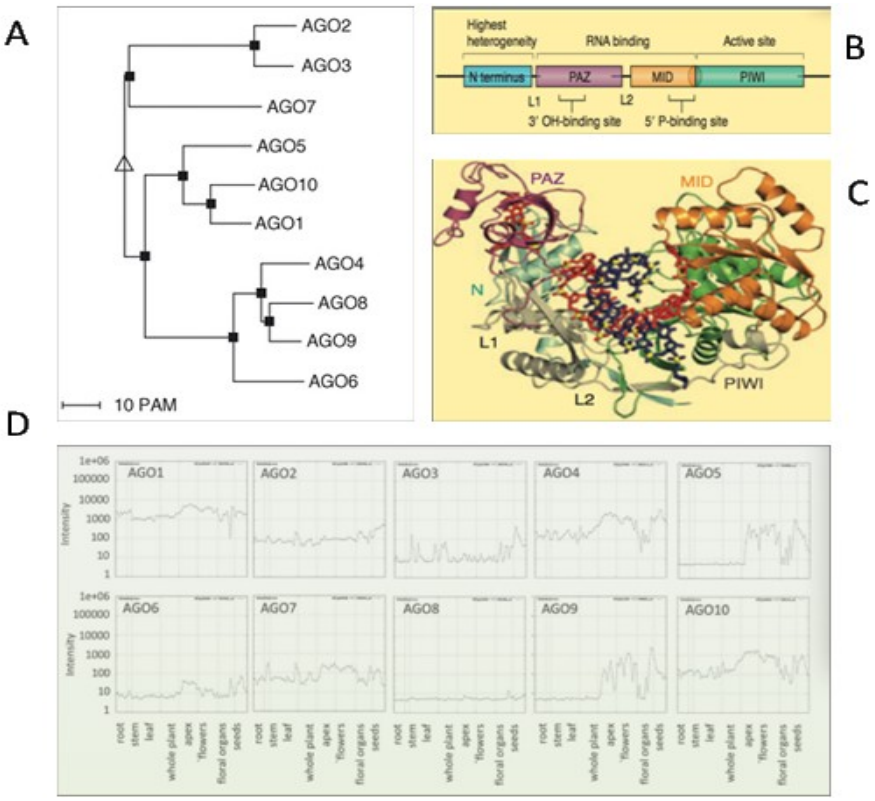

Fig. 1-4 Information on Argonaute proteins

A, Phylogenetic classification of Arabidopsis AGO proteins into three clades (Vaucheret 2008); B, Domain structure of an Argonaute protein (EnderMeister 2010); C, Crystal structure of the Argonaute protein from *Thermos thermophile*.s (EnderMeister 2010); D, Expression Intensities of the 10 *Arabidopsis* AGO genes at various developmental stages and in different tissues (MalloryVaucheret 2010)

1.2.3 RDR proteins and other proteins involved in RNA silencing

The activity of plant RNA-dependent RNA polymerases (RdRPs) was first reported in Chinese cabbage in 1971 (Astier-Manifacier et al 1971). Since then, RdRPs have been found in a number of plants including *Arabidopsis* (Dalmay et al 2000; Mourrain et al 2000). Arabidopsis plants contain at least six active RdRP genes, termed RDR1-RDR6 (RDR6 also known as SDE1/SGS2) (Schwach et al 2005) and they function both differently and redundantly (Yu et al 2003). A likely role of RDRs in RNA silencing is to produce dsRNA that is cleaved by DCL proteins in plants. SDE1, an RNA-dependent RNA polymerase gene in *Arabidopsis* is required for PTGS mediated by a transgene not by a virus. The role of SDE1 is to produce a dsRNA activator of PTGS (Dalmay et al 2000). *Arabidopsis* SGS2 encode a protein that is similar to an RdRPs and SGS3 encodes a novel plant-specific protein. The isolation of *sgs2* and *sgs3 Arabidopsis* mutants impaired in PTGS, SGS2/SDE1 and SGS3 were also reported to be required for juvenile development and the production of trans-acting siRNAs in *Arabidopsis* (Mourrain et al

2000; Peragine et al 2004). Thus RDR6 is thought to recognize, and to use as templates, certain transgene transcripts with aberrant features that include a lack of 5' capping. This favours their conversion into dsRNA by RDR6 and the subsequent degradation of all transgene transcripts through the S-PTGS pathway (Brodersen and Voinnet 2006). RDR2 is required for the production of siRNAs from endogenous transcripts, but is not required for virus resistance. RDR1 is induced upon viral infection and limits virus replication, but has no apparent role in the silencing of endogenous transcripts (Xie et al 2004). RdRPs were first implicated in regulating virus accumulation in plants through the analysis of the sgs2 and sgs3 mutant *Arabidopsis* lines. The *sgs2* and *sgs3* mutants show enhanced susceptibility to CMV but not to TuMV or TVCV Infection (Mourrain et al 2000). Plants with compromised RDR6 function are hyper-susceptible to several viruses (Brodersen and Voinnet 2006). The ortholog of RDR1 has been shown to contribute to defense against *Tobacco mosaic virus* (TMV) and PVX in *N. tabacum* (Mandadi and Scholthof 2013) and the lack of a functional ortholog of this enzyme is at least partly responsible for the hyper-susceptibility of *N. benthamiana* plants to TMV. SGS2/SDE1 and SGS3 were reported to be required for virus induced gene silencing (VIGS) of endogenous genes using a geminivirus CaLCuV vector.

Except for the proteins described above, a number of other proteins in *Arabidopsis* have also been shown to play roles in RNA silencing pathways (Table1-3).

1.3 The antiviral role of RNA silencing

Plants have developed diverse mechanisms to defend virus infections. One mechanism is through RNA silencing. Two lines of evidence indicate that RNA silencing has a role for antiviral defense in plants (Baulcombe 2004). Firstly, virus-derived siRNAs (viRNAs) accumulate during virus infections. Secondly, Plant viruses have elaborated a variety of counter-defensive measures to overcome the host silencing response. One of these strategies is to produce proteins called viral suppressors of RNA silencing (VSRs) that target different steps of RNA silencing such as DCL, RISC, or small RNA. Thirdly, Plants lacking of RNA silencing components are more susceptible to some virus infection (Voinnet et al 1999).

Table 1-3 Other proteins involved in *Arabidopsis* sRNA pathways
(BrodersenVoinnet 2006)

Proteins	Domains and motifs	Biochemical activity	Pathway
HYL1	dsRNA binding domnian	dsRNA binding	miRNA pathway
HST	RanGTP binding	Putative exportin	miRNA pathway
HEN1	sRNA binding domnian Lupus La RNA binding S-adenosyl binding	sRNA Methyltranseferase	All sRNA pathways
WEX	3'–5' exonuclease	Putative 3'–5' exonuclease	S-PTGS
SDE3	DEAD Helicase	Putative RNA helicase	S-PTGS /Transitivity
NRPD1a	RNA Polymerase	Referred DNA dependent RNA Polymerase	Chromosome/nat-siRNA
NRPD1b	RNA Polymerase	Referred DNA dependent RNA Polymerase	Chromosome
NRPD2	RNA Polymerase	Referred DNA dependent RNA Polymerase	Chromosome
HDA6	Deacetylase	Putative histone deacetylase	Chromosome
DRD1	SNF2-related DNA and ATP binding Helicase	Putative chromatin remodeling	Chromosome
CMT3	Cytosine DNA Methyltranseferase Chromodomain Brom adjacent domain	Cytosine DNA Methyltranseferase	Chromosome
DRM1/2	Cytosine DNA Methyltranseferase	Cytosine DNA Methyltranseferase	Chromosome
MET1	Cytosine DNA Methyltranseferase Bromo-adjacent domain	Cytosine DNA Methyltranseferase	Chromosome
KYP	SET domain ZnII-binding domain Pre-SET domain Post-SET domain YDG domain EF-hand	H3 K9 Methyltranseferase	Chromosome
SUVH	SET domain ZnII-binding pre-SET domain YDG domain	H3 K9 Methyltranseferase	Chromosome

1.4 Virus-encoded VSRs

RNA silencing suppressors were first identified because of the study of the *potexvirus* and *potyvirus* synergistic interaction, which led to the identification of the potyviral Helper HC-Pro of potyvirus as the synergism determinant in this interaction (Pruss et al 1997). Subsequently HC-Pro and CMV-2b were identified as the first silencing suppressor proteins (Anandalakshmi et al 1998; Brigneti et al 1998; Kasschau and Carrington 1998). A subsequent survey of more than 15 viruses further confirmed that suppression of RNA silencing is a general property for plant viruses to counter-plant defense (Voinnet et al 1999). Interestingly, all the suppressors identified from plant viruses have a high diversity in sequence and protein structure, suggesting that they function by diverse mechanisms. Different suppressors suppress different steps of the RNA silencing pathway and a number of recent reviews have discussed plant RNA silencing suppressors and their different behavior in plant (Dalmay et al 2000; Voinnet 2001; MacDiarmid 2005; Qu and Morris 2005; Voinnet 2005a; Scholthof 2006; Ding and Voinnet 2007; Song et al 2011; Incarbone and Dunoyer 2013) (Fig. 1-5).

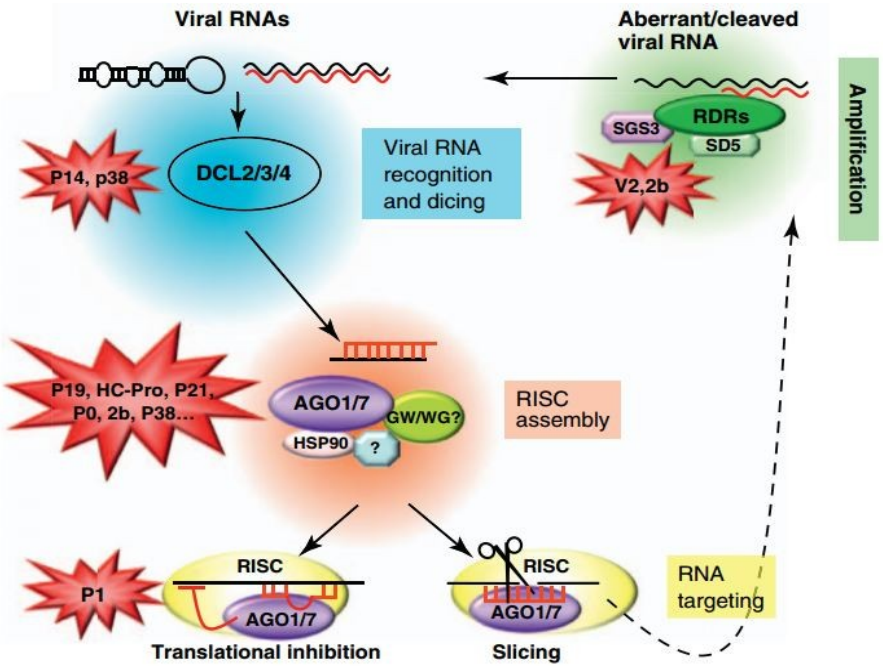

Fig. 1-5 Current model of antiviral RNA silencing in plants and its VSRs
Viral-silencing suppressors can disrupt RNA silencing pathways at multiple points, thereby preventing the assembly of different effectors or inhibiting their actions. The points at which certain VSRs (i.e. P14, P38, V2, 2b, P19, HC-Pro, P21, P0 and P1) interact with the silencing pathways are depicted (Burgyán Havelda 2011)

1.5 *Tobacco rattle virus* TRV

TRV, which forms rod-shaped particles (MacFarlane 1999) and is transmitted by nematodes (Taylor and Brown 1997), has a bipartite, positive-sense single-stranded RNA (+ssRNA) genome and is a type member of the genus *Tobravirus* (family Virgaviridae). TRV genome consists of two RNA molecules, RNA1 and RNA2, in which RNA1 is conserved in size and gene content while RNA2 displays a high sequence variation (MacFarlane 1999). RNA1 encodes four proteins, 134 and 194 kDa replicase proteins (including the methyltransferase, helicase, and RNA-dependent RNA polymerase domains), a 29 kDa movement protein and a 16 kDa cysteine-rich protein (CRP), respectively. The replicase proteins are translated directly from the genomic RNA while the 29 K and 16 K are expressed from respective subgenomic RNAs (sgRNA) and both of them function as a suppressor of RNA silencing (Ghazala et al 2008; Martinez-Priego et al., 2008 Deng et al 2013). Depending on the strains, TRV RNA2 can vary in size and gene content and serial passage of TRV under different selection conditions results in deletion of structural and nonstructural genes in RNA2 (Hernandez et al 1996). However, it always encodes a coat protein (CP), which encapsidates RNA1 and RNA2 into different rod-shaped particles (MacFarlane 1999). RNA2 also encodes the proteins 2b and 2c, which are involved in transmission of TRV by root nematodes (Hernandez et al 1997; MacFarlane 1999), and 2b also involved in invasion of meristems in roots (Valentine et al 2004). All proteins encoded by RNA2 are translated from sgRNAs (MacFarlane 1999). The host range of TRV is very wide, natural infection has been reported in more than 100 species, when inoculation with sap, about 400 species in more than 50 dicotyledonous and monocotyledonous families can be infected. The disease symptoms induced by TRV are affected by environmental conditions, which include necrotic or chlorotic spots, rings, vein necrosis, etc.

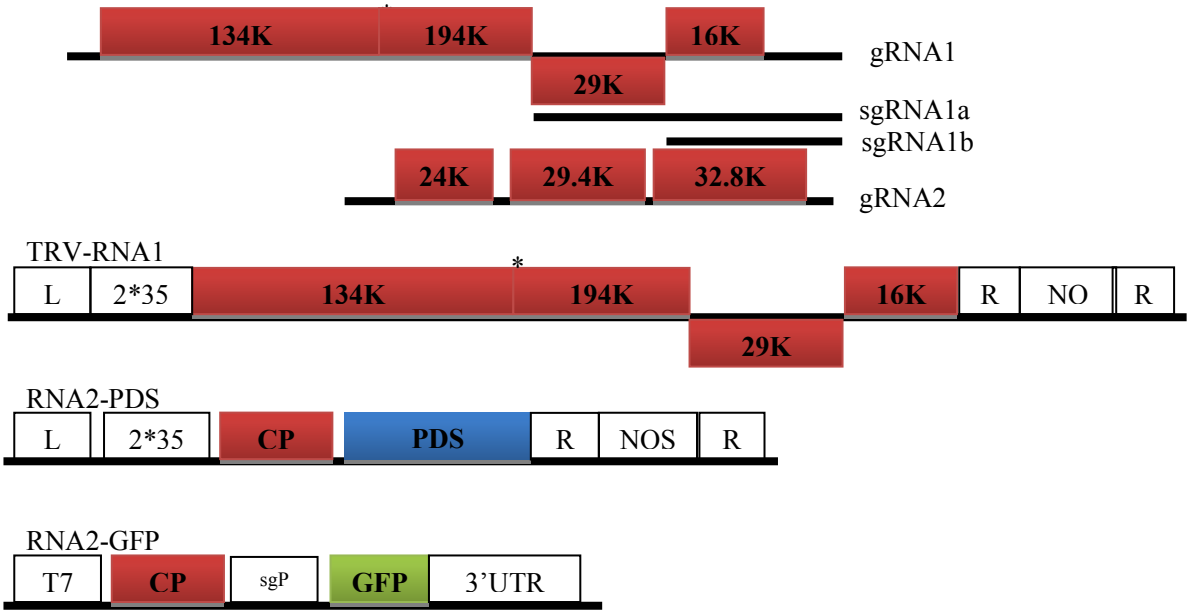

Fig. 1-6 The genome structure of Tobacco rattle virus (TRV) and derivative vectors
1) Wild type TRV; 2) In TRV-RNA1 vector, TRV cDNA clones were placed in between the duplicated CaMV 35S promoter (2×35S) and the nopaline synthase terminator (NOSt) in a T-DNA vector. Rz refers to self-cleaving ribozyme, LB and RB refer to left and right borders of T-DNA; 3) In TRV-RNA2-PDS, whereas the two genes involved in nematode transmission of TRV (*2b* and *2c*) have been removed and replaced with a multiple cloning site (Mcs), PDS was inserted into the Mcs (Liu et al 2002); 4) In RNA2-GFP, the 2b and 2c genes encode nonstructural proteins involved in nematode transmission and are deleted from the vector constructs, GFP was inserted into the Mcs, and the CP subgenomic RNA promoter (sgP) derived from *Pea early-browning virus* has been added upstream of *GFP* (MacFarlane and Popovich 2000)

1.6 Recovery

Recovery was first described by Wingard S. A. in 1928 and is typified by systemic virus infection with associated symptoms followed by decrease and disappearance of symptoms in young leaves (MacDiarmid 2005). Recovery occurs within some natural virus infections (e.g, nepoviruses, AlMV, TRV, CaMV and geminiviruses) (Covey et al 1997; Ratcliff et al 1997; Ratcliff et al 1999; Szittya et al 2002) and transgenic plants engineered for viral resistance (Smith et al 1994; Carlsbecker et al 2010). The recovered plants are immune to the same or closely related strains of the initially infecting virus and this resistance shown by the recovered tissue is sequence specific (Covey et al 1997; Ratcliff et al 1997; Ratcliff et al 1999).

For a long time recovery of plants from natural virus infection or transgenic plants following the primary virus infection is described as a consequence of RNA silencing

(Ratcliff et al 1997; Baulcombe 2004), and there are two lines of evidence for this. One is that the recovered plants are observed to associate with activation of RNA silencing and increased viral siRNA (Szittya et al 2002; Jovel et al 2007). Another is that loss of expression of viral silencing suppressors in mutant viruses results in a recovery-like phenotype instead of nonrecovery (Ding et al 1995; Szittya et al 2002). However, several lines of evidence suggest that activation of virus RNA silencing in infected plants is insufficient to ensure recovery: 1) TRV and *Potato virus X* (PVX) induced RNA silencing provides a sequence-specific cross-protection in *Nicotiana benthamiana* plants, however, only the TRV-infected plants recover (Ratcliff et al 1999); 2) many viruses encode VRSs to counter defense the host RNA silencing antiviral defense including the recover and nonrecovery viruses; 3) for some viruses (e.g., *Tomato ringspot virus*, *Tobacco streak virus*) viral clearance by RNA silencing may not be essential for the initiation of host recovery (Xin and Ding 2003; Jovel et al 2007). Thus, these data collectively argue that host recovery is not an inevitable consequence of activation of the RNA silencing in infected plants and that other factors may play a key role in the initiation of recovery.

There is an association between recovery and meristem exclusion in that most natural recovery viruses can invade the apical growing point while the nonrecovery viruses cannot (Ratcliff et al 1997; Schwach et al 2005). Meristem exclusion is thought to be a variation of the recovery process; classical meristem exclusion would be recovery that is restricted to the growing point of the infected plant, whereas recovery would be meristem exclusion that operated not only in the meristem but also in the uppermost leaves of the plant (Schwach et al 2005). There is also evidence that meristem exclusion is involved in RNA silencing. Firstly, based on the study of the virus-derived gene transgenic plants challenged with the original virus (Smith et al 1994; Carlsbecker et al 2010), scientists found that different transgenic lines exhibited differently, recovery or the normal response to virus infection, which could be influenced by the different expression level of the virus-derived gene in different transgene lines. Frank Schwach et.al (2006) attributed this different exhibition to the amount of silencing signal produced by the virus and the nature of the viral silencing suppressor protein(s) (Schwach et al 2005). Secondly, the nonrecovery virus PVX acquires the ability to invade meristems if it is inoculated on plants expressing viral suppressors of silencing (Foster et al 2002). Thirdly, PVX acquires the ability to invade meristems in *N. benthamiana* line in which *NbRDR6* was down regulated, and the RDR6 is involved RNA silencing (Schwach et al 2005).

Little is known about how host recovery is initiated in virus infected plants, which occurs only in certain host-virus interaction systems. The entire mechanism of recovery is not understood but may simply be an example of completely successful RNA silencing antiviral defense or maybe the ability of viruses to infect the meristem of the plant may also trigger an additional host response that results in recovery.

1.7 Virus-induced gene silencing VIGS

The term Virus-induced gene silencing (VIGS) was first used to describe the phenomenon of recovery from virus infection (Van Kammen et al 1997), so VIGS may in fact be a kind of recovery. Nowadays, VIGS is often used as an RNA silencing based technique used for down regulating a host gene through the use of a recombinant virus. The dsRNA replication intermediates of the viruses is processed into small interfering siRNA in the infected cell that correspond to different parts of the viral vector genome, including the insertion fragments. The host gene derived-siRNAs can mediate degradation of related endogenous gene transcripts, resulting in silencing of target gene expression. This virus-based technique can also be used to explore the plant defense system against viruses. VIGS also was developed as a reverse genetics approach for gene function study. There are several advantages of VIGS when compared to the traditionally approaches, such as chemical or physical mutagenesis, tilling, T-DNA insertion, and transposon tagging. Firstly, VIGS is labour and time saving. It can identify a specific gene function within a single plant generation in a month. Also, VIGS avoids plant transformation, which is labour and time consuming and sometimes, unpredictable. Second, VIGS overcomes gene functional redundancy. By using an inserted sequence derived from the most highly conserved region of a gene family, it is possible to silence all or most of members of a given family. In contrast, specific member of a gene family can be targeted by selecting unique sequence of this member. Third, VIGS allows rapid comparisons of gene function between species because some VIGS vector can infect different plant species (Godge et al 2008). Despite its advantages, there are some limitations for VIGS. Firstly, you need to know the gene sequence of the targets, it is hard to work with plant species that lack sequenced genomes. Second, VIGS does not always result in the complete loss of expression of a target gene and it is hard to say with certainty that the reduced expression of target the gene is not enough to produce at least some functional protein. Third, some VIGS vectors produce disease symptoms and sometimes it can be hard to tell the silenced gene phenotypes from the disease symptoms. Finally, the levels

of silencing can vary between plants and experiments, which introduces an element of variability (Godge et al 2008).

So far, several viruses have been developed as VIGS vectors in plants (Godge et al 2008; Igarashi et al 2009), including TMV (Kumagai et al 1995), PVX (Ruiz et al 1998), *Tomato golden mosaic virus* (TGMV) (Kjemtrup et al 1998), TRV (Ratcliff et al 2001), and *Apple latent spherical virus* (ALSV) (Igarashi et al 2009). These VIGS vectors have successfully silenced endogenous genes like phytoene desaturase (PDS) in *N.benthamiana* plants. Except for being a VIGS vectors, many of these VIGS vector-viruses could also be used as expression vectors to highly express a gene by inserting the gene to the viral genome, but the recombinant viruses often express foreign gene in 2-4 days after inoculation while VIGS a host gene often costs one month. For TRV VIGS and GFP vector, the *2b* and *2c* genes are removed from RNA2, and the GFP gene and the PDS gene was introduced to the RNA2 (Fig. 1-6) (MacFarlane and Popovich 2000; Ratcliff et al 2001; Liu et al 2002). TRV-derived vectors can be used for VIGS in *Solanum* species including tomato, potato, *N. benthamiana*, as well as *Arabidopsis thaliana*. ALSV is a new VIGS vector and does not induce any obvious symptoms in most host plants, and can effectively VIGS endogenous genes among a broad range of plant including different *Nicotiana* species, *Solanum lycopersicum*, *Arabidopsis thaliana*, different *cucurbit* species, and different *legume* species (Igarashi et al 2009).

To be a good VIGS vector, first, the recombinant virus should have a broad range of hosts. Second, they should not cause obvious disease symptoms on inoculated plants, which make interpretation of some genes VIGS phenotypes difficult. Third, these viruses should not be excluded from the growing points or meristems of their hosts, if not, which will preclude effective silencing of genes in those tissues. Finally, they should not suppress RNA silencing too efficiently, because that would negatively affect gene silencing (Godge et al 2008; Igarashi et al 2009). The limitations of host range and meristem exclusion were overcome by the TRV and ALSV based VIGS vectors (Ratcliff et al 2001; Igarashi et al 2009). TRV and ALSV is able to spread more vigorously throughout the entire plant, including meristem tissue, yet the overall symptoms of infection are mild compared with other viruses, and also they both have a broad range of hosts.

1.8 *Foveavirus*

Foveavirus, *Allexivirus*, *Potexvirus*, *Carlavirus*, *Trichovirus*, *Vitivirus*, *Capillovirus*, *Mandarivirus*, *Citrivirus*, and some genuses of undefined viruses such as *Banana mild mosaic virus* (BMMV), *Cherry green ring mottle virus* (CGRMV), *Cherry necrotic rusty mottle virus* (CNRMV), Potato virus T (PVT) and *Sugarcane striate mosaic-associated virus* (SSMaV) were classified into the family of *Flexiviridae* in 2007 (Martelli et al 2007). However, in 2009 the family of *Flexiviridae* were further divided into *Alphaflexiviridae* (*α-flexiviridae*), *Betaflexiviridae* (*β-flexiviridae*) and *Gammaflexiviridae* (ɾ-*flexiviridae*) accorrding to the documents of International Committee on Taxonomy of Viruses (ICTV), these three family and *Tymoviridae* were classified into Tymovirales (Carstens 2009). *Foveavirus* was belong to the family of *Betaflexiviridae*, which included *Apple stem pitting virus* (ASPV) (Jelkmann et al 1994), Apricot latent virus (ApLV) (Nemchinov et al 2000), Grapevine rupestris stem pitting-associated virus (GRSPaV) (Martelli and Jelkmann 1998), Asian prunus virus 1 (APV-1) (ICTV, 2013), Rubus canadensis virus 1 (RuCV-1) (ICTV, 2014).

Viruses in *Foveavirus* genuspositive single-stranded RNA with polyA tail, and virus particles of *Foveavirus* filamentous, 800~1000 nm long and 12~15 nm wide. Usually their genome sizes ranged from 8.4 to 9.3 kb, which contained five open reading frame (ORF1- ORF5) and 5' and 3' untranslated region (UTR) and with CP sizes from 28 to 44 KDa. ORF1 encoded replicase, ORF2-ORF4 encoded Triple gene block (TGB1-TGB3) movement proteins, and ORF5 encoded coat proteins (CP).

TGB (TGB1-TGB3) genes of *Foveavirus* encoded TGBp1 (24~26 KDa), TGBp2 (12~24 KDa), TGBp3 (7~11 KDa), respectively (Solovyev et al 2000), those of whom involved in transporting viral RNAs to the adjacent cells. TGBp1 contained a conservative ATP-GTP binding domain (Wong et al 1998). Both TGBp2 and TGBp3 consisted a hydrophobic functional domains, wherein TGBp2 encoded by all TGB containing viruses has a conserbative core area with two hydrophobic domains aside, however, domains composition of TGBp3 by different viruses were relatively variable, for example, TGBp3 encoded by *Foveavirus* only has one hydrophobic domain at N . TGBp1 functioned as binding single strand RNA (ssRNA) (Morozov and Solovyev 2003), suppressing RNA silencing (Verchot-Lubicz 2005) and increasing the plasmodesmata permeability to help virus particles transport, whereas TGBp2 and TGBp3 functioned as membrane-bound proteins (Krishnamurthy et al 2003).

ASPV distributes worldwide and its natural hosts are largely restricted to *Maloideae* species, including pear and apple. There are also recent evidence of ASPV detection in cherry and in sour cherry in India (Dhir et al 2010) and wild *Rosaceae* (*Cydonia japonica, Pyrus calleryana* and *P. amygdaliformis*) in Greece (Mathioudakis and Katis 2006) as well as in grapevine in South Africa (Goszczynski, Genbank). ASPV infected apple trees often remain symptomless, however, it causes visible symptoms on susceptible rootstocks (Jelkmann 1994; Jelkmann and Keim Konrad 1997) and xylem pits in the stem of *Malus pumila* Virginia Crab, as well as epinasty and decline of *M. domestica* Spy227 (Jelkmann 1994; Komorowska et al 2010). In many pear varieties, ASPV infection results in vein yellow (Wu et al 2010), red mottling (Komorowska et al 2011) or necrotic spot (PNS) or stony pit (Mathioudakis et al 2009). ASPV frequently infected in combination with other viruses: *Apple chlorotic leaf spot virus* (ACLSV), *Apple stem grooving virus* (ASGV) as well as *Apple mosaic virus* (ApMV). Complex infection of these viruses caused significant decrease in yield quality and quantity of fruit products. There is no known insect vector reported for ASPV (Martelli and Jelkmann 1998).

1.9 Purpose and objectives of our projects

For a long time of evolution, plants have developed a series of mechanisms to defend themselves against viruses including Resistance (R) gene-mediated responses, RNA silencing, Lectin protein-mediated response and some other host proteins such as translational initiation factors. However, plant viruses also involved a variety of mechanisms to survive from hosts, either through molecular evolution (mutations, recombinations, selection pressure or gene flow), or through encoding proteins (e.g., VSRs) to defense against plant immunity. Our study focused on genetic dissection of plant-virus interactions:

- On one hand, we explored how virus counter-defense plant immunity by using ASPV. China has the largest pear cultivated area, however, pear plants in China were commonly infected with ASPV. ASPV was the type species of *Foveavirus*, *Betaflexiviridae*. The objectives of our study include: 1) Investigating ASPV incidence on pear in China; 2) Analyzing genetic diversity of ASPV population obtained from pear isolates by sequencing functional important genes (TGB and CP); 3) Inferring ASPV evolution mechanisms; 4) To make clear the biological, serological and pathogenic diversity induced by ASPV molecular diversity. Our results could greatly enrich data set of ASPV sequences and allow to develop reliable diagnostic methods in clean-plant programs.
- On the other hand, we study how plant defense against virus by exploring how *Arabidopsis* defend against TRV. *Arabidopsis* AGO proteins can be divided into three main clades comprised of: AGOs 1, 5, 10; AGOs 2, 3, 7; and AGOs 4, 6, 8, 9. Although some AGOS have partially overlapping functions with other clade members, many do not, instead playing roles in specific RNA silencing-related phenomena. We have obtained single mutants for all ten Arabidopsis AGO genes, as well as some double and triple mutants for a subset of AGO genes. In this study, we will test all the mutants by infecting plants with TRV-PDS, through this we will determine which AGO protein(s) are involved in virus-induced gene silencing (VIGS), whereby endogenous plant genes are silenced by small RNAs generated from a viral vector. By infecting with TRV-GFP, we would know AGO protein(s) are involved in the phenomenon known as Recovery, wherein the plant is able to silence the expression of the viral genetic material.

Chapter 2 - Genetic diversity and evolution of *Apple stem pitting virus* isolates from pear in China

2.1 Abstract

To make clear population structure and molecular evolution mechanisms of *Apple stem pitting virus* (ASPV) pear isolates in China, four hundred fifty-one samples from different pear production regions in China were collected，wherein one hundred forty-five samples tested ASPV positive. Complete *coat protein* (CP) and *triple gene block* (TGB) of some of those ASPV positive isolates were sequenced. In our study, we obtained forty-eight unique CP sequences from thirty-one ASPV pear isolates, sixty-six unique TGB sequences from ASPV forty-four pear isolates. Phylogenetic trees analysis based on these unique sequences and corresponding sequences from GenBank suggested that: 1) ASPV grouping in phylogenetic trees were related to their hosts (apple, pear and Korla pear), no matter which ASPV genes was used; 2) ASPV pear isolates could be divided into six evolutionary divergent subgroups (A-F) based on their CP sequences, wherein two new subgroups (B and F) were identified in our study; 3) ASPV isolates could be divided into five evolutionary divergent groups based on their TGB sequences. Multiple alignments analysis indicated continuous nucleotides insertions or deletions were exited in CP of ASPV pear isolates in China. Recombination events were detected in CP and TGB sequences in our study. Results suggested that ASPV CP and TGB genes were under negative selection. Our study suggested insertions or deletions mutations, selection pressure and recombination played important roles in genetic diversity of ASPV pear isolates in China.

Keywords ASPV, CP, TGB, Phylogenetic analysis, Selection Pressure, Recombination

---

This chapter has been reformatted and reprinted from: An original article already submitted to *Canadian Journal of Plant Pathology*. Xiaofang Ma, Ni Hong, Guoping Wang. (2015) Genetic diversity and evolution of *Apple stem pitting virus* isolates from pear in China.

2.2 Introduction

ASPV is the type species of genus *Foveavirus* in the family *Betaflexiviridae* (Carstens 2009). The flexible filamentous particles approximately 12-15 nm in width and 800 nm in length, which can form end-to-end aggregates in host cells. The single-stranded positive-sense RNA (+ssRNA) genome of ASPV has about 9,300 nucleotides (nts), which acontains five open reading frames (ORFs, ORF1-ORF5) and the 5' untranslated region (UTR) and 3' UTR. ORF1 encoded the viral *RNA-dependent RNA polymerase* (RdRP), ORF2-ORF4 encoded *triple gene block* proteins (TGBps) and ORF5 encoded *coat protein* (CP) (Jelkmann 1994). RNA viruses have high mutation rates, which result in accumulation of abundant genetic variations in viral populations (Holmes 2010). Liu et al (2012) reported that all the five genes of ASPV had large genetic variability, especially in the CP, which provided strong motive to study the diversity of ASPV based on CP. Studies showed that there was conserved C-terminal and variable N-terminal of CP (Wu et al 2010; Yoon et al 2014). CP of different ASPV isolates were highly variable, which lead to different CP sizes, ranging from 1125 to 1245 nt (Komorowska et al 2011; Yoon et al 2014). Significant genetic variability of ASPV isolates was also reported by analyzing partial region of *RdRp* (Mathioudakis et al 2010). In additional, previous results indicated that ASPV genetic variations did not correlate to geographic regions, but to the host (Liu et al 2012). To date, 11 ASPV whole genomes were sequenced, wherein 8 isolates were from apple and 3 isolates were from Korla pear (Liu et al 2012). In addition, almost fifty complete ASPV *CP* sequences have been available in Genbank (about 33 sequnces were from apple isolates, 4 from Korla pear and 10 from pear isolates) (Wu et al 2010; Komorowska et al 2011; Yoon et al 2014). Most studies on ASPV genetic diversity conducted so far have involved the whole or part of ASPV CP from apple isolates (Komorowska et al 2011; Yoon et al 2014), nevertheless, sequences characteristics from pear isolates have been poorly understood.

China has relatively larger pear cultivation area in the world, however, pear plants are seriously damaged by ASPV in China (Wang et al 1994; Liu et al 2012). The objectives of our study include: 1) Investigating ASPV incidence on pear in China; 2) Analyzing genetic diversity of ASPV population obtained from pear isolates by sequencing functional important genes (TGB and CP); 3) Inferring ASPV evolution mechanisms. Our results could greatly enrich data set of ASPV sequences and allow to develop reliable diagnostic methods in clean-plant programs.

2.3 Materials and methods

2.3.1 Sample collection

A field survey on ASPV occurrence was carried out from August 2009 to June 2012 in seventeen orchards located in twelve provinces in China. A total of four hundred sixty-five samples (four hundred fifty-one pear samples and fourteen apple samples), were randomly collected to test for ASPV (Table 2-1). The pear samples included leaves or fruits of pear (*Pyrus* spp.), most of which were symptomless while some showed vein yellow in leaf or stony pit in fruit. Virus-free leaves from seedlings of *Pyrus betulifolia* Bge were used as a negative control.

Table 2-1 Incidence of ASPV in different areas in China surveyed in this study

Geographic area	Total samples	ASPV positive	Host	Collected Date
Enshi, Hubei province (HB)[a]	5	2	Pear	2009-08
Wuhan, HB	83	28	Pear	2010-03
ChongYang, HB	38	12	Pear	2011-04
Wuhan, HB	23	12	Pear	2012-04
Xiangyang, HB	9	9	Pear	2012-06
Yunnan province (YN)	4	1	Pear	2010-02
Hangzhou, Zhejiang	46	2	Pear	2010-05
Zhengzhou, Henan province	25	9	Pear	2010-11
Guiyang, Guizhou province	9	4	Pear	2011-09
Yingtan, Jiangxi province	10	9	Pear	2012-04
Nanchang, JX	10	10	Pear	2012-04
Xingcheng, Liaoning province (LN)	117	22	Pear	2012-04
Ganshu province (GS)	5	1	Pear	2012-04
Shanxi province (SX)	28	6	Pear	2012-05
Chongqing (CQ)	13	4	Pear	2012-05
Xinjiang province (XJ)	14	10	Pear	2012-06
Yantai, Shandong province	12	4	Pear	2012-06
Total samples from pear	451	145		
Xingcheng, LN	3	2	Apple	2010-09
Yantai, SD	3	2	Apple	2010-10
Zhengzhou, HN	1	1	Apple	2010-11
Wuhan, HB	3	3	Apple	2011-04
Guiyang, GZ	2	1	Apple	2011-09
Yantai, SD	2	2	Apple	2012-06
Total samples from pear	14	11		

a, We use HB to represent Hubei province in the whole article and isolates from Hubei province named beginning with HB

2.3.2 RT-PCR, cloning and sequencing

Total RNA extracted from 0.1 g leaves with cetyl-triethylammonium bromide (CTAB) method (Li et al 2008) was used as a template for the detecting ASPV and the amplification of fragments containing CP and TGB genes of ASPV by RT-PCR. The primer sequences used for ASPV detection were 370-F/370-R (Menzel 2002) (Table 2-2). The primers pairs used for amplifying fragments containing complete *CP* were D-F/D-R (Jelkmann et al 1997). Fragments sizes amplified by primers D-F/A-R ranging from 1,430 to 1,552 bp (Fig. 2-1), including entire CP and the 221 and 78 bp upstream and downstream of CP, respectively. The primer pairs for amplifying fragments containing *TGB* genes were MP-F/MP-R, which were designed based on TGB genes sequences available on the GenBank (Accession No: D21829, AB045371 and EU095327), could amplified a fragment with expected size of 1,203 bp.

First-strand cDNA synthesis was performed using 0.5 mM of random primer (6 mer) (TaKaRa, Dalian, China) and M-MLV reverse transcriptase (Promega, Madison, USA) at 37 °C for 1.5 hour. PCR reactions were taken in a 25 µl volume with reaction mixtures containing 2.5 µl 10×PCR buffer, 0.5 mM dNTP, 1 mM specific primer, 0.15µl of 5 U/lL rTaq DNA polymerase (TaKaRa, Dalian, China), and corresponding templates (3 µl first-strand cDNA). The PCR cycling parameters were set as follows: pre-activation at 94°C for 5 min, followed by 35 cycles of denaturation (94°C for 30 s), annealing (30 s at a certain temperature for each primer pairs: annealing temperature for D-F/A-R is 54°C, 370-F/370-R is 56°C, and MP-F/MP-R is 50°C), and extension (1 min at 72°C), final extension (1 cycle of 72°C for 10 min). The PCR reaction was conducted in a 96-well PCR Thermal Cycler (T-100TM, BIO-RAD, USA). The PCR products were analyzed on 1% agarose gels and visualized in a UV transilluminator by Ethidium bromide (1 µl/ml) staining.

All amplified PCR products were cloned individually into pMD18-T simple vector (TaKaRa, Dalian, China) according to the manufacturer's instruction. To exclude in vitro RT-PCR errors, at least three clones from each ASPV isolates were sequenced in both forward and reverse orientations. If the three independent clones showed ≥98% similarity, then a consensus sequence was obtained, which was named ‘unique sequence’. If there was <98% nucleotide similarity between the three initially sequenced clones, additional clones would be sequenced to investigate the possible occurrence of molecular variants mixtures within individual pear.

Table 2-2 Primers used in this study for detecting the often occurred virus on apple and pear

Virus detection	Primer names	Primer sequences (5'-3')	Position	Fragment lengths	Reference
ASGV	499-F	CCCGCTGTTGGATTTGATACACCTC	5871-5895nt	499 bp	James 1999
	499-R	GGAATTTCACACGACTCCTAACCCTCC	6344-6370nt		
ACLSV	677-F	TTCATGGAAAGACAGGGGCAA	6860-6880nt	677 bp	Song 2011
	677-R	AAGTCTACAGGCTATTTATTATAAGTCTAA	7507-7536nt		
ASPV	370-F	ATGTCTGGAACCTCATGCTGCAA	8869-8895nt	370 bp	Menzel 2002
	370-R	TTGGGATCAACTTTACTAAAAAGCATAA	9211-9238nt		
	D-F	GTACATGAGTAACTCGAGCC	7708-7728nt	1500 bp（CP）	Jelkmann et al 1997
	A-R	ATAGCCGCCCCGGTTAGGTT	9239-9258nt		
	MP-F	GTGTGTAAGCATATTAGG	6656-6664nt	1200 bp（TGB）	This study
	MP-R	CTACACCCTAACCTAATG	7832-7850nt		

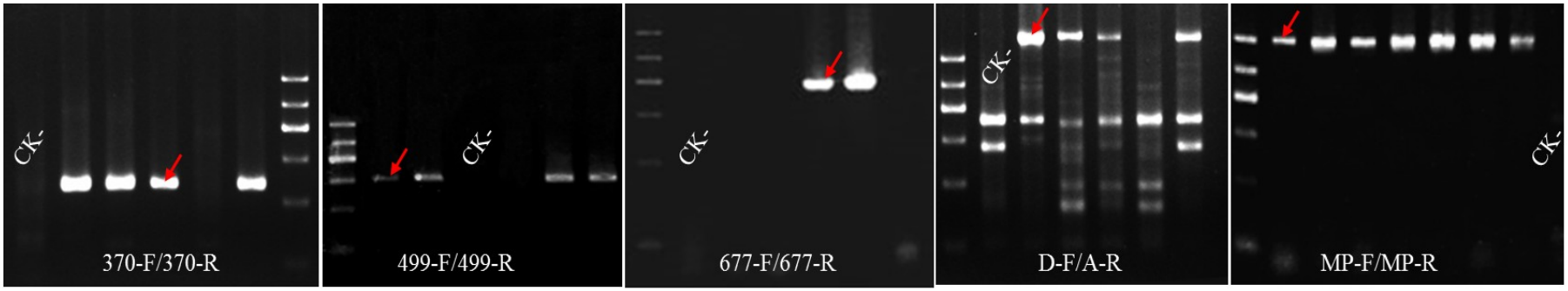

Fig. 2-1 1.0% agarose gel electrophoresis of RT-PCR products of fragments amplified by primers pair in Table 2-2

2.3.3 Sequence alignments, phylogenetic and recombination analysis

The nucleotides sequence alignments were carried out by using ClustalX 1.81 (Thompson et al 1997) with default settings and adjusted manually for the correct open reading frames. The corresponding sequences of ASPV isolates available in the GenBank were also included for analysis (Table 2-3). Corresponding genes of *Apple green crinkle associated virus* (AGCaV) were used as outgroup for phylogenetic analysis. Phylogenetic and virus molecular evolutionary analysis were conducted by using MEGA 6.06 through using the neighbor-joining method with 1,000 bootstrap replicates and bootstrap values <60% were omitted (Tamura et al 2013). The genetic distances (the average number of nucleotide substitutions between two randomly selected sequences in a population) of different ASPV genes within and between phylogenetic groups and subgroups were calculated by MEGA 6.06 (Tamura et al 2013). The CP and TGB sequences of each isolate were also subjected to recombination analysis. Possible recombination events were detected by using programs RDP (Heath et al 2006): GENECONV (Padidam et al 1999), BOOTSCAN (Martin et al 2005), Maximum Chi Square (MAXCHI) (Smith 1992), CHIMAERA (Posada and Crandall 2001), 3SEQ (Boni et al 2007), Sister Scanning (SISCAN) (Posada and Crandall 2001).

2.2.4 Selection pressure and neutrality tests analysis

The selection pressure was estimated by dN/dS ratio, where dN/dS represented the average number of nucleotide substitutions per site between two sequences. The values of dN and dS were estimated separately by using the software DnaSP 5.10 (Librado and Rozas 2009). The gene is under positive (or diversifying) selection when dN/dS ratio is >1, neutral selection when dN/dS ratio =1 and negative (or purifying) selection when dN/dS ratio <1. DnaSP 5.10 was also used to estimate Tajima's D, Fu & Li's D and F statistical tests, haplotype (gene) diversity (Hd) and nucleotide diversity (Pi) (Rozas et al 2004; Librado and Rozas 2009). Tajima's D, Fu & Li's D and F statistical tests hypothesize that all mutations are selectively neutral. Haplotype diversity refers to the frequency and number of haplotypes in the population. Nucleotide diversity estimates the average pairwise differences among sequences.

Table 2-3 Origin and GenBank accession numbers of ASPV isolates analyzed in our study

Isolates	Hosts	Origin	Accession No.	References
N1	Apple	Poland	AF491931.1	Komorowska et al, direct submission
GNKIII/45	Pear	Poland	AF491929.1	Komorowska et al, direct submission
ST181	Apple	Poland	AF495382.1	Komorowska et al, direct submission
MT24	Apple	Poland	AF438522.1	Komorowska et al, direct submission
ST113	Pear	Poland	AF345895.1	Komorowska et al, direct submission
MT32	Apple	Poland	AF438521.1	Komorowska et al, direct submission
ST132	Pear	Poland	AF345894.1	Komorowska et al, direct submission
GNKVII/34	Pear	Poland	AF345893.1	Komorowska et al, direct submission
ST54	Pear	Poland	AF345892.1	Komorowska et al, direct submission
ws	Apple	China	EU314950.1	Dong et al, direct submission
24	Apple	China	FJ619188.1	Li et al, direct submission
38	Apple	China	FJ619187.1	Li et al, direct submission
ASPV-p1	Pear	China	EU708018.1	Li et al, direct submission
PR1	Pear	China	EU095327.1	Zhao et al, direct submission
PA66	Apple	Germany	D21829.1	Jelkmann et al, direct submission
Hannover	Apple	Germany	KF321967.1	Arntjen et al, direct submission
PM8	Apple	Germany	KF319056.1	Liebenberg et al, direct submission
PB66	Apple	Germany	KF321966.1	Arntjen et al, direct submission
PSA-H	Pear	Germany	D21828.1	Jelkmanm et al, direct submission
Palampur	Apple	India	FN433599.1	Dhir et al, direct submission
br1	-	Brasil	AY572458.1	Nickel et al., direct submission
VY1	Pear	Taiwan	HM352767.1	Wu et al, 2010
Rohru	Apple	India	HM352767.1	Dhir et al, direct submission
IF38	Apple	Japan	AB045371.1	Yoshikawa et al, direct submission
KL1	Pear	China	JF946775.1	Liu et al 2012
KL9	Pear	China	JF946772.1	Liu et al 2012
KL2	Pear	China	JF946774.1	Liu et al, direct submission
Y2	Pear	China	JF946774.1	Liu et al, direct submission
YT	Apple	China	KF915809.1	Chen et al, direct submission
PV2	Apple	China	HM125157.1	Li et al, direct submission
PV7	Apple	China	HM125158.1	Li et al, direct submission
PV9	Apple	China	HM125153.1	Li et al, direct submission
PV11	Apple	China	HM125156.1	Li et al, direct submission
NJS-HJ-GW	Apple	South Korea	KC791790.1	Yoon et al 2014
KHS-HR-SJ	Apple	South Korea	KC791789.1	Yoon et al 2014
KJH-HR-JS3	Apple	South Korea	KC791788.1	Yoon et al 2014
KJH-HR-JS2	Apple	South Korea	KC791787.1	Yoon et al 2014
KJH-HR-JS1	Apple	South Korea	KC791786.1	Yoon et al 2014
SJY-HR-YC2	Apple	South Korea	KC791785.1	Yoon et al 2014
SJY-HR-YC1	Apple	South Korea	KC791784.1	Yoon et al 2014
JGH-HR-YC	Apple	South Korea	KC791783.1	Yoon et al 2014

2.4 Results

2.4.1 Genetic diversity of ASPV pear isolates from China

RT-PCR was used to detect ASPV among four hundred fifty-one pear samples, however, we also tested the often occurred viruses (ACLSV and ASGV) on pear, viruses detection primers used in our study are listed in Table 2-2. Of the four hundreds fifty-one samples analyzed, one hundred forty-five samples were ASPV positive detecting by RT-PCR. There was no apparent difference in infection rate among samples with different geographic origins (Table 2-1). However, infection rates of pear and apple samples had a great difference with a 78.6% (11/14) of apple verse 32.3% (145/451) of pear, although the number of samples from apple tree need to be more in the future study (Table 2-1).

CP sequences from thirty-two ASPV isolates (thirty-one pear isolates and 1 apple isolates) and TGB sequences from fifty-two (forty-four pear isolates and 8 apple isolates) ASPV isolates were selected to analyze the genetic diversity of ASPV isolates. For most of those isolates, the three initially sequenced clones within a single pear showed ≥98.0 % similarity, except for fourteen ASPV CP isolates (Appendix 3) and sixteen ASPV TGB isolates (Appendix 4). In total, fifty CP sequences and seventy-five TGB sequences obtained in this study were considered as ‘unique sequences’. These ‘unique sequences’ of these isolates were deposited in GenBank (Appendix 3, Appendix 4).

To estimate genetic variability for CP and TGB, we calculated population genetic parameters of all available CP and TGB sequences on the basis of variant groups and geographical distributions (Table 2-7). The parameters of TGB were calculated only based on Chinese isolates due to the lack of enough TGB sequences from other countries. Based on variant groups, the overall haplotype diversity (Hd) values were around 0.900-1.000, which indicated highly genetic diversity within groups. However, their nucleotide sequence diversities (Pi) values were varied among different groups and subgroups. The relatively higher Pi value (high value indicates higher sequences diversity) in Gp1 (0.1487) than Gp2 (0.1396) and Gp3 (0.1450) indicated higher sequences diversity of CP sequences from pear isolates, however, for TGB, it was in contrast. Pi values of sequences from apple in Gp4 (0.1624) and from Korla pear in Gp5 (0.1504) were higher than sequences from pear in Gp1-Gp3. Based on geographical origin, higher Pi values were observed in sequences from Poland (0.1915) and China (0.16616) as compared to that of South Korea (0.15123) and Germany (0.00261).

2.4.2 Phylogenetic analysis of ASPV pear isolates from China

Fifty unique CP sequences from our study and relative sequences obtained from GenBank (Table 2-3) were used to reconstruct phylogenic tree by using neighbor-joining method (Fig. 2-2 A). Results revealed that all CP sequences in our study clustered into Gp1 and Gp2, two of the three well defined groups (Gp1, Gp2 and Gp3) in previous studies (Rozas et al 2004; Wu et al 2010; Liu et al 2012). Gp1 consisted of isolates from pear except a German isolate PA66 (D21829.1), which was divided into five subgroups (A~E); Gp2 consisted of isolates majority from apple, however, 10 isolates from pear Gp2 formed a subgroup F; Five previously reported isolates (KRL1, KL1, KL2, KL9 and Y2) from Korla pear (*Pyrus sinkiangensis* Yü) (Liu et al 2012), formed a group Gp3. Group Gp2 have the highest genetic distance (0.2005±0.0109), followed by group Gp1 (0.1822±0.0096), group Gp3 (0.1602±0.0105). The genetic distance between the three groups arranged from 0.2824±0.0164 to 0.3821±0.0234. Subgroup D had the highest genetic distance (0.1475±0.0064), followed by subgroup C (0.0754±0.0065), and lowest in subgroup F (0.0370±0.0032). The genetic distances between subgroups ranged from 0.1482±0.0129 to 0.3281±0.0178 (Table 2-4).

For TGB, seventy-five TGB sequences from our study and relative sequences obtained from GenBank (Table 2-3) were used to reconstruct phylogenic tree (Tree topologies based on TGB1, TGB2 and TGB3 were highly similar, therefore, only phylogenic tree based on the whole TGB was show here) (Fig. 2-2 B). Results revealed that all TGB sequences clustered into five groups, designated as Gp1-Gp5. Gp1, Gp2 and Gp3 mainly consisted of isolates from pear (except for an India isolate Palampur and SD-AP1-1 from our study both from apple, but were clustered in Gp1); most of isolates in Gp4 are from apple (except for ZJ-YG2-5 and ZJ-YG1-1 from our study both from pear); Gp5 consisted of 4 isolates from Korla pear (KL1, KL9, PR1 and XJ-5-5, wherein XJ-5-5 from our study was also isolated from Kolar pear). The genetic distance of ASPV TGB within the variant groups was highest in group Gp4 (0.1941±0.011), followed by group Gp5 (0.1690±0.0104), group Gp2 (0.1653±0.0105), group Gp1 (0.1404±0.0086) and group Gp3 (0.0906±0.0063). The genetic distance between variant groups ranged from 0.2398±0.0137 to 0.2721±0.0149.

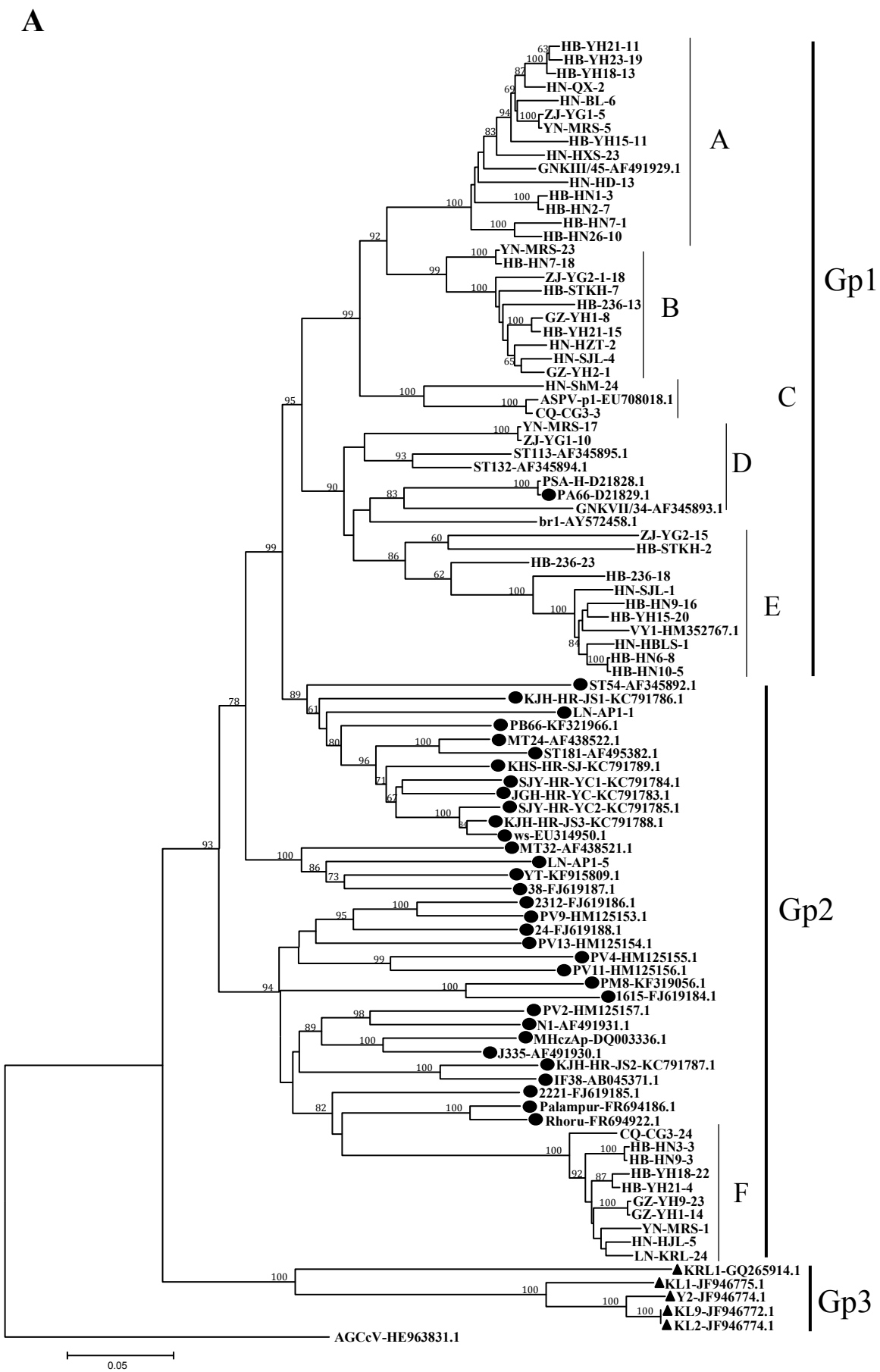
A
HB-YH21-11
HB-YH23-19
HB-YH18-13
HN-QX-2
HN-BL-6
ZJ-YG1-5
YN-MRS-5
HB-YH15-11
HN-HXS-23
GNKIII/45-AF491929.1
HN-HD-13
HB-HN1-3
HB-HN2-7
HB-HN7-1
HB-HN26-10
YN-MRS-23
HB-HN7-18
ZJ-YG2-1-18
HB-STKH-7
HB-236-13
GZ-YH1-8
HB-YH21-15
HN-HZT-2
HN-SJL-4
GZ-YH2-1
HN-ShM-24
ASPV-p1-EU708018.1
CQ-CG3-3
YN-MRS-17
ZJ-YG1-10
ST113-AF345895.1
ST132-AF345894.1
PSA-H-D21828.1
PA66-D21829.1
GNKVII/34-AF345893.1
br1-AY572458.1
ZJ-YG2-15
HB-STKH-2
HB-236-23
HB-236-18
HN-SJL-1
HB-HN9-16
HB-YH15-20
VY1-HM352767.1
HN-HBLS-1
HB-HN6-8
HB-HN10-5
ST54-AF345892.1
KJH-HR-JS1-KC791786.1
LN-AP1-1
PB66-KF321966.1
MT24-AF438522.1
ST181-AF495382.1
KHS-HR-SJ-KC791789.1
SJY-HR-YC1-KC791784.1
JGH-HR-YC-KC791783.1
SJY-HR-YC2-KC791785.1
KJH-HR-JS3-KC791788.1
ws-EU314950.1
MT32-AF438521.1
LN-AP1-5
YT-KF915809.1
38-FJ619187.1
2312-FJ619186.1
PV9-HM125153.1
24-FJ619188.1
PV13-HM125154.1
PV4-HM125155.1
PV11-HM125156.1
PM8-KF319056.1
1615-FJ619184.1
PV2-HM125157.1
N1-AF491931.1
MHczAp-DQ003336.1
J335-AF491930.1
KJH-HR-JS2-KC791787.1
IF38-AB045371.1
2221-FJ619185.1
Palampur-FR694186.1
Rhoru-FR694922.1
CQ-CG3-24
HB-HN3-3
HB-HN9-3
HB-YH18-22
HB-YH21-4
GZ-YH9-23
GZ-YH1-14
YN-MRS-1
HN-HJL-5
LN-KRL-24
KRL1-GQ265914.1
KL1-JF946775.1
Y2-JF946774.1
KL9-JF946772.1
KL2-JF946774.1
AGCcV-HE963831.1
0.05
A
B
C
D
E
F
Gp1
Gp2
Gp3

B

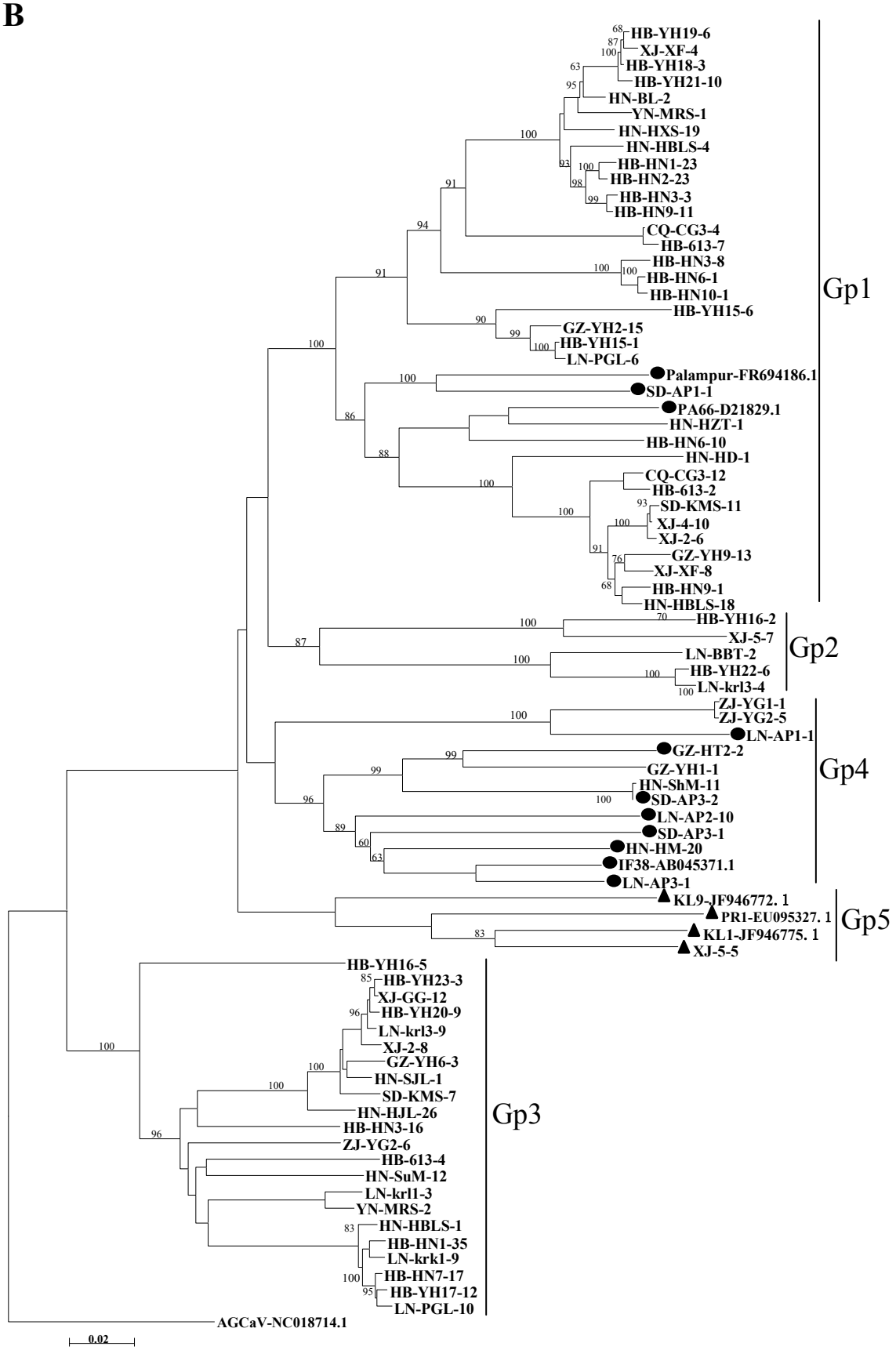
HB-YH19-6
XJ-XF-4
HB-YH18-3
HB-YH21-10
HN-BL-2
YN-MRS-1
HN-HXS-19
HN-HBLS-4
HB-HN1-23
HB-HN2-23
HB-HN3-3
HB-HN9-11
CQ-CG3-4
HB-613-7
HB-HN3-8
HB-HN6-1
HB-HN10-1
HB-YH15-6
GZ-YH2-15
HB-YH15-1
LN-PGL-6
Palampur-FR694186.1
SD-AP1-1
PA66-D21829.1
HN-HZT-1
HB-HN6-10
HN-HD-1
CQ-CG3-12
HB-613-2
SD-KMS-11
XJ-4-10
XJ-2-6
GZ-YH9-13
XJ-XF-8
HB-HN9-1
HN-HBLS-18
Gp1
HB-YH16-2
XJ-5-7
LN-BBT-2
HB-YH22-6
LN-krl3-4
Gp2
ZJ-YG1-1
ZJ-YG2-5
LN-AP1-1
GZ-HT2-2
GZ-YH1-1
HN-ShM-11
SD-AP3-2
LN-AP2-10
SD-AP3-1
HN-HM-20
IF38-AB045371.1
LN-AP3-1
Gp4
KL9-JF946772.1
PR1-EU095327.1
KL1-JF946775.1
XJ-5-5
Gp5
HB-YH16-5
HB-YH23-3
XJ-GG-12
HB-YH20-9
LN-krl3-9
XJ-2-8
GZ-YH6-3
HN-SJL-1
SD-KMS-7
HN-HJL-26
HB-HN3-16
ZJ-YG2-6
HB-613-4
HN-SuM-12
LN-krl1-3
YN-MRS-2
HN-HBLS-1
HB-HN1-35
LN-krk1-9
HB-HN7-17
HB-YH17-12
LN-PGL-10
Gp3
AGCaV-NC018714.1
0.02

Continued

Fig. 2-2 Phylogenetic tree of complete CP (A) and TGB (B) sequences of ASPV isolates
Reference isolates are named through their isolate name with GenBank accession numbers after. Isolates in our study are indicated by isolate abbreviation and number after isolate names representing sequenced CP or TGB clones name. Sequences from the host apple have symbol ● in front, whereas sequences from Korla pear with a symbol ▲ in front and sequences from the host pear without symbols in front. The tree was constructed by the neighbor joining method implemented by MEGA6. Bootstrap analysis with 1000 replicates was performed. Only ≥50% bootstrap values are shown, and branch lengths are proportional to the genetic distances. Bar, 0.05 substitutions per site

Table 2-4 Genetic distance between and within groups and subgroup clustered in phylogenetic trees based on ASPV CP and TGB sequences

Gene		Between and within-group diversity (±SE)					
		Gp1	Gp2	Gp3			
	Gp1	0.1822±0.0096					
	Gp2	0.2824±0.0164	0.2005±0.0109				
	Gp3	0.3736±0.0228	0.3821±0.0234	0.1602±0.0105			
		A	B	C	D	E	F
CP	A	0.0586±0.0038					
	B	0.1482±0.0129	0.0511±0.0038				
	C	0.1718±0.0105	0.1543±0.0092	0.0754±0.0065			
	D	0.2186±0.0102	0.2187±0.0109	0.2156±0.0104	0.1475±0.0064		
	E	0.2285±0.0117	0.2167±0.0116	0.2307±0.0130	0.1745±0.0082	0.0540±0.0036	
	F	0.3071±0.0160	0.2997±0.0165	0.3199±0.0174	0.3023±0.0150	0.3281±0.0178	0.0370±0.0032
		Gp1	Gp2	Gp3	Gp4	Gp5	
	Gp1	0.1404±0.0086					
TGB	Gp2	0.2398±0.0133	0.1653±0.0105				
	Gp3	0.2604±0.0150	0.2656±0.0157	0.0906±0.0063			
	Gp4	0.2398±0.0137	0.2598±0.0146	0.2721±0.0149	0.1941±0.0112		
	Gp5	0.2545±0.0138	0.2653±0.0149	0.2678±0.0158	0.2642±0.0144	0.1690±0.0104	

2.4.3 A new type of continuous insertion in the 5' terminal of CP

The CP sizes of different ASPV isolates fluctuated from 1,125 nt to 1,245 nt (Wu et al 2010). Normally, it was 1,194 nt and 1,191 nt long for Korla pear (Liu et al 2012) and apple isolates (Liu et al 2012; Yoon et al 2014), respectively, although there were some exceptions (for example, it was 1,188 nt long for apple isolate PV7). Our results revealed that CP sizes for ASPV pear isolates varied according to the subgroups in the phylogenic tree (Fig.2-3 A): It was 1,185 nt long for sequences in subgroups A~C, 1,125 nt long for sequences in subgroup D and 1,233 nt long for sequences in subgroups E and F. Multiple alignment with LN-AP1-1 from apple (1,191 nt) as reference sequence showed that amino acids insertions or deletions or mutations occurred at the 5' terminal of CP, however, the 3' terminal was relatively conserved (Fig. 2-3), which was consistent with previous results (Wu et al 2010; Yoon et al 2014). In different subgroups, different amino acids insertions or deletions existed at different position of 5' terminal: 2 amino acids deleted after position 507 nt (5'-3') for sequences in subgroups A~C; 22 amino acids deleted after position 246 nt (5'-3') for sequences in subgroup D; 14 amino acids inserted after the position 135 nt (5'-3') for sequences in subgroup E; 15 amino acids inserted after position 135 nt (5'-3') and 1 amino acids deleted after position 507 nt (5'-3') for sequences in subgroup F. Although CP size and insertion position were the same for sequences in subgroups E and F, the insertion amino acids were not the same. Insertion type in subgroup E was reported once (isolate VY1, HM352767.1) (Wu et al 2010), however, the insertion type in subgroup F was reported for the first time. Surprisingly, there were no deletions or insertions were found in TGB.

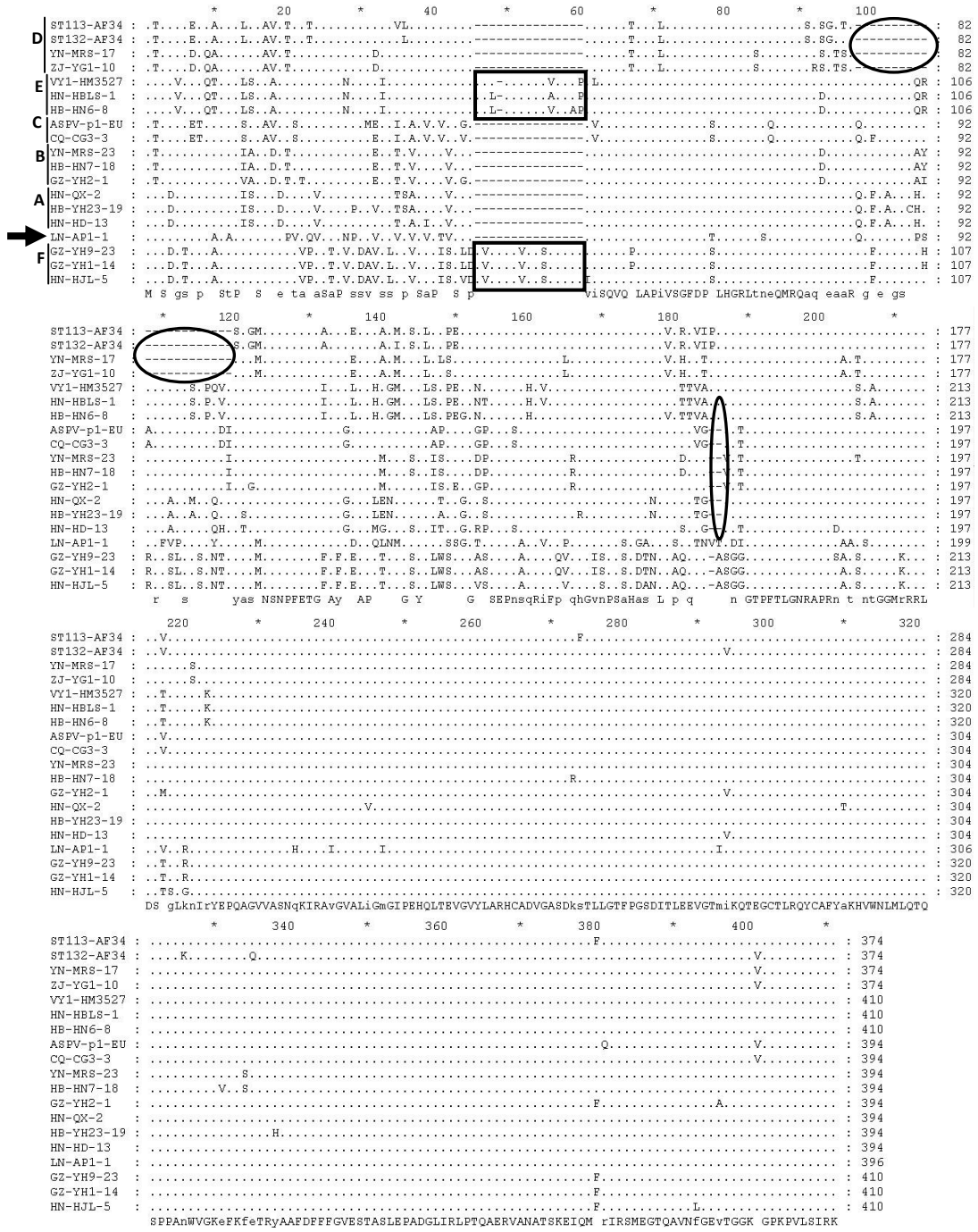

Fig. 2-3 Multiple alignment of amino acids of 16 representative ASPV CP sequences

2-3 sequences from each subgroup in phylogenetic tree in Fig.2-3 A were selected. LN-AP1-1 (arrow) from an apple isolate was used as a reference sequence. The deletion regions are represented by rectangular boxes and the insertion regions are represented by oval boxes

2.4.4 Novel recombination events in the ASPV CP and TGB

There were some discordant clustering sequences in CP and TGB based phylogenetic trees, suggesting the possible recombination events. A total of five putative recombinant events were detected by seven programs in RDP software with default settings (Fig.2-4, Table 2-5). Two CP recombinants HB-HN7-18 and YN-MRS-23 had the same parental variants from subgroup A (YN-MRS-3) and subgroup B (HN-HZT-2), as well as the same statistical values and crossing over sites. For TGB, HB-YH15-6 (in group Gp2) was a recombinant of variants in Gp3 (HB-HN6-10) and Gp2 (LN-PGL-6), HN-BL-2 (Gp1) was a recombinant of variants in Gp5 (HN-SJL-1) and Gp1 (HB-HN2-23), while the previously reported sequence PR1 (EU095327) (Gp7) was a recombinant of variants in Gp7 (XJ-5-5) and Gp3 (PA66, D21829). These three recombinant sequences had different break points: break and end point for HB-YH15-6 crossed over the entire TGB, whereas that of HN-BL-2 located at TGB*1* and that of PR1 located at TGB3.

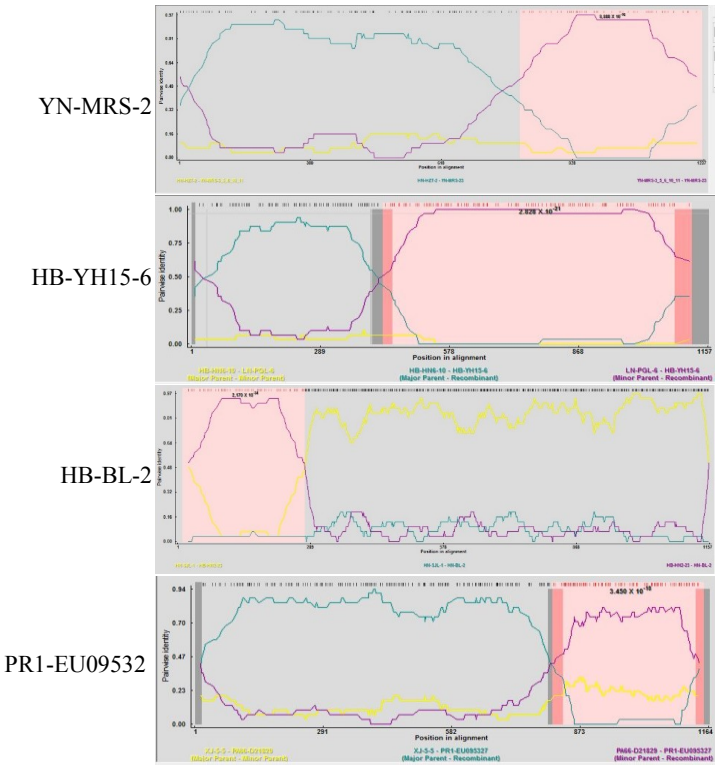

Fig. 2-4 Recombinant events ASPV genes by using RDP software

Table 2-5 List of putative recombination events among ASPV CP and TGB sequences

Gene	Recombinant Isolates	Parental isolate		Break Point		Recombination detection methods						
		Major	Minor	Start	End	RDP	GeneConv	Bootscan	MaxChi	CHIMAERA	SiScan	3SEQ
						Av. P-Value						
CP	**YN-MRS-23**	HN-HZT-2	YN-MRS-3	752	1179	7.670×10^{-15}	5.958×10^{-13}	3.498×10^{-15}	7.009×10^{-10}	1.854×10^{-10}	2.871×10^{-11}	6.641×10^{-21}
CP	**HB-HN7-18**	HN-HZT-2	YN-MRS-3	752	1179	7.670×10^{-15}	5.958×10^{-13}	3.498×10^{-15}	7.009×10^{-10}	1.854×10^{-10}	2.871×10^{-11}	6.641×10^{-21}
TGB	**HB-YH15-6**	HB-HN6-10	LN-PGL-6	428	1149	2.413×10^{-16}	1.391×10^{-10}	8.021×10^{-17}	5.408×10^{-14}	8.358×10^{-14}	9.612×10^{-26}	7.840×10^{-29}
TGB	**HN-BL-2**	HN-SJL-1	HB-HN2-23	11	274	2.170×10^{-34}	4.939×10^{-34}	3.315×10^{-27}	1.607×10^{-10}	1.545×10^{-10}	7.422×10^{-44}	1.787×10^{-14}
TGB	**PR1-EU095327**	XJ-5-5	PA66-D21829	810	1185	2.994×10^{-13}	7.068×10^{-08}	5.037×10^{-13}	3.978×10^{-15}	4.198×10^{-14}	2.343×10^{-09}	5.145×10^{-35}

Notes, P-values >0.05 were considered significant; 'Minor' and 'Major' parents refer to the parental isolates contributing the smaller and larger portions of the recombinant's sequence, respectively

2.4.5 Selection pressure and neutrality tests analysis

The dN/dS ratios have been commonly used to estimate the selection pressure under which viral gene suffered (Zhang et al 2011; Liu et al 2012; Farooq et al 2013). To estimate selection pressure for CP and TGB, we calculated dN/dS ratios of ASPV CP, TGB1, TGB2 and TGB3 on the basis of all available sequences. The dN/dS ratios for all the tested genes were <1, indicating that TGB and CP were under negative selection. The higher dN/dS ratio of CP and TGB3 compared to that of TGB1 and TGB2 suggested that the evolution constraint on TGB1 and TGB2 be higher than CP and TGB3 (Table 2-6).

In neutrality tests, the Tajima's *D*, Fu and Li's *D* and *F* values for subpopulations from Groups Gp1, Gp2, Gp3 based on CP and groups Gp1, Gp3 and Gp5 based on TGB were negative (Table 2-7), suggesting these subpopulations be in a state of increasing. However, all of them were not significant (P-value >0.05), which indicated the result was not conclusive. The Tajima's *D*, Fu and Li's *D* and *F* values of subpopulations from groups Gp2 and Gp4 based on TGB were positive, which seemed to suggest these two subpopulations in a state of decreasing, but also not convincing.

Table 2-6 Selection pressures (dN/dS) of different ASPV genes

Genes	Nnumber of Sequences	dS	dNS	dNS/dS
CP	87	0.5695	0.1177	0.2067
TGB*1*	81	0.66430	0.04721	0.07107
TGB*2*	81	0.66285	0.05170	0.0780
TGB*3*	81	0.28095	0.07920	0.2819

Table 2-7 Population genetic parameters and neutrality tests calculated for ASPV CP and TGB based on geographic origins or variant groups

Genes	Lineage	n	Hd	Pi	Tajima's *D*	Fu and Li's *D**	Fu and Li's *F**
CP Host	All	95	1.000	0.1717	-0.2610	-1.1853	-0.8538
	Gp1 (pear)	47	1.000	0.1487	-0.3836	-1.0547	-0.8690
	Gp2 (apple)	43	1.000	0.1396	-0.9266	-0.4101	-0.7193
	Gp3 (Korla pear)	5	0.900	0.1450	-0.8872	-0.7507	-0.8484
CP Geographic origins	China	76	0.9994	0.16616	-0.2958	-0.6272	-0.5521
	South Korea	8	1.0000	0.15123	-0.9181	-0.6853	-0.8270
	Poland	9	1.0000	0.1915	-0.4401	0.0017	-0.1189
	Germany	2	1.0000	0.00261	-	-	-
TGB Variant groups	All	81	1.000	0.1834	0.0395	0.3131	0.2295
	Gp1	38	1.000	0.1344	-0.0816	0.3669	0.2607
	Gp2	5	1.000	0.0636	0.0579	0.4967	0.4435
	Gp3	22	1.000	0.0818	-0.5895	-1.3386	-1.2911
	Gp4 (apple)	12	1.000	0.1624	0.2825	0.6697	0.6476
	Gp5 (Korla pear)	4	1.000	0.1504	-0.7348	-0.4073	-0.5034

Notes: Fu & Li's and Tajima's D statistic were performed using DnaSP software version 5.10.01. Values for neutrality tests were not significant (ns) in all cases (P > 0.05)

2.5 Discussion

To investigate ASPV incidence and to provide a clear of phytosanitation status of pear plants in China, four hundred fifty-one pear samples from different geographical areas of China were collected to detect ASPV in our study. ASPV incidence detected by RT-PCR in pear was 32.3%, which was greatly different from previous results (Syrgianidis 1989; Jelkmann 1994; Jelkmann and Keim Konrad 1997; Klerks et al 2001; Kundu 2003; Aglayan et al 2006; Mathioudakis et al 2009; Mathioudakis et al 2010; Youssef et al 2010). Possible reasons account for the different ASPV detection rate between different studies were different primer pairs corresponding to different regions of ASPV genome or different detection methodologies were used (Komorowska et al 2010), or different viral titer at different time of a year (Mathioudakis et al 2009) or using different tissues of the plants (Klerks et al 2001). Therefore, more reliable and sensitive methods such as RT-nPCR, real-time PCR and RT loop-mediated isothermal amplification (RT-LAMP), are required for ASPV detection. It was interesting that ASPV incidence in apple plants (78.6%) was significant higher than that in pear plants (32.3%), which was in accordance with two previous surveys in Greece (Syrgianidis 1989; Mathioudakis et al 2010). ASPV infection prevalence showed some host preferences similar to that of *Tobacco etch virus* (TEV) (Estevan et al 2014), however, mechanisms account for this phenomenon have been not determined yet.

A previous study showed that ASPV isolates grouping in phylogenetic tree seemed related with their hosts (Liu et al 2012), however, they result were not supported by enough sequences data, since previous study mainly focused on CP molecular characteristics of ASPV isolates from apple and Kolar pear (Komorowska et al 2010; Wu et al 2010; Liu et al 2012; Yoon et al 2014), here we confirmed this result here by sequencing large number of CP and TGB sequences from different ASPV pear isolates. Our results showed no matter which ASPV genes (CP or TGB) were used to construct phylogenetic tree, ASPV isolates grouping was related with their hosts (apple, pear and Kolar pear). Here we consider pear and Kolar pear (specifically grown in Xinjiang province, north-western China) were different hosts for ASPV, since ASPV isolates from Kolar pear always formed a single group in phylogenetic tree. For example, ASPV isolates in Gp3 (CP) shared a similarity of 89.9-100% at at the nucleotide level and 92.7-100% at amino acid level within-group, however, they had very low identities with isolates in other groups, ranging from 66.4 to 72.2% (nt) and 68.6 to 78.20% (aa). These

values were out of the limits of species demarcation criteria in the family *Flexiviridae*, wherein isolates sharing greater than 72% nt or 80% aa sequence identities between their CP were considered one specie (Adams et al 2014). This probably suggested that ASPV isolates from Kolar pear reported previously could be a new species of virus， which was closely related to ASPV. However, not all ASPV isolates followed the rule that genetic position in the phylogenetic tree related with their hosts, there were always some exceptions. For CP, it was interesting that subgroup F was closed to ASPV apple isolates in phylogenetic tree. The ten isolates in subgroup F shared a similarity of 94.8-99.7% at nt level and 94.9-100% at the amino acid (aa) level, at the same time, genetic distance in subgroup F was the lowest (0.0370±0.0032) among the six subgroups, which indicated sequences in this subgroup were not obtained by chance or by mistakes during sequencing progress. These results may indicated that ASPV isolates from different host evolved from the same ancestor.

Our results indicated that ASPV isolates from pear in China had great genetic diversity. For CP, ASPV pear isolates formed six subgroup (A-F), wherein two subgroups B and F, which did not correspond to any previously reported variant groups, were identified from Chinese ASPV pear isolates. There are a lot of pear varieties cultivated in China, at least including *Pyrus ussuriensis* Maxim., *P. bretschneideri* Rehd, *P. pyrifolia*, *P. communis* L. and *P. sinkiangensis* T. T. Yu. Top grafting frequently using in the new variety of pear cultivation, combination with frequent regional and international exchange of propagating materials, may have played a major role in the great genetic diversity of ASPV pear isolates.

Recombination represents a successfully evolutionary phenomenon (Glasa et al 2004), which play a role in the ability of various viruses to acquire sequence diversity allowing faster adaptation to new host, environment changes or overcoming host resistance (Valli et al 2007; Martín et al 2009; Seo et al 2009). Nowadays, more and more recombination events are detected in RNA viruses from fruit trees (Alabi et al 2010; Zhang et al 2011; Farooq et al 2013). The recombination events of ASPV CP from apple isolates have already been reported in two previous studies (Komorowska et al 2011; Yoon et al 2014), however, our study reported recombination events of ASPV CP and TGB from Chinese pear isolates. Recombination events were detected in both CP (two out of fifty unique CP sequences) and TGB (two out of seventy-five unique TGB sequences) in our study, but the recombination events were unlikely to be artificial effects, because most of the

detected recombination sites located within CP and TGB, and also all the recombination events detected in our study were combination between ASPV isolates from different geographical regions. The two recombinants in CP shared exactly the same recombination site, which implied that they were probably the progeny of one successful recombination. Nevertheless, these results indicated that recombination played a role in ASPV genomic diversity.

The dN/dS ratios of four ASPV genes indicated that all of them were under negative selection. In comparison, TGB1 was under the strongest selection pressure, followed by TGB2. TGB1 like proteins have been reported to play many roles in interactions between viruses and plants including movement in plants and suppressing RNA silencing (Voinnet et al 2000; Senshu et al 2009; Solovyev et al 2012), but the functions of ASPV TGB have been not studied at all. Transport of TGB1 protein to plasmodesmata is generally accepted to require the functions of TGB2 and TGB3 proteins (Solovyev et al 2013; Verchot-Lubicz et al 2010). Higher constraints on these genes help the proteins protect their structures and fulfill their functions.

Chapter 3 - Diversity analysis of ASPV CP

3.1 Abstract

Full length of ASPV pear isolate (*Pyrus pyrifolia*) (Wuhan city, HuBei province) was sequenced in our study, which was named HB-HN1. HB-HN1 was 9,270 nt in length (excluding polyA tail). HB-HN1 shared 72.4%-80.0% similarity with 11 other reported ASPV isolates at nt leve. However, Results patterns were different if different genes were used. The 5' UTR (Untranslated Region) of ASPV was relatively conserved while the 3' UTR region were highly variable. Phylogenetic tree analysis based on these 12 full length sequences also suggested different ASPV isolates grouping was related to hosts (apple, pear and Korla pear). Results of ASPV-vsiRNAs analysis indicated ASPV positive and negative strand RNAs contributed equally to generated vsiRNAs and these vsiRNAs distributed onto whole ASPV genome. It was interesting to find that 5' teminal of ASPV-vsiRNAs had a C bias.

ASPV CP sequences (HB-HN1-3, HB-HN7-18, HB-HN6-8, HB-HN9-3, YN-MRS-17, LN-AP-1) from five pear isolates and 1 apple isolate were selected to express fused CP in Prokaryotes in certain conditions (30℃, in LB medium containing 50 mg/L Kan, induced 6 h by 1 mM/L IPTG), in which three were selected to produce recombinant antibody for further analyzing serological reactivity. These three produced polyclonal antiserums were named PAb-HB-HN9-3, PAb-HB-HN6-8 and PAb-YN-MRS-17. Western blot indicated different extent of serological reactivity between these three antibodies and six fused CP expressed in Prokaryotes. Different isolates of ASPV CP expressed by PVX vector (PVX-ASPV-CP) were found to have VSRs (viral supressor of RNA silencing) founction. Also PVX-ASPV-CP infected *Nicotiana occiden*talis dispalyed severe symptoms compared to PVX (wt) infected ones. We also confirmed that VSR function and pathogenicity of ASPV CP were not affected by molecular variation.

Keywords ASPV, vsRNAs, CP, recombinant antibody, VSR, pathogenicity

---

This chapter has not been published yet. Xiaofang Ma, Ni Hong, Peter Moffett, Guoping Wang. (2015). Coat protein of *Apple stem pitting virus* possessed viral RNA silencing suppressor activity. *Manuscript preparing.*

3.2 Introduction

ASPV can induce pear leaves vein yellow (Fig 3-1A), red mottling (Fig 3-1D) or necrotic spot (PNS) (Fig 3-1B) or fruit stony pit (Fig 3-1C) (Jelkmann 1994, Jelkmann and Keim Konrad, 1997)), however, ASPV is usually latent infection in apple. Results in Chapter 2 suggested that ASPV grouping in the phylogenetic tree was related with their hosts (pear, apple and Korla pear), which indicated that ASPV induced symptoms diversity seemed have a kind of relationship with its molecular diversity. To date, full length of 11 ASPV isolates (8 apple isolates and 3 Korla pear isolates) have been reported, apple isolate PA66 (D21829.2) from Germany, Hannover (KF321967.1) and PM8 (KF319056.1), apple isolate IF38 (AB045371.1) from Japan, apple isolate PB66 (KF321966.1) from United Kingdom, apple isolate Palampur (FR694186.1) from India, apple isolate YL (KJ522472.1) and YT (KF915809.1) from China, Korla pear isolates PR1(EU095327.1), KL1 (JF946775.1) and KL9 (JF946772.1) from China. However, no ASPV isolates from pear have been reported yet.

The objectives of our study were to make clear the biological, serological and pathogenic diversity induced by ASPV molecular diversity.

Fig. 3-1 Different symptoms induced by *Apple stem pitting virus* on pear

3.3 Materials and Methods

3.3.1 RT-PCR, cloning and sequencing

Total RNAs extracted from 0.1 g leaves of HB-HN1, which was an ASPV pear (*pyrus pyrifolia* Nakai) isolate identified in **chapter 2** by using cetyl-triethylammonium bromide (CTAB) method (Li et al 2008). Then the extracted total RNAs were used as

template for amplification of fragments containing different regions of ASPV. The primer sequences used for amplifying the whole genome of ASPV are listed in Table 3-1. The primers desiged in this study according to the cDNA sequence of ASPV from GenBank D21829.2. Fig. 3-2 indicaetd the ASPV whole genome amplification strategy.

First-strand cDNA synthesis was performed using 0.5 mM of random primer (6 mer) (TaKaRa, Dalian, China) and M-MLV reverse transcriptase (Promega, Madison, USA) at 37 °C for 1.5 hour. PCR reactions were undertaken in a 25 μl volume with reaction mixtures containing 2.5 μl 10×PCR buffer, 0.5 mM dNTP, 1 mM specific primer, 0.15μl of 5 U/lL rTaq DNA polymerase (TaKaRa, Dalian, China), and corresponding templates (3 μl first-strand cDNA). The PCR cycling parameters were set as follows: pre-activation at 94°C for 5 min, followed by 35 cycles of denaturation (94°C for 30 s), annealing (30 s at a certain temperature for each primer pairs, and extension (1 min or more at 72°C), final extension (1 cycle of 72°C for 10 min). The PCR reaction was conducted in a 96-well PCR Thermal Cycler (T-100TM, BIO-RAD, USA). The PCR products were analyzed on 1% agarose gels and visualized in a UV transilluminator by Ethidium bromide (1 μl/ml) staining. The 5'- and 3'-terminal sequences of HB-HN1 were determined using 5'- and 3'-RACE Kits (TaKaRa, Dalian, China), respectively, and following the instruction manual.

All amplified PCR products were cloned individually into pMD18-T simple vector (TaKaRa, Dalian, China) according to the manufacturer's instruction. To exclude in vitro RT-PCR errors, at least three clones from each ASPV isolates were sequenced in both forward and reverse orientations. If the three independent clones showed ≥98% similarity, then a consensus sequence was obtained, which was named ‘unique sequence’. If there was <98% nucleotide similarity between the three initially sequenced clones, additional clones would be sequenced to investigate the possible occurrence of molecular variants mixtures within individual pear.

Table 3-1 The primers used for amplifying fragments of ASPV (HB-HN1) full genome

Primer names	Primer sequence (5'-3')	Fragment Name	Length (bp)	Position	Reference
P1-F	GCAGAGGAAGTAATCGCATC	P1	2727	83-103 nt	This study
P1-R	GAACTCTTGAACTGGAGCACT			2800-2820 nt	
P2-F	GAGCATGATGATTCAGATG	P2	2722	2577-2595 nt	This study
P2-R	CACGATTCTTGCTGTGAT			6719-6737 nt	
6-F	TTCCTGAATTGGTCCATGA	6	620	4151-4170 nt	This study
6-R	GACAATCCTTACGACCCAT			4753-4772 nt	
P3-F	ATCACAGCAAGAATCGTGGTCAAG	P3	1399	5339-5362 nt	Niu et al 2012
P3-R	TCAACTGTTCTCTCAAAGCCAAAT			6714-6738 nt	
P4-F	GTGTGTAAGCATATTAGG	P4	1203	6656-6664 nt	This study
P4-R	CTACACCCTAACCTAATG			7832-7850 nt	
P5-F	GTACATGAGTAACTCGAGCC	P5	1484	7708-7728 nt	W.Jelkamnn 1997
P5-R	ATAGCCGCCCCGGTTAGGTT			9239-9258 nt	
5'RACE GSP Inner Primer	AAGAAGCCACCATACCT	ASPV-5'	507	5'UTR	This study
5'RACE GSP Outer Primer	CCCTCCATACATCCTGGAAT				
3'RACE GSP Outer Primer	GGACATTACACTGGAGGAG	ASPV-3'	200	3'UTR	This study
3'RACE GSP Inner Primer	GCCTGTTCTATCCATTAAG				

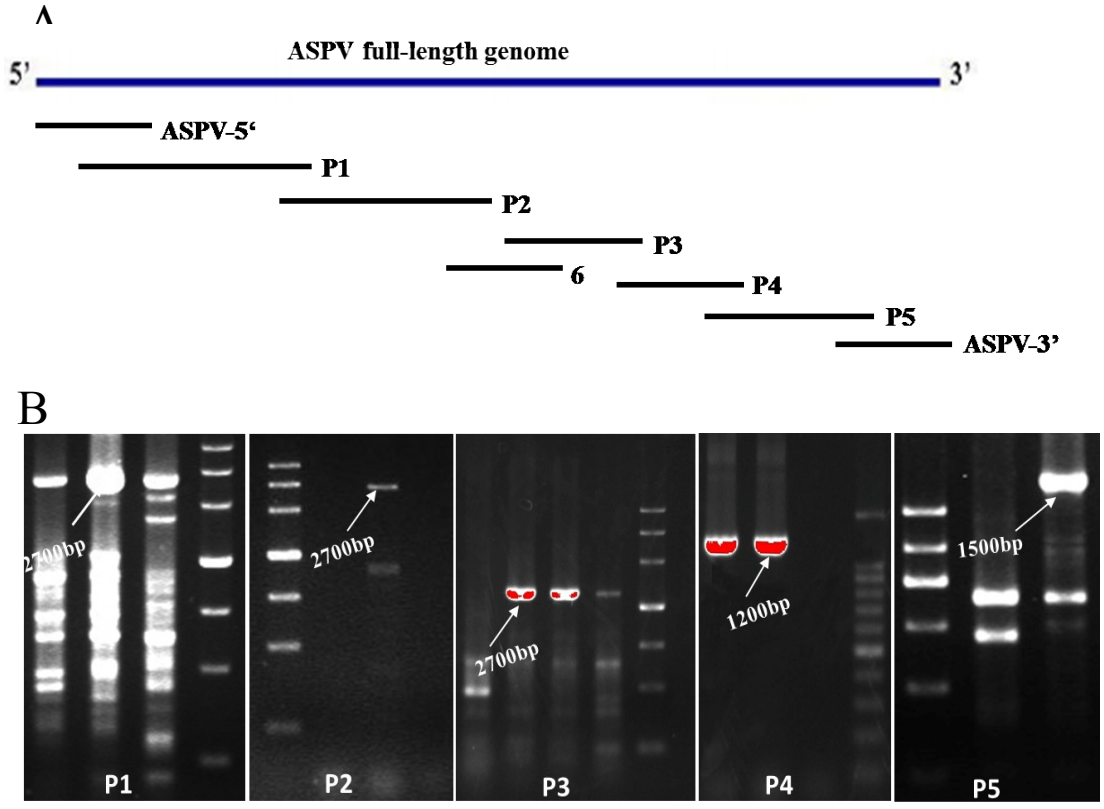

Fig. 3-2 Full genome amplification of ASPV

A, The 8 selected cDNA fragments and their relative genomic position; B, 1.0% agarose gel electrophoresis of RT-PCR products of fragments (P1-P5) from ASPV full genome

3.3.2 Sample preparation and deep sequencing

Leaves of HB-HN1 were frozen in liquid nitrogen, and then preserved in carbon dioxide ice blocks and shipped to BGI Company (Shenzhen, China) for deep sequencing. One microgram of total RNA was extracted, unique, barcoded adaptors were added, RT-PCR was performed and the product was purified via polyacrylamide gel electrophoresis (PAGE) for sRNA library construction and sequencing in an Illumina HiSeq™2000 (Illumina, USA) (Fig. 3-3).

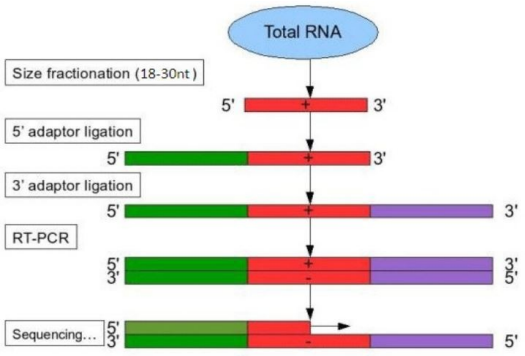

Fig.3-3 Small RNAs sequencing strategy for plant

3.3.4 Expression of ASPV CP in *Escherichia coli*

Based on phylogenetic analysis of ASPV CP gene in **Chapter 2**, unique CP sequences of five ASPV pear isolates (HB-HN1-3, HB-HN7-18, HB-HN6-8, HB-HN9-3, YN-MRS-17) were selected to produce recombinant proteins, which would be used for analysis of electrophoretic mobility and serological reactivity. The unique CP sequence LN-AP-1 from apple isolate was used as reference. Sequences of primers used for constructing ASPV CP prokaryotic expression vectors were listed in Table 3-2. HB-HN9-3 was cloned into BamHI and HindIII sites of pET-28a (+) (Novagen, Madison, WI, USA), and HB-HN1-3, HB-HN7-18, HB-HN6-8, LN-AP-1 and YN-MRS-17 were cloned into SacI and SalI sites of pET-28a(+). The constructed recombinant expression vectors were named as pET-HB-HN1-3, pET-HB-HN7-18, pET-HB-HN6-8, pET-HB-HN9-3, pET-YN-MRS-17 and pET-LN1-AP-1, respectively. Then these constructs were transformed to *Escherichia coli* (*E. coli*) strain BL21 (DE3). Recombinant CP (rCP) productions were induced for 6 h in Luria-Bertani (LB) medium containing 50 mg/L kanamycin and 1 mM/L isopropyl-β -d-thiogalactoside (IPTG) at 30°C, and then evaluated by 10.5% SDS-PAGE. Gels were stained with 0.25% Coomassie blue G250 solution.

Table 3-2 List of primers with Restriction Enzyme cutting site used for constructing vectors that could express fused CP with a His tag in *Escherichia Coli* BL21 (DE3)

Clone names	Primers with Restriction Enzyme cutting site (5'-3')	Enzyme names	Fragment length	Host
HB-HN9-3	*Forward*: GG*GGATCC*ATGGCTTCCGATGGTACT	*Bam*HI	1233 bp	Pear
	Reverse: GGG*AAGCTT*TCACTTCCTAATTGATAG	*Hin*dI		
HB-HN1-3	*Forward*: GGG*GAGCTC*ATGGCATCCGATGGCTCT	*Sac*I	1185 bp	Pear
	Reverse: GG*GTCGAC*TTACTTCTTAATGGATAG	*Sal*I		
HB-HN6-8	*Forward*: GGG*GAGCTC*ATGGCTTCCAATGTATCC	*Sac*I	1233 bp	Pear
	Reverse: GG*GTCGAC*TTACTTCCTAATGGATAA	*Sal*I		
HB-HN7-18	*Forward*: GGG*GAGCTC*ATGACTTCCAATGGTTCC	*Sac*I	1185 bp	Pear
	Reverse: GG*GTCGAC*TTACTTCCTAATGGATAA	*Sal*I		
YN-MRS-17	*Forward*: GGG*GAGCTC*ATGACTTCTAATGGATCC	*Sac*I	1125 bp	Pear
	Reverse: GG*GTCGAC*TTACTTCCTAATGGATAG	*Sal*I		
LN-AP1-1	*Forward*: GGG*GAGCTC*ATGGCTTCCAATGGTTCC	*Sac*I	1191 bp	Apple
	Reverse: GG*GTCGAC*TTACTTCCTGATGGATAG	*Sal*I		

3.3.5 Preparation of antiserum against ASPV rCP and Western blot

Antiserum against ASPV rCP expressed by pET-HB-HN6-8, pET-HB-HN9-3 and pET-YN-MRS-17 were prepared and purified on the basis of methods reported previously in our lab (Xu et al 2006; Song et al 2011). The raised antiserum were named PAb-HB-HN6-8, PAb-HB-HN9-3, PAb-YN-MRS-17.

Western blot was used to detect expressed in *E. coli* with three antibodies PAb-HB-HN6-8, PAb-HB-HN9-3, PAb-YN-MRS-17. For western blot: Total induced proteins from *E. coli* cells were separated on 10.5% resolving gels and transferred onto a PVDF membrane (BIORAD, USA), followed by blocked with 5% (w/v) skimmed milk in 1x PBST (0.01 M PBS, 0.05-0.1% Tween-20, pH 7.4) at 37°C for 2 h or 4°C overnight; then the membranes were incubated with purified primary antibodies at dilutions of 1:500 for PAb-HB-HN6-8, YN-MRS-17 and PAb-HB-HN9-3; then incubated with secondary antibody Alkaline phosphatase (AP) conjugated goat anti-rabbit IgG (Sigma, Germany) diluted at 1:5,000; Antigen-antibody reactions were visualized by incubation in BCIP/NBT substrate solution (Amresco, USA). Image J was used to quantify reaction signals on the blots.

3.3.6 Expression of ASPV CP in *planta*

Again the six unique CP sequences (HB-HN1-3, HB-HN7-18, HB-HN6-8, HB-HN9-3, YN-MRS-17 and LN-AP-1) were selected to express ASPV CP in *planta.* All sequences for ASPV CP expression vectors were cloned into ClaI and SalI sites of

pGR106, which was modified from *Potato virus X* (PVX) vector. Primer sequences used for constructing these vectors were listed in Table 3-3. The constructed vectors were named PVX-CP (HB-HN1-3/HB-HN7-18/HB-HN6-8/HB-HN9-3/YN-MRS-17/LN-AP-1). Then these constructs were transformed to *Agrobacterium Tumefaciens* strain GV3101. *Agrobacterium Tumefaciens* strain GV3101 containing these six constructs were grown at 28°C in Luria-Bertani (LB) medium containing 50 mg/L Kanamycin, 5 mg/L Tetracycline, 10 mM/L 2-(4-Morpholino) ethanesulfonic acid (MES) and 20 mM/L Acetosyringone (AS), until optical density at 600 nm (OD600)=0.5. Plasmids 35S-GFP, and 35S-P19 have been previously described (Voinnet et al 2003). GFP transgene *N. benthamiana* line 16C or *N. occidentails* plants were infiltrated with *Agrobacterium tumefaciens* (Agroinfiltration). GFP expression was monitored under UV light using a handheld lamp (BLAK RAY, UVP). GFP transgene *N. benthamiana* line 16C or *N. occidentails* plants were germinated and grown in a glasshouse maintained at 26℃with 16 h day and 8 h night.

Table 3-3 List of primers with Restriction Enzyme cutting site used for constructing PVX vectors that could express ASPV coat protein in *N. benthamiana*

Clone names	Primers with Restriction Enzyme cutting site (5'-3')	Enzyme names
HB-HN9-3	*Forward*: GGATCGATATGGCTTCCGATGGTACT	*Cla*I
	Reverse: GGGTCGACTCACTTCCTAATTGATAG	*Sal*I
HB-HN1-3	*Forward*: GGATCGATATGGCATCCGATGGCTCT	*Cla*I
	Reverse: GGGTCGACTTACTTCTTAATGGATAG	*Sal*I
HB-HN6-8	*Forward*: GGATCGATATGGCTTCCAATGTATCC	*Cla*I
	Reverse: GGGTCGACTTACTTCCTAATGGATAA	*Sal*I
HB-HN7-18	*Forward*: GGATCGATATGACTTCCAATGGTTCC	*Cla*I
	Reverse: GG*GTCGAC*TTACTTCCTAATGGATAA	*Sal*I
YN-MRS-17	*Forward*: GGATCGATATGACTTCTAATGGATCC	*Cla*I
	Reverse: GGGTCGACTTACTTCCTAATGGATAG	*Sal*I
LN1-AP-1	*Forward*: GGATCGATATGGCTTCCAATGGTTCC	*Cla*I
	Reverse: GGGTCGACTTACTTCCTGATGGATAG	*Sal*I

3.4 Results and Discussion

3.4.1 Analysis of the whole genome of HB-HN1

The complete genomic sequences of pear isolates HB-HN1 was 9270 nt excluding poly (A) tail at 3' end. Sequences analysis revealed that genome of HB-HN1 exhibited the common properties of the genome of *Foveaviruses*, which contained five ORFs. ORF1-ORF5 were 6522 bp, 672 bp, 363 bp, 228 bp and 1185 bp, respectively. The 3' and 5' untranslate regions (UTR) were 60 and 130 nt, respectively (Table 3-4). Full length of HB-HN1 and the other reported 11 ASPV isolates shared the similarity ranged from 68.1%-92.4% at nt level (Fig. 3-4 A), wherein isolates KL1 and KL9 from Korla pear in Xinjiang province in China shared the highest indentity (92.4%), however, Korla pear isolate PR1 and German apple isolates Hannover shared the lowest indentity (68.1%). Pear isolate HB-HN1 in our study shared the hightest indentity with apple isolate PB66 from United Kingdom (80.0%), and lowest indentity with Korla pear isolate PR1 (72.4%). The identities of RdRp, TGB1, TGB2, TGB3, and CP gene of HB-HN1 with other 11 ASPV isolates were 70.3%–79.2%, 78.7%–81.8%, 75.2%–86.6%, 79.8%–92.1% and 69.0%–80.8% at nt levels, respectively (Fig. 3-4 B-F). The 5' and 3' UTR showed identities of 82.8–100% and 67.7–85.0% with other 11 ASPV isolates, respectively (Fig. 3-4 G, H). Phylogenetic analysis of the full genomes of 12 ASPV isolates at nt sequence revealed ASPV phylogenetic grouping was also related to their hosts, isolates from apple excepting for PB66 and Palampur) formed a group, isolates from Korla pear formed another group, however, HB-HN1 in our study from sand pear (there were no other isolates from pear) did not belong to any defined groups (Fig. 3-5). This result confirmed our result in Chapter 2.

Table 3-4 The Host, origin, full length of ASPV genome and different genes on GneBank

Accession Number	IsolatesIsolates	HostHost	Source	Full Length (bp)	Length Of *RdRP* (bp)	Length Of *MP* (bp)			Length Of *CP* (bp)
						TGB1	TGB2	TGB3	
D21829.2	PA66	Apple	Germany	9332	6552	672	363	213	1245
KF321966.1	PB66	Apple	United Kingdom	9363	6552	672	366	231	1191
AB045371.1	IF38	Apple	Japan	9293	6558	672	363	228	1191
FR694186.1	Palampur	Apple	India	9267	6552	672	363	228	1191
KF915809.1	YT	Apple	China	9270	6552	672	363	213	1188
KJ522472.1	YL	Apple	China	9262	6552	672	363	228	1191
KF319056.1	PM8	Apple	Germany	9284	6567	672	363	228	1191
KF321967	Hannover	Apple	Germany	9324	6561	672	363	213	1221
EU095327.1	PR1	Korla Pear	China	9336	6552	672	369	228	1209
JF946775.1	KL1	Korla Pear	China	9265	6555	672	363	213	1194
JF946772.1	KL9	Korla Pear	China	9265	6555	672	363	213	1194
-	HB-HN1	Pear	This study	9270	6552	672	363	228	1185

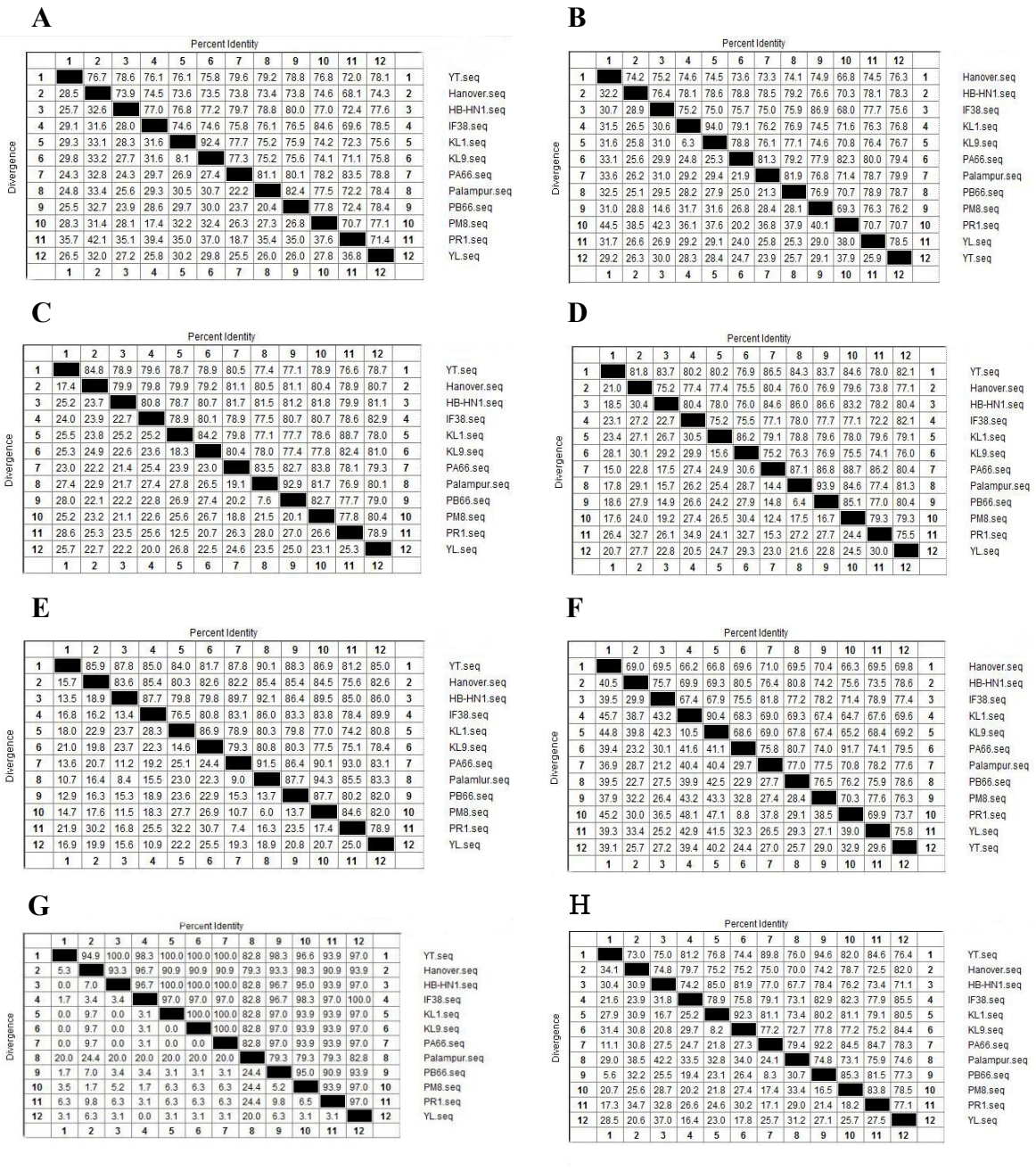

Fig.3-4 Phylogenetic tree of whole genome sequences of HB-HN1 and global isolates

A, Similarity of full ASPV genome of diferent isolates; B, Similarity of RdRP gene of diferent isolates; C, Similarity of TGB1 gene of diferent isolates; D, Similarity of TGB2 gene of diferent isolates; E, Similarity of TGB3 gene of diferent isolates; F, Similarity of CP gene of diferent isolates; G, Similarity of 5'-UTR (Untranslated Region) of diferent isolates; H, Similarity of 3'-UTR of diferent isolates. Similarity values were calculated by software MegAlign

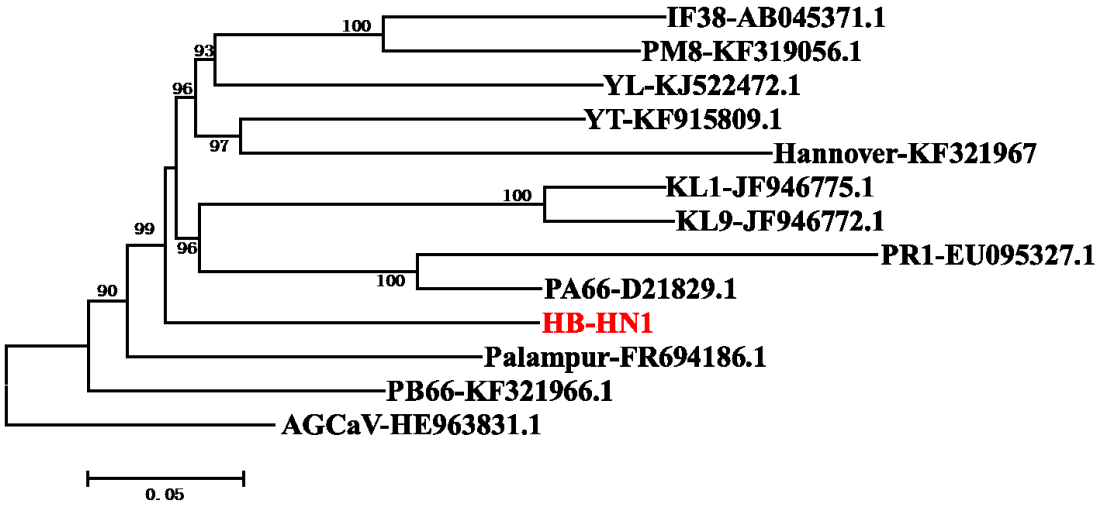

Fig.3-5 Phylogenetic tree of whole genome sequences of HB-HN1 and global isolates
Reference isolates are named through their isolate name with GenBank accession numbers after. The tree was constructed by the neighbor joining method implemented by MEGA6. Bootstrap analysis with 1000 replicates was performed. Only ≥50% bootstrap values are shown, and branch lengths are proportional to the genetic distances. Bar, 0.05 substitutions per site

3.4.2 Analysis of vsiRNAs derived from ASPV pear isolate HB-HN1

A total of 12,845,169 clean reads with size 14-29 nt (after removing adapter sequences and selected by size differences) were obtained from HB-HN1 pear plants. The sRNAs profile was evaluated base on the obtained ASPV full genome sequences (Small RNA reads were mapped to ASPV genome using Bowtie (1.0) software, and only those having sequences identical or complementary to viral genomic sequence less than 2 mismatches were identified as viral derived small RNAs (vsRNAs)). In total, 55,499 vsRNAs reads accounting for 0.432% of total reads matched onto the genome of HB-HN1. The size classes of vsRNAs were mainly 18-26 nt with 21 nt being a highest accumulation (31,349, 56.49%) followed by 22 nt (17,706, 31.90%) (Fig. 3-6 A).

Among the 55,499 ASPV-vsiRNAs, 59.1% (32,782) of which distributed onto ASPV positive strand and 40.9% (22,717) of which distributed onto ASPV negtive strand. Generally, these ASPV-vsRNAs distributed continuously but unevenly along both sense and antisense strands of the viral genome (Fig. 3-6 B).

Analysis of the 5' terminus of ASPV-vsRNAs indicated U was the most abundant nucleotide, followed by A and C, and G was the least abundant (Fig. 3-6 C).

A

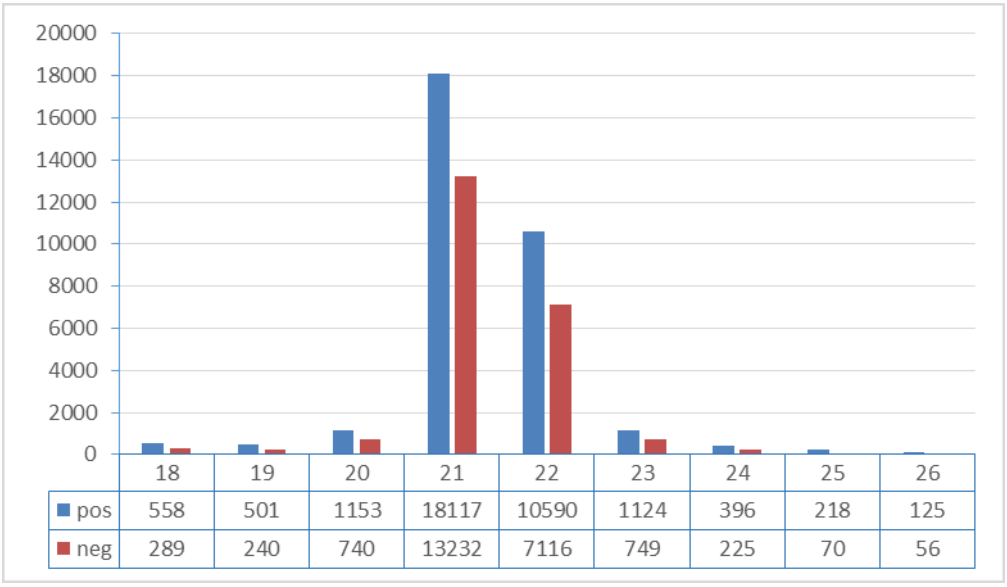

	18	19	20	21	22	23	24	25	26
pos	558	501	1153	18117	10590	1124	396	218	125
neg	289	240	740	13232	7116	749	225	70	56

B

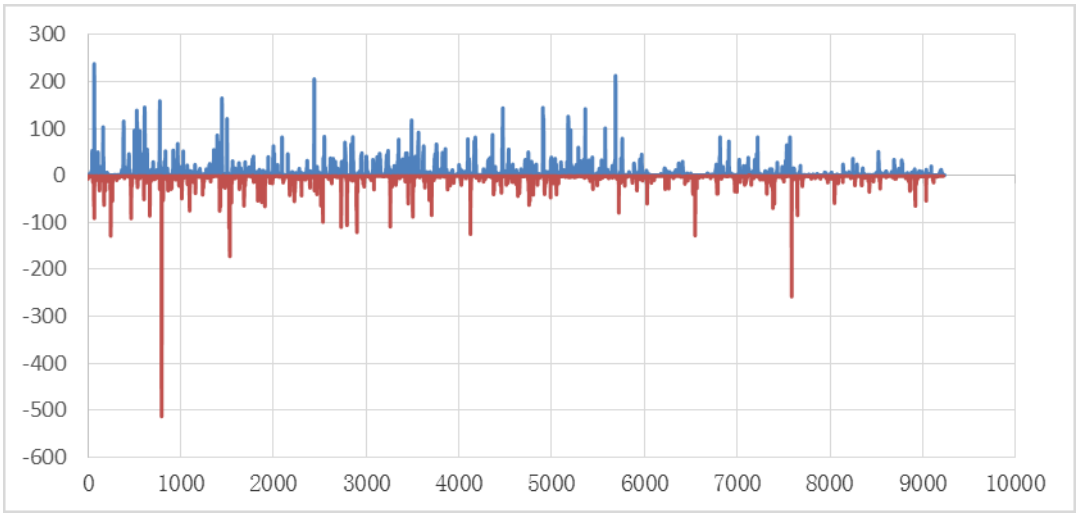

C

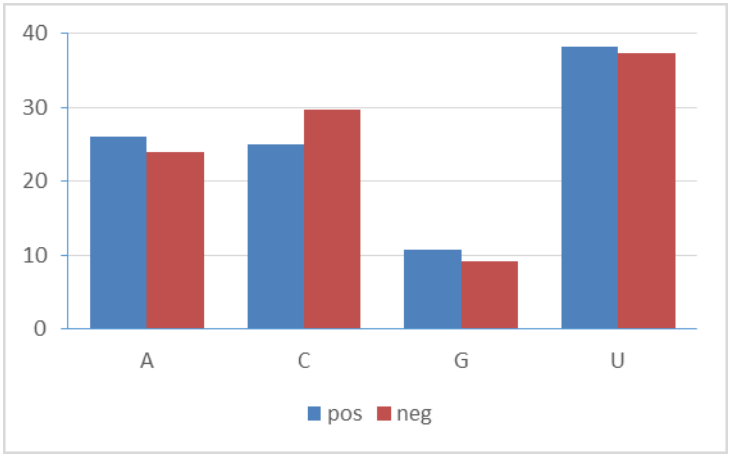

Fig.3-6 ASPV-vsiRNAs analysis obtained from pear plant HB-HN1

A, Size distribution of ASPV-vsiRNAs in library prepared from pear plant HB-HN1; B, Genome-wide map of ASPV-vsiRNA at single nucleotide resolution; C, Relative frequency of 5' terminal nucleotide of vsRNA in pear plant HB-HN1. pos indicated positive strand，neg indicated negative strand

3.4.3 Differences in symptoms induced by different ASPV isolates in *N. occidentails*

Pear (names and cultivars of these isolates were HB-HN6, *P. bretschneideri* cv. Xuehuali; HB-HN9, *P. pyrifolia* cv. Fengshui; HB-HN7, *P. pyrifolia* cv. Fengshui; HB-HN10, *P. pyrifolia* cv. Fengshui; HB-HN2, *P. pyrifolia* cv. Ershishiji, respectively) or apple (HB-AP, unknown cultivar) samples, which were tested ASPV positive by RT-PCR, were sap inoculated onto *N. occidentails*. Symptoms induced on leaves of *N. occidentails* at 14 days post inoculation were pictures listed in Fig. 3-3: A, irregular faded green spots; B, regular faded green circular spots; C and E, secondary veins yellowing; D and F, secondary veins necrosis.

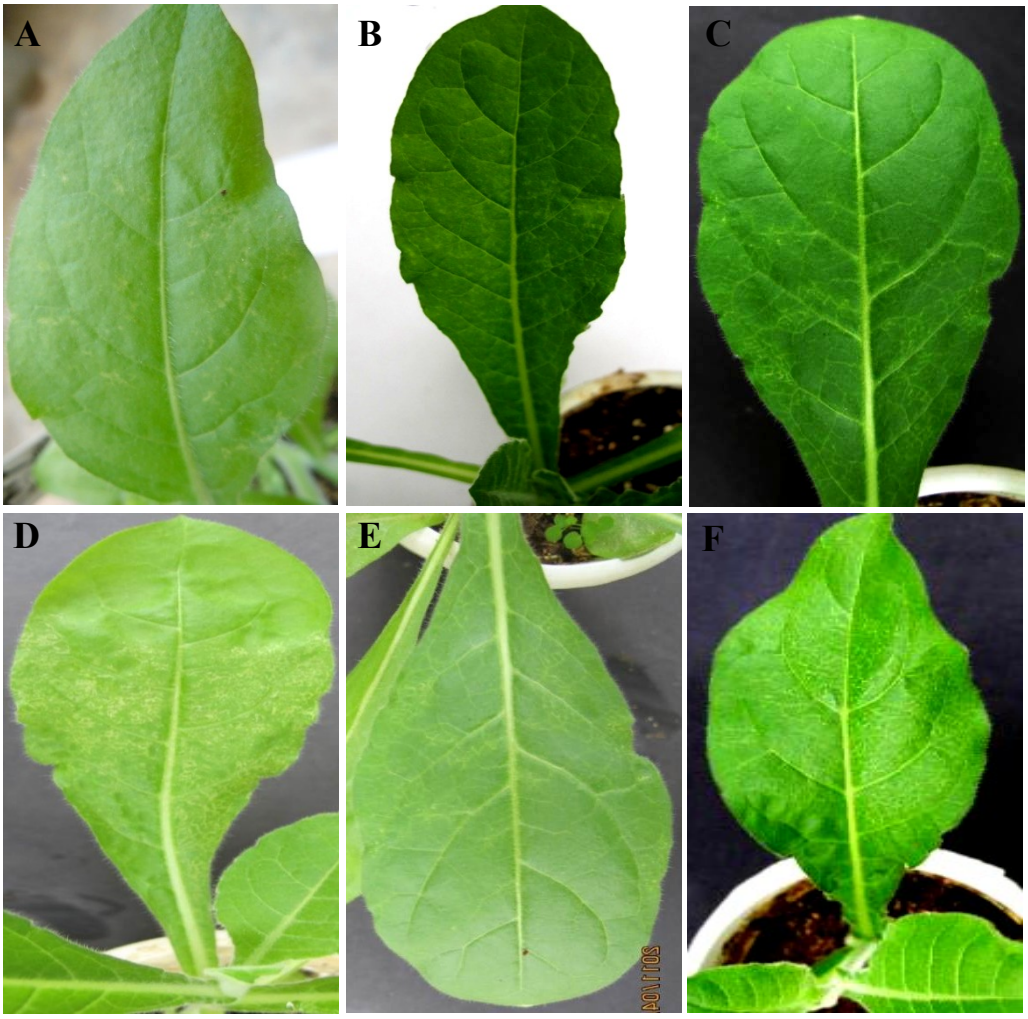

Fig. 3-7 Symptoms induced by different ASPV isolates on *N. occidentails*
A-F, Symptoms induced on *N. occidentails* by ASPV pear (A-E) or apple (F) isolates at 14 days post inoculation (dpi). The samples were collected from an orchard in Wuhan city, Hubei province.

3.4.4 Differences in serological reactivity among rCPs of different ASPV isolates

The selected unique CP sequences of six ASPV isolates (HB-HN1-3, HB-HN7-18, HB-HN6-8, HB-HN9-3, YN-MRS-17 and LN-AP1-1) shared similarity ranged from 72.5% to 87.8% at nt level and 78.2%~88.8% at aa level (Table 3-5). Prediction results of secondary structure (Table 3-6) and B cell epitope(s) (Appendix 5) of CP encoded by the selected six unique CP sequences indicated molecular variation of different ASPV isolates result in great differences in predicted secondary structure and epitopes of CP. To make clear whether the different secondary structures and B cell epitope(s) affected serological features (antibodes-antigens interaction), the following experiments were conducted. The six selected CP sequences were into pET-28a (+), which could express rCPs in *Escherichia coli* BL21 (DE3). SDS-PAGE analysis indicated the six rCPs were efficiently expressed (Fig. 3-8A). The predicted molecular sizes (by online software: ProMACC, *http://www.proteomics.com.cn/tools/mwcal/MyMW.asp*) of these CPs were 43.38 KDa (HB-HN9-3) > 43.27 KDa (HB-HN6-8) > 42.16 KDa (LN-AP1-1) > 41.99 KDa (HB-HN7-18) > 41.54 KDa (HB-HN1-3) > 39.63 KDa (YN-MRS-17), however, electrophoretic mobility results from SDS-PAGE seems different with the predicted ones, which is HB-HN1-3 > YN-MRS-17 > LN-AP1-1 > HB-HN7-18 > HB-HN6-8 > HB-HN9-3.

Table 3-5 Nucleotides and amino acids similarity among the six selected CP sequences

	HB-HN1-3	HB-HN6-8	HB-HN7-18	HN-HN9-3	LN-AP1-1	YN-MRS-17
HB-HN1-3	100%	85.5%	88.8%	81.7%	83.8%	86.6%
HB-HN6-8	80.9%	100%	87.1%	78.2%	81.8%	88.5%
HB-HN7-18	87.8%	80.4%	100%	82.7%	83.0%	88.7%
HN-HN9-3	74.9%	72.5%	74.9%	100%	81.5%	83.1%
LN-AP1-1	74.9%	78.9%	78.8%	74.2%	100%	83.7%
YN-MRS-17	80.9%	86.2%	81.1%	76.2%	80.6%	100%

Note, Lower left and upper right represented nucleotides and amino acids similarity between each two clones, respectively

Table 3-6 Secondary structures prediction of the six selected CP sequences encoded proteins by using software SOPMA

Different CP isolates name	Alpha helix	Extended strand	Random coil	Beta turn
HB-HN6-8	12 (30.49%)	45 (10.98%)	223 (54.39%)	17 (4.15%)
HB-HN1-3	104 (26.40%)	46 (11.68%)	22 (57.61%)	17 (4.31%)
HN-HN7-18	11 (27.92%)	42 (10.66%)	222 (56.35%)	20 (5.08%)
YN-MRS-17	109 (29.14%)	36 (9.63%)	209 (55.88%)	20 (5.35%)
LN-AP1-1	116 (29.29%)	48 (12.12%)	222 (56.06%)	10 (2.53%)
HB-HN9-3	120 (29.27%)	55 (13.41%)	213 (51.95%)	22 (5.37%)

Three polyclonal antibodies PAb-HB-HN9-3, PAb-HB-HN6-8 and PAb-YN-MRS-17

were made against purified rCP expressed in *Escherichia coli* BL21 (DE3). The rCPs of six ASPV isolates were analyzed by western blot (Fig. 3-8B-D) with the three antibodies PAb-HB-HN9-3, PAb-HB-HN6-8 and PAb-YN-MRS-17, respectively. Hybridization signals on the blots were quantified using Image J software to compare the serological reactivity between rCPs of the six isolates. Results showed that the rCPs of the six ASPV isolates could react with the three antibodies, but intensities of the reaction signals were different, however, the reaction intensities was positive related to amino acides similarity among different isolates. Our results indicated that molecular variation of differernt ASPV isolates not only results in differences in amino acides but also in serological reactivity, which probably through epitope(s) modifications.

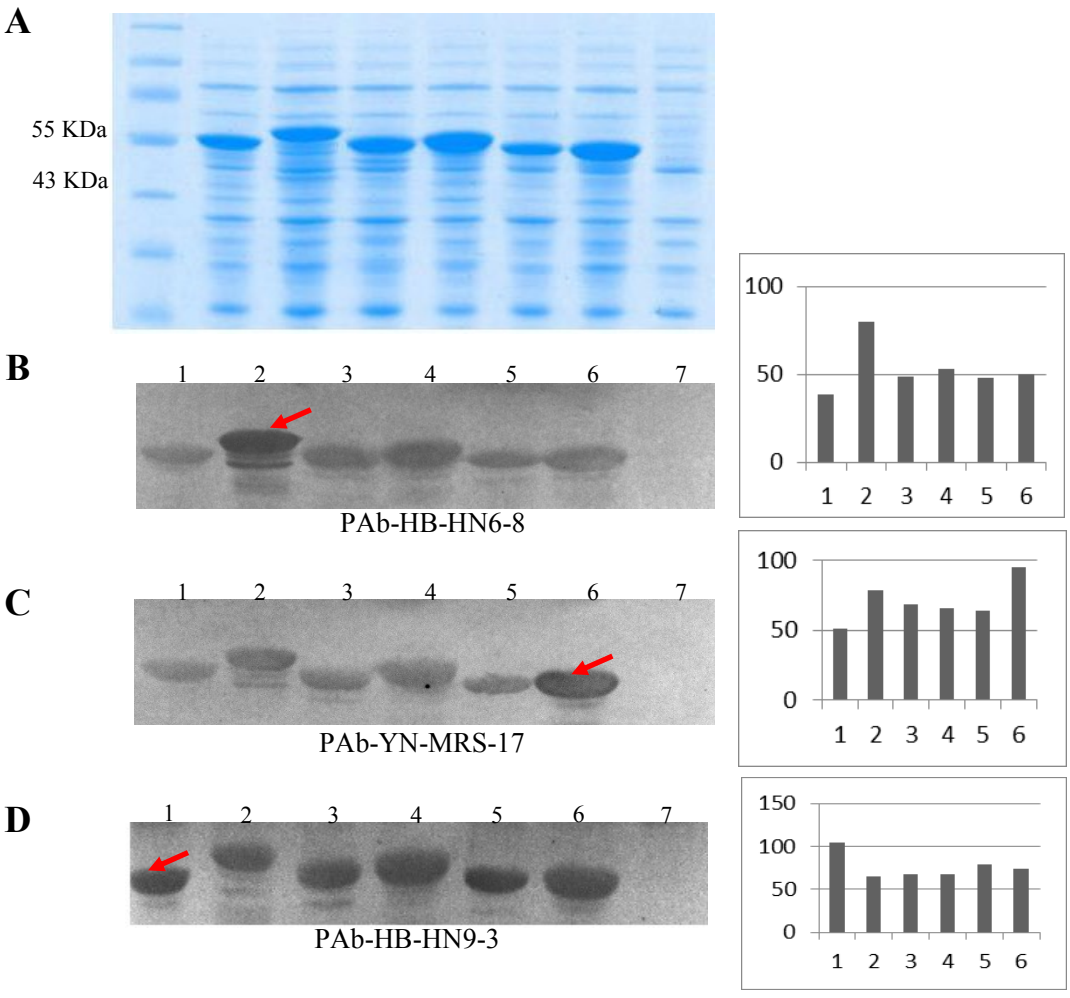

Fig. 3-8 SDS-PAGE and Western blot analyzed the fused CP from different ASPV isolates expressed in *Escherichia Coli* BL21 (DE3)

M, Molecular weight marker; Lane 1-7，The *Escherichia Coli* BL21 (DE3) with constructed vectors pET-YN-MRS-17, pET-HB-HN1-3, pET-HB-HN7-18, pET-LN-AP1-1, pET-HB-HN6-8, pET-HB-HN9-3 and the empty vector pET-28a (+) , respectively, were induced for 6 h in LB medium with 1mM/L IPTG at 30℃ to express the fused CP. Hybridization signals on western blots were quantified by Image J software (right column of B~D)

3.4.5 ASPV CP possesses VSR activity

The ASPV TGBp1 is homologous to the PVX P25 protein, which possesses VSR activity that could suppress systemic RNA silencing but not local RNA silencing (Voinnet et al 2000). However, ASPV TGBp1 in our study did not possess VSR activity, which was tested by *Agrobacterium* mediated transient expression (agroinfiltration) assay (data not shown). The theoretical basis of this VSR identification assay was in the standard that takes advantage of the fact that transiently expressed transgenes are subjected to RNA silencing, and that this silencing is suppressed by many VSRs (Voinnet et al 2003).

Transient expression of 35S-GFP by agroinfiltration in *N. benthamiana* line 16c leaves results in bright fluorescence visible at 3 day post infiltration (dpi). However, by 5 dpi, GFP expression is silenced and fluorescence only faintly visible. Coexpression of GFP with PVX-CP (HB-HN9-3, HB-HN6-8, HB-HN7-18, YN-MRS-17, LN1-AP-1), resulted in strong GFP fluorescence at 5 dpi, whereas coexpression of GFP with PVX (wt) had no effect on GFP persistence (Fig. 3-9A). PVX encodes P25, which could only suppress systemic RNA silencing (Voinnet et al 2000). Our results suggested ASPV CP possesses VSR activity, however, VSR activity of different ASPV isolates displayed no differences.

Previous studies indicated that viruses encoded VSRs usually were pathogenic determinants (Voinnet 2005b). To test whether ASPV CP consisted of pathogenicity, we agroinfiltration *N.occidentails* with PVX-CP and PVX (wt) as a negtive control. Results showed that PVX-CP infected *N.occidentails* plants displayed more serious syptoms at 30 dpi than PVX (wt) infected plants (Fig. 3-9B-D). This result indicated that ASPV CP was also a pathogenic determinant.

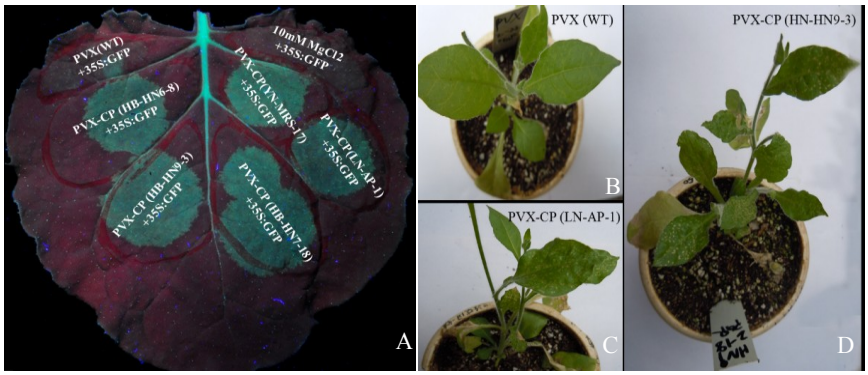

Fig. 3-9 VSR activity test of ASPV CP

A, Suppressor activity of ASPV CP (different isolates) on local RNA silencing. GFP was transiently expressed via agroinfiltration under 35S promoter in *N. benthamiana* line 16c, together with either PVX-CP (different clones from different isolates), PVX wild type or 10 mM $MgCl_2$. GFP signal was monitored by UV illumination at 5 dpi after infiltration; B-D, Symptoms displayed on *N. occidentails* plants infected with PVX or PVX-CP at 30 d.

Chapter 4 - Different roles for RNA silencing and RNA processing components in virus recovery and virus-induced gene silencing in plants

4.1 Abstract

A major antiviral mechanism in plants is mediated by RNA silencing, which relies on the cleavage of viral double-stranded RNA into virus-derived small interfering RNAs (vsiRNAs) by DICER-like (DCL) enzymes. Members of the Argonaute (AGO) family of endonucleases then use these vsiRNA as guides to target viral RNA. This can result in a phenomenon known as recovery, whereby the plant silences viral gene expression and recovers from viral symptoms. Endogenous mRNAs can also be targeted by vsiRNAs in a phenomenon known as virus-induced gene silencing (VIGS). Although related to other RNA silencing mechanisms, it has not been established if recovery and VIGS are mediated by the same molecular mechanisms. We have used *Tobacco rattle virus* carrying a fragment of the *PDS* gene (TRV-PDS) or expressing GFP (TRV-GFP) as readouts for VIGS and recovery, respectively, in *Arabidopsis ago* mutants. Our results demonstrate roles for AGO2 and AGO4 in susceptibility to TRV, whereas VIGS of endogenous genes appears to be largely mediated by AGO1. However, recovery appears to be mediated by different components, as all the aforementioned mutants were able to recover from TRV-GFP. TRV RNAs from recovered plants associate less with ribosomes, suggesting that recovery involves translational repression of viral transcripts. Translationally repressed RNAs often accumulate in RNA processing bodies (PBs), where they are eventually processed by decapping enzymes. Consistent with this, we find that viral recovery induces increased PB formation and that a decapping mutant (*DCP2*) shows increased VIGS and virus RNA accumulation, indicating an important role for PBs in eliminating viral RNA.

Keywords: Argonaute, VIGS, RNA silencing, *Arabidopsis*, *Tobacco rattle virus*, *DCP2*.

This chapter has been reformatted and reprinted from: *J Experimental Botany*, Xiaofang Ma, Marie-Claude N., Louis-Valentin Meteignier, Ni Hong, Guoping Wang and Peter Moffett. (2014) Different roles for RNA silencing and RNA processing components in virus recovery and virus-induced gene silencing in plants.

4.2 Introduction

Plants have developed diverse mechanisms to defend themselves against viral infections, including RNA silencing. RNA silencing is a sequence-specific RNA mechanism that regulates the expression of endogenous genes as well as exogenous genetic elements, including viruses, transgenes, and transposable elements (BolognaVoinnet, 2014, IncarboneDunoyer, 2013). As a defense against viruses in plants, RNA silencing relies on the recognition of viral double-stranded RNA by DICER-like (DCL) enzymes, which cleave the dsRNA into virus-derived small interfering RNAs (vsiRNA) 21-24nt in length. These vsiRNAs in turn bind to RNA-induced silencing complexes (RISC) complexes, which contain Argonaute (AGO) proteins that use the vsiRNAs as guides to target single stranded RNAs (Mallory and Vaucheret 2010). The targeting of viral RNAs is thought to largely involve RNA cleavage, although RNA silencing mechanisms can target endogenous genes by translational repression (Brodersenet al, 2008, Carbonellet al, 2012, Lanetet al, 2009). Given the strong pressure exerted by RNA silencing, plant viruses have evolved viral suppressors of RNA silencing (VSRs), which interfere with the RNA silencing machinery at multiple steps (Pumplin and Voinnet 2013).

The *Arabidopsis* genome encodes for ten AGO proteins and four DCL proteins, which play roles in multiple RNA silencing related phenomena. DCL1 is reported to mainly process endogenous micro RNAs (miRNAs) (BolognaVoinnet, 2014) that target cellular transcripts and does not appear to produce significant amounts of vsiRNAs upon infection with *Cucumber mosaic virus* (CMV) or *Turnip crinkle virus* (TCV) (Deleriset al, 2006, Vaucheretet al, 2004). Both DCL2 and DCL4 play roles in antiviral defenses against (+) single stranded RNA viruses, whereas DCL3 is thought to play a minor role in defense against RNA viruses (Deleriset al, 2006, Garcia-Ruizet al, 2010, Quet al, 2008). A number of AGO proteins show direct antiviral activity and multiple VSRs have been shown to target AGO proteins (Pumplin and Voinnet 2013; Schuck et al 2013). Genetic analyses have reported a role for AGO1 in resistance to CMV and TCV (Morel et al 2002; Azevedo et al 2010) while AGO2 has been shown to play a role in resistance to CMV and TCV, as well as to *Potato virus X* (PVX), *Tomato bushy stunt virus* (TBSV) and *Turnip mosaic virus* (TuMV) (Azevedo et al 2010; Harvey et al 2011; Jaubert et al 2011; Scholthof et al 2011; Wang et al 2011; Carbonell et al 2012; Zhang et al 2012).

The phenomenon of recovery is typified by systemic virus infection with associated

symptoms, followed by a decrease and disappearance of symptoms in young leaves (MacDiarmid 2005). Recovered plants are subsequently resistant to further inoculations by the same virus, despite the continued presence of viral RNA in some cases (Jovel et al 2007). Recovery can also provide resistance against sequence-related viruses, a phenomenon known as cross-protection (Ratcliff et al 1999; Folimonova 2013). Recovery occurs in a number of plant-virus interactions, including *Tobacco rattle virus* (TRV) (Ratcliff et al 1997; Ratcliff et al 1999). Although traditionally defined by symptomology, in the latter case, the term recovery is used to describe a situation wherein TRV expressing GFP (TRV-GFP) accumulates in *N. benthamiana* with few symptoms except green fluorescence, followed by a loss of fluorescence and a dramatic decrease in virus abundance (Ratcliff et al 1999). Recovery is thought to be a consequence of RNA silencing as it can induce sequence specific gene silencing (Ratcliff et al 1999; Jovel et al 2007) and mutations in a viral VSR can result in viruses that undergo recovery and induce cross protection (Lin et al 2007). Likewise, the resistance of plants to VSR-defective viruses resembles recovery and this has been shown to be dependent on RNA silencing components (Deleris et al 2006; Azevedo et al 2010; Garcia-Ruiz et al 2010; Carbonell et al 2012). Furthermore, the NbAgo1 protein has been reported as being required for recovery to *Tomato ringspot virus* (ToRSV) in *N. benthamiana* (Ghoshal and Sanfacon 2014).

Mechanisms related to virus recovery are thought to be involved in virus-induced gene silencing (VIGS), a technique used to down regulate a host gene through the use of a recombinant virus carrying a fragment of the host gene of interest. Upon infection, vsiRNAs are produced from the host gene fragment that can in turn target the gene for degradation (Ratcliff et al 2001; Burch-Smith et al 2004). A small number of RNA silencing mutants have been tested, but only mutants in *HEN1* and *DCL2*/*DCL4* have been reported to be dramatically affected in VIGS, suggesting either redundancy or distinct mechanisms in VIGS, as compared to other RNA silencing pathways (Deleris et al 2006; Dunoyer et al 2007). Thus, although VIGS and virus recovery are related to other RNA silencing mechanisms, the genetic requirements for these phenomena have not been extensively studied. In particular, it is unclear if they employ the same AGO proteins that mediate other RNA silencing phenomena.

Likewise, little is known about the fate of viral RNAs upon recovery and we have investigated the possibility that this RNA silencing-related phenomenon might involve translational repression. RNA processing bodies (P-bodies) are cytoplasmic foci where

translationally repressed mRNAs accumulate and are eventually processed by decapping enzymes and exoribonucleases (Parker and Sheth 2007). In animals and yeast, mRNAs subjected to translational repression accumulate in PBs and increases in translation repression can result in an increase in the number of PBs in the cell (Balagopal and Parker 2009; Franks and Lykke-Andersen 2008). In plants, the major enzymatic components of PBs are well conserved (Weber et al 2008; Maldonado-Bonilla 2014). Several PB component mutants have enhanced RNA silencing phenotypes, which are thought to be due to an accumulation of "aberrant" RNAs, which subsequently become substrates for the RNA silencing machinery (Souret et al 2004; Gy et al 2007; Thran et al 2012).

We have used TRV to investigate the role of individual AGO proteins in VIGS and recovery using *Arabidopsis* mutants. Although *ago2-1* and *ago4-2* mutants were initially more susceptible to TRV, none of the ten single *ago* mutant lines were compromised in virus recovery whereas the *ago1-27* mutant was compromised for VIGS, suggesting that VIGS and recovery are mediated by different components of the RNA silencing machinery. At the same time, we find that TRV RNAs in recovered plants show reduced association with ribosomes, suggesting translational repression of viral RNAs. Consistent with this, plants expressing a PB marker showed increased numbers of PBs after recovery from TRV, but not upon infection with TCV, from which *Arabidopsis* does not recover. These results indicated a connection between virus recovery, VIGS and translational repression.

4.3 Materials and Methods

4.3.1 Plants and viruses

Arabidopsis thaliana wild-type (Col-0 and Ler) and the following previously described mutant lines were used (Table 4-1): *ago1-27* (Morel et al 2002), *ago2-1*, *ago3-2*, *ago6-3*, *ago8-1*, *ago10-2* (Takeda et al 2008), *ago5*, *ago7*, *ago9* (Katiyar-Agarwal et al 2007), *ago4-1* (Zilberman et al 2003), *ago4-2* (Agorio and Vera 2007), triple dicer mutant *dcl2-1/dcl3-1/dcl4-2* (Deleris et al 2006), *ago1/2*, *ago1/5, ago1/7, ago1/5/10* (Wang et al 2011), *its1* (Thran et al 2012). *Arabidopsis* wild type and mutant plants were grown from seed in soil (Agromix, Fafard) in a growth chamber at 23 °C for three weeks with 12 h day and 12 h night. Three weeks post-germination, seedlings were rub-inoculated with sap from *N. benthamiana* infected with either TRV-GFP (MacFarlane and Popovich, 2000) (Fig. 4-1) or TRV-PDS (Liu et al 2002) (Fig. 4-2). After TRV inoculation, plants were grown in a growth chamber at 19 °C as dictated by established protocols (Deng et al

2013), except where indicated otherwise. GFP was visualized by using a handheld UV lamp (BLAK RAY, UVP).

Table 4-1 The Arabidopsis mutants and its origin used in this study

***Arabidopsis* Mutants**	
Wild type	Col-0 , Ler
Single mutants	*ago1-27* (Morel et al, 2002) *ago2-1, ago3-2, ago6-3, ago8-1, ago10-2* (Takeda et al, 2008) *ago5,ago7, ago9* (Katiyar-Agarwal et al, 2007) *ago4-1(Ler)* (Zilberman et al, 2003) *ago4-2*(Col) (Agorio, 2007) *rdr1-1, rdr6-15* (Garcia-Ruiz et al, 2010) *its1* (Thran et al, 2012)
Double mutants	*ago1/2*，*ago1/5, ago1/7* (Wang et al, 2011) *rdr1/6* (Garcia-Ruiz et al, 2010)
Triple mutants	*ago1/2/7*，*ago1/2/10*，*ago1/5/10* (Wang et al, 2011) *dcl2-1/dcl3-1/dcl4-2* (Deleris et al, 2006)

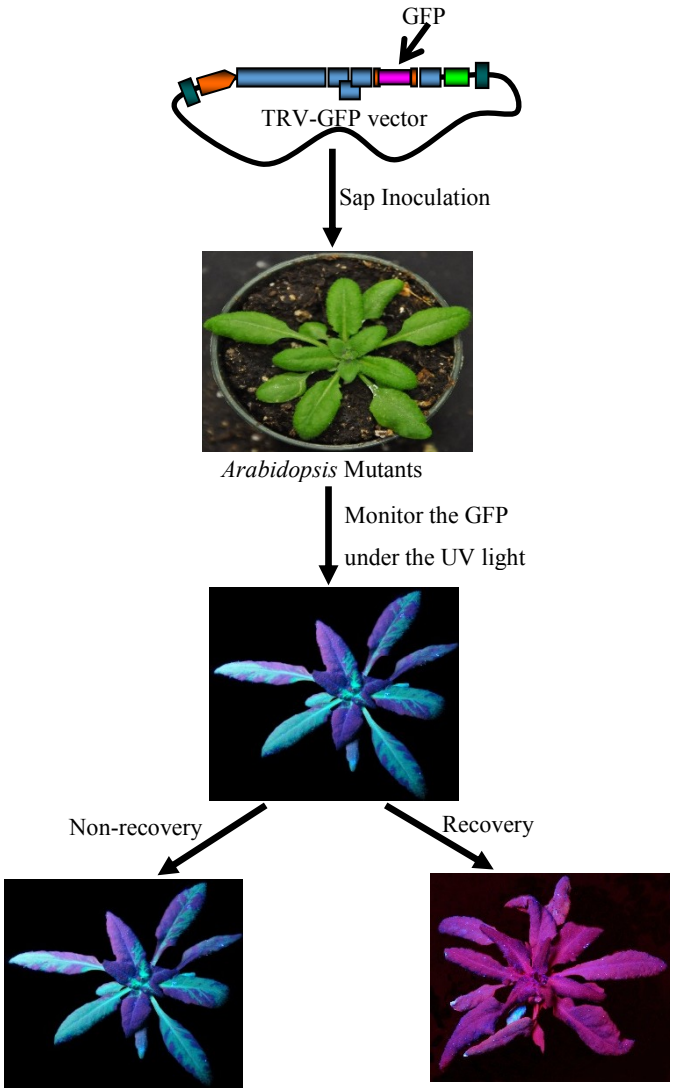

Fig. 4-1 Schematic representation of the various stages of recovery experiment
The candidate gene (*green fluorescent protein, GFP*) was cloned into the RNA2-based TRV vector under the control of a constitutive promoter. This was used to inoculate *N. benthamiana*, from which infectious sap was harvested. The infectious sap was then sap-inoculated on wild-type and mutants of *Arabidopsis thaliana*. Then, the GFP fluorescence was monitored under UV light through time course to see whether this fluorescence recovery or non-recovery

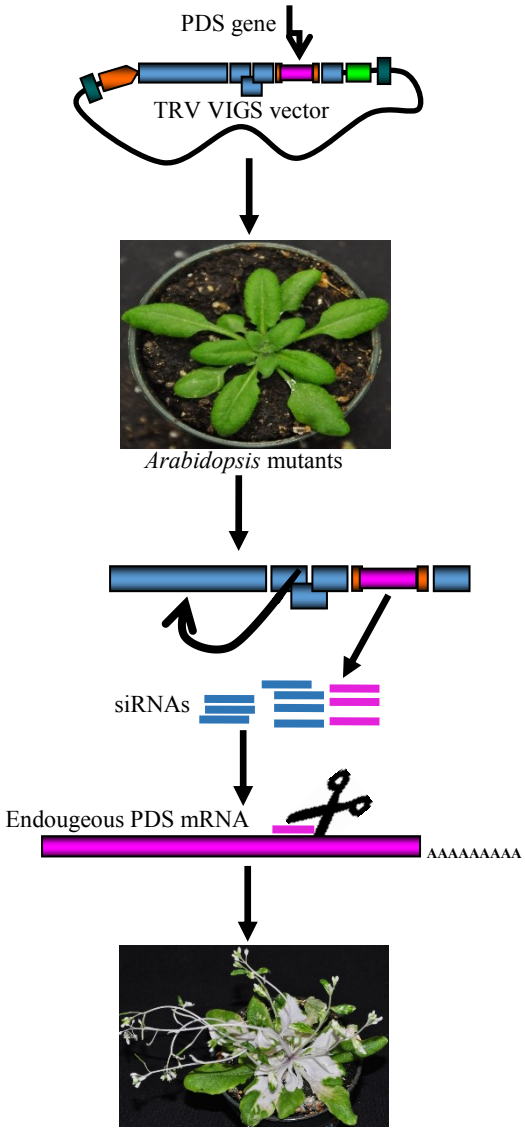

Fig. 4-2 Schematic representation of the various stages involved in VIGS with the TRV-PDS
The candidate gene (*phytoene desaturase, PDS*) was cloned into the RNA2-based TRV VIGS vector under the control of a constitutive promoter. This is used to inoculate *N. benthamiana*, from which infectious sap was harvested. The infectious sap was then sap-inoculated on wild-type and mutants of *Arabidopsis thaliana*. Then, through the RNA silencing mechanisms the host mRNA is degraded, leading to a photobleaching phenotype.

4.3.2 RNA extraction and northern blotting

Total RNA was extracted from pools of 6 to 8 plants using Trizol reagent as per the manufacturer's instructions (Invitrogen). 15-20 μg of total RNA was separated on a 1.2% (w/v) formaldehyde agarose gel by electrophoresis, and then transferred to a positively charged nylon membrane (Roche) and cross-linked with UV light (Spectro linker, XL-1000 UV Crosslinker). Pre-hybridization, hybridization (Roche, DIG Easy Hyb) and washing (Roche, DIG Wash and Block Buffer Set) were performed by following the manufacturer's instructions. DNA probes labeled with Dig-11-dUTP (Roche, PCR DIG

Probe Synthesis Kit) corresponding to the coat protein of TRV RNA2 or the GFP insert were PCR amplified using primer pairs CP-F/CP-R (forward primer: 5'-atgggagatatgtacgatgaatcatt-3' and reverse primer: 5'-ctagggattaggaggtatcggacctc-3') or GFP-F/GFP-R (forward primer: 5'-gtcagtggagagggtgaaggtg-3' and reverse primer: 5'-gtctgctagttgaacgcttccat-3') (Table 4-2, Fig. 4-3), and were used to detect TRV RNA2-PDS and TRV RNA2-GFP, respectively. Signals were revealed by CDP-Star ready-to-use (Roche). Signal intensities were quantified using Image J software.

Table 4-2 Primers used for making Northern blot probes to detect TRV

Primer names	Primer sequences (5'-3')	Gene	Fragment length	Reference
CP-F	ATGGGAGATATGTACGATGAATCATT	CP	615 bp	In this study
CP-R	CTAGGGATTAGGAGGTATCGGACCTC			
GFP-F	GTCAGTGGAGAGGGTGAAGGTG	GFP	454 bp	In this study
GFP-R	GTCTGCTAGTTGAACGCTTCCAT			

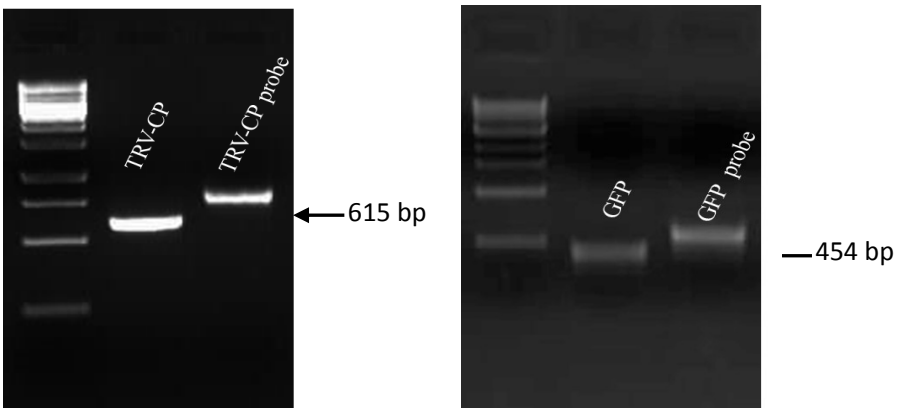

Fig. 4-3 1.2% agarose gel electrophoresis for detecting PRC labeling DNA probes that detects TRV viral Northern blot process (Table 4-2)

4.3.3 SDS-PAGE Western Blotting

The entire above ground portion of individual *Arabidopsis* plants were ground in liquid nitrogen and 50 mg of the ground powder was mixed with 50 µl 1.5x sample buffer (18 µM Tris-HCl pH 6.8, 7.5% glycerol, 0.6% SDS, 0.3 mg/ml Bromophenol blue, 5% β-mercaptoethanol [v/v]), and incubated at 95 °C for 5 min. Protein samples from total leaf tissue extracts were separated by SDS-PAGE on 10.5% resolving gels and transferred onto a polyvinylidenedifluoride membrane (BioRad), followed by incubations with the HRP conjugated GFP antiserum (Rockland Immunochemicals) and proteins were revealed by western blotting luminol reagent (Santa Cruz Biotechnology).

4.3.4 Polysome RNA isolation

Polysome extraction assays were performed as described previously (Mustroph et al 2009), with some minor modifications (Fig. 4-4). Briefly, tissues from the infiltrated leaf areas were ground to a fine powder in liquid nitrogen, resuspended in polysome extraction buffer (0.2M Tris-HCl, pH 9.0, 0.2 M KCl, 25 mM EGTA, 35 mM $MgCl_2$, 1% Detergent mix [1% (w/v) polyoxyethylene (23) lauryl ether (Brij-35), 1% (v/v) Triton X-100, 1% (v/v) octylphenyl-polyethylene glycol (Igepal CA630), 1% (v/v) polyoxyethylene sorbitan monolaurate 20], 1% deoxycholic acid sodium salt, 1% Polyoxyethlene (10) tridecyl ether, 5mM DTT, 1 x protease inhibitors, 50 μg/ml Cycloheximide, 50 μg/ml Chloramphenicol) and clarified by centrifugation at 14,000 rpm for 15 minutes at 4 °C. Extracts were overlaid on a 1.6 M sucrose cushion solution (0.4 M Tris-HCl, pH 9.0, 0.2 M KCl, 5mM EGTA, 35 mM $MgCl_2$, 1.7 M sucrose, 5 mM DDT, 50 μg/mL Cycloheximide, 50 μg/ml Chloramphenicol) and ultracentrifuged (Beckman SW70Ti) at 116 000g for 18 h at 4 ℃. RNA pellets were resuspended in resuspension buffer (0.2 M Tris-HCl, pH 9.0, 0.2M KCl, 25 mM EGTA, 35 mM $MgCl_2$, 5 mM DDT, 50 μg/mL Cycloheximide, 50 μg/ml Chloramphenicol). Aliquots from the input and from the pellet fractions were subsequently isolated with an equal volume of 8 M guanidine HCl and three volumes of ethanol, and quantified. For polysome profiles, RNA pellets were overlaid on sucrose gradients (4.5 mL linear sucrose gradient of 15%–60% sucrose [w/v], supplemented with 10 mM Tris-HCl at pH 7.5, 140 mM KCl, 1.5 mM MgCl2, 100 μg/mL Chloramphenicol and 100 μg/mL Cycloheximide) and ultracentrifuged (Beckman SW55Ti) at 50,000 rpm for 2 h at 4 ℃. Seventeen fractions (300 μl/fraction) were collected and an equal volume of 8 M guanidine HCl and three volumes of ethanol were added to each fraction to precipitate RNA.

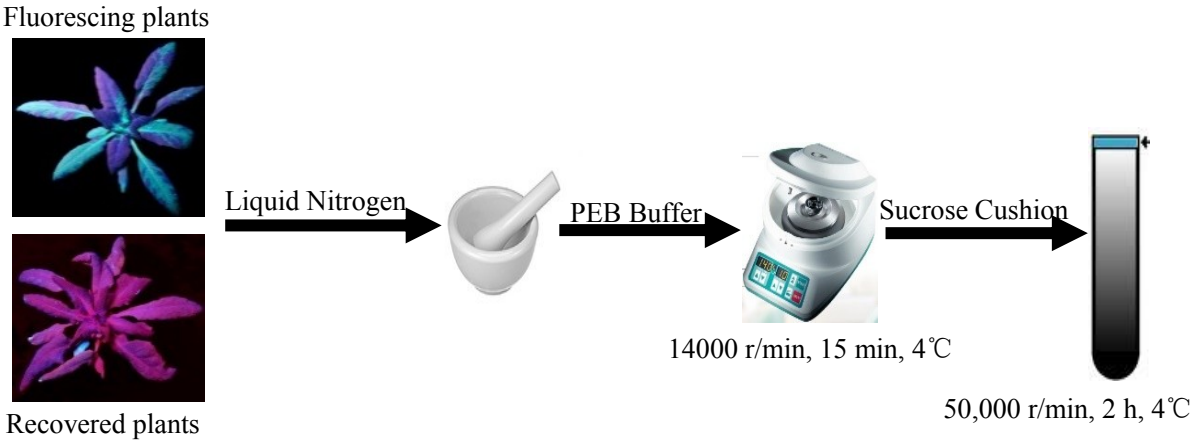

Fig. 4-4 Schematic representation of the protocol allowing isolation of polysome-bound mRNAs from *Arabidopsis* samples

1-The treated plants are quickly frozen under liquid nitrogen and then are grounded to powder in a mortar under liquid nitrogen; 2-The powder is transferred to a micro-centrifuge tube and lysed with PEB buffer; 3-14000 rpm, 15min, 4 ℃; 4-The supernatant is loaded onto a sucrose cushion, 50,000 rpm 2 h, 4℃; 5-Prepare RNA by precipitation with ethanol

4.3.5 Microscopy and quantification

Confocal laser scanning microscopy was performed on a FV300 imaging system (Olympus). YFP was excited using a 488 nm argon laser and emission was detected using a 510-530 band-pass filter. Granules were counted from images of equal areas (244 x 244 μm) from each treatment using Cell-Profiler software (Jones et al 2008). In this study, each image represents a Z stack of 0.5 μm. Representative images are shown from experiments repeated at least three times.

4.4 Results

4.4.1 Recovery from TRV in Arabidopsis RNA silencing mutants

TRV is widely used as a VIGS vector in a variety of plant species (MacFarlane 2010) and is one of the only VIGS vectors based on an RNA virus to function in Arabidopsis (Deng et al 2013). We have previously used TRV to silence AGO-encoding genes in *N. benthamiana* (Bhattacharjee et al 2009; Scholthof et al 2011). The latter experiments may seem paradoxical if AGO proteins are required for VIGS and so we investigated which AGO proteins are required for viral recovery and VIGS by TRV in *Arabidopsis*. In certain cases, virus recovery is characterized by a continued presence of viral RNA but a dramatic decrease in viral protein translation (Ghoshal and Sanfacon 2014; Jovel et al 2007). TRV engineered to express GFP (TRV-GFP) (MacFarlane and Popovich 2000) has previously been used as a read out for recovery in *N. benthamiana* (Ratcliff et al 1999). In TRV-GFP infected *Arabidopsis* Col-0 plants, GFP fluorescence was observed on the

inoculated leaves 2-3 days post-inoculation (dpi, Fig. 4-5 A). At 5 dpi, GFP fluorescence appeared on the systemic leaves above the inoculated leaf (Fig. 4-5 A). However, at 8 dpi, GFP fluorescence was no longer apparent on either the infected or the newly emerging leaves (Fig. 4-5 A). Likewise immun-blotting showed reduced levels of GFP protein over time, indicating that the plant had recovered from TRV-GFP (Fig. 4-5 B). Northern blotting indicated a peak of viral RNA accumulation at 5 dpi with decreased viral RNA levels thereafter (Fig. 4-5 C).

To explore the role of RNA silencing components in TRV recovery we first infected a "triple dicer" (TD; *dcl2/dcl3/dcl4*) mutant line. The TD mutant has been reported to be dramatically compromised in its ability to generate vsiRNAs and to be hyper susceptible to viruses (Deleris et al 2006; Jaubert et al 2011). Visibly, TD plants showed a faster and more extensive accumulation of GFP fluorescence compared to wt plants (Fig. 4-5 A). Likewise, TD plants showed increased levels of viral RNA accumulation, accumulated GFP protein for a longer time period relative to WT plants, and showed viral symptoms in the form stunted growth and leaf curling (Fig. 4-5 D). Nonetheless, TD plants still recovered to a certain extent in that GFP fluorescence still disappeared at eleven dpi and GFP protein and viral RNA decreased over time, albeit a later time points than WT (Fig. 4-5 A, B, C). Thus, although the TD mutant can eventually down regulate TRV-GFP expression, the virus appears to accumulate sufficiently (or long enough) to induce symptoms. We next infected WT and *AGO* mutant lines. These included the hypomorphic *ago1-27* allele, as *ago1* null mutants are lethal (Morel et al 2002), as well as T-DNA insertional null alleles for the *AGO2* through *AGO10* genes. Upon infection with TRV-GFP, GFP was detectable visually and by immun-blotting at 3-5 dpi in all genotypes (Fig. 4-7 D). Nonetheless, all ten *ago* mutant lines still underwent recovery from TRV-GFP in that GFP fluorescence subsided 8-11 days post infection (Table 5-3, Fig. 4-7 A, B, C).

The fact that all mutant lines tested showed a loss of GFP fluorescence could be caused by properties inherent to the replication/expression strategies of TRV rather than by RNA silencing. To test whether TRV has the intrinsic ability to undergo sustained GFP expression, we co-infected WT plants with TRV-GFP and wt TCV, which encodes a strong VSR, P38 (Qu et al 2003). Plants infected with both TRV-GFP and TCV showed dramatically increased GFP fluorescence after eight days, compared to TRV-GFP alone (Fig. 4-6). GFP fluorescence was observable up to 17 days, at which point the infected plants died (data not shown). Although we cannot rule out the possibility that TCV causes

this effect via other mechanisms, the simplest interpretation of this result is that TRV can undergo sustained expression in *Arabidopsis* if RNA silencing mechanisms are fully inhibited by a more virulent virus.

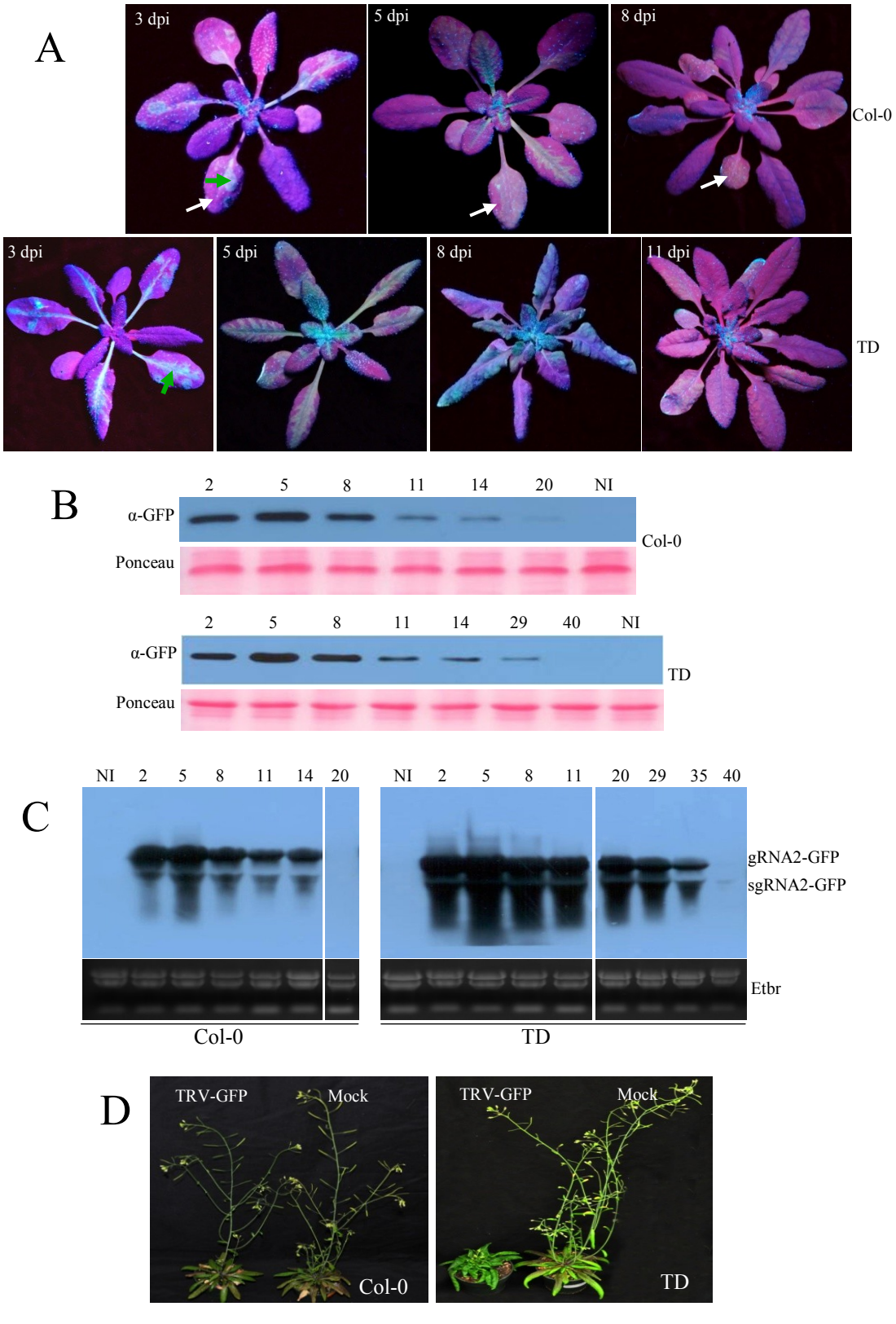

Continued

Fig. 4-5 TRV-GFP as a model for virus recovery in *Arabidopsis*

A, Several leaves of wild-type (Col-0; upper panels) and Triple dicer mutant (TD; lower panels) *Arabidopsis* were infected with TRV-GFP and representative leaves are indicated with white arrows. GFP fluorescence (representative fluorescent areas indicated by green arrows) was photographed under UV illumination at 3, 5, 8 and 11 days post inoculation (dpi). B, Protein extracts from non-infected (NI) and TRV-GFP-infected Col-0 (upper panel) and TD mutant plants (lower panel), sampled at the indicated time points, were subjected to anti-GFP immune-blotting. Ponceau staining is shown to demonstrate equal loading. Each lane corresponds to a pool of 5-6 inoculated plants. C, Total RNA was extracted from plants infected with TRV-GFP-infected Col-0 (left panel) or TD mutant plants (right panel) at the time points indicated and subjected to northern blotting with an anti-GFP probe. TRV RNA2 genomic (g) and subgenomic (sg) are indicated. Ethidium bromide stained RNA (prior to transfer) is shown as a loading control. D, Symptoms in non-infected (Mock) and TRV-GFP infected *Arabidopsis*. Photographs were taken three weeks after infection

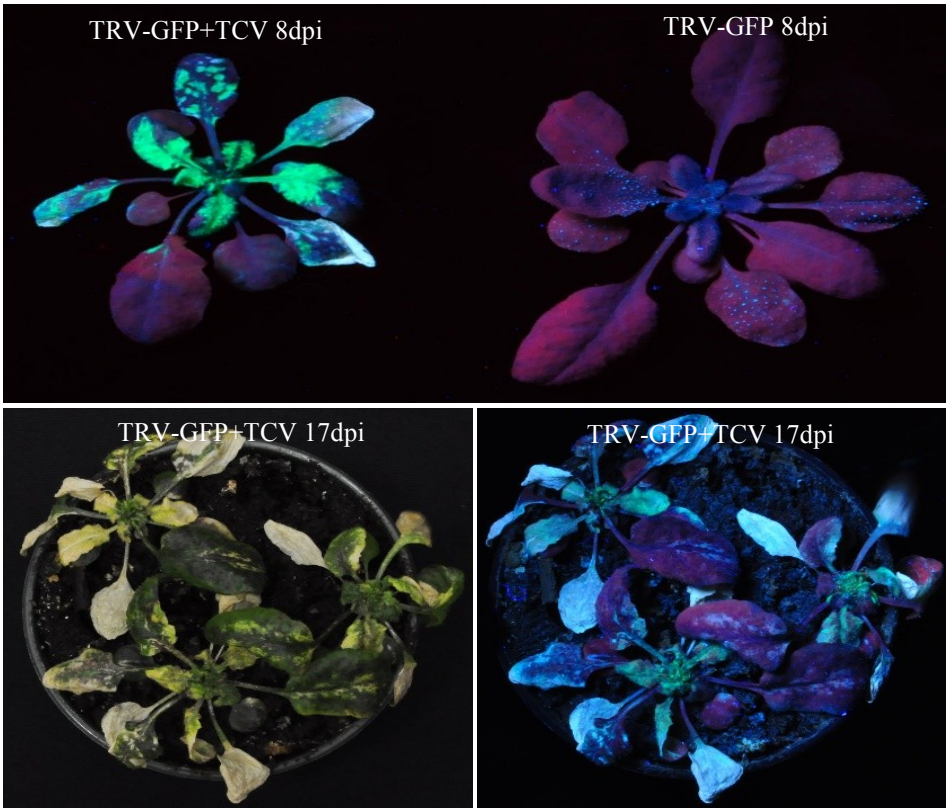

Fig. 4-6 Wild-type Arabidopsis were co-infected with TRV-GFP and TCV

GFP fluorescence was photographed under UV illumination at 8 dpi and 17 dpi. All experiments were repeated 3 times and representative results are shown

A

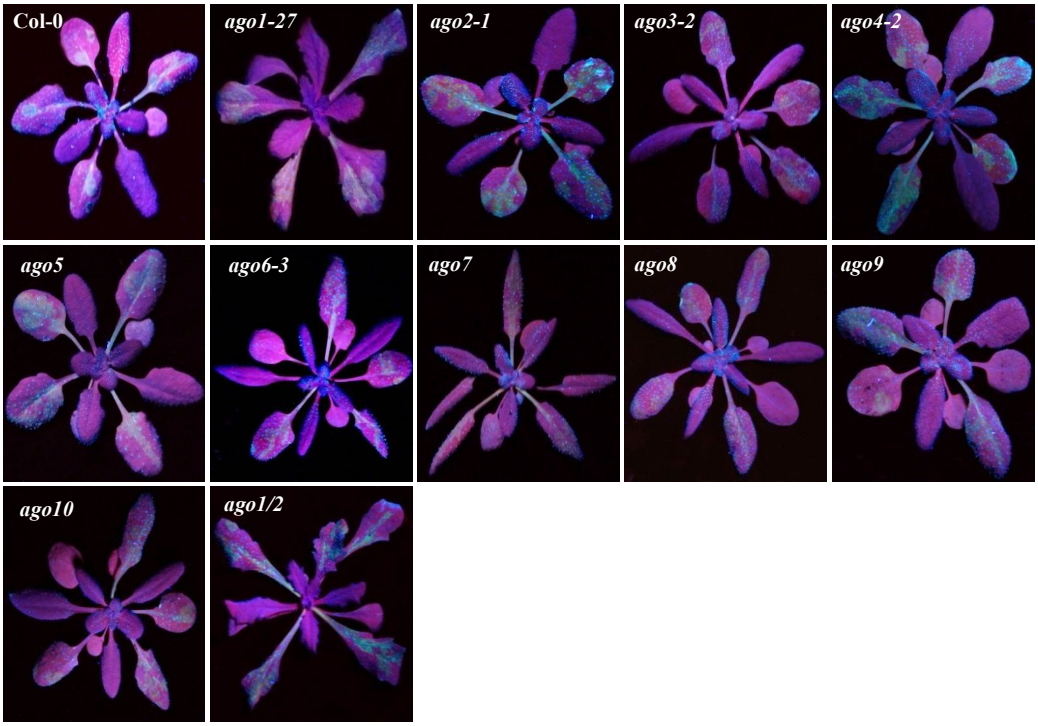
Col-0
ago1-27
ago2-1
ago3-2
ago4-2
ago5
ago6-3
ago7
ago8
ago9
ago10
ago1/2

B

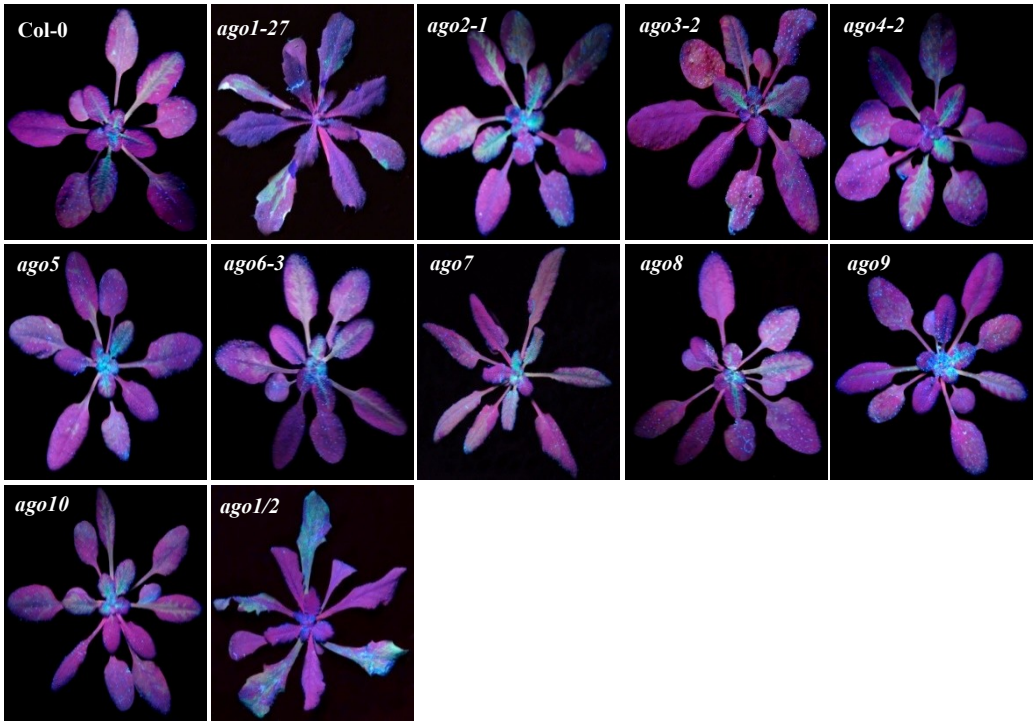
Col-0
ago1-27
ago2-1
ago3-2
ago4-2
ago5
ago6-3
ago7
ago8
ago9
ago10
ago1/2

C

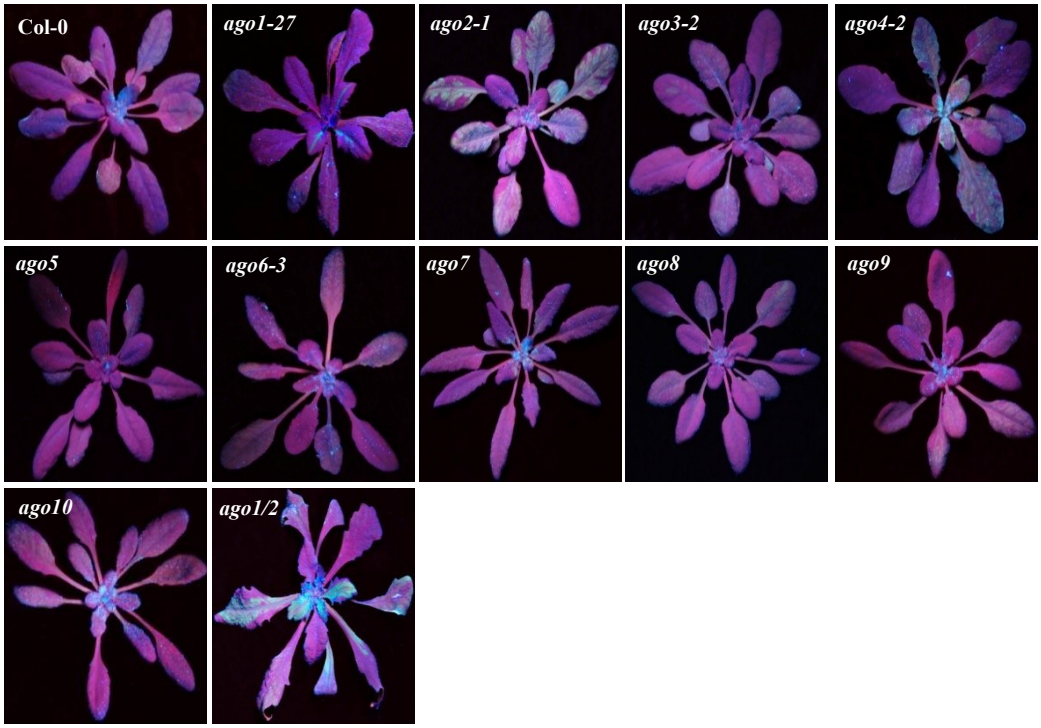

D

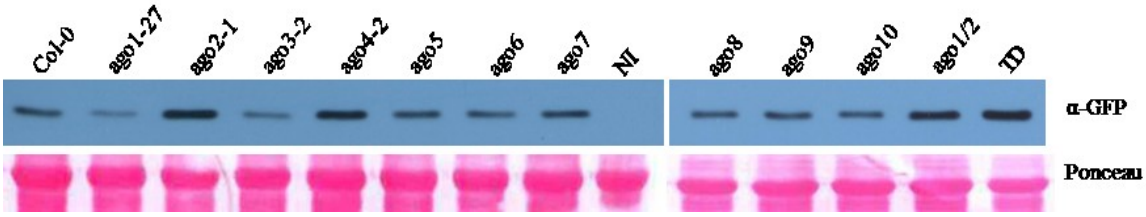

Fig. 4-7 TRV-GFP susceptibility and recovery in *Arabidopsis* RNA silencing mutants

A-D, The indicated mutant *Arabidopsis* lines were infected with TRV-GFP by rub inoculating four leaves per plant. GFP fluorescence was photographed under UV illumination at 3, 5, 8 and 11 days post inoculation (dpi), respectively. E, Total protein extracts were prepared from infected plants at 5 dpi and subjected to anti-GFP immunoblotting. Ponceau staining is shown as a loading control. Each lane corresponds to a pool of the 5-6 infected *Arabidopsis* plants. The results shown are representative of five separate experiments in which at least ten plants were tested for each mutant lines

Table 4-3 Summary of phenotypes observed in mutant lines tested in this study

Mutants	GFP intensity[1)]	PDS VIGS intensity[2)]	TRV-GFP Recovery
Col-0	++	++	8 dpi
ago2–1	+++	++	10 dpi
ago3-2	++	++	8 dpi
ago4-2	+++	++	10 dpi
ago5	++	++	8 dpi
ago6-3	++	++	8 dpi
ago7	++	++	8 dpi
ago8-1	++	++	8 dpi
ago9	++	++	8 dpi
ago10	++	++	8 dpi
its1	++	++++	8 dpi
dcl2-1/dcl3-1/dcl4-2	+++++	+/-[3)]	11dpi
Ler	++	+	8 dpi
ago4-1 (Ler)	+++	+	10 dpi
ago1–27	+	+	8 dpi
ago1/5/10	+	+	8 dpi
ago1/7	+	+	8 dpi
ago1/2	++++	+	11 dpi
ago1/2/7	++++	+	11 dpi
ago1/2/10	++++	+	11 dpi

1) GFP intensity is based on visual assessment at 5 dpi of at least thirty plants of a given genotype using Col-0 as a standard (++). Examples of varying degrees of fluorescence (+, *ago1-27*; +++, *ago2-1*; +++++, TD) are shown in Figure 5-6 A-C;

2) VIGS intensity is based on visual assessment of the relative extent (portion of entire plant) of photobleaching at 13 dpi of at least thirty plants of a given genotype using Col-0 as a standard (++). Examples of varying degrees of VIGS intensity (+/-, TD; +, *ago1-27*; ++++, *its1*) are shown in Figures 5-9 A-B;

3) At 19°C only.

4.4.2 AGO2 and AGO4 mutants show increased TRV susceptibility

Upon infection with TRV-GFP, we observed increased GFP intensity on both the inoculated and systemic leaves of *ago2-1* and *ago4-2* mutant plants compared to Col-0 (Fig. 4-7 A, B, C). This was also confirmed by anti-GFP immune-blotting (Fig. 4-7 D) and northern blotting (Fig. 4-8 C, D). The role of AGO2 in virus defense is well established, but to confirm the role of AGO4 in TRV susceptibility, we tested an additional *ago4* mutant allele. Upon infection of the *ago4-1* mutant, present in the Landsberg (ler) background, and wild type ler plants, we observed the same result as with the *ago4-2* allele in the Col-0 background (Fig. 4-8 A). Despite these initial increased GFP levels, however, both *ago2* and *ago4* mutant plants still recovered, eventually losing GFP expression (Table 5-3, Fig. 4-7 A, B, C). At the same time, *ago1-27* plants consistently showed less GFP and viral RNA accumulation and systemic movement of TRV-GFP proceeded more slowly in this mutant (Fig. 4-7 A, Fig. 4-11). We also inoculated a double mutant, possessing the *ago1-27* allele and an *ago2* mutant allele (*ago1/ago2*), with TRV-GFP. In this mutant, we observed increased GFP, visually and by immune-blotting, similar to that seen in the *ago2* single mutant (Fig. 4-7 A, B, C). However, virus infection progressed more slowly in this mutant, as seen in *ago1-27* plants, with the virus moving into systemic leaves at 6-8 dpi, compared to 5 dpi for WT plants (Fig. 4-7 A, B, C).

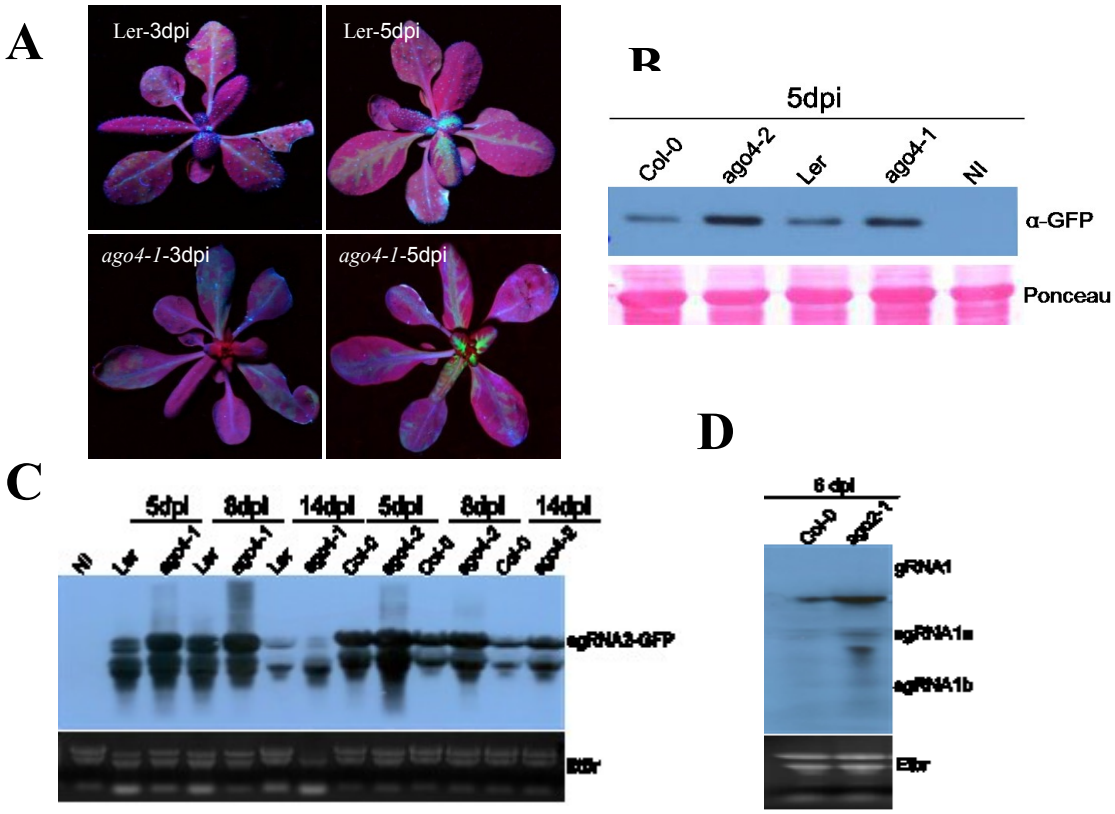

Fig. 4-8 AGO2 and AGO4 play anti-viral roles against TRV-GFP

A, Wild-type Ler and *ago4-1* mutant *Arabidopsis* plants were infected with TRV-GFP and GFP fluorescence was monitored visually daily for 11 days. Plants were photographed under UV illumination at 3 and 5 days post inoculation (dpi), as indicated. Increased GFP fluorescence was observed in the *ago4-1* mutant at all time points, as compared to Col-0. B, Protein extracts from non-infected (NI) or TRV-GFP infected Ler and *ago4-1* mutant plants at 5 dpi were subjected to anti-GFP immune-blotting. Ponceau staining is shown to demonstrate equal loading. Each lane corresponds to a pool of 5-6 inoculated plants; C, Total RNA was extracted from NI plants as well as from Col-0 and *ago4-2* plants infected with TRV-GFP at 5 dpi and subjected to northern blotting with an anti-GFP probe. Ethidium bromide stained RNA (prior to transfer) is shown as a loading control (EtBr). Images are representative of experiments biologically repeated at least three times; D, Total RNA was extracted from Col-0 and *ago2* plants infected with TRV-GFP at 6 dpi and subjected to northern blotting with an anti-GFP probe. Ethidium bromide stained RNA (prior to transfer) is shown as a loading control

4.4.3 TRV VIGS in *Arabidopsis* RNA silencing mutants

Virus recovery differs from VIGS in that the former targets viral RNAs, whereas the latter is due to the targeting of endogenous mRNAs by vsiRNAs. To determine if these mechanisms might use different components, we infected the same mutant lines with TRV carrying an insert from the *Arabidopsis Phytoene Desaturase* (*PDS*) gene (TRV-PDS) (Liu et al 2002). Consistent with the results observed with TRV-GFP, *ago2* and *ago4* mutant plants showed increased levels of TRV-PDS viral RNAs, although this was not accompanied by an altered VIGS phenotype (Fig. 4-9, Table 5-3). Indeed, with the exception of *ago1-27*, all single *ago* mutant lines showed similar VIGS phenotypes, as assessed visually by the intensity and extent of photobleaching (Fig. 4-9A-B). VIGS in *ago1-27* and in several double and triple mutants with the *ago1-27 allele* (*ago1/2, ago1/ago5/ago10, ago1/ago7, ago1/ago5*) (Fig. 4-10A) was compromised, with greatly reduced photobleaching, which was restricted to areas around primary veins (Fig. 4-9 A-B, Fig. 4-10A). This decrease in VIGS efficiency was similar to, but not as severe, as in the TD mutant (Table 5-3), in which VIGS was has been previously been reported to be severely compromised (Deleris et al 2006). Surprisingly, whereas TRV-GFP showed decreased accumulation of viral RNA in the *ago1-27* mutant (Fig. 4-11), we consistently observed an increase in TRV-PDS RNA accumulation in this mutant compared to the wild type (Fig. 3B). At the same time, viral TRV-PDS RNA levels were even higher in the *ago1/2* mutant (Fig. 4-10B). These observations suggest independent functions of AGO1 and AGO2 in defense against TRV-PDS. They also suggest differences in the mechanisms that inhibit viral gene expression (recovery) versus those that regulate viral RNA accumulation and the targeting of endogenous genes for silencing.

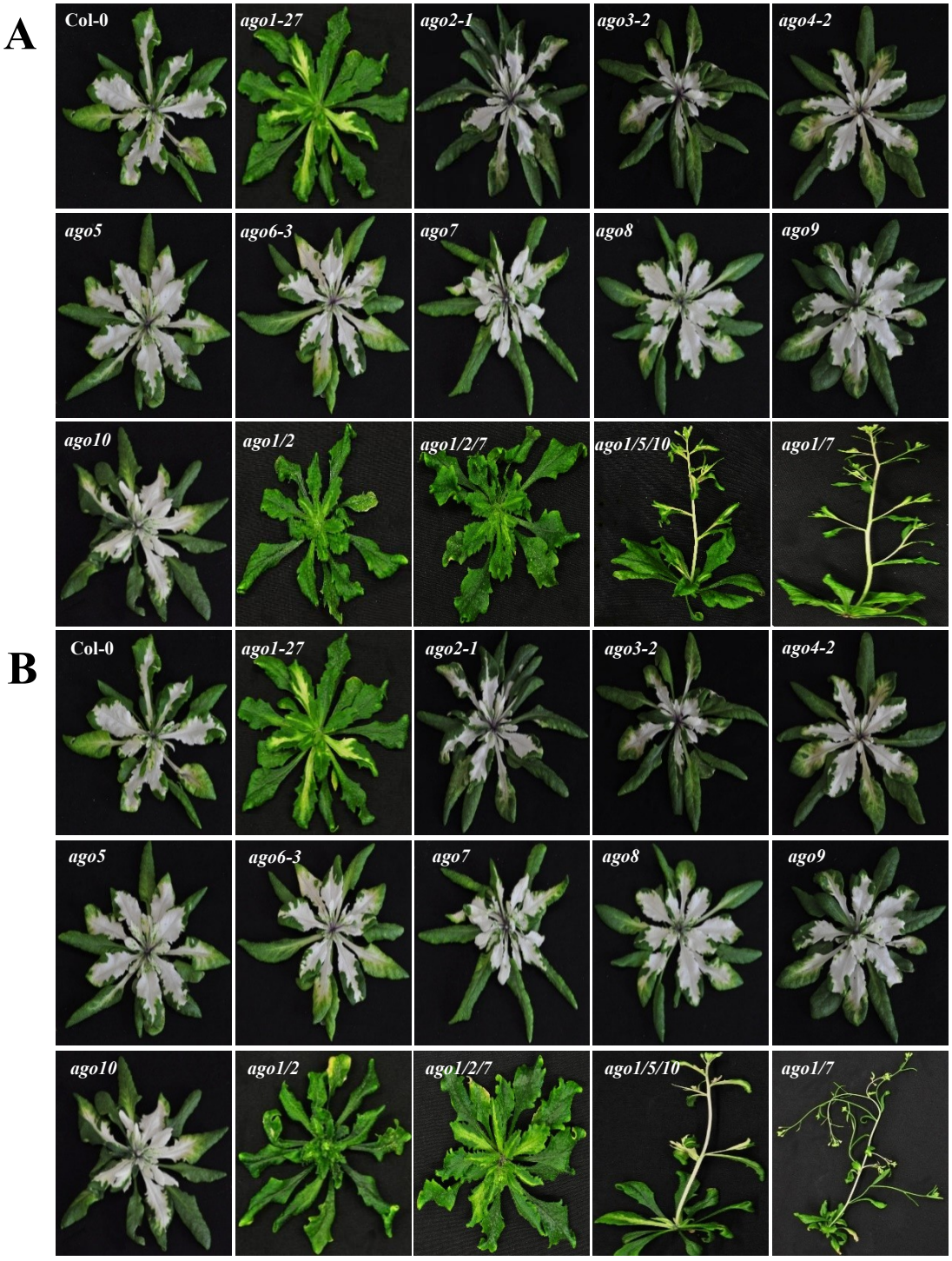
A
Col-0
ago1-27
ago2-1
ago3-2
ago4-2
ago5
ago6-3
ago7
ago8
ago9
ago10
ago1/2
ago1/2/7
ago1/5/10
ago1/7
B
Col-0
ago1-27
ago2-1
ago3-2
ago4-2
ago5
ago6-3
ago7
ago8
ago9
ago10
ago1/2
ago1/2/7
ago1/5/10
ago1/7

Continued

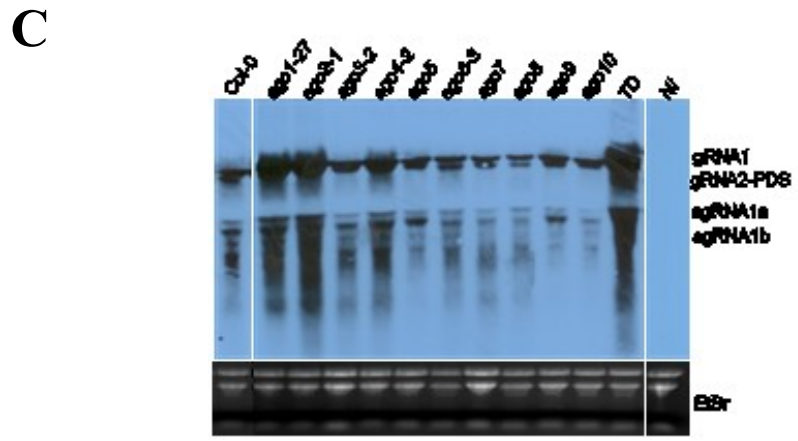

Fig. 4-9 AGO1 is required for optimal VIGS by TRV-PDS

A-B, The indicated mutant *Arabidopsis* lines were infected with TRV-PDS and photographed 13, 17 days post inoculation (dpi), respectively. C, Total RNA was extracted from plants infected with TRV-PDS at 17 dpi and subjected to northern blotting with an anti-TRV *CP* probe. TRV genomic (g) and subgenomic (sg) RNAs are indicated. Ethidium bromide stained RNA (prior to transfer) is shown as a loading control. Each lane corresponds to a pool of the 5-6 inoculated *Arabidopsis* plants. Images have been cropped from a larger gel for representation purpose, but originate from the same experiment and exposure times

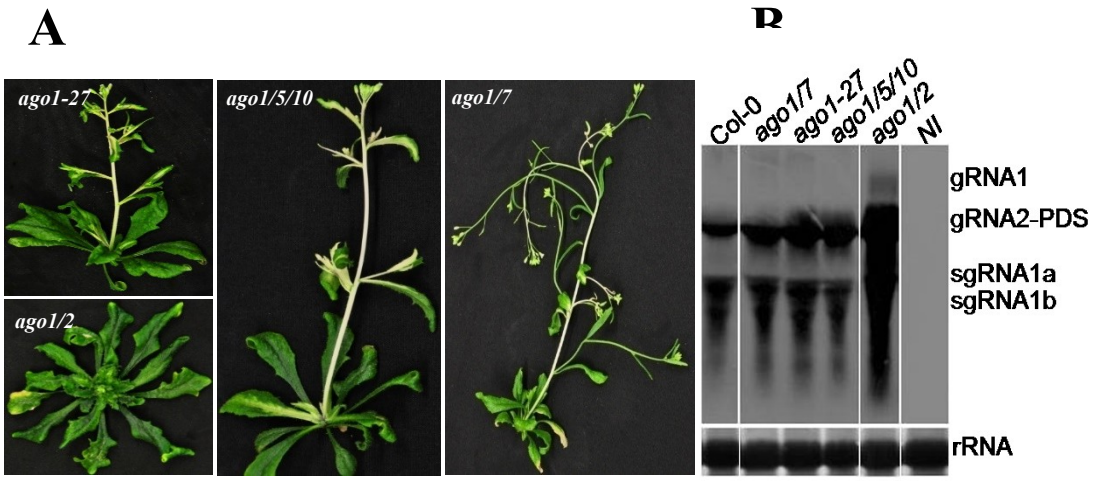

Fig. 4-10 VIGS phenotypes in *ago1* and compound mutants

A, The indicated mutant *Arabidopsis* lines were infected with TRV-PDS and photographed 17 days post inoculation (dpi). B, Total RNA was extracted from plants infected with TRV-PDS at 11 dpi and subjected to northern blotting with an anti-TRV CP probe. Each lane corresponds to the pool of the 5-6 inoculated *Arabidopsis* plants. Methylene Blue stained RNA (after transfer) is shown as a loading control. Images have been cropped from a larger gel for representation purpose, but originate from the same experiment and exposure times. Images are representative of experiments biologically repeated at least three times

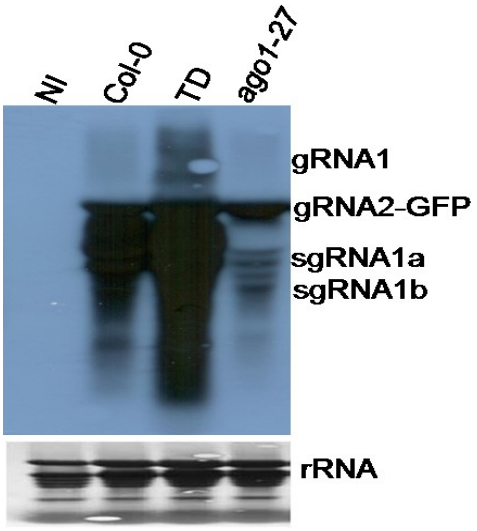

Fig. 4-11 Reduced TRV-GFP viral RNA in the *ago1-27* mutant
Total RNA was extracted from uninfected WT plants and from plants of the indicated genotypes infected with TRV-GFP at 13 dpi and subjected to northern blotting with an anti-TRV CP probe. Each lane corresponds to the pool of the 5-6 inoculated Arabidopsis plants. Methylene Blue stained RNA (after transfer) is shown as a loading control. Images are representative of experiments biologically repeated at least three times

4.4.4 VIGS intensity of *dcl2/dcl3/dcl4* plants is temperature dependent

Previous studies have shown that environmental conditions such as elevated temperature can enhance silencing efficiency against RNA viruses, often resulting in decreased symptom development and/or enhanced recovery (Szittya et al 2003; Qu et al 2005; Velázquez et al 2010; Zhang et al 2012; Ghoshal and Sanfacon 2014). As the TD and *ago1-27* mutants showed reduced VIGS intensity in the experiments outlined above (at 19 °C), we repeated TRV-PDS infections at 19 °C and 26 °C. As shown in Figure 5-12, growing infected plants at 26 °C resulted in a significantly increased photobleaching in TD mutant plants compared to plants grown at 19 °C. The *ago1-27* showed a slight increase in VIGS efficiency, but not to the same extent as the TD mutant at 26 °C (Fig. 4-12). These results further indicate that AGO1 is a limiting factor in silencing endogenous genes by VIGS and suggest that the Dicer protein remaining in the TD mutant, DCL1, can function in VIGS under certain circumstances.

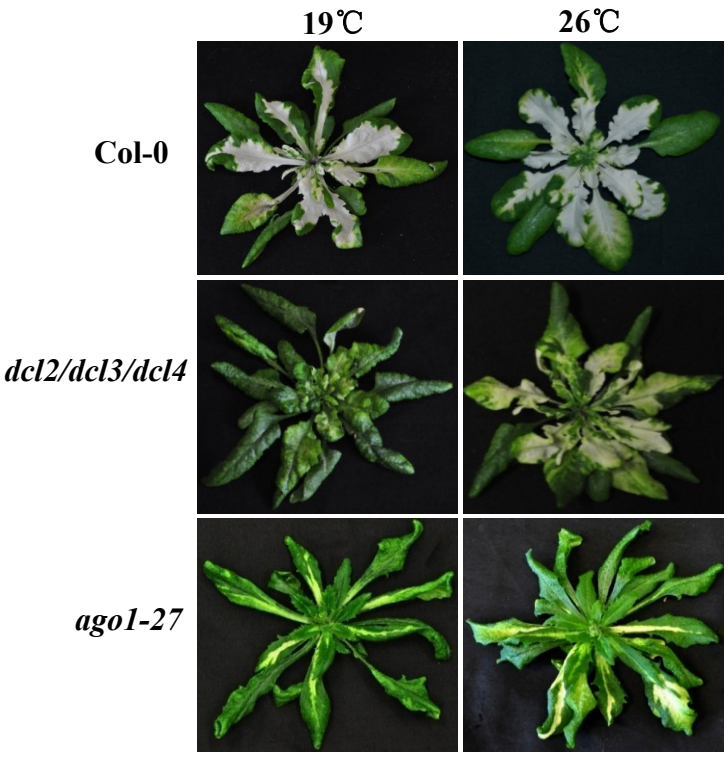

Fig. 4-12 TRV-PDS VIGS in the triple DICER mutant is temperature-dependent
The indicated mutant *Arabidopsis* lines plants were infected with TRV-PDS by rub inoculation. After infection, plants were grown in growth chambers where the temperature was 19℃ or 26℃, as indicated. Photographs were taken 17 days after infection. Shown are representative images of results obtained consistently from experiments that were repeated at least three independent times, including at least ten plants for each genotype and for each treatment

4.4.5 TRV recovery involves translational repression and PB formation

Plants that have recently recovered from TRV-GFP infection contain significant levels of viral RNA (Fig. 4-5C), begging the question of why these RNAs do not produce greater amounts of GFP protein. A recent report suggests that recovery involves the repression of translation of viral proteins (Ghoshal and Sanfacon 2014). To test this possibility in our experimental system we analyzed the association of TRV-GFP transcripts with actively translating ribosomes. We performed polysome profiling by sucrose density gradient fractionation on plants infected with TRV-GFP showing green fluorescence (5 dpi) and recovered plants (8 dpi). As seen, in Figure 5A, total polysome profiles did not differ between uninfected, fluorescing and recovered plants, indicating that recovery is not associated with a global repression of translation (Fig. 4-13A). Polysome profiling protocols for plant ribosomes include a ribosome pelleting step in which extracts are passed through a 1.6 M sucrose cushion to pellet all ribosomes prior to separation on a sucrose gradient (Mustroph et al 2009). Initial attempts at polysome profiling of TRV RNAs however were hampered by low amounts of RNA in the

ribosome pellets from recovered plant samples. As shown in figure 5-13B, northern blotting showed a mild reduction in total RNA in recovered versus non-recovered plants. However, much less viral RNA was present in the ribosome pellets of recovered plants. In the northern blots shown in Figure 5-13B, which is a representative result from three biological repetitions, we observed that in non-recovered plants the ratio of signal in total versus ribosome pellet RNAs was 1.4:1, whereas in recovered plants the ratio was 3.1:1. Thus, when compared to total viral RNA, TRV-GFP RNAs were reduced more than two-fold in the ribosomal pellet in recovered plants compared to non-recovered plants. These results indicate that after recovery, a significant proportion of TRV-GFP RNAs do not associate with ribosomes, suggesting that their translation may be inhibited.

RNAs subjected to translational repression often accumulate in PBs prior to degradation (Maldonado-Bonilla 2014). The decapping protein DCP1 is a well-established marker for PBs in *Arabidopsis* (Xu et al 2006; Weber et al 2008; Xu and Chua 2009). We investigated the role of PBs in virus recovery using transgenic *Arabidopsis* plants expressing DCP1 fused to YFP (YFP-DCP1) from the *DCP1* promoter (Merret et al 2013). Plants were infected with TRV (with no insert) or with TCV (from which *Arabidopsis* does not recover) on day 0, followed by infection of a second batch of plants of the same age four days later. PBs were then visualized eight days later as, based on the results found with TRV-GFP (Fig. 4-5A-B), the first batch of infected plants would have recovered from TRV, whereas the second batch would not. PBs, as indicated by foci of YFP-DCP1, were observed by confocal microscopy in inoculated leaves and the number of PBs in a fixed area (244 x 244 μm) were counted. Uninfected plants showed very few PBs and we observed no significant difference in PB numbers in plants infected with TRV for four days, or in plants infected with TCV for four or eight days, as compared to uninfected plants (Fig. 4-14). However, we observed a dramatic increase in the average number of PBs in TRV recovered plants (eight days infected), suggesting that viral RNAs in recovered plants contribute to an increase in PB activity, likely due to their translational repression (Fig. 4-13).

To further investigate the role of PB components in virus recovery/VIGS, we infected the *Arabidopsis increased transgene silencing* (*its1*) mutant (Thran et al 2012) with TRV-PDS and TRV-GFP. Most mutants in genes encoding components of the decapping complex have severe or lethal phenotypes (Maldonado-Bonilla 2014). However, the *its1* phenotype is caused by a hypomorphic mutation in *DECAPPING 2* (*DCP2*) which encodes for the catalytic subunit of the decapping complex found in PBs (Xu et al 2006).

We observed an increase in the time of onset, intensity and the extent of TRV-PDS VIGS in the *its1* mutant (Fig. 4-15A). In contrast, the timing and extent of infection by TRV-GFP, as well as recovery, was not noticeably different from WT except for a slight increase in GFP protein accumulation (Fig. 4-15B-C). However, the *its1* mutant consistently accumulated much higher levels of TRV-GFP and TRV-PDS RNA compared to Col-0 (Fig. 4-15C-D).

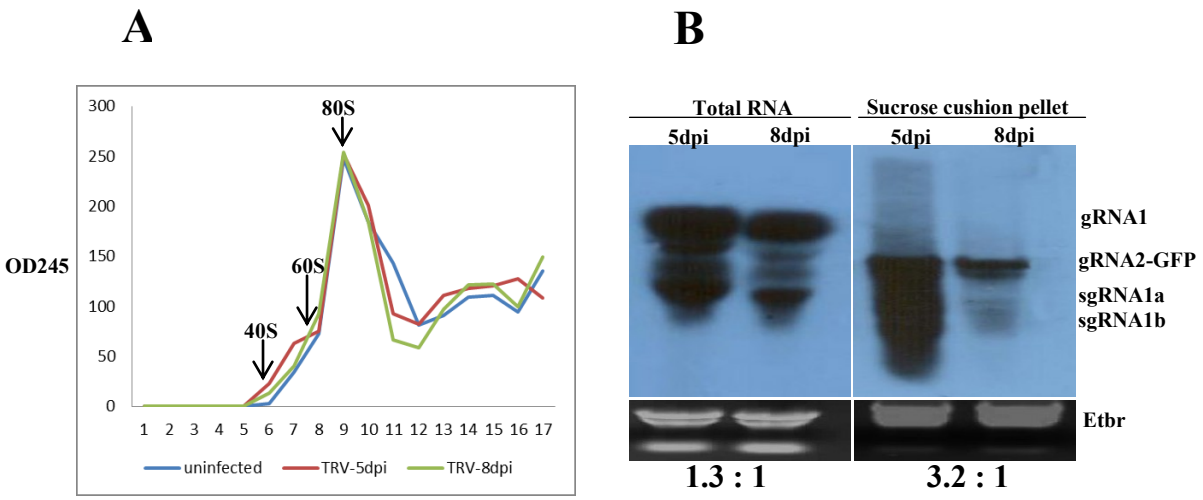

Fig. 4-13 Reduction in ribosome association of TRV RNAs after recovery

A, Typical sucrose gradient (15-60%) absorbance (245nm) profiles of ribosome complexes obtained from TRV-GFP uninfected Col-0 plants or plants infected with TRV-GFP for 5 (5 dpi) or 8 days (8 dpi). Positions of peaks corresponding to 40S ribosomal subunits, 60S ribosomal subunits and 80S monosomes are indicated (arrowheads). B, Total RNA was extracted from plants infected with TRV-GFP for 5 or 8 days. RNA was subjected to either Trizol extraction (total RNA) or to ribosomal pelleting (pellet) by ultracentrifugation through a sucrose cushion, followed by RNA extraction. RNAs were then subjected to northern blotting using a probe corresponding to the CP gene of TRV. Genomic and subgenomic RNAs are indicated and ethidium bromide stained RNA (prior to transfer) is shown as a loading control. Images shown are representative results from at least three biological repeats

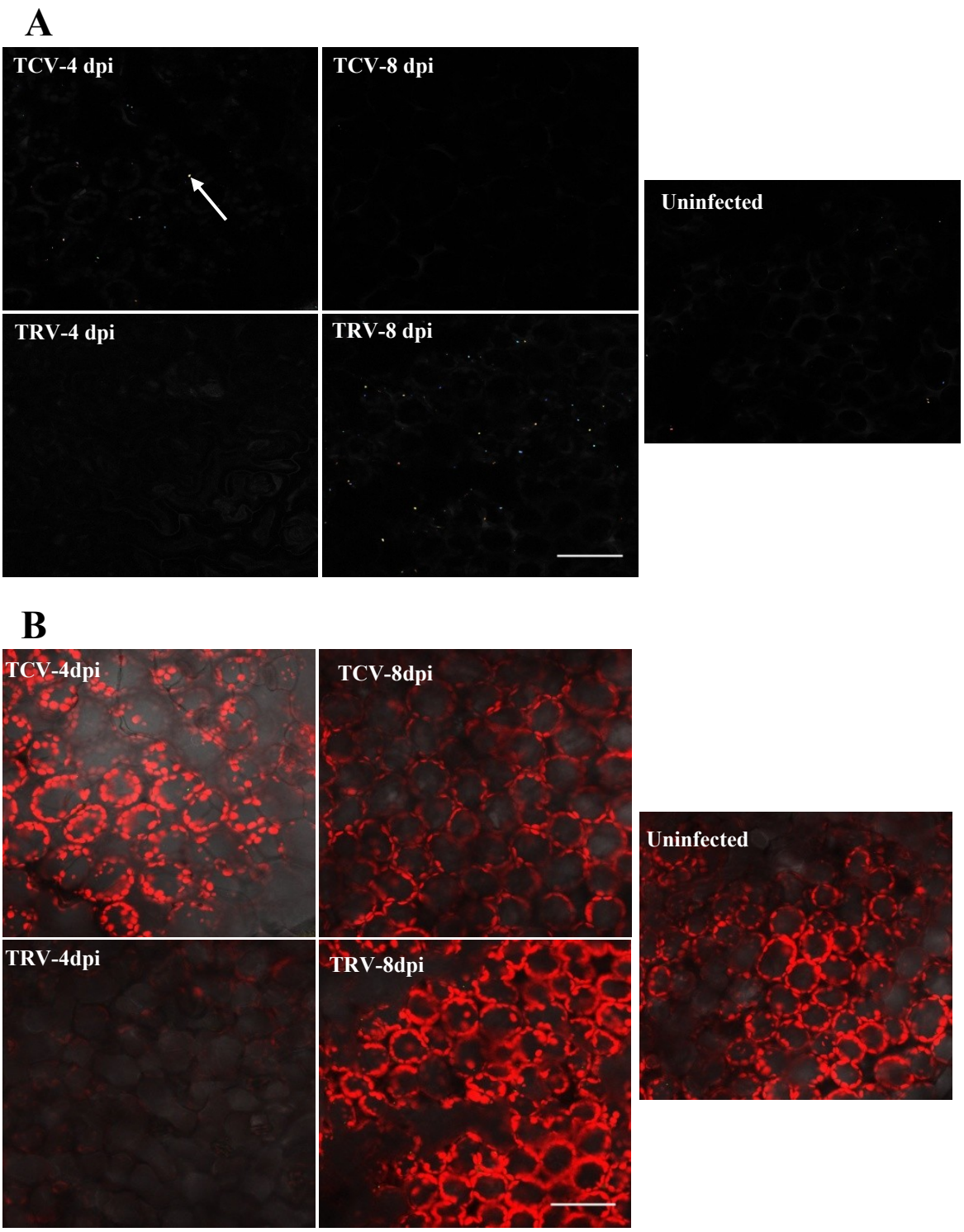
A
TCV-4 dpi
TCV-8 dpi
Uninfected
TRV-4 dpi
TRV-8 dpi
B
TCV-4dpi
TCV-8dpi
Uninfected
TRV-4dpi
TRV-8dpi

Continued

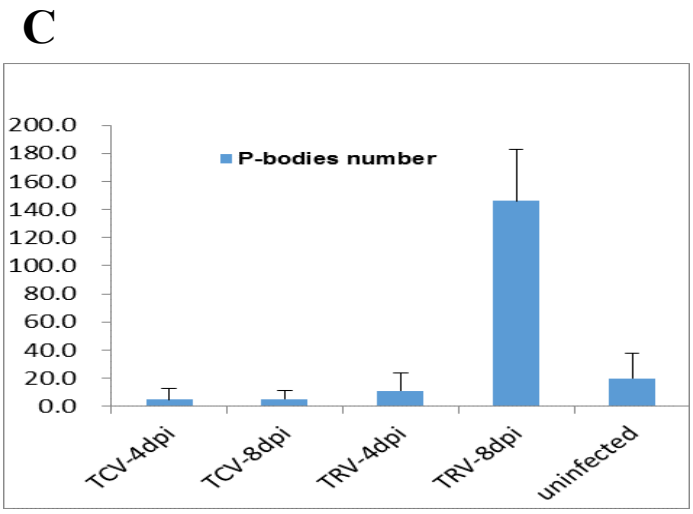

Fig. 4-14 TRV recovery induces an increase in PB formation

Transgenic *Arabidopsis* plants expressing YFP-DCP1 were infected with TCV or TRV and monitored for YFP fluorescence at 4 and 8 days. A, Confocal images of YFP fluorescence in mesophyll cells of virus-infected or uninfected plants. A representative PB is indicated with a white arrow. YFP fluorescence was pseudocolored using the software Cell-Profiler. B, Transmission images of transgenic *Arabidopsis* mesophyll cells expressing YFP-DCP1. Scale bars = 50 mm. Images are representative of experiments biologically repeated at least three times. C, The number of YFP-expressing bodies was quantified using software Cell-Profiler and represented graphically

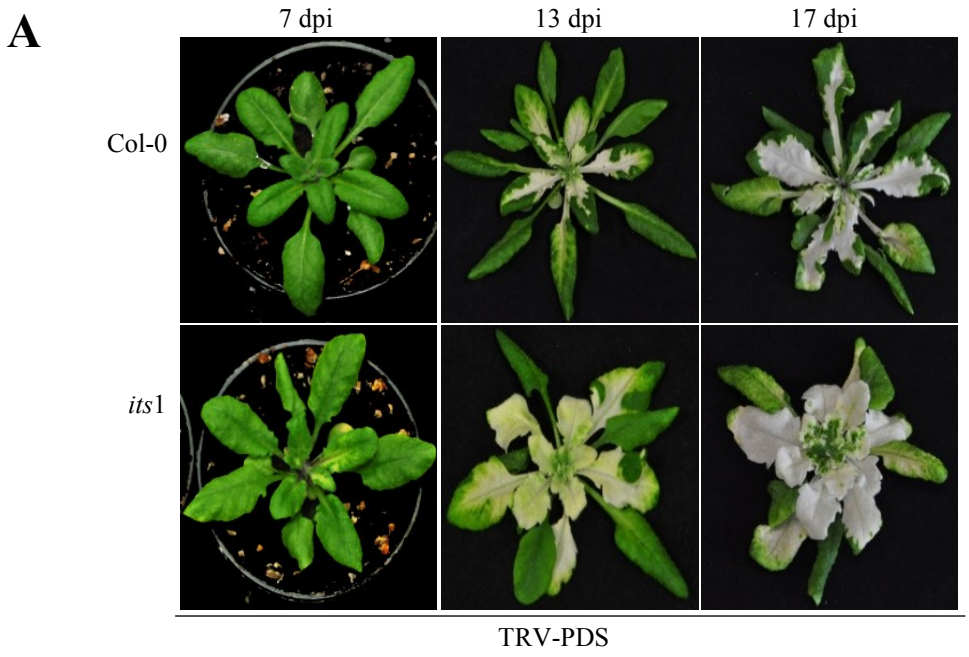

Continued

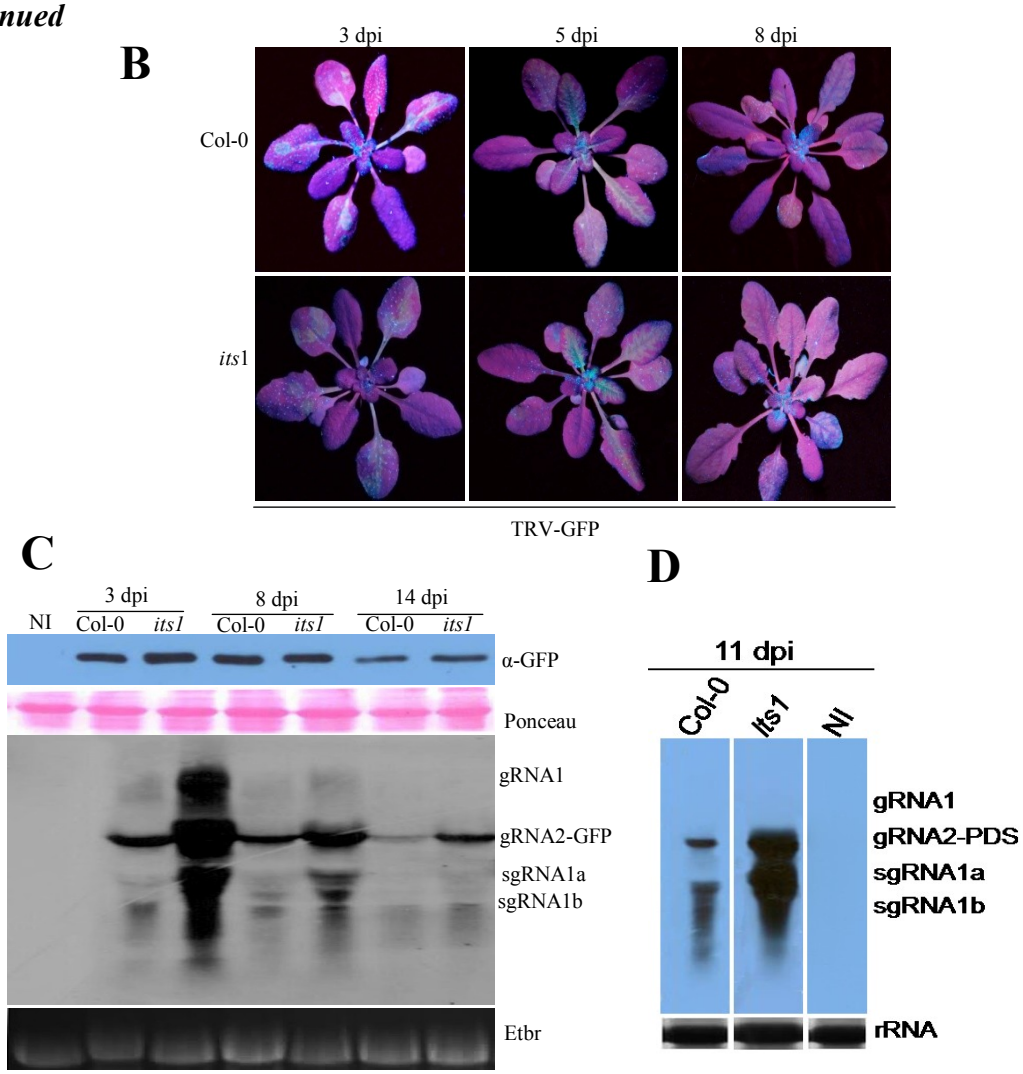

Fig. 4-15 VIGS and recovery in the *Arabidopsis its1* mutant

A, Col-0 and *its1* mutant *Arabidopsis* plants were infected with TRV-PDS and photographed at the indicated number of days post inoculation (dpi). B, Col-0 and *its1* mutant *Arabidopsis* plants were infected with TRV-GFP and photographed under UV illumination at the indicated number of days post inoculation (dpi). C, Total protein and total RNA was extracted from plants of the indicated genotypes that were either non-infected (NI) or infected with TRV-GFP at the time points indicated. Samples were subjected to anti-GFP immune-blotting (upper panels) and northern blotting with an anti-TRV CP probe (lower panels). Ponceau staining and Ethidium bromide stained RNA (prior to transfer) are shown as a loading control. D, Total RNA was extracted from non-infected Col-0 plants (NI) or from Col-0 or *its1* mutant plants, as indicated, eleven days post infection (dpi) with TRV-PDS. RNA was subsequently subjected to northern blotting with an anti-TRV CP probe. Each lane corresponds to the pool of the 5-6 inoculated *Arabidopsis* plants. Methylene Blue stained RNA (after transfer) is shown as a loading control. Images have been cropped from a larger gel for representation purpose, but originate from the same experiment and exposure times. Images are representative of experiments biologically repeated at least three times

4.5 Discussion

In the first systematic study of the involvement of AGO proteins in VIGS and recovery, we find that these phenomena are surprisingly robust, in contrast to other RNA silencing mechanisms. Although the TD, *ago2* and *ago4* mutants show delayed recovery

(Table 5-3), this is likely due to increased initial levels of virus and GFP. Thus, either recovery involves non RNA silencing mechanisms, or the involvement of DCL and AGO proteins in recovery is highly redundant. We do not rule out the former possibility, but the fact that co-infection with TCV allows TRV to escape recovery, presumably by providing a strong VSR in *trans*, suggests that recovery is mediated by RNA silencing-related mechanisms. The TCV VSR, P38 interferes with AGO activity and has been reported to co-immunoprecipitate with AGO1, but not AGO4 or AGO7 (Azevedo et al 2010). Our data suggest that in addition to AGO1, P38 must also inhibit whichever other AGO proteins mediate recovery. For example, of the AGO proteins tested, AGO1, AGO2 and AGO5, but not AGO4 and AGO7, bind vsiRNAs derived from viruses (TCV and CMV) with VSRs that target AGOs (Zhang et al 2006; Takeda et al 2008; Azevedo et al 2010; Hamera et al 2012). At the same time AGO1, AGO2, AGO3, AGO4, AGO5, and AGO9 are able to bind to siRNAs derived from a viroid, which does not encode a VSR (Minoia et al 2014). These results suggest that in the absence of VSR, most AGO proteins are able to bind siRNAs. Thus, given the relatively weak activity of the TRV VSR (Martin-Hernandez and Baulcombe 2008), it is possible that multiple unrelated AGO proteins target TRV. Likewise, although DCL2 and DCL4 are thought to be the most important Dicers for defense against viruses, TD mutants infected with TRV do nonetheless produce small amounts of TRV-derived siRNAs (Deleris et al 2006). Thus, although the latter Dicers may normally mediate anti-viral defense, our results indicate that DCL1 does have some capacity to mediate recovery. The fact that VIGS in the TD mutant is temperature dependant is consistent with the temperature-dependent property of RNA silencing, which has been well documented in previous studies (Szittya et al 2003; Qu et al 2005; Tuttle et al 2008; Zhang et al 2012).

The *ago2* and *ago4* mutants show an initial increase in susceptibility to TRV, as indicated by increased protein and RNA levels (Fig. 4-6 and Fig. 4-8). The antiviral role of AGO2 has been well established in previous studies (Harvey et al 2011; Jaubert et al 2011; Scholthof et al 2011; Wang et al 2011) and appears to function through direct slicing of viral RNAs (Carbonell et al 2012). However, increased susceptibility of the *ago4* mutants to a virus is novel. The role of AGO4 in TRV infection is less clear as AGO4 is best characterized for its role in RNA-directed DNA methylation (RdDM) and transcriptional gene silencing (TGS) of transposons and repeats (Zilberman et al 2004; Li et al 2006; Li et al 2008; Ye et al 2012; Bologna and Voinnet 2014). This activity may play a general role in plant defenses as *ago4* mutants are also more susceptible to the

bacterium *Pseudomonas syringae* (Agorio and Vera 2007). Nonetheless, the *ago2* and *ago4* mutants still undergo recovery, suggesting a temporal aspect to antiviral defenses and that susceptibility (i.e. the ability of the virus to initially accumulate in plant cells) and recovery may be carried out by different molecular mechanisms. That is, AGO2 and AGO4 may play important roles in restricting viruses early in infection whereas other AGO proteins (or other mechanisms) may later mediate recovery. This idea is consistent with DCL proteins having differential effects in local and systemic infection, in that DCL4 alone is required for defence against TuMV in inoculated leaves whereas both DCL4 and DCL2 are required later in infection, in systemic tissues (Garcia-Ruiz et al 2010). The *ago1-27* mutant shows decreased susceptibility to TRV-GFP, as indicated by reduced GFP intensity (Fig. 4-6) and reduced viral RNAs level in TRV-GFP infected plants (Fig. 4-11). This phenotype contrasts with the increased susceptibility of *ago1* mutants to CMV and VSR-defective TCV (Vaucheret et al 2004; Deleris et al 2006) and with the requirement for *NbAgo1* for recovery to ToRSV (Ghoshal and Sanfacon 2014). On the other hand, it is consistent with a lack of requirement for *NbAgo1* for recovery from a VSR-deficient TBSV (Scholthof et al 2011), a lack of increased susceptibility to PVX in *ago1-27* plants (Jaubert et al 2011) and a slower infection of *NbAgo1*-silenced plants by ToRSV (Ghoshal and Sanfacon 2014). AGO1 regulates the expression of *AGO2*, which is targeted by a miRNA, and consequently AGO2 protein levels increase in *ago1* mutants (Harvey et al 2011). The *ago1/ago2* double mutant allows for GFP expression from TRV similar to the *ago2* mutant (Fig. 4-6) and greater accumulation of TRV-PDS RNA (Fig. 4-6), suggesting that *ago1-27* phenotypes may be due to increased AGO2. However, TRV-GFP still moves more slowly in *ago1/ago2* plants, indicating that this mutant is still somewhat more resistant to TRV. This observation is consistent with previous reports showing that silencing or mutation of *AGO1* can result in constitutive expression of defense related-genes and enhanced R gene responses (Yi and Richards 2007; Bhattacharjee et al 2009; Li et al 2010; Li et al 2012; Shivaprasad et al 2012).

To date, only mutations in *DCL2*, *DCL4* and *HEN1* have been reported to have dramatic effects on VIGS (Deleris et al 2006; Dunoyer et al 2007). In contrast to recovery, we are able to identify one AGO protein, AGO1, that appears to be the major effector of VIGS (Fig. 4-9). The *ago1-27* mutant shows some residual VIGS, although this may be due to the fact that this allele encodes a hypomorphic allele (Morel et al 2002). A role for AGO1 in VIGS is in agreement with the fact that AGO1 appears to be the major effector of miRNA-mediated control of endogenous gene expression (Bologna and Voinnet 2014).

This result underlines an important difference between recovery and VIGS in that the former targets viral RNAs, whereas the latter targets cellular transcripts. Our results suggest that although both AGO1 and AGO2 can bind vsiRNAs (Takeda et al 2008), they somehow distinguish between different types of target RNA. That is, even though virus infection results in massive production of vsiRNAs, AGO2 (and possibly others) appear to use these guide RNAs only to target viral RNAs, whereas AGO1 can be loaded with vsiRNAs but largely targets cellular mRNA, at least in the case of TRV. Our speculation is supported by a recent report indicating the existence of two distinct pools of cellular AGO1 that are specifically loaded by siRNAs and miRNAs, respectively (Schott et al 2012).

Surprisingly, in contrast to the decreased susceptibility to TRV-GFP (Fig. 4-6), we observed increased TRV-PDS viral RNA level in *ago1-27* and *ago1* double and triple mutants plants compared to wild type plants (Fig. 4-11). This result is similar in part to that seen with TCV; whereas TCV lacking its VSR (TCVΔCP) accumulated to higher levels in an *ago1* mutant, TCV-ΔCP-GFP accumulated to lower levels (Qu et al 2008). The reason for this difference is not yet clear although it is possible that the GFP insert, due to some as yet undefined characteristic(s), makes the virus more susceptible to the increase in AGO2 caused by a lack of AGO1. Qu *et al* (2008) suggest that this may be due to a lack of secondary structure in the GFP insert, although the PDS insert would likewise be predicted to have less structure than viral RNA. Nonetheless, this result implies that different viruses may be more or less affected by different AGO proteins due to the intrinsic properties of their RNA genomes.

A recent study has shown that recovery of *N. benthamiana* from ToRSV was not accompanied by reduced viral RNA levels (Jovel et al 2007), but was associated with an AGO1-dependent mechanism that represses the translation of viral RNA2 (Ghoshal and Sanfacon 2014; Karran and Sanfacon 2014). In our case the TRV-GFP recovery in both WT and TD plants was accompanied by both reduced viral RNA and viral protein levels (Fig. 4-5). Although this might indicate that the recovery mechanisms against TRV and ToRSV differ, this may only be a matter of degree as highly efficient repression of viral translation would disallow further virus replication, leading to less steady-state RNA levels. Indeed, in wild type plants that have recovered from TRV, the percentage of viral RNA associated with active ribosomes is reduced compared to that of non-recovered plants (Fig. 4-13B). Although this could indicate that viral RNAs are shifted to encapsidation, it nonetheless indicates that they are shifted away from active translation.

Studies in other systems suggest that the formation of PBs depends on free cytoplasmic mRNA or mRNA that is translationally repressed and that PB numbers increase in response to increased amounts of translationally repressed mRNAs (Teixeira et al 2005; Parker and Sheth 2007). Although it is possible that different types of DCP1-containing granules exist, DCP1 does not localize to stress granules, heat stress granules or siRNA bodies in plants (Weber et al 2008; Jouannet et al 2012). As such, DCP1 is generally accepted to be a well-established reference marker for PBs in plants (Xu et al 2006; Iwasaki et al 2007; Weber et al 2008; Balagopal and Parker 2009; Xu and Chua 2009; Perea-Resa et al 2012; Merret et al 2013; Moreno et al 2013; Maldonado-Bonilla 2014). Recovery from TRV is associated with a reduction in TRV RNA association with ribosomes and induces increased numbers of PBs (Fig. 4-13, Fig. 4-14). This result is consistent with a scenario wherein viral RNAs are subjected to translational repression and in turn accumulate in PBs where they are eventually degraded.

A role for the decapping complex in viral defense is also seen with the hypomorphic *DCP2* mutant *its1* (Fig. 4-15). This mutation does not affect recovery to TRV-GFP. However, *its1* shows greatly increased accumulation of RNA from TRV-GFP (Fig. 4-15C) and TRV-PDS (Fig. 4-15D). Unlike *ago1-27*, however, *its1* plants underwent VIGS to a much faster and greater extent. This phenotype is similar to the original increased transgene silencing phenotype (Thran et al 2012). The *its1* mutation plants have less uncapped RNAs and transgenes have a greater tendency to undergo silencing and to give rise to siRNAs. This is thought to be due to a buildup of "aberrant" RNAs that feed into a siRNA production/amplification mechanism based on RNA-dependent RNA polymerase 6, thus producing more siRNAs, which can in turn target the source gene. In contrast, however, whereas transgene RNAs decrease in *its1*, TRV-GFP RNA increases. This suggests that the decapping/PB pathway may be an important mechanism for degrading viral RNA. Indeed, in contrast to the TD, *ago2* and *ago4* mutants, the greatly increased TRV-GFP RNA accumulation in *its1* plants was not reflected in a similar increase in GFP protein (Fig. 4-6, Fig. 4-15). This suggests that much of the "excess" viral RNA represents aberrant or non-translating RNA that would normally be degraded in PBs. Whether this degradation activity is linked to RNA silencing or represents an independent mechanism for clearing viral RNA remains to be determined. At the same time, the *its1* mutant is, to our knowledge, the only mutant described with an increased efficiency of VIGS and this mutant could be useful in functional genomics approaches in *Arabidopsis*.

Chapter 5 - Conclusions and Perspectives

ASPV defends against it hosts' defenses

To live in host cells or to escape from host immunity, plant viruses involved a series of defense strategies. Here we investigated ASPV population structures and molecular diversity of ASPV pear isolates based on its function important gene CP and TGB in China, so as to infer the evolutionary mechanisms of ASPV. Our study showed that mutations (including insertions or deletions), purifying selection, and recombination were important factors driving ASPV evolutions in China or maybe even in the world. And also ASPV defends against it hosts by encoding a VSR, which was its CP. Surprisingly, the great molecular diversity of ASPV CP isolates did not affect its VSR activity and pathogenicity. But how ASPV CP protected its VSR function and how the VSR function need to be further studied.

Our results indicate that ASPV has great molecular diversity among its hosts (pear, apple, Korla pear), probably because when a virus adapts to a new host, it was primarily manifested as amino acid substitutions, which could allow more efficient virus entry into the new host, block interactions with host proteins or promote escape from both the new and the old host's immune responses (Moya et al 2004; Boulila 2010; Bandín and Dopazo 2011). However, interactions between ASPV and its hosts have been not studied yet and further studies of these interactions will need to be explored. Molecular diversity of a virus may result in dramatic changes in the biological properties of the virus, which included the appearance of resistance-breaking strains or the acquisition of broader host ranges. Here we showed that ASPV molecular diversity not only induced different biological properties on its herbaceous host *N. occidentails* but also resulted in antigenic variation of different ASPV CP isolates, which leaded to their differences in serological reactivity among rCPs of different ASPV isolates. However, unfortunately we did not furture expore how the molecular variation affected those results, which will need more studies.

VsiRNAs derived from ASPV detected by deep suquencing and VSR activity of ASPV CP indicated that RNA silencing of pear plant play a role in defending against ASPV. The pear genome sequence were recently reported (Wu et al 2013), which provides a great advantage to further study the RNA silencing components of pear plant defending against ASPV.

Arabidopsis thaliana defends against TRV

Plants have developed a series of mechanisms to defend themselves against viruses. Here we have investigated which elements of the *Arabidopsis* RNA silencing machinery are required to defend against TRV (Chapter 4). Our results are summerized in Figure 5-1 (Fig. 5-1).

Firstly, we have shown that VIGS intensity of *dcl2/dcl3/dcl4* plants correlated positively with temperature, which propably indicated that DCL1 also could target TRV dsRNAs. This result was inconsistent with previous results that atDCL1 was not involved in TRV-PDS VIGS (Deleris et al 2006). Explaination for this contradiction was that probably the expression level of DCL1 correlated positively with temperature: at low temperature the expression level of DCL1 was not enough to involve in targeting TRV dsRNAs, as the temperature became high DCL1 expression level was increased.

Secondly, we have shown that TRV susceptibility, recovery and VIGS appear to be separable phenomena, with AGO2 and AGO4 playing important roles in initial susceptibility to TRV, AGO1 playing an important role in VIGS. These results suggest the existence of distinct RISC complexes that target different RNA populations within the cell and over time, which was cleary showed in Figure 5-1: AGO2 and AGO4 containing RISC complexes specially targeted TRV viral RNA, however, AGO1 containing RISC complexes specially targeted endogenous *PDS* mRNA. However, in our results it seemed as yet unidentified players mediating recovery, but our results indicated either the involvement of RNA silencing components in recovery is highly redundant or additional mechanisms was involved in TRV-GFP recovery. A recent study showed that TRV induced nonrecovery symptoms on *N. tabacum* plants that Coilin gene was knocked down, whereas TRV infected wildtype *N. tabacum* plants went recovery (Shaw et al 2014). Coilin is a key component of Cajal bodies (CBs) and also the scaffolding protein essential for CB formation and function (Collier et al 2006). CBs are distinct nuclear bodies physically and functionally associated with the nucleolus. In addition to their traditional function in coordinating maturation of certain nuclear RNAs, CBs participate in cell cycle regulation, development and regulation of stress responses. CBs have been identified in many orgnisms including *Arabidopsis* and *Arabidopsis* also encoed Coilin protein (Collier et al 2006). It is not clear whether Coilin plays a role in an as-yet unknown RNA silencing mechanism or whether it triggers a separate defense response that restricts virus accumulation concomitantly with RNA silencing (Ghoshal et al 2015). Thus, the interplay

of RNA silencing and other plant defense responses may regulate the establishment of symptom recovery in some plant-virus interactions, which need to be further tested.

Thirdly, results in our study indicated that homologous viral RNAs were targeted by two ways, either by slicing activity or by translationl repression and the part of translationl repressed TRV RNAs went to the PBs structure. Probably translational repression of viral RNAs likely plays an important role in restricting viral RNAs accumulation and that PB function plays an important role in clearing viral RNA from the cell. The fact that PBs are induced only at later stages of infection again suggests a temporal aspect to virus resistance. If we accept that an increase in PBs is indicative of increased translational repression, then the lack of PB induction at early time points would suggest that RNA silencing defenses against TRV are largely mediated through slicing activity, most likely mediated by AGO2, followed by translational repression mediated by additional AGO proteins. Decapping complexes are not thought to participate directly in translational repression, but rather in the processing of repressed mRNAs or producing aberrant RNAs and thus DCP2 would necessarily act downstream of AGO proteins.

Finally, the *its1* mutant here was the only mutant described with an increased VIGS intensity and this mutant could be useful in functional genomics approaches in *Arabidopsis* in the furture. In the hypomorphic *DCP2* mutant *its1* plants, increased accumulation of TRV-GFP and TRV-PDS viral RNAs suggests that the decapping/PB pathway may be an important mechanism for degrading viral RNA. However, increased TRV-GFP RNAs accumulated in *its1* plants was not associated with increased GFP protein, which indicated that much of the “excess” viral RNA represents aberrant or non-translating RNA.

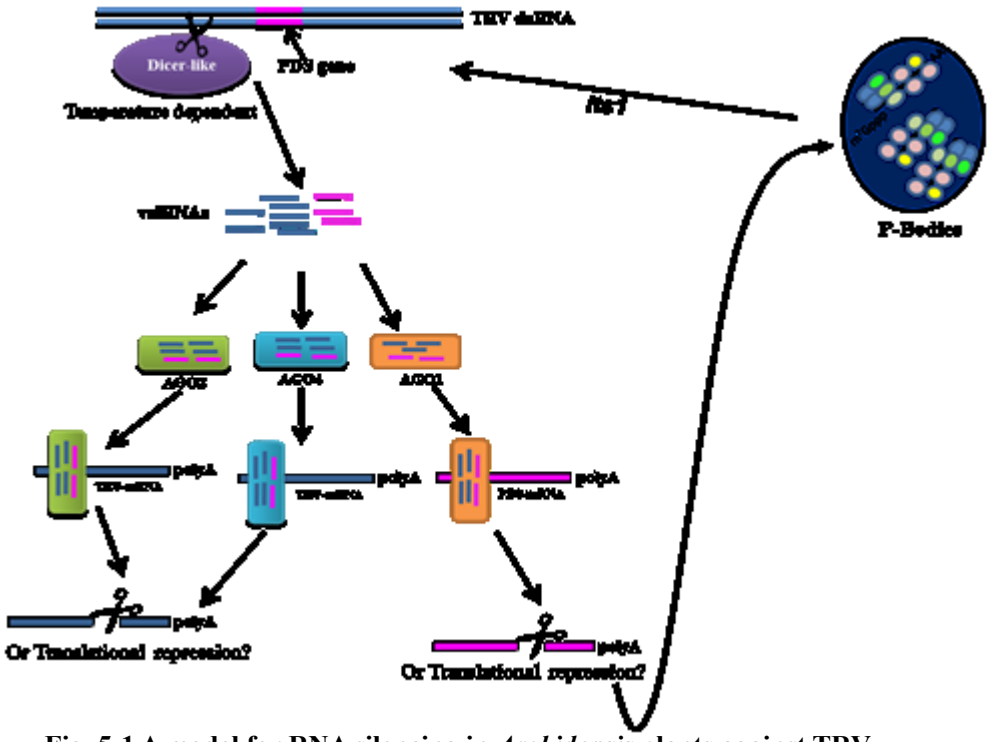

Fig. 5-1 A model for RNA silencing in *Arabidopsis* plants against TRV

Once *Arabidopsis* was infected with TRV, TRV Replicative intermediate dsRNAs were recognized by DCL2, DCL3 and DCL4, and were cut into vsiRNAs (if exogenous factors were inserted into TRV vector, for example, *PDS*, there would be also PDS derived siRNAs). However, at high temperature (26 ℃), DCL1 may be involved in defending against TRV-PDS. TRV derived siRNAs were loaded into AGO2 and AGO4 containing slicing complex, specially targeting TRV viral RNA, however, PDS derived siRNAs were loaded into AGO1 containing slicing complex, specially targeting endogenous *PDS* mRNA. Results in our study indicated that homologous RNAs were targeted by two ways, either by slicing or by translationl repression. Our results indicated that those translationl repression RNAs went to P-bodies. In *its1* mutant, temporary storaged TRV viral RNA in P-bodies went back to RNA silencing pathway, which could induce an increaed VIGS phenotype

Appendix 1 Genome structures of viruses or virus vector used in this study

Turnip Crinkle Virus (TCV)

+ssRNA virus, genus *Carmovirus*, family *Tombusviridae*

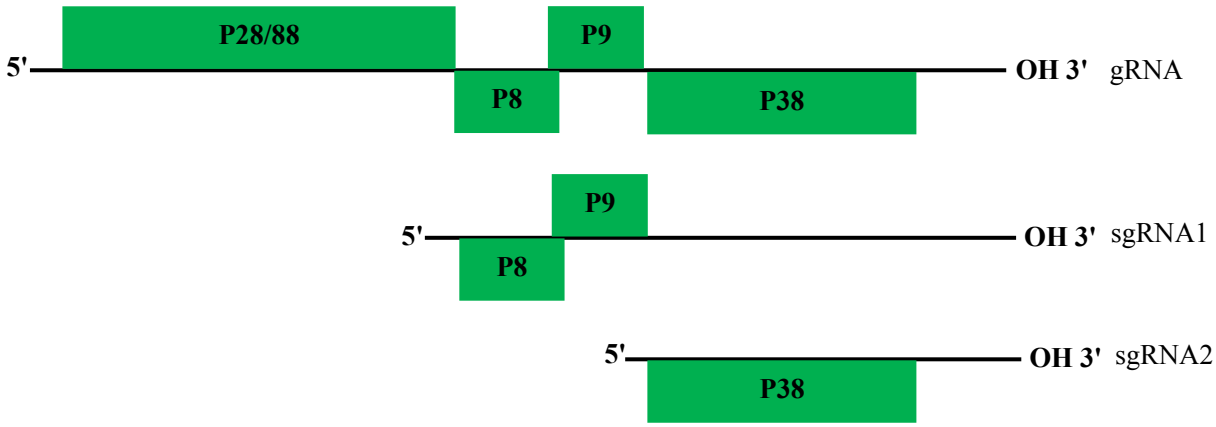

Apple stem pitting virus (ASPV)

+ssRNA virus, genus *Foveavirus*, family *Betaflexiviridae*

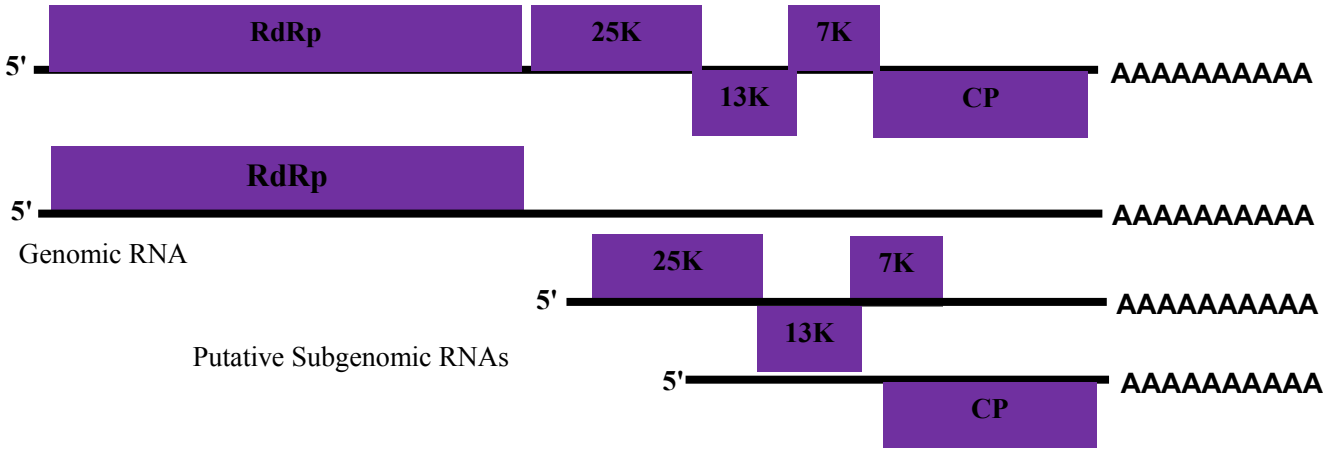

Apple stem grooving virus (ASGV)

+ssRNA virus, genus *Capillovirus*, family *Betaflexiviridae*

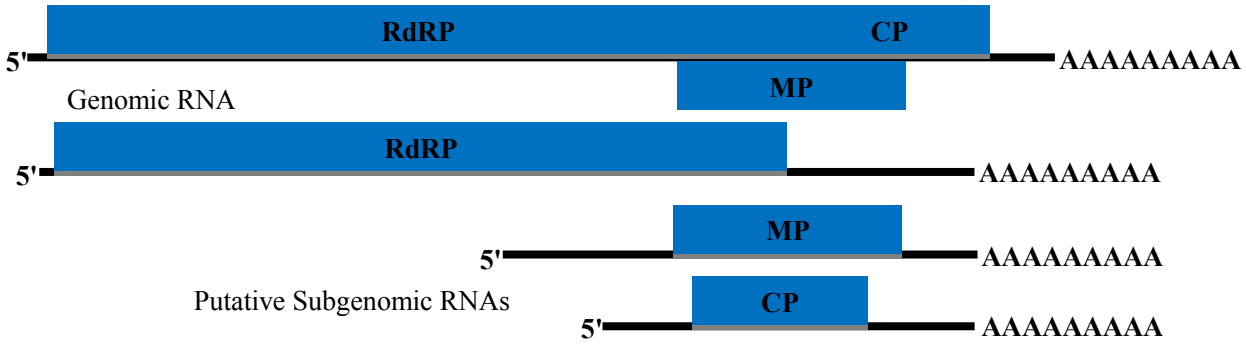

Apple chlorotic leaf spot virus (ACLSV)

+ssRNA virus, genus *Trichovirus*, family *Betaflexiviridae*

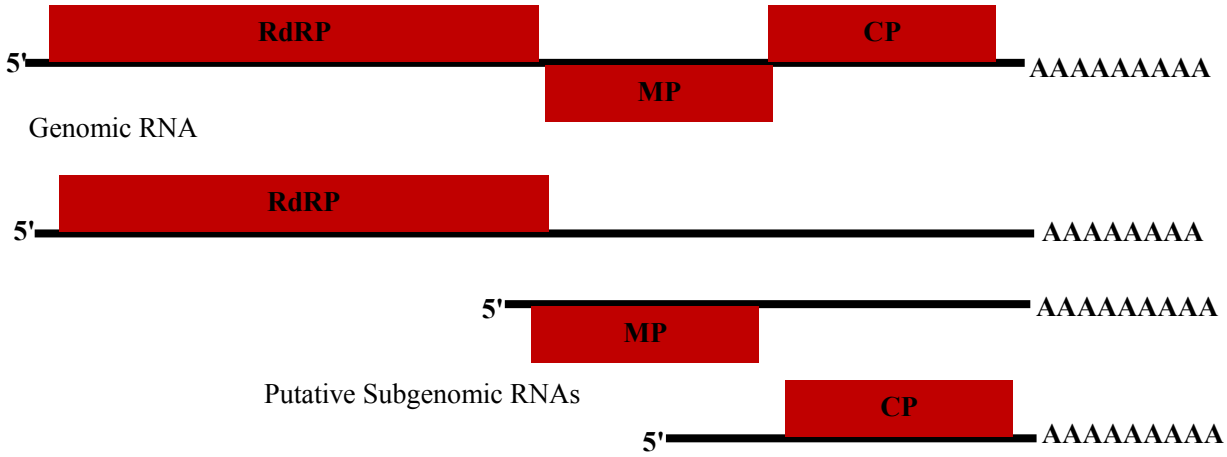

Appendix 2 Statistical Table for detection of three often occurred viruseson pome fruit trees by RT-PCR

Sample NO.	Cultivars	Source	Collected Date	viruses detection			symptoms
				ASPV	ASGV	ACLSV	
1-HB-UN	-*	Enshi.HuBei	08/2009	+	N**	N	-***
2-HB-UN	-	Enshi.HuBei	08/2009	+	N	N	-
3-HB-UN	-	Enshi.HuBei	08/2009	-	N	N	-
4-HB-UN	-	Enshi.HuBei	08/2009	-	N	N	-
5-HB-UN	-	Enshi.HuBei	08/2009	-	N	N	-
1-HN-HBLS	Hong bei lei sha	Zhengzhou.Henan	08/2010	+	N	N	-
2-HN-SJL	Shui jing li	Zhengzhou.Henan	08/2010	+	N	N	-
3-HN-BL	Ba li	Zhengzhou.Henan	08/2010	+	N	N	-
4-HN-NSL	Nan shui li	Zhengzhou.Henan	08/2010	-	N	N	-
5-HN-BL-1	Ba li	Zhengzhou.Henan	08/2010	-	N	N	-
1-YN-MRS	Mei ren su	Yunnan	02/2010	+	N	N	-
2-YN-MRS	Mei ren su	Yunnan	02/2010	-	N	N	-
3-YN-ZBM	Zao bai mi	Yunnan	02/2010	-	N	N	-
4-YN-ZBM	Zao bai mi	Yunnan	02/2010	-	N	N	-
1-HB-HN1	Er shi shi ji	Wuhan.Huebei	02/2010	+	N	N	-
2-HB-HN2	Er shi shi ji	Wuhan.Huebei	10/2010	+	N	N	-
3-HB-HN3	Feng shui	Wuhan.Huebei	10/2010	+	N	N	-
4-HB-HN4	Feng shui	Wuhan.Huebei	10/2010	-	N	N	-
5-HB-HN5	Huang hua	Wuhan.Huebei	10/2010	-	N	N	-
6-HB-HN6	Xue hua li	Wuhan.Huebei	10/2010	+	N	N	-
7-HB-HN7	Feng shui	Wuhan.Huebei	10/2010	+	N	N	-
8-HB-HN8	-	Wuhan.Huebei	10/2010	-	N	N	-
9-HB-HN9	-	Wuhan.Huebei	10/2010	+	N	N	-
10-HB-HN10	-	Wuhan.Huebei	10/2010	+	N	N	-
11-HB-HN11	-	Wuhan.Huebei	25/11/2010	-	N	N	-
12-HB-HN12	-	Wuhan.Huebei	25/11/2010	-	N	N	-
13-HB-HN13	-	Wuhan.Huebei	25/11/2010	-	N	N	-
14-HB-HN14	-	Wuhan.Huebei	25/11/2010	-	N	N	-
15-HB-HN15	-	Wuhan.Huebei	25/11/2010	-	N	N	-
16-HB-HN16	-	Wuhan.Huebei	25/11/2010	+	N	N	-
17-HB-HN17	-	Wuhan.Huebei	25/11/2010	-	N	N	-
18-HB-HN18	-	Wuhan.Huebei	25/11/2010	-	N	N	-
19-HB-HN19	-	Wuhan.Huebei	25/11/2010	+	N	N	-
20-HB-HN20	-	Wuhan.Huebei	25/11/2010	-	N	N	-
21-HB-HN21	-	Wuhan.Huebei	25/11/2010	-	N	N	-
22-HB-HN22	-	Wuhan.Huebei	25/11/2010	+	N	N	-
23-HB-HN23	-	Wuhan.Huebei	25/11/2010	+	N	N	-
24-HB-HN24	-	Wuhan.Huebei	25/11/2010	-	N	N	-
25-HB-HN25	-	Wuhan.Huebei	25/11/2010	-	N	N	-
26-HB-HN26	-	Wuhan.Huebei	25/11/2010	+	N	N	-
27-HB-HN27	-	Wuhan.Huebei	25/11/2010	-	N	N	-
28-HB-HN28	-	Wuhan.Huebei	25/11/2010	-	N	N	-
29-HB-HN29	-	Wuhan.Huebei	25/11/2010	-	N	N	-

Sample NO.	Cultivars	Source	Collected Date	viruses detection			symptoms
				ASPV	ASGV	ACLSV	
30-HB-HN30	-	Wuhan.Huebei	25/11/2010	-	N	N	-
31-HB-HN31	-	Wuhan.Huebei	23/12/2010	-	N	N	-
32-HB-HN32	-	Wuhan.Huebei	23/12/2010	-	N	N	-
33-HB-HN33	-	Wuhan.Huebei	23/12/2010	+	N	N	-
34-HB-HN34	-	Wuhan.Huebei	23/12/2010	+	N	N	-
35-HB-HN35	-	Wuhan.Huebei	23/12/2010	-	N	N	-
36-HB-HN36	-	Wuhan.Huebei	23/12/2010	-	N	N	-
37-HB-HN37	-	Wuhan.Huebei	23/12/2010	+	N	N	-
38-HB-HN38	-	Wuhan.Huebei	23/12/2010	-	N	N	-
39-HB-HN39	-	Wuhan.Huebei	23/12/2010	-	N	N	-
40-HB-HN40	-	Wuhan.Huebei	23/12/2010	+	N	N	-
41-HB-HN41	-	Wuhan.Huebei	23/12/2010	+	N	N	-
42-HB-HN42	-	Wuhan.Huebei	23/12/2010	+	N	N	-
43-HB-HN43	-	Wuhan.Huebei	23/12/2010	+	N	N	-
44-HB-HN44	-	Wuhan.Huebei	23/12/2010	+	N	N	-
1-LN-AP1	-	Xingcheng.Liaoning	09/2010	+	+	+	-
2-LN-AP2	-	Xingcheng.Liaoning	09/2010	+	+	+	-
3-LN-AP3	-	Xingcheng.Liaoning	09/2010	-	N	N	-
1-SD-AP1	Hong fu shi	Yantai.Shandong	10/2010	+	+	+	-
2-SD-AP2	Hong fu shi	Yantai.Shandong	10/2010	-	+	-	-
3-SD-AP3	Hong fu shi	Yantai.Shandong	10/2010	+	+	+	-
1-ZJ-CG	Cui guan	Zhejiang.Hangzhou	01/05/2010	-	+	+	CL
2-ZJ-CG	Cui guan	Zhejiang.Hangzhou	01/05/2010	-	-	-	CL
3-ZJ-CG	Cui guan	Zhejiang.Hangzhou	01/05/2010	-	-	+	CL
4-ZJ-CG	Cui guan	Zhejiang.Hangzhou	01/05/2010	-	+	-	CL
5-ZJ-CG	Cui guan	Zhejiang.Hangzhou	01/05/2010	-	+	+	CL
6-ZJ-CG	Cui guan	Zhejiang.Hangzhou	01/05/2010	-	-	+	CL
7-ZJ-CG	Cui guan	Zhejiang.Hangzhou	01/05/2010	-	-	+	CL
8-ZJ-CG	Cui guan	Zhejiang.Hangzhou	01/05/2010	-	+	-	CL
9-ZJ-CG	Cui guan	Zhejiang.Hangzhou	01/05/2010	-	-	+	-
10-ZJ-CG	Cui guan	Zhejiang.Hangzhou	01/05/2010	-	+	+	CL+VY
11-ZJ-CG	Cui guan	Zhejiang.Hangzhou	01/05/2010	-	+	+	CL
12-ZJ-CG	Yu guan	Zhejiang.Hangzhou	01/05/2010	-	+	+	CL
13-ZJ-CG	Yu guan	Zhejiang.Hangzhou	01/05/2010	-	+	-	CL
14-ZJ-CG	Yu guan	Zhejiang.Hangzhou	01/05/2010	-	+	+	CL
15-ZJ-CG	Cui guan	Zhejiang.Hangzhou	01/05/2010	-	+	+	CL
16-ZJ-CG	Cui guan	Zhejiang.Hangzhou	01/05/2010	-	-	-	CL
17-ZJ-CG	Cui guan	Zhejiang.Hangzhou	01/05/2010	-	+	+	CL
18-ZJ-CG	Cui guan	Zhejiang.Hangzhou	01/05/2010	-	-	-	CL
19-ZJ-CG	Cui guan	Zhejiang.Hangzhou	01/05/2010	-	-	-	CL
20-ZJ-CG	Cui guan	Zhejiang.Hangzhou	01/05/2010	-	+	-	CL
21-ZJ-CG	Cui guan	Zhejiang.Hangzhou	01/05/2010	-	-	-	CL
22-ZJ-CG	Chu xia lv	Zhejiang.Hangzhou	01/05/2010	-	+	+	-
23-ZJ-CG	Cui guan	Zhejiang.Hangzhou	01/05/2010	-	+	+	-
24-ZJ-CG	Chu xia lv	Zhejiang.Hangzhou	01/05/2010	-	+	+	-
25-ZJ-CG	Cui guan	Zhejiang.Hangzhou	01/05/2010	-	+	-	CL

Sample NO.	Cultivars	Source	Collected Date	viruses detection			symptoms
				ASPV	ASGV	ACLSV	
26-ZJ-CG	Cui guan	Zhejiang.Hangzhou	01/05/2010	-	-	-	-
27-ZJ-CG	Cui guan	Zhejiang.Hangzhou	01/05/2010	-	-	+	CL
28-ZJ-CG	Cui guan	Zhejiang.Hangzhou	01/05/2010	-	-	-	CL
29-ZJ-CG	Cui guan	Zhejiang.Hangzhou	01/05/2010	-	+	-	CL
30-ZJ-CG	Chu xia lv	Zhejiang.Hangzhou	01/05/2010	-	+	-	CL
31-ZJ-CG	Cui guan	Zhejiang.Hangzhou	01/05/2010	-	+	+	CL
32-ZJ-CG	Cui guan	Zhejiang.Hangzhou	01/05/2010	-	+	+	CL
33-ZJ-CG	Cui guan	Zhejiang.Hangzhou	01/05/2010	-	+	-	CL
34-ZJ-CG	Yu guan	Zhejiang.Hangzhou	01/05/2010	-	+	-	-
35-ZJ-CG	Cui guan	Zhejiang.Hangzhou	01/05/2010	-	+	+	-
36-ZJ-CG	Cui guan	Zhejiang.Hangzhou	01/05/2010	-	-	-	CL
37-ZJ-CG	Cui guan	Zhejiang.Hangzhou	01/05/2010	-	-	+	-
38-ZJ-CG	Cui guan	Zhejiang.Hangzhou	01/05/2010	-	+	+	CL
40-ZJ-YG	Yu guan	Zhejiang.Hangzhou	01/05/2010	+	-	+	VY
41-ZJ-YG	Yu guan	Zhejiang.Hangzhou	01/05/2010	+	-	+	VY
42-ZJ-YG	Yu guan	Zhejiang.Hangzhou	01/05/2010	-	+	-	CL
43-ZJ-CG	Cui guan	Zhejiang.Hangzhou	01/05/2010	-	-	+	CL
44-ZJ-CG	Cui guan	Zhejiang.Hangzhou	01/05/2010	-	+	+	CL
45-ZJ-CG	Cui guan	Zhejiang.Hangzhou	01/05/2010	-	-	-	-
46-ZJ-YH	Yuan huang	Zhejiang.Hangzhou	01/05/2010	-	-	+	CL
47-ZJ-YG	Yu guan	Zhejiang.Hangzhou	01/05/2010	-	+	+	CL
1-HB-HGL	Huang gai li	Wuhan.Hubei	12/03/2010	-	N	N	-
2-HB-STL	Shi tang li	Wuhan.Hubei	12/03/2010	-	N	N	-
3-HB-EL2H	E li 2 hao	Wuhan.Hubei	12/03/2010	-	N	N	-
4-HB-ZX	Zao xia	Wuhan.Hubei	12/03/2010	-	N	N	-
5-HB-HPXL	Huang pi xue li	Wuhan.Hubei	12/03/2010	-	N	N	-
6-HB-BDTZL	Ba dong tong zi li	Wuhan.Hubei	12/03/2010	-	N	N	-
7-HB-WNDHL	Wei ning da huang li	Wuhan.Hubei	12/03/2010	+	N	N	-
8-HB-XZ	Xia zhi	Wuhan.Hubei	12/03/2010	-	N	N	-
9-HB-QB	Qiu bai	Wuhan.Hubei	12/03/2010	-	N	N	-
10-HB-HPCBL	Huang pi chang ba tang li	Wuhan.Hubei	12/03/2010	-	N	N	-
11-HB-BTGZ	Bai tang geng zi	Wuhan.Hubei	12/03/2010	-	N	N	-
12-HB-QY	Qing yu	Wuhan.Hubei	12/03/2010	-	N	N	-
13-HB-XLML	Xing long ma li	Wuhan.Hubei	12/03/2010	-	N	N	-
14-HB-HL1H	Hua li 1hao	Wuhan.Hubei	12/03/2010	-	N	N	-
15-HB-J20SJ	Jin 20 shi ji	Wuhan.Hubei	12/03/2010	-	N	N	-
16-HB-SL	Shuai li	Wuhan.Hubei	12/03/2010	-	N	N	-
17-HB-AD	Ai dan	Wuhan.Hubei	12/03/2010	-	N	N	-
18-HB-JQ	Jing qiu	Wuhan.Hubei	12/03/2010	-	N	N	-
19-HB-XZL	Xi zi lv	Wuhan.Hubei	12/03/2010	-	N	N	-
20-HB-BYH	Ba yue hong	Wuhan.Hubei	12/03/2010	-	N	N	-
21-HB-MBL	Mian bao li	Wuhan.Hubei	12/03/2010	-	N	N	-
22-HB-JH	Jin hua	Wuhan.Hubei	12/03/2010	-	N	N	-
23-HB-61-7-7	61-7-7	Wuhan.Hubei	12/03/2010	-	N	N	-
24-HB-HPXL	Huang pi xi li	Wuhan.Hubei	12/03/2010	-	N	N	-
25-HB-MJ	Ming jiang	Wuhan.Hubei	12/03/2010	+	N	N	-

Sample NO.	Cultivars	Source	Collected Date	viruses detection			symptoms
				ASPV	ASGV	ACLSV	
26-HB-CBL	Chang ba li	Wuhan.Hubei	12/03/2010	-	N	N	-
27-HB-AS20SJ	Ao sa 20 shi ji	Wuhan.Hubei	12/03/2010	-	N	N	-
28-HB-STXHL	Shao tong xiao huang li	Wuhan.Hubei	12/03/2010	-	N	N	-
29-HB-SPL	Sang pi li	Wuhan.Hubei	12/03/2010	-	N	N	-
30-HB-HPEL	Huang pi e li	Wuhan.Hubei	12/03/2010	-	N	N	-
1-HN-BL	Ba li	Zhengzhou.Henan	04/11/2010	+	N	N	-
2-HN-DGL	Dong guo li	Zhengzhou.Henan	04/11/2010	-	N	N	-
3-HB-HD	Ha dai	Zhengzhou.Henan	04/11/2010	+	N	N	-
4-HN-SJL	Shui jing li	Zhengzhou.Henan	04/11/2010	+	N	N	-
5-HN-HBLS	Hong bei lei sha	Zhengzhou.Henan	04/11/2010	+	N	N	-
6-HN-HM	Hua mei	Zhengzhou.Henan	04/11/2010	+	N	N	-
7-HN-XHL	Xue hua li	Zhengzhou.Henan	04/11/2010	-	N	N	-
8-HN-LZCB	Lan zhou chang ba	Zhengzhou.Henan	04/11/2010	-	N	N	-
9-HN-DSS	Dang shan su	Zhengzhou.Henan	04/11/2010	-	N	N	-
10-HN-SM	Su mei	Zhengzhou.Henan	04/11/2010	+	N	N	-
11-HN-DSS	Dang shan su	Zhengzhou.Henan	04/11/2010	-	N	N	-
12-HN-HXS	Hong xiang su	Zhengzhou.Henan	04/11/2010	+	N	N	-
13-HN-YL	Ya li	Zhengzhou.Henan	04/11/2010	-	N	N	-
14-HN-GZCB	Gui de chang ba	Zhengzhou.Henan	04/11/2010	-	N	N	-
15-HN-KXY	Kao xi	Zhengzhou.Henan	04/11/2010	-	N	N	-
16-HN-QX	Qing xiang	Zhengzhou.Henan	04/11/2010	+	N	N	-
17-HN-REL	Ruan er li	Zhengzhou.Henan	04/11/2010	-	N	N	-
18-HN-BX	Ba xing	Zhengzhou.Henan	04/11/2010	-	N	N	-
19-HN-BLX	Ba li xiang	Zhengzhou.Henan	04/11/2010	-	N	N	-
20-HN-WX	Wu xiang	Zhengzhou.Henan	04/11/2010	-	N	N	-
21-HN-XMY	Man yuan xiang	Zhengzhou.Henan	04/11/2010	-	N	N	-
22-HN-DXS	Da xiang shui	Zhengzhou.Henan	04/11/2010	-	N	N	-
23-HN-CG	Cui guan	Zhengzhou.Henan	04/11/2010	-	N	N	-
24-HN-HXS	Hong xiang su	Zhengzhou.Henan	04/11/2010	-	N	N	-
25-HN-HJL	Haung jin li	Zhengzhou.Henan	04/11/2010	+	N	N	-
26-HN-ShM	Sheng ma	Zhengzhou.Henan	04/11/2010	+	N	N	-
1-HB-FS	Feng shui	Xianning.Hubei	19/04/2011	-	N	N	-
2-HB-FS	Feng shui	Xianning.Hubei	19/04/2011	+	+	-	-
3-HB-FS	Feng shui	Xianning.Hubei	19/04/2011	+	-	-	-
4-HB-FS	Feng shui	Xianning.Hubei	19/04/2011	-	+	-	-
5-HB-FS	Feng shui	Xianning.Hubei	19/04/2011	-	+	+	-
6-HB-FS	Feng shui	Xianning.Hubei	19/04/2011	-	+	-	-
7-HB-FS	Feng shui	Xianning.Hubei	19/04/2011	-	+	-	-
8-HB-FS	Feng shui	Xianning.Hubei	19/04/2011	+	+	-	-
9-HB-FS	Feng shui	Xianning.Hubei	19/04/2011	-	-	-	-
10-HB-FS	Feng shui	Xianning.Hubei	19/04/2011	-	-	-	-
11-HB-FS	Feng shui	Xianning.Hubei	19/04/2011	-	-	-	-
12-HB-FS	Feng shui	Xianning.Hubei	19/04/2011	-	-	-	-
13-HB-FS	Feng shui	Xianning.Hubei	19/04/2011	+	-	-	-
14-HB-FS	Feng shui	Xianning.Hubei	19/04/2011	+	+	-	-
15-HB-FS	Feng shui	Xianning.Hubei	19/04/2011	-	-	-	-

Sample NO.	Cultivars	Source	Collected Date	viruses detection			symptoms
				ASPV	ASGV	ACLSV	
16-HB-FS	Feng shui	Xianning.Hubei	19/04/2011	-	+	-	-
17-HB-FS	Feng shui	Xianning.Hubei	19/04/2011	+	-	-	-
18-HB-FS	Feng shui	Xianning.Hubei	19/04/2011	-	-	-	-
19-HB-FS	Feng shui	Xianning.Hubei	19/04/2011	-	-	-	-
20-HB-FS	Feng shui	Xianning.Hubei	19/04/2011	+	+	-	-
21-HB-FS	Feng shui	Xianning.Hubei	19/04/2011	+	+	-	-
22-HB-FS	Feng shui	Xianning.Hubei	19/04/2011	-	+	-	-
23-HB-FS	Feng shui	Xianning.Hubei	19/04/2011	-	+	-	-
24-HB-FS	Feng shui	Xianning.Hubei	19/04/2011	-	-	-	-
25-HB-FS	Feng shui	Xianning.Hubei	19/04/2011	-	-	-	-
26-HB-LYX	Liu yue xian	Xianning.Hubei	19/04/2011	+	+	-	-
27-HB-LYX	Liu yue xian	Xianning.Hubei	19/04/2011	-	+	-	-
28-HB-LYX	Liu yue xian	Xianning.Hubei	19/04/2011	-	+	-	-
29--HB-LYX	Liu yue xian	Xianning.Hubei	19/04/2011	-	+	-	-
30-HB-LYX	Liu yue xian	Xianning.Hubei	19/04/2011	-	-	-	-
31-HB-YH	Yuan huang	Xianning.Hubei	19/04/2011	-	-	-	-
32-HB-YH	Yuan huang	Xianning.Hubei	19/04/2011	+	-	-	-
33-HB-YH	Yuan huang	Xianning.Hubei	19/04/2011	-	-	-	-
34-HB-YH	Yuan huang	Xianning.Hubei	19/04/2011	-	-	-	-
35-HB-XS	Xing shui	Xianning.Hubei	19/04/2011	+	+	+	-
36-HB-XS	Xing shui	Xianning.Hubei	19/04/2011	-	-	-	-
37-HB-HH	Haung hua	Xianning.Hubei	19/04/2011	-	+	-	-
38-HB-HJL	Huang jin li	Xianning.Hubei	19/04/2011	+	+	+	-
1-HB- LJHPL	Li jiang huang pi li	Wuhan.Hubei	05/05/2011	-	-	-	-
2-HB-JXCL	Jiu xiang ci li	Wuhan.Hubei	05/05/2011	-	+	-	-
3-HB-HYSL	Han yuan suan li	Wuhan.Hubei	05/05/2011	+	+	+	-
4-HB-SKHT	Si ke hong ta	Wuhan.Hubei	04/2011	+	N	N	-
5-HB-HG	Huang guan	Wuhan.Hubei	04/2011	+	N	N	-
6-HB-XZL	Xi zi lv	Wuhan.Hubei	04/2011	+	N	N	-
7-HB-JH	Jin hua	Wuhan.Hubei	04/2011	+	N	N	-
8-HB-HJL	Huang jin li	Wuhan.Hubei	04/2011	+	N	N	-
9-HB-CL	Cui lv	Wuhan.Hubei	04/2011	+	N	N	-
1-GZ-HT	Hai tang	Guiyang.Guizhou	17/09/2011	+	-	-	-
2-GZ-HT	Hai tang	Guiyang.Guizhou	17/09/2011	+	-	-	-
3-GZ-DGSJ	Da guo shui jing	Guiyang.Guizhou	17/09/2011	-	-	-	-
4-GZ-HJL	Huang jin li	Guiyang.Guizhou	17/09/2011	+	-	-	-
5-GZ-YH	Yuang huang	Guiyang.Guizhou	17/09/2011	+	-	-	FP
6-GZ-YH	Yuang huang	Guiyang.Guizhou	17/09/2011	-	+	-	-
7-GZ-YH	Yuang huang	Guiyang.Guizhou	17/09/2011	-	-	-	-
8-GZ-YH	Yuang huang	Guiyang.Guizhou	17/09/2011	-	-	-	-
9-GZ-YH	Yuang huang	Guiyang.Guizhou	17/09/2011	-	-	-	-
10-GZ-YH	Yuang huang	Guiyang.Guizhou	17/09/2011	-	+		-
11-GZ-YH	Yuang huang	Guiyang.Guizhou	17/09/2011	-	-	-	-
12-GZ-YH	Yuang huang	Guiyang.Guizhou	17/09/2011	-	-	-	-
13-GZ-YH	Yuang huang	Guiyang.Guizhou	17/09/2011	+	+	-	FP
1-HB-HG	Huang guan	Wuhan.Hubei	16/04/2012	-	N	N	-

Sample NO.	Cultivars	Source	Collected Date	viruses detection			symptoms
				ASPV	ASGV	ACLSV	
2-HB-KD	Kang de	Wuhan.Hubei	16/04/2012	-	N	N	-
3-HB-HJ	Huang jin	Wuhan.Hubei	16/04/2012	+	N	N	-
4-HB-AN1H	An nong 1 hao	Wuhan.Hubei	16/04/2012	-	N	N	-
5-HB-JJ	Jin jing	Wuhan.Hubei	16/04/2012	+	N	N	-
6-HB-XHL	Xiang hua li	Wuhan.Hubei	16/04/2012	+	N	N	-
7-HB-DSX	De sheng xiang	Wuhan.Hubei	16/04/2012	-	N	N	-
8-HB-CG	Cui guan	Wuhan.Hubei	16/04/2012	+	N	N	-
9-HB-HL1H	Hua li1hao	Wuhan.Hubei	16/04/2012	+	N	N	-
10-HB-XSJ	Xin shi ji	Wuhan.Hubei	16/04/2012	-	N	N	-
11-HB-HL	Hong li	Wuhan.Hubei	16/04/2012	-	N	N	-
12-HB-XS	Xing shui	Wuhan.Hubei	16/04/2012	-	N	N	-
13-HB-ZL1H	Zhong li 1hao	Wuhan.Hubei	16/04/2012	+	N	N	-
14-HB-KFLS	Kang fu lun si	Wuhan.Hubei	16/04/2012	+	N	N	-
15-HB-FX	Feng xiang	Wuhan.Hubei	16/04/2012	-	N	N	-
16-HB-SMJSL	San men jiang sha li	Wuhan.Hubei	16/04/2012	+	N	N	-
17-HB-JS1H	Jin shui 1 hao	Wuhan.Hubei	16/04/2012	+	N	N	-
18-HB-FS	Feng shui	Wuhan.Hubei	16/04/2012	+	N	N	-
19-HB-YH	Yuan huang	Wuhan.Hubei	16/04/2012	+	N	N	-
20-HB-JH	Jin hua	Wuhan.Hubei	16/04/2012	+	N	N	-
21-HB-JS1H	Jin shui 1 hao	Wuhan.Hubei	16/04/2012	-	N	N	-
22-HB-JS1H	Jin shui 1 hao	Wuhan.Hubei	16/04/2012	-	N	N	-
23-HB-JS1H	Jin shui 1 hao	Wuhan.Hubei	16/04/2012	-	N	N	-
1-JX-HH	Huang hua	Yingtan.Jiangxi	18/04/2012	+	N	N	-
2-JX-JS2H	Jin shui 2 hao	Yingtan.Jiangxi	18/04/2012	+	N	N	-
3-JX-HH	Huang hua	Yingtan.Jiangxi	18/04/2012	-	N	N	-
4-JX-HH	Huang hua	Yingtan.Jiangxi	18/04/2012	+	N	N	-
5-JX-HH	Huang hua	Yingtan.Jiangxi	18/04/2012	+	N	N	-
6-JX-HH	Huang hua	Yingtan.Jiangxi	18/04/2012	+	N	N	-
7-JX-JS2H	Jin shui 2 hao	Yingtan.Jiangxi	18/04/2012	+	N	N	-
8-JX-JS2H	Jin shui 2 hao	Yingtan.Jiangxi	18/04/2012	+	N	N	-
9-JX-JS2H	Jin shui 2 hao	Yingtan.Jiangxi	18/04/2012	+	N	N	-
10-JX-JS2H	Jin shui 2 hao	Yingtan.Jiangxi	18/04/2012	+	N	N	-
11-JX-QX	Qing xiang	Nanchang.Jiangxi	18/04/2012	+	N	N	-
12-JX-QX	Qing xiang	Nanchang.Jiangxi	18/04/2012	+	N	N	-
13-JX-QX	Qing xiang	Nanchang.Jiangxi	18/04/2012	+	N	N	-
14-JX-QX	Qing xiang	Nanchang.Jiangxi	18/04/2012	+	N	N	-
15-JX-CG	Cui guan	Nanchang.Jiangxi	18/04/2012	+	N	N	-
16-JX-CG	Cui guan	Nanchang.Jiangxi	18/04/2012	+	N	N	-
17-JX-CG	Cui guan	Nanchang.Jiangxi	18/04/2012	+	N	N	-
18-JX-CG	Cui guan	Nanchang.Jiangxi	18/04/2012	+	N	N	-
19-JX-CG	Cui guan	Nanchang.Jiangxi	18/04/2012	+	N	N	-
20-JX-CG	Cui guan	Nanchang.Jiangxi	18/04/2012	+	N	N	-
1-LN-KKJJ	Kui ke ju ju	Liaoning.Xingcheng	27/04/2012	-	N	N	-
2-LN-ZS	Zao shu	Liaoning.Xingcheng	27/04/2012	+	N	N	-
3-LN-KKJJ	Kui ke ju ju	Liaoning.Xingcheng	27/04/2012	-	N	N	-
4-LN-SRKF	Se er ke fu	Liaoning.Xingcheng	27/04/2012	+	N	N	-

Sample NO.	Cultivars	Source	Collected Date	viruses detection			symptoms
				ASPV	ASGV	ACLSV	
5-LN-ZSJJ	Zao shu ju ju	Liaoning.Xingcheng	27/04/2012	-	N	N	-
6-LN-XJHL	Xin jiang hua li	Liaoning.Xingcheng	27/04/2012	-	N	N	-
7-LN-HNR	Hong na er	Liaoning.Xingcheng	27/04/2012	-	N	N	-
8-LN-SRKF	Se er ke fu	Liaoning.Xingcheng	27/04/2012	-	N	N	-
9-LN-LJJ	Lv ju ju	Liaoning.Xingcheng	27/04/2012	-	N	N	-
10-LN-NXBT	Nai xi bu te	Liaoning.Xingcheng	27/04/2012	-	N	N	-
11-LN-HNR	Hong na er	Liaoning.Xingcheng	27/04/2012	-	N	N	-
12-LN-BBT	Ba bu te	Liaoning.Xingcheng	27/04/2012	+	N	N	-
13-LN-XJHL	Xin jiang huang li	Liaoning.Xingcheng	27/04/2012	-	N	N	-
14-LN-NXBT	Nai xi bu te	Liaoning.Xingcheng	27/04/2012	-	N	N	-
15-LN-NXBT	Nai xi bu te	Liaoning.Xingcheng	27/04/2012	-	N	N	-
16-LN-KKJJ	Kui ke ju ju	Liaoning.Xingcheng	27/04/2012	+	N	N	-
17-LN-JK61	Jie ke 61	Liaoning.Xingcheng	27/04/2012	-	N	N	-
18-LN-LYS	Lu yi si	Liaoning.Xingcheng	27/04/2012	-	N	N	-
19-LN-JK62	Jie ke 62	Liaoning.Xingcheng	27/04/2012	+	N	N	-
20-LN-BL15	Bo li 15	Liaoning.Xingcheng	27/04/2012	-	N	N	-
21-LN-LYS	Jie ke 62	Liaoning.Xingcheng	27/04/2012	-	N	N	-
22-LN-BL11	Bo li 11	Liaoning.Xingcheng	27/04/2012	-	N	N	-
23-LN-BL	Ba li	Liaoning.Xingcheng	27/04/2012	-	N	N	-
24-LN-AGLM	An ji lie mu	Liaoning.Xingcheng	27/04/2012	-	N	N	-
25-LN-CT	Che tou	Liaoning.Xingcheng	27/04/2012	-	N	N	-
26-LN-CT	Che tou	Liaoning.Xingcheng	27/04/2012	-	N	N	-
27-LN-CT	Che tou	Liaoning.Xingcheng	27/04/2012	-	N	N	-
28-LN-BL15	Bo li 15	Liaoning.Xingcheng	27/04/2012	-	N	N	-
29-LN-RMH	Ri mian hong	Liaoning.Xingcheng	27/04/2012	-	N	N	-
30-LN-B10	Bo 10	Liaoning.Xingcheng	27/04/2012	-	N	N	-
31-LN-RMH	Ri mian hong	Liaoning.Xingcheng	27/04/2012	+	N	N	-
32-LN-AGLM	An ji lie mu	Liaoning.Xingcheng	27/04/2012	-	N	N	-
33-LN-DHT	Da huang tou	Liaoning.Xingcheng	27/04/2012	-	N	N	-
34-LN-SHX	Shui hong xiao	Liaoning.Xingcheng	27/04/2012	-	N	N	-
35-LN-WJX	Wu jiu xiang	Liaoning.Xingcheng	27/04/2012	-	N	N	-
36-LN-SHX	Shui hong xiao	Liaoning.Xingcheng	27/04/2012	-	N	N	-
37-LN-FHX	Fen hong xiao	Liaoning.Xingcheng	27/04/2012	-	N	N	-
38-LN-FHX	Fen hong xiao	Liaoning.Xingcheng	27/04/2012	-	N	N	-
39-LNFHX	Fen hong xiao	Liaoning.Xingcheng	27/04/2012	-	N	N	-
40-LN-LYRL	Lai yang ren li	Liaoning.Xingcheng	27/04/2012	-	N	N	-
41-LN-MTH	Ma ti huang	Liaoning.Xingcheng	27/04/2012	-	N	N	-
42-LN-LYRL	Lai yang ren li	Liaoning.Xingcheng	27/04/2012	-	N	N	-
43-LN-BZMY	Bai zhi mu yang	Liaoning.Xingcheng	27/04/2012	-	N	N	-
44-LN-BZMY	Bai zhi mu yang	Liaoning.Xingcheng	27/04/2012	-	N	N	-
45-LN-LYRL	Lai yang ren li	Liaoning.Xingcheng	27/04/2012	-	N	N	-
46-LN-LYRL	Lai yang ren li	Liaoning.Xingcheng	27/04/2012	-	N	N	-
47-LN-MTH	Ma ti huang	Liaoning.Xingcheng	27/04/2012	-	N	N	-
48-LN-SHX	Shui hong xiao	Liaoning.Xingcheng	27/04/2012	-	N	N	-
49-LN-WJX	Wu jiu xiang	Liaoning.Xingcheng	27/04/2012	-	N	N	-
50-LN-WJX	Wu jiu xiang	Liaoning.Xingcheng	27/04/2012	-	N	N	-

Sample NO.	Cultivars	Source	Collected Date	viruses detection			symptoms
				ASPV	ASGV	ACLSV	
51-LN-RRL	Ruan er li	Liaoning.Xingcheng	27/04/2012	-	N	N	-
52-LN-RRL	Ruan er li	Liaoning.Xingcheng	27/04/2012	-	N	N	-
53-LN-WSJ	Wan san ji	Liaoning.Xingcheng	27/04/2012	+	N	N	-
54-LN-XC	Xing cang	Liaoning.Xingcheng	27/04/2012	-	N	N	-
55-LN-JCZ	Jin chui zi	Liaoning.Xingcheng	27/04/2012	+	N	N	-
56-LN-XC	Xing cang	Liaoning.Xingcheng	27/04/2012	-	N	N	-
57-LN-JL	Jin li	Liaoning.Xingcheng	27/04/2012	-	N	N	-
58-LN-JL	Jin li	Liaoning.Xingcheng	27/04/2012	+	N	N	-
59-LN-JCZ	Jin chui zi	Liaoning.Xingcheng	27/04/2012	-	N	N	-
60-LN-MDX	Man ding xue	Liaoning.Xingcheng	27/04/2012	-	N	N	-
61-LN-ETL	E tou li	Liaoning.Xingcheng	27/04/2012	-	N	N	-
62-LN-SM	Su mu	Liaoning.Xingcheng	27/04/2012	+	N	N	-
63-LN-MDX	Man ding xue	Liaoning.Xingcheng	27/04/2012	-	N	N	-
64-LN-DY	Da yan	Liaoning.Xingcheng	27/04/2012	-	N	N	-
65-LN-GHX	Gaun hong xiao	Liaoning.Xingcheng	27/04/2012	-	N	N	-
66-LN-YL	You li	Liaoning.Xingcheng	27/04/2012	-	N	N	-
67-LN-YL	Ya li	Liaoning.Xingcheng	27/04/2012	-	N	N	-
68-LN-YL	Ya li	Liaoning.Xingcheng	27/04/2012	-	N	N	-
69-LN-ETL	E tou li	Liaoning.Xingcheng	27/04/2012	-	N	N	-
70-LN-DSS	Dang shan su	Liaoning.Xingcheng	27/04/2012	-	N	N	-
71-LN-QB	Qiu bai	Liaoning.Xingcheng	27/04/2012	-	N	N	-
72-LN-DDG	Da dong guo	Liaoning.Xingcheng	27/04/2012	-	N	N	-
73-LN-YL	You li	Liaoning.Xingcheng	27/04/2012	+	N	N	-
74-LN-QB	Qiu bai	Liaoning.Xingcheng	27/04/2012	-	N	N	-
75-LN-YL	Ya li	Liaoning.Xingcheng	27/04/2012	-	N	N	-
76-LN-FXJT	Fen xian ji tui	Liaoning.Xingcheng	27/04/2012	-	N	N	-
77-LN-QB	Qiu bai	Liaoning.Xingcheng	27/04/2012	-	N	N	-
78-LN-ETL	E tou li	Liaoning.Xingcheng	27/04/2012	-	N	N	-
79-LN-DSS	Dang shan su	Liaoning.Xingcheng	27/04/2012	-	N	N	-
80-LN-JL	Jin li	Liaoning.Xingcheng	27/04/2012	-	N	N	-
81-LN-JCZ	Jin chui zi	Liaoning.Xingcheng	27/04/2012	-	N	N	-
82-LN-SM	Su mu	Liaoning.Xingcheng	27/04/2012	-	N	N	-
83-LN-SM	Su mu	Liaoning.Xingcheng	27/04/2012	-	N	N	-
84-LN-FXJT	Feng xian ji tui	Liaoning.Xingcheng	27/04/2012	-	N	N	-
85-LN-DSS	Dang shan su	Liaoning.Xingcheng	27/04/2012	+	N	N	-
86-LN-MYX	Man yuan xiang	Liaoning.Xingcheng	27/04/2012	+	N	N	-
87-LN-LYX	Liu yue xian	Liaoning.Xingcheng	27/04/2012	-	N	N	-
88-LN-TQZ	Tian qiu zi	Liaoning.Xingcheng	27/04/2012	-	N	N	-
89-LN-QZ	Qiu zi	Liaoning.Xingcheng	27/04/2012	-	N	N	-
90-LN-JB	Jian ba	Liaoning.Xingcheng	27/04/2012	-	N	N	-
91-LN-XXS	Xiao xiang shui	Liaoning.Xingcheng	27/04/2012	-	N	N	-
92-LN-LYX	Liu yue xian	Liaoning.Xingcheng	27/04/2012	-	N	N	-
93-LN-JB	Jian ba	Liaoning.Xingcheng	27/04/2012	-	N	N	-
94-LN-QZ	Qiu zi	Liaoning.Xingcheng	27/04/2012	-	N	N	-
95-LN-MYX	Man yuan xiang	Liaoning.Xingcheng	27/04/2012	-	N	N	-
96-LN-QZ	Qiu zi	Liaoning.Xingcheng	27/04/2012	-	N	N	-

Sample NO.	Cultivars	Source	Collected Date	viruses detection			symptoms
				ASPV	ASGV	ACLSV	
97-LN-DXS	Da xiang shui	Liaoning.Xingcheng	27/04/2012	-	N	N	-
98-LN-MYX	Man yuan xiang	Liaoning.Xingcheng	27/04/2012	-	N	N	-
99-LN-BLX	Ba li xiang	Liaoning.Xingcheng	27/04/2012	+	N	N	-
100-LN-MS	Mian suan	Liaoning.Xingcheng	27/04/2012	-	N	N	-
101-LN-LYX	Liu yue xian	Liaoning.Xingcheng	27/04/2012	-	N	N	-
102-LN-DXS	Da xiang shui	Liaoning.Xingcheng	27/04/2012	+	N	N	-
103-LN-BLX	Ba li xiang	Liaoning.Xingcheng	27/04/2012	-	N	N	-
104-LN-DXS	Da xiang shui	Liaoning.Xingcheng	27/04/2012	+	N	N	-
105-LN-TQZ	Tain qiu zi	Liaoning.Xingcheng	27/04/2012	+	N	N	-
106-LN-MS	Mian suan	Liaoning.Xingcheng	27/04/2012	-	N	N	-
107-LN-LYX	Liu yue xiang	Liaoning.Xingcheng	27/04/2012	-	N	N	-
108-LN-JX	Jin xiang	Liaoning.Xingcheng	27/04/2012	-	N	N	-
109-LN-PGL	Ping guo li	Liaoning.Xingcheng	27/04/2012	-	N	N	-
110-LN-BJL	Jing bai li	Liaoning.Xingcheng	27/04/2012	-	N	N	-
111-LN-BJL	Jing bai li	Liaoning.Xingcheng	27/04/2012	-	N	N	-
112-LN-NG	Nan guo li	Liaoning.Xingcheng	27/04/2012	-	N	N	-
113-LN-PGL	Pingguo li	Liaoning.Xingcheng	27/04/2012	+	N	N	-
114-LN-PGL	Pingguo li	Liaoning.Xingcheng	27/04/2012	+	N	N	-
116-LN-KRL	Korla	Liaoning.Xingcheng	27/04/2012	+	N	N	-
117-LN-KRL	Korla	Liaoning.Xingcheng	27/04/2012	+	N	N	-
118-LN-KRL	Korla	Liaoning.Xingcheng	27/04/2012	+	N	N	-
1-GS-ZS	Zao su	Gansu Province	25/04/2012	-	N	N	-
2-GS-ZS	Zao su	Gansu Province	25/04/2012	-	N	N	-
3-GS-ZS	Zao su	Gansu Province	25/04/2012	-	N	N	-
4-GS-ZS	Zao su	Gansu Province	25/04/2012	+	N	N	-
5-GS-ZS	Zao su	Gansu Province	25/04/2012	-	N	N	-
1-SX-XHL	Xue hua li	Taigu.Shanxi	04/05/2012	-	N	N	-
2-SX-YL	Ya li	Taigu.Shanxi	04/05/2012	-	N	N	-
3-SX-NGL	Nan guo li	Taigu.Shanxi	04/05/2012	-	N	N	-
4-SX-HG	Huang guan li	Taigu.Shanxi	04/05/2012	-	N	N	-
5-SX-KRL	Korla	Taigu.Shanxi	04/05/2012	+	N	N	-
6-SX-YLX	Yu lou xiang	Taigu.Shanxi	04/05/2012	+	N	N	-
7-SX-SL	Su li	Taigu.Shanxi	04/05/2012	-	N	N	-
8-SX-BL	Ba li	Taigu.Shanxi	04/05/2012	+	N	N	-
9-SX-HJL	Huang jin li	Taigu.Shanxi	04/05/2012	-	N	N	-
10-SX-PGL	Ping guo li	Taigu.Shanxi	04/05/2012	-	N	N	-
11-SX-FS	Feng shui	Taigu.Shanxi	04/05/2012	-	N	N	-
12-SX-ABTX	A ba te xi	Taigu.Shanxi	04/05/2012	-	N	N	-
13-SX-YLX	Yu lou xiang	Taigu.Shanxi	04/05/2012	-	N	N	-
14-SX-YLX	Yu lou xiang	Taigu.Shanxi	04/05/2012	-	N	N	-
15-SX-YLX	Yu lou xiang	Taigu.Shanxi	04/05/2012	-	N	N	-
16-SX-YLX	Yu lou xiang	Taigu.Shanxi	04/05/2012	+	N	N	-
17-SX-YLX	Yu lou xiang	Taigu.Shanxi	04/05/2012	+	N	N	-
18-SX-XHL	Xue hua li	Taigu.Shanxi	04/05/2012	-	N	N	-
19-SX-YL	Ya li	Taigu.Shanxi	04/05/2012	-	N	N	-
20-SX-XHL	Xue hua li	Taigu.Shanxi	04/05/2012	+	N	N	-

Sample NO.	Cultivars	Source	Collected Date	viruses detection			symptoms
				ASPV	ASGV	ACLSV	
21-SX-XHL	Xue hua li	Taigu.Shanxi	04/05/2012	-	N	N	-
22-SX-XHL	Xue hua li	Taigu.Shanxi	04/05/2012	-	N	N	-
23-SX-SL	Su li	Taigu.Shanxi	04/05/2012	-	N	N	-
24-SX-SL	Su li	Taigu.Shanxi	04/05/2012	-	N	N	-
25-SX-SL	Su li	Taigu.Shanxi	04/05/2012	-	N	N	-
26-SX-SL	Xue hua li	Taigu.Shanxi	04/05/2012	-	N	N	-
27-SX-SL	Su li	Taigu.Shanxi	04/05/2012	-	N	N	-
28-SX-SL	Su li	Taigu.Shanxi	04/05/2012	-	N	N	-
1-SD-H1	-	YanTai.Shandong	06/25/2012	+	N	N	-
2-SD-H2	-	YanTai.Shandong	06/25/2012	-	N	N	-
3-SD-H3	-	YanTai.Shandong	06/25/2012	-	N	N	-
4-SD-H4	-	YanTai.Shandong	06/25/2012	-	N	N	-
5-SD-H5	-	YanTai.Shandong	06/25/2012	+	N	N	-
6-SD-H6	-	YanTai.Shandong	06/25/2012	+	N	N	-
7-SD-J1	-	YanTai.Shandong	06/25/2012	+	N	N	-
8-SD-J2	-	YanTai.Shandong	06/25/2012	-	N	N	-
9-SD-J3	-	YanTai.Shandong	06/25/2012	-	N	N	-
10-SD-J4	-	YanTai.Shandong	06/25/2012	-	N	N	-
11-SD-DL	Du li	YanTai.Shandong	06/25/2012	-	N	N	-
12-SD-KMS	Kao mi si	YanTai.Shandong	06/25/2012	-	N	N	-
13-SD-FS	Fu shi	YanTai.Shandong	06/25/2012	+	N	N	-
14-SD-HQFS	Hong qian fu shi	YanTai.Shandong	06/25/2012	+	N	N	-
15-SD-XG	Xin gao	YanTai.Shandong	06/25/2012	-	N	N	-
1-XJ-D-7-8	Dong-7-8	Xinjiang Province	06/22/2012	-	N	N	-
2-XJ-D-3-1	Dong-3-1	Xinjiang Province	06/22/2012	+	N	N	-
3-XJ-D-5-6	Dong-5-6	Xinjiang Province	06/22/2012	+	N	N	-
4-XJ-D-6-5	Dong-6-5	Xinjiang Province	06/22/2012	+	N	N	-
5-XJ-D-1-3	Dong-1-3	Xinjiang Province	06/22/2012	+	N	N	-
6-XJ-D-2-3	Dong-2-3	Xinjiang Province	06/22/2012	+	N	N	-
7-XJ-XL7H	Xin li 7 hao	Xinjiang Province	06/22/2012	-	N	N	-
8-XJ-XL8H	Xin li 8 hao	Xinjiang Province	06/22/2012	-	N	N	-
9-XJ-QS	Qing song	Xinjiang Province	06/22/2012	-	N	N	-
10-XJ-LY	Lv yun	Xinjiang Province	06/22/2012	+	N	N	-
11-XJ-XY	Xin ya	Xinjiang Province	06/22/2012	+	N	N	-
12-XJ-XF	Xue fang	Xinjiang Province	06/22/2012	+	N	N	-
13-XJ-GG	Gui guan	Xinjiang Province	06/22/2012	+	N	N	-
14-XJ-XX	Xue xin	Xinjiang Province	06/22/2012	+	N	N	-
1-HB-YH	Yuan huang	Xiangyang.Hubei	06/22/2012	+	N	N	-
2-HB-YH	Yuan huang	Xiangyang.Hubei	06/22/2012	+	N	N	-
3-HB-YH	Yuan huang	Xiangyang.Hubei	06/22/2012	+	N	N	-
4-HB-YH	Yuan huang	Xiangyang.Hubei	06/22/2012	+	N	N	-
5-HB-YH	Yuan huang	Xiangyang.Hubei	06/22/2012	+	N	N	-
6-HB-YH	Yuan huang	Xiangyang.Hubei	06/22/2012	+	N	N	-
7-HB-YH	Yuan huang	Xiangyang.Hubei	06/22/2012	+	N	N	-
8-HB-YH	Yuan huang	Xiangyang.Hubei	06/22/2012	+	N	N	-
9-HB-YH	Yuan huang	Xiangyang.Hubei	06/22/2012	+	N	N	-

Sample NO.	Cultivars	Source	Collected Date	viruses detection			symptoms
				ASPV	ASGV	ACLSV	
1-CQ-HG	Huang guan	Chongqing City	05/15/2012	+	+	-	-
2-CQ-HG	Huang guan	Chongqing City	05/15/2012	-	+	-	-
2-CQ-HG	Huang guan	Chongqing City	05/15/2012	-	-	-	-
4-CQ-HG	Huang guan	Chongqing City	05/15/2012	+	-	-	-
5-CQ-CG	Cui guan	Chongqing City	05/15/2012	-	+	-	-
6-CQ-CG	Cui guan	Chongqing City	05/15/2012	+	+	+	-
7-CQ-HH	Huang hua	Chongqing City	05/15/2012	-	+	-	-
8-CQ-HH	Huang hua	Chongqing City	05/15/2012	-	+	-	-
9-CQ-HH	Huang hua	Chongqing City	05/15/2012	-	-	+	-
10-CQ-CG	Cui guan	Chongqing City	05/15/2012	-	-	-	-
11-CQ-CG	Cui guan	Chongqing City	05/15/2012	-	+	+	-
12-CQ-CG	Cui guan	Chongqing City	05/15/2012	-	+	-	-
13-CQ-CG	Huang hua	Chongqing City	05/15/2012	+	+	-	-

Note, * indicated unknown var.;

** indicated virus not detected;

*** indicated no obvious syptoms;

+ indicated viruses were tested positive;

- indicated viruses were tested negtive;

CY: chlorisis leaf;

VY: vein yellow;

FP: Fruit Pitting

Appendix 3 Summary of GenBank Acession number of sequenced ASPV CP 'unique sequences' in this study

Sequence ID	Acesssion Number	Host	Isolate	Clones	Collection Date
HB-HN1-3	JX673791	Pear	HB-HN1	HB-HN1-3	19/Oct/2010
HB-HN2-7	JX673792	Pear	HB-HN2	HB-HN2-7	19/Oct/2010
HB-HN3-3	JX673793	Pear	HB-HN3	HB-HN3-3	19/Oct/2010
HB-HN7-1	JX673795	Pear	HB-HN7	HB-HN7-1	19/Oct/2010
HB-HN7-18	JX673796	Pear	HB-HN7	HB-HN7-18	19/Oct/2010
HB-HN9-16	JX673813	Pear	HB-HN9	HB-HN9-16	19/Oct/2010
HB-HN9-3	JX673797	Pear	HB-HN9	HB-HN9-3	19/Oct/2010
HB-HN10-5	JX673814	Pear	HB-HN10	HB-HN10-5	19/Oct/2010
HB-HN6-8	JX673794	Pear	HB-HN	HB-HN6-8	19/Oct/2010
HB-HN26-10	JX673815	Pear	HB-HN26	HB-HN26-10	19/Oct/2010
HB-STKH-2	JX673816	Pear	HB-STKH	HB-STKH-2	19/Oct/2010
HB-STKH-7	JX673817	Pear	HB-STKH	HB-STKH-7	19/Oct/2010
ZJ-YG1-5	JX673784	Pear	ZJ-YG1	ZJ-YG1-5	06/May/2010
ZJ-YG1-10	JX673828	Pear	ZJ-YG1	ZJ-YG1-10	06/May/2010
ZJ-YG2-1	JX673786	Pear	ZJ-YG2	ZJ-YG2-1	06/May/2010
ZJ-YG2-15	JX673829	Pear	ZJ-YG2-15	ZJ-YG2-15	06/May/2010
YN-MRS-1	JX673901	Pear	YN-MRS	YN-MRS-1	05/Feb/2010
YN-MRS-5	JX673788	Pear	YN-MRS	YN-MRS-5	05/Feb/2010
YN-MRS-17	JX673789	Pear	YN-MRS	YN-MRS-17	05/Feb/2010
YN-MRS-23	JX673790	Pear	YN-MRS	YN-MRS-23	05/Feb/2010
HN-HBLS-1	JX673781	Pear	HN-HBLS	HN-HBLS-1	07/Nov/2010
HN-SJL-1	JX673783	Pear	HN-SJL	HN-SJL-1	07/Nov/2010
HN-SJL-4	JX673787	Pear	HN-SJL	HN-SJL-4	07/Nov/2010
HN-HZT-2	JX673785	Pear	HN-HZT	HN-HZT-2	07/Nov/2010
HN-BL-6	JX673826	Pear	HN-BL	HN-BL-6	07/Nov/2010
HN-HXS-23	JX673799	Pear	HN-HXS	HN-HXS-23	07/Nov/2010
HN-HJL-5	JX673798	Pear	HN-HJL	HN-HJL-5	07/Nov/2010
HN-QX-2	JX673801	Pear	HN-QX	HN-QX-2	07/Nov/2010
HN-HD-13	JX673800	Pear	HN-HD	HN-HD-13	07/Nov/2010
HN-ShM-24	JX673802	Pear	HN-ShM	HN-ShM-24	07/Nov/2010
GZ-YH9-23	JX673805	Pear	GZ-YH9	GZ-YH9-23	18/Sep/2011
GZ-YH1-8	JX673806	Pear	GZ-YH1	GZ-YH1-8	18/Sep/2011
GZ-YH1-14	JX673807	Pear	GZ-YH1	GZ-YH1-14	18/Sep/2011
GZ-YH2-1	JX673808	Pear	GZ-YH2	GZ-YH2-15	18/Sep/2011
CQ-CG3-3	JX673807	Pear	CQ-CG3	CQ-CG3-3	19/May/2012
CQ-CG3-24	JX673810	Pear	CQ-CG3	CQ-CG3-24	19/May/2012
HB-236-18	JX673830	Pear	HB-236	HB-236-18	21/Jun/2012
HB-236-23	JX673812	Pear	HB-236	HB-236-23	21/Jun/2012
HB-YH15-11	JX673818	Pear	HB-YH15	HB-YH15-11	21/Jun/2012
HB-YH15-20	JX673819	Pear	HB-YH15	HB-YH15-20	21/Jun/2012

Sequence ID	Acesssion Number	Host	Isolate	Clones	Collection Date
HB-YH18-13	JX673820	Pear	HB-YH18	HB-YH18-13	21/Jun/2012
HB-YH18-22	JX673821	Pear	HB-YH18	HB-YH18-22	21/Jun/2012
HB-YH21-4	JX673822	Pear	HB-YH21	HB-YH21-4	21/Jun/2012
HB-YH21-11	JX673823	Pear	HB-YH21	HB-YH21-11	21/Jun/2012
HB-YH21-15	JX673824	Pear	HB-YH21	HB-YH21-15	21/Jun/2012
HB-YH23-19	JX673825	Pear	HB-YH23	HB-YH23-19	21/Jun/2012
LN-KRL-24	JX673827	Pear	LN-KRL	LN-KRL-24	21/Jun/2012
LN-AP1-1	JX673803	Apple	LN-AP1	LN-AP1-1	19/Oct/2010
LN-AP1-5	JX673804	Apple	LN-AP1	LN-AP1-5	19/Oct/2010
HB-236-13	JX673811	Pear	HB-236	HB-236-13	21/Jun/2012

Appendix 4 Summary of GenBank Acession number of sequenced ASPV TGB 'unique sequences' in this study

Sequence ID	Accession Number	Host	Isolate	Clones	Collection Date
CQ-CG3-12	JX673832	Pear	CQ-CG3	CQ-CG3-12	15/May/2012
CQ-CG3-4	JX673831	Pear	CQ-CG3	CQ-CG3-4	15/May/2012
GZ-HT1-12	JX673833	Apple	GZ-HT1	GZ-HT1-12	18/Sep/2011
GZ-HT2-12	JX673835	Apple	GZ-HT2	GZ-HT2-12	18/Sep/2011
GZ-HT2-2	JX673834	Apple	GZ-HT2	GZ-HT2-2	18/Sep/2011
GZ-YH1-1	JX673836	Pear	GZ-YH1	GZ-YH1-1	18/Sep/2011
GZ-YH2-15	JX673837	Pear	GZ-YH2	GZ-YH2-15	18/Sep/2011
GZ-YH6-3	JX673838	Pear	GZ-YH6	GZ-YH6-3	18/Sep/2011
GZ-YH9-13	JX673839	Pear	GZ-YH9	GZ-YH9-13	18/Sep/2011
HB-613-2	JX673840	Pear	HB-613	HB-613-2	18/Nov/2011
HB-613-4	JX673841	Pear	HB-613	HB-613-4	18/Nov/2011
HB-613-6	JX673842	Pear	HB-613	HB-613-6	18/Nov/2011
HB-HN1-23	JX673843	Pear	HB-HN1	HB-HN1-23	19/Oct/2010
HB-HN1-35	JX673844	Pear	HB-HN1	HB-HN1-35	19/Oct/2010
HB-HN10-1	JX673854	Pear	HB-HN10	HB-HN10-1	19/Oct/2010
HB-HN2-23	JX673845	Pear	HB-HN2	HB-HN2-23	19/Oct/2010
HB-HN3-16	JX673848	Pear	HB-HN3	HB-HN3-16	19/Oct/2010
HB-HN3-3	JX673846	Pear	HB-HN3	HB-HN3-3	19/Oct/2010
HB-HN3-8	JX673847	Pear	HB-HN3	HB-HN3-8	19/Oct/2010
HB-HN6-1	JX673849	Pear	HB-HN6	HB-HN6-1	19/Oct/2010
HB-HN6-10	JX673850	Pear	HB-HN6	HB-HN6-10	19/Oct/2010
HB-HN7-17	JX673851	Pear	HB-HN7	HB-HN7-17	19/Oct/2010
HB-HN9-1	JX673852	Pear	HB-HN9	HB-HN9-1	19/Oct/2010
HB-HN9-11	JX673853	Pear	HB-HN9	HB-HN9-11	19/Oct/2010
HB-YH15-1	JX673855	Pear	HB-YH15	HB-YH15-1	21/Jun/2012
HB-YH15-6	JX673856	Pear	HB-YH15	HB-YH15-6	21/Jun/2012
HB-YH16-2	JX673857	Pear	HB-YH16	HB-YH16-2	21/Jun/2012
HB-YH16-5	JX673858	Pear	HB-YH16	HB-YH16-5	21/Jun/2012
HB-YH17-12	JX673859	Pear	HB-YH17	HB-YH17-12	21/Jun/2012
HB-YH18-3	JX673860	Pear	HB-YH18	HB-YH18-3	21/Jun/2012
HB-YH19-6	JX673861	Pear	HB-YH19	HB-YH19-6	21/Jun/2012
HB-YH20-9	JX673862	Pear	HB-YH20	HB-YH20-9	21/Jun/2012
HB-YH21-10	JX673863	Pear	HB-YH21	HB-YH21-10	21/Jun/2012
HB-YH22-6	JX673864	Pear	HB-YH22	HB-YH22-6	21/Jun/2012
HB-YH23-3	JX673865	Pear	HB-YH23	HB-YH23-3	21/Jun/2012
HN-BL-2	JX673866	Pear	HN-BL	HN-BL-2	07/Nov/2010
HN-HBLS-1	JX673867	Pear	HN-HBLS	HN-HBLS-1	07/Nov/2010
HN-HBLS-18	JX673869	Pear	HN-HBLS	HN-HBLS-18	07/Nov/2010
HN-HBLS-4	JX673868	Pear	HN-HBLS	HN-HBLS-4	07/Nov/2010
HN-HD-1	JX673870	Pear	HN-HD	HN-HD-1	07/Nov/2010

Sequence ID	Accession Number	Host	Isolate	Clones	Collection Date
HN-HJL-26	JX673871	Pear	HN-HJL	HN-HJL-26	07/Nov/2010
HN-HM-20	JX673872	Apple	HN-HM	HN-HM-20	07/Nov/2010
HN-HXS-19	JX673873	Pear	HN-HXS	HN-HXS-19	07/Nov/2010
HN-HZT-1	JX673874	Pear	HN-HZT	HN-HZT-1	07/Nov/2010
HN-ShM-11	JX673875	Pear	HN-ShM	HN-ShM-11	07/Nov/2010
HN-SJL-1	JX673876	Pear	HN-SJL	HN-SJL-1	07/Nov/2010
HN-SuM-12	JX673877	Pear	HN-SuM	HN-SuM-12	07/Nov/2010
LN-BBT-2	JX673880	Pear	LN-BBT	LN-BBT-2	27/Apr/2012
LN-KRL1-3	JX673882	Pear	LN-KRL1	LN-KRL1-3	27/Apr/2012
LN-KRL1-9	JX673883	Pear	LN-KRL1	LN-KRL1-9	27/Apr/2012
LN-KRL3-4	JX673884	Pear	LN-KRL3	LN-KRL3-4	27/Apr/2012
LN-KRL3-9	JX673885	Pear	LN-KRL3	LN-KRL3-9	27/Apr/2012
LN-PGL-10	JX673887	Pear	LN-PGL	LN-PGL-10	27/Apr/2012
LN-PGL-6	JX673886	Pear	LN-PGL	LN-PGL-6	27/Apr/2012
LN-AP1-1	JX673878	Apple	LN-AP1	LN-AP1-1	17/Sep/2010
LN-AP2-10	JX673879	Apple	LN-AP2	LN-AP2-10	17/Sep/2010
LN-AP3-1	JX673880	Apple	LN-AP3	LN-AP3-1	17/Sep/2010
SD-AP1-1	JX673888	Apple	SD-AP1	SD-AP1-1	17/Oct/2010
SD-AP3-1	JX673889	Apple	SD-AP3	SD-AP3-1	17/Oct/2010
SD-AP3-2	JX673890	Apple	SD-AP3	SD-AP3-2	17/Oct/2010
SD-KMS-11	JX673891	Pear	SD-KMS	SD-KMS-11	22/Jun/2012
SD-KMS-7	JX673892	Pear	SD-KMS	SD-KMS-7	22/Jun/2012
XJ-2-6	JX673893	Pear	XJ-2	XJ-2-6	22/Jun/2012
XJ-2-8	JX673894	Pear	XJ-2	XJ-2-8	22/Jun/2012
XJ-4-10	JX673895	Pear	XJ-4	XJ-4-10	22/Jun/2012
XJ-5-5	JX673896	Pear	XJ-5	XJ-5-5	22/Jun/2012
XJ-5-7	JX673897	Pear	XJ-5	XJ-5-7	22/Jun/2012
XJ-GG-12	JX673898	Pear	XJ-GG	XJ-GG-12	22/Jun/2012
XJ-XF-4	JX673899	Pear	XJ-XF	XJ-XF-4	22/Jun/2012
XJ-XF-8	JX673900	Pear	XJ-XF	XJ-XF-8	22/Jun/2012
YN-MRS-1	JX673901	Pear	YN-MRS	YN-MRS-1	05/Feb/2010
YN-MRS-2	JX673902	Pear	YN-MRS	YN-MRS-2	05/Feb/2010
ZJ-YG1-1	JX673903	Pear	ZJ-YG1	ZJ-YG1-1	06/May/2010
ZJ-YG2-5	JX673904	Pear	ZJ-YG	ZJ-YG2-5	06/May/2010
ZJ-YG2-6	JX673905	Pear	ZJ-YG2	ZJ-YG2-6	06/May/2010

Appendix 5 Prediction of B cell epitope(s) of ASPV CP obtained from six isolates by using on line software ABCPred

YN-MRS-17 Start Position-Sequence (Score)	HB-HN9-3 Start Position-Sequence (Score)	HB-HN6-8 Start Position-Sequence (Score)	HB-HN1-3 Start Position-Sequence (Score)	HB-HN7-18 Start Position-Sequence (Score)	LN-AP1-1 Start Position-Sequence (Score)
56-LVSGFDPNLHGRLSNE (0.92)	140-TSLGSYPFWSGSGASS (0.93)	373-SKEIQMYRIRSMEGTQ (0.91)	21-TAAVSAPISSVAGSTP (0.94)	125-MSLGSYPISFGSGDPS (0.93)	171-TGDIGTPFTLGNRAPR
337-SKEIQMYRIRSMEGTQ (0.91)	216-TGLRNIRYEPQAGVVA (0.91)	21-TAAASAPNSSVAISAP (0.91)	357-SKEIQMYRIRSMEGTQ (0.91)	357-SKEIQMYRIRSMEGTQ (0.91)	359-SKEIQMYRIRSMEGTQ (0.91)
320-DGLIRLPTQAERVANA (0.89)	71-IVSGFDPSLHGRLTNE(0.90)	70-IVSGFDPNLHGRLTNE (0.90)	89-SRHNQRSTSSMAAQNN (0.90)	78-DEAARKGYEEGSRAYQ (0.90)	133-FSSGGTASEPNAQRVF
5-GSDPQASTPMVSAVET (0.87)	185-ASGGGTPFTLGNRAPR (0.90)	356-DGLIRLPTQAERVANA (0.89)	56-IVSGFDPNLHGRLTNE (0.90)	56-IVSGFDPNLHGRLTNE (0.90)	342-DGLIRLPTQAERVANA (0.89)
254-GTMIKQTEGCTLRQYC (0.86)	356-DGLIRLPTQAERVANA (0.89)	216-TGLKNIKYEPQAGVVA (0.89)	125-ESLGPYPTAFGGGSSS (0.90)	340-DGLIRLPTQAERVANA (0.89)	275-VGTIIKQTEGCTLRQY
149-GGNAGTPFTLGNRAPR (0.86)	165-VQHGVSPSSHDANLAT (0.88)	161-IFPQQHGVNPSAHASD (0.89)	340-DGLIRLPTQAERVANA (0.89)	30-SVESSTPVSAPAVSEP (0.89)	150-PQHGVNPSSHGADLAS (0.88)
112-SGSGSASEPNSQRIFP (0.86)	373-SKEIQMFRIRSMEGTQ (0.87)	30-SVAISAPTSAPAASEP (0.88)	274-GTMIKQTEGCTLRQYC (0.86)	116-GTAYSGAPRMSLGSYP (0.89)	267-GSDITLEEVGTIIKQT (0.86)
76-AQSETSRYASMNSNPF (0.85)	21-TVPASTPVSDAVSLAP (0.87)	147-FPEGGNASEPNSHRIF (0.87)	166-NQTGGNTGTPFTLGNR (0.86)	4-NGSQPPSSTPIASVDE (0.88)	202-VGLRNIRYEPQAGVVA (0.86)
356-FGEVTGGKVGPKPVLS (0.85)	290-GTMIKQTEGCTLRQYC (0.86)	290-GTMIKQTEGCTLRQYC (0.86)	240-VGVYLARHCADVGASD (0.85)	147-IFPQRHGVNPSAHASD (0.87)	242-VGVYLARHCADVGASD (0.85)
220-VGVYLARHCADVGASD(0.85)	256-VGVYLARHCADVGASD (0.85)	185-GGNAGTPFTLGNRAPR (0.86)	265-GSDITLEEVGTMIKQT (0.83)	274-GTMIKQTEGCTLRQYC (0.86)	82-RQGYEEGSRPSQRFVP (0.83
180-IGLKSIRYEPQAGVVA (0.85)	110-SSLSTSANTNYASMSS (0.85)	256-VGVYLARHCADVGASD (0.85)	224-GVALIGMGIPEHQLTE (0.83)	21-TAAASAPISSVESSTP (0.86)	226-GVALIGIGIPEHQLTE (0.83)
141-LVPHQATSGGNAGTPF (0.84)	4-DGTQPPASTPMVSVEE (0.83)	200-RNVTSNAGGMRRRLDS (0.85)	117-TAYGGAPLESLGPYPT (0.82)	240-VGVYLARHCADVGASD (0.85)	163-LASNQTNVTGDIGTPF (0.82)
245-GSDITLEEVGTMIKQT (0.83)	281-GSDITLEEVGTMIKQT (0.83)	281-GSDITLEEVGTMIKQT(0.83)	82-RQGFEAGSRHNQRSTS (0.81)	265-GSDITLEEVGTMIKQT (0.83)	14-MVSVEEPVAQVSAPNP (0.82)
204-GVALIGMGIPEHQLTE (0.83)	240-GVALIGMGIPEHQLTE (0.83)	240-GVALIGMGIPEHQLTE(0.83)	200-IGLKNIRYEPQAGVVA (0.81)	224-GVALIGMGIPEHQLTE (0.83)	56-IVSGFDPTLHGRLTSE (0.80)
168-TNTGGMRRRLDSIGLK (0.83)	206-TGGMRRRLDSTGLRNI (0.82)	137-PHVGMGPYLSFPEGGN (0.83)	147-IFPLQHGVNPSAHASN (0.80)	133-SFGSGDPSEPNSQRIF (0.83)	186-RNAAASTGGMRRRLDS (0.80)
125-IFPLQHGVNPSAHASD (0.83)	151-SGASSEPNAQRIFQVQ (0.80)	119-YASINSNPFETGIAYS (0.83)	329-GVESTASLEPADGLIR (0.79)	317-SETRYAAFDFFFGVES (0.82)	97-PSTAAYNNYASMNSNP (0.79)
30-SVDSSAPTSAPAASEP (0.82)	51-PVGTSAASEFIVSQVQ (0.79)	128-ETGIAYSLAPHVGMGP (0.82)	7-QPPSSTPISSVEDSTA (0.78)	200-IGLKNIRYEPQAGVVA (0.81)	331-GVESTASLEPADGLIR (0.79)
103-ASMGPYLTLSGSGSAS (0.81)	345-GVESTASLEPADGLIR (0.79)	92-DEAARKGYEEGSRQRQ (0.81)	49-QVQSLAPIVSGFDPNL (0.78)	92-YQRSTSSTAAHNIYAS (0.80)	192-TGGMRRRLDSVGLRNI (0.79)
21-TAAASAPISSVDSSAP (0.80)	100-FEEGSRSNRRSSLSTS (0.79)	206-AGGMRRRLDSTGLKNI (0.81)	133-AFGGGSSSEPNSQRIF (0.78)	329-GVESTASLEPADGLIR (0.79)	156-PSSHGADLASNQTNVT (0.79)
155-PFTLGNRAPRNATTNT (0.80)	200-RNATSNTGGMRRRLDS (0.78)	36-PTSAPAASEPASLAPA (0.79)	282-GCTLRQYCAFYAKHVW (0.77)	49-QVQSLAPIVSGFDPNL (0.78)	141-EPNAQRVFPPQHGVNP (0.79)
309-GVESTASLEPADGLIR (0.79)	298-GCTLRQYCAFYAKHVW (0.77)	345-GVESTASLEPADGLIR (0.79)	153-GVNPSAHASNFAPNQT (0.77)	311-VGKVFKSETRYAAFDF (0.78)	112-PFETGTAYSDAPQLNM (0.79)
262-GCTLRQYCAFYAKHVW (0.77)	333-FETRYAAFDFFFGVES (0.76)	63-QVQSLAPIVSGFDPNL (0.78)	317-FETRYAAFDFFFGVES (0.76)	169-SVNTGTPFTLGNRAPR (0.78)	284-GCTLRQYCAFYAKHVW (0.77)
90-PFETGTAYSEAPRASM (0.76)	93-GEAARKGFEEGSRSNR (0.75)	77-NLHGRLTNEQMRQAQD (0.77)	30-SVAGSTPASVPAVSGP (0.75)	63-NLHGRLTNEQMRQAQD (0.77)	4-NGSQPPASAPMVSVEE (0.76)
49-QVQTLAPLVSGFDPNL (0.76)	191-PFTLGNRAPRNATSNT (0.75)	7-QPQTSTPLSSVAESTA (0.77)	175-PFTLGNRAPRNVTANT (0.75)	282-GCTLRQYCAFYAKHVW (0.77)	319-FETRYAAFDFFFGVES (0.76)
297-FETRYAAFDFFFGVES (0.760)	327-VGKEFKFETRYAAFDF (0.74)	298-GCTLRQYCAFYAKHVW (0.77)	311-VGKEFKFETRYAAFDF (0.74)	141-EPNSQRIFPQRHGVNP (0.77)	89-SRPSQRFVPSTAAYNN (0.75)
291-VGKEFKFETRYAAFDF (0.74)	393-GEVTGGKIGPKPVLSI (0.72)	109-STSSSAPHVNYASINS (0.77)	206-RYEPQAGVVASNQKIS (0.74)	105-YASINSNPFETGTAYS (0.77)	49-QVQSLAPIVSGFDPTL (0.74)

YN-MRS-17 Start Position-Sequence (Score)	HB-HN9-3 Start Position-Sequence (Score)	HB-HN6-8 Start Position-Sequence (Score)	HB-HN1-3 Start Position-Sequence (Score)	HB-HN7-18 Start Position-Sequence (Score)	LN-AP1-1 Start Position-Sequence (Score)
96-AYSEAPRASMGPYLTL (0.71)	250-EHQLTEVGVYLARHCA (0.71)	333-FETRYAAFDFFFGVES (0.76)	188-ANTGGMRRRLDSIGLK (0.74)	175-PFTLGNRAPRNVTANT (0.75)	313-VGKEFKFETRYAAFDF (0.74)
214-EHQLTEVGVYLARHCA (0.71)	382-RSMEGTQAVNFGEVTG (0.69)	175-SDLVPTTVASGGNAGT (0.75)	182-APRNVTANTGGMRRRL (0.74)	188-ANTGGMRRRLDSIGLK (0.74)	21-VAQVSAPNPSVVSSVP (0.74
36-PTSAPAASEPVISQVQ (0.70)	34-LAPVSAPISSVNAVSS (0.69)	327-VGKEFKFETRYAAFDF (0.74)	159-HASNFAPNQTGGNTGT (0.74)	182-APRNVTANTGGMRRRL (0.74)	29-PSVVSSVPVSVPTVSE (0.73)
346-RSMEGTQAVNFGEVTG (0.69)	315-LMLQTQSPPANWVGKE (0.69)	393-GEVTGGKIGPKPVLSI (0.72)	377-GEVTGGKIGPKPVLSI (0.72)	10-SSTPIASVDETTAAAS (0.73)	177-PFTLGNRAPRNAAAST (0.73)
279-LMLQTQSPPANWVGKE (0.69)	363-TQAERVANATSKEIQM (0.68)	191-PFTLGNRAPRNVTSNA (0.72)	43-SGPVISQVQSLAPIVS (0.71)	377-GEVTGGKIGPKPVLSI (0.72)	125-LNMGPYPTFSSGGTAS (0.73)
327-TQAERVANATSKEIQM (0.68)	339-AFDFFFGVESTASLEP (0.68)	250-EHQLTEVGVYLARHCA (0.71)	234-EHQLTEVGVYLARHCA (0.71)	234-EHQLTEVGVYLARHCA (0.71)	379-GEVTGGKIGPKPVLSI (0.72)
303-AFDFFFGVESTASLEP (0.680	304-YCAFYAKHVWNLMLQT (0.66)	153-ASEPNSHRIFPQQHGV (0.71)	97-SSMAAQNNYASINSNP (0.70)	43-SEPVISQVQSLAPIVS (0.69)	236-EHQLTEVGVYLARHCA (0.71)
63-NLHGRLSNEQMRQAQS (0.67)	86-EQMRQAQGEAARKGFE (0.65)	222-KYEPQAGVVASNQKIR (0.70)	366-RSMEGTQAVNFGEVTG (0.69)	366-RSMEGTQAVNFGEVTG (0.69)	43-SEPVISQVQSLAPIVS (0.69)
268-YCAFYAKHVWNLMLQT (0.66)	58-SEFIVSQVQSLAPIVS (0.65)	382-RSMEGTQAVNFGEVTG (0.69)	299-LMLQTQSPPANWVGKE (0.69)	299-LMLQTQSPPANWVGKV (0.69)	368-RSMEGTQAVNFGEVTG (0.69)
133-NPSAHASDLVPHQATS (0.66)	40-PISSVNAVSSAPVGTS (0.64)	315-LMLQTQSPPANWVGKE (0.69)	347-TQAERVANATSKEIQM (0.68)	347-TQAERVANATSKEIQM (0.68)	301-LMLQTQSPPANWVGKE (0.69)
82-RYASMNSNPFETGTAY (0.63)	131-GFAFSEAPRTSLGSYP (0.64)	363-TQAERVANATSKEIQM (0.68)	323-AFDFFFGVESTASLEP (0.68)	323-AFDFFFGVESTASLEP (0.68)	349-TQAERVANATSKEIQM (0.68)
186-RYEPQAGVVASNQKIR (0.63)	222-RYEPQAGVVASNQKIR (0.63)	339-AFDFFFGVESTASLEP (0.68)	194-RRRLDSIGLKNIRYEP (0.68)	194-RRRLDSIGLKNIRYEP (0.68)	325-AFDFFFGVESTASLEP (0.68)
119-EPNSQRIFPLQHGVNP (0.630	176-ANLATQQASASGGGTP (0.62)	53-TPVASAPVISQVQSLA (0.67)	288-YCAFYAKHVWNLMLQT (0.66)	288-YCAFYAKHVWNLMLQT (0.66)	71-EQMRQAQGEAARQGYE (0.66)
12-TPMVSAVETTAAASAP (0.62)	121-ASMSSNPFETGFAFSE (0.62)	45-PASLAPASTPVASAPV (0.67)	141-EPNSQRIFPLQHGVNP (0.63)	160-ASDLAPDQASVNTGTP (0.66)	290-YCAFYAKHVWNLMLQT (0.66)
197-NQKIRAVGVALIGMGI (0.61)	233-NQKIRAVGVALIGMGI (0.61)	304-YCAFYAKHVWNLMLQT (0.66)	105-YASINSNPFETGTAYG (0.63)	36-PVSAPAVSEPVISQVQ (0.65)	63-TLHGRLTSEQMRQAQG (0.63)
235-DKSTLLGTFPGSDITL (0.59)	78-SLHGRLTNEQMRQAQG (0.60)	233-NQKIRAVGVALIGMGI (0.61)	217-NQKISAVGVALIGMGI (0.62)	255-DRSTLLGTFPGSDITL (0.63)	36-PVSVPTVSEPVISQVQ (0.63)
	271-DKSTLLGTFPGSDITL (0.59)	271-DKSTLLGTFPGSDITL (0.59)	63-NLHGRLTNEQMRQAQG (0.59)	206-RYEPQAGVVASNQKIR (0.63)	208-RYEPQAGVVASNHKIR (0.62)
			255-DKSTLLGTFPGSDITL (0.59)	217-NQKIRAVGVALIGMGI (0.61)	257-DKSTLLGTFPGSDITL (0.59)
			13-PISSVEDSTAAVSAPI (0.57)	248-CADVGASDRSTLLGTF (0.58)	
				305-SPPANWVGKVFKSETR (0.51)	

Appendix 6 Determination of work concentration of the polyclonal antibodies made in our study by indirect ELISA

Antigen Diluted Concentration	OD_{450}* (Negtive)	PAb-HB-HN6-8		OD_{450} (Negtive)	PAb-YN-MRS-17		OD_{450} (Negtive)	PAb-HB-HN9-3	
		OD_{450}	P/N		OD_{450}	P/N		OD_{450}	P/N
1:1000	0.081	1.365	16.957	0.018	0.613	34.028	0.262	1.272	4.864
1:2000	0.071	1.155	16.376	0.018	0.505	28.829	0.136	0.991	7.314
1:4000	0.037	0.895	24.521	0.010	0.381	38.100	0.068	0.748	10.993
1:8000	0.031	0.581	19.049	0.011	0.304	27.591	0.043	0.465	10.814
1:16000	0.014	0.316	23.370	0.019	0.185	10.000	0.027	0.228	8.426
1:32000	0.036	0.156	4.380	0.008	0.120	15.000	0.005	0.118	23.600
1:64000	0.022	0.095	4.295	0.010	0.067	7.000	0.005	0.116	23.100
1:128000	0.029	0.054	1.877	0.003	0.046	18.400	0.000	0.021	——
1:256000	0.005	0.048	9.600	0.009	0.012	1.412	-0.009	0.020	-2.294
1:512000	0.008	0.026	3.400	0.013	0.012	0.960	-0.010	-0.005	0.500
1:1024000	0.0045	0.022	4.788	0.016	0.011	0.656	0.002	-0.011	-5.500

Notes, OD_{450}*indicated the absorbance under the wavelength of 450 nm.

Appendix 7 Determination of work concentration of PAb-HB-HN6-8 to detected ASPV CP fused proteins expressed in prokaryote by indirect ELISA

Antigen	Treatment	Blank	Diluted Concentration										
			1:1000	1:2000	1:4000	1:8000	1:16000	1:32000	1:64000	1:128000	1:256000	1:512000	1:102400
Negitive HB-HN6-8	1	-0.017	0.074	0.094	0.045	0.030	0.016	0.034	0.032	0.042	0.009	0.015	0.007
	2	-0.032	0.087	0.047	0.028	0.031	0.011	0.037	0.012	0.015	0.001	0.000	0.002
	Average	-0.025	0.081	0.071	0.037	0.031	0.014	0.036	0.022	0.029	0.005	0.008	0.0045
HB-HN6-8	1	0.000	1.362	1.218	1.031	0.698	0.356	0.149	0.092	0.056	0.081	0.027	0.020
	2	-0.030	1.368	1.091	0.759	0.464	0.275	0.162	0.097	0.051	0.015	0.024	0.023
	Average	-0.015	1.365	1.155	0.895	0.581	0.316	0.156	0.095	0.054	0.048	0.026	0.022
	P/N	-	16.957	16.376	24.521	19.049	23.370	4.380	4.295	1.877	9.600	3.400	4.778
HB-HN9-3	1	0.000	0.961	0.657	0.419	0.246	0.165	0.104	0.023	0.017	-0.005	0.003	-0.011
	2	0.031	1.112	0.762	0.477	0.302	0.239	0.107	0.041	0.022	0.006	0.002	-0.005
	Average	0.016	1.037	0.710	0.448	0.274	0.202	0.106	0.032	0.020	0.001	0.003	-0.008
	P/N	-	12.876	10.064	12.274	8.984	14.963	2.972	1.455	0.684	0.100	0.333	-1.778
YN-MRS-17	1	0.000	0.608	0.368	0.230	0.150	0.082	0.035	0.022	0.015	0.014	0.002	0.009
	2	-0.005	0.666	0.454	0.263	0.131	0.074	0.024	0.023	0.004	-0.001	-0.004	-0.001
	Average	-0.003	0.637	0.411	0.247	0.141	0.078	0.030	0.023	0.010	0.007	-0.001	0.004
	P/N	-	7.913	5.830	6.753	4.607	5.778	0.831	1.023	0.333	1.300	-0.133	0.889

Appendix 8 Determination of work concentration of PAb-HB-HN9-3 to detected ASPV CP fused proteins expressed in prokaryote by indirect ELISA

Antigen	Treatment	Blank	Diluted Concentration										
			1:1000	1:2000	1:4000	1:8000	1:16000	1:32000	1:64000	1:128000	1:256000	1:512000	1:102400
Negive HB-HN9-3	1	0.017	0.265	0.134	0.073	0.048	0.036	0.010	0.000	-0.004	-0.011	-0.008	0.009
	2	-0.008	0.258	0.137	0.063	0.038	0.018	0.000	0.010	0.004	-0.006	-0.012	-0.005
	Average	0.005	0.262	0.136	0.068	0.043	0.027	0.005	0.005	0.000	-0.009	-0.010	0.002
HB-HN9-3	1	0.013	1.204	0.937	0.729	0.436	0.228	0.115	0.153	0.014	0.016	-0.002	-0.016
	2	0.008	1.340	1.045	0.766	0.494	0.227	0.121	0.078	0.027	0.023	-0.008	-0.006
	Average	0.011	1.272	0.991	0.748	0.465	0.228	0.118	0.116	0.021	0.020	-0.005	-0.011
	P/N	-	4.864	7.314	10.993	10.814	8.426	23.600	23.100	-	-2.294	0.500	-5.500
YN-MRS-17	1	0.002	0.855	0.659	0.395	0.242	0.172	0.108	0.049	0.020	-0.004	-0.012	0.002
	2	-0.007	0.928	0.789	0.415	0.265	0.139	0.069	0.024	0.008	-0.007	-0.017	-0.007
	Average	-0.003	0.892	0.724	0.405	0.254	0.156	0.089	0.037	0.014	-0.006	-0.015	-0.003
	P/N	-	3.409	5.343	5.956	5.895	5.759	17.700	7.300	-	0.647	1.450	-
HB-HN6-8	1	-0.005	1.513	1.478	1.276	0.908	0.536	0.294	0.166	0.060	0.030	0.012	-0.005
	2	0.006	1.684	1.455	1.333	0.995	0.632	0.348	0.186	-0.044	0.039	0.065	0.006
	Average	0.001	1.599	1.467	1.305	0.952	0.584	0.321	0.176	0.008	0.035	0.039	0.001
	P/N	-	6.113	10.823	19.184	22.128	21.630	64.200	35.200	-	-4.059	-3.850	-

Appendix 9 Determination of work concentration of PAb-YN-MRS-17 to detected ASPV CP fused proteins expressed in prokaryote by indirect ELISA

Antigen	Treatment	Blank	Diluted Concentration										
			1:1000	1:2000	1:4000	1:8000	1:16000	1:32000	1:64000	1:128000	1:256000	1:512000	1:102400
Negtive YN-MRS-17	1	-0.005	0.025	0.022	0.008	0.007	0.021	0.008	0.011	0.008	0.009	0.012	0.023
	2	0.027	0.011	0.013	0.012	0.015	0.016	0.008	0.008	-0.003	0.008	0.013	0.009
	Average	0.011	0.018	0.018	0.010	0.011	0.019	0.008	0.010	0.003	0.009	0.013	0.016
YN-MRS-17	1	-0.001	0.586	0.506	0.402	0.357	0.185	0.142	0.074	0.048	0.009	0.016	0.013
	2	0.001	0.639	0.503	0.360	0.250	0.185	0.098	0.059	0.044	0.015	0.008	0.008
	Average	0.000	0.613	0.505	0.381	0.304	0.185	0.120	0.067	0.046	0.012	0.012	0.011
	P/N	-	34.028	28.829	38.100	27.591	10.000	15.000	7.000	18.400	1.412	0.960	0.656
HB-HN9-3	1	0.002	0.478	0.398	0.258	0.208	0.119	0.051	0.034	0.024	0.009	0.010	0.013
	2	-0.003	0.452	0.352	0.236	0.149	0.106	0.050	0.034	0.025	0.005	0.000	0.004
	Average	-0.001	0.465	0.375	0.247	0.179	0.113	0.051	0.034	0.025	0.007	0.005	0.009
	P/N	-	25.833	21.429	24.700	16.227	6.081	6.313	3.579	9.800	0.824	0.400	0.531
HB-HN6-8	1	0.000	0.521	0.429	0.321	0.270	0.201	0.091	0.049	0.045	0.022	0.028	0.009
	2	0.006	0.606	0.474	0.426	0.292	0.157	0.108	0.054	0.035	0.024	0.011	0.006
	Average	0.003	0.564	0.452	0.374	0.281	0.179	0.100	0.052	0.040	0.023	0.020	0.008
	P/N	0.273	31.306	25.800	37.350	25.545	9.676	12.438	5.421	16.000	2.706	1.560	0.469

Appendix 10 pGEM®-T vector information

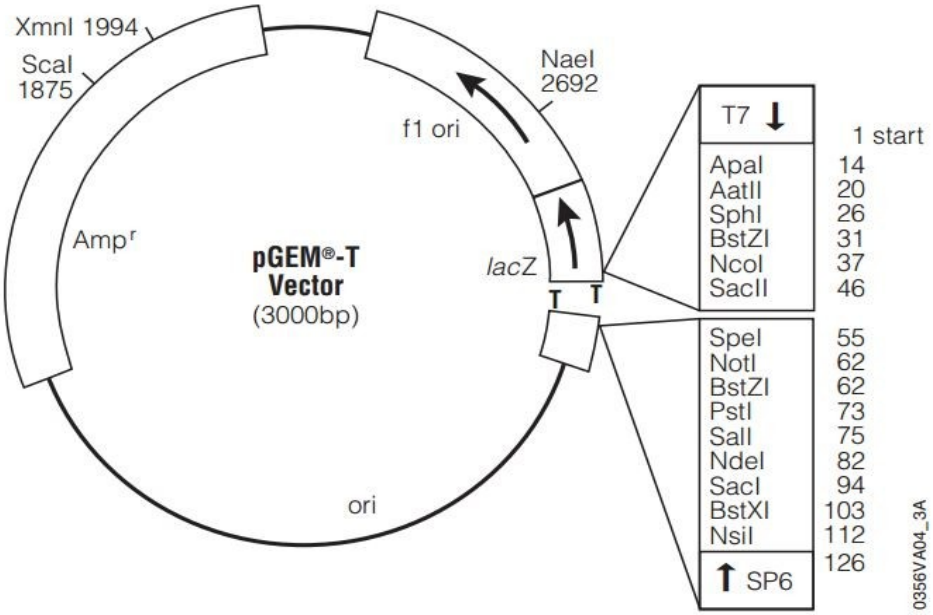

pGEM®-T Vector sequence reference points:

T7 RNA polymerase transcription initiation site	1
Multiple cloning region	10–113
SP6 RNA polymerase promoter (–17 to +3)	124–143
SP6 RNA polymerase transcription initiation site	126
pUC/M13 Reverse Sequencing Primer binding site	161–177
*lac*Z start codon	165
lac operator	185–201
β-lactamase coding region	1322–2182
phage f1 region	2365–2820
lac operon sequences	2821–2981, 151–380
pUC/M13 Forward Sequencing Primer binding site	2941–2957
T7 RNA polymerase promoter (–17 to +3)	2984–3

Note: Inserts can be sequenced using the SP6 Promoter Primer, T7 Promoter Primer, pUC/M13 Forward Primer, or pUC/M13 Reverse Primer.

Appendix 11 pET-28a (+) vector information

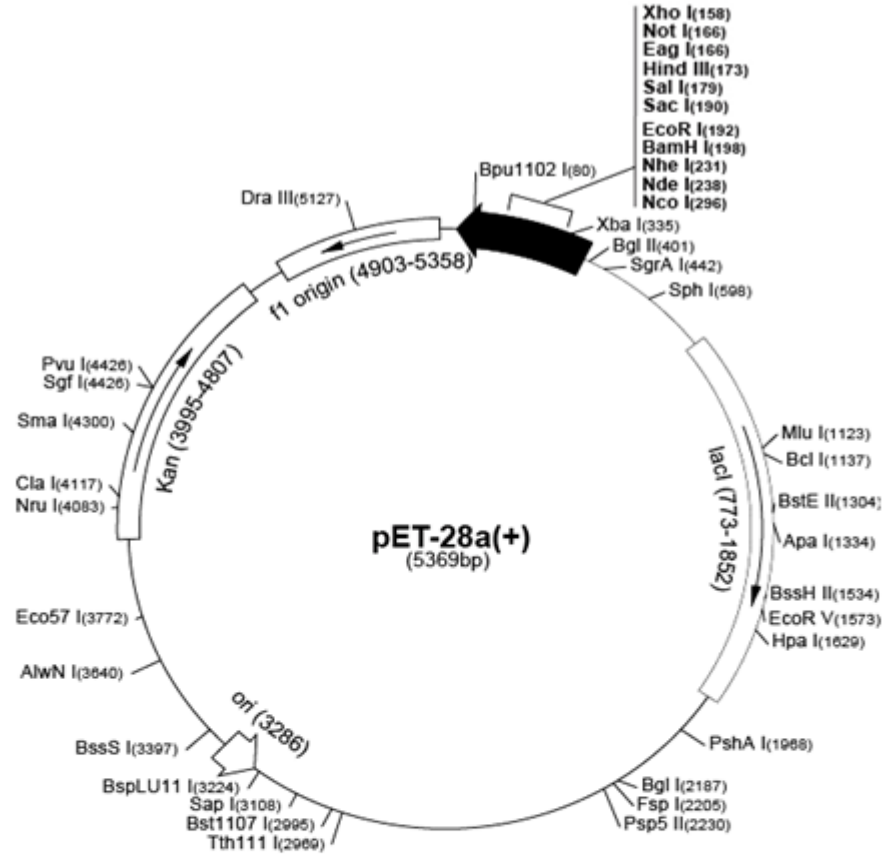

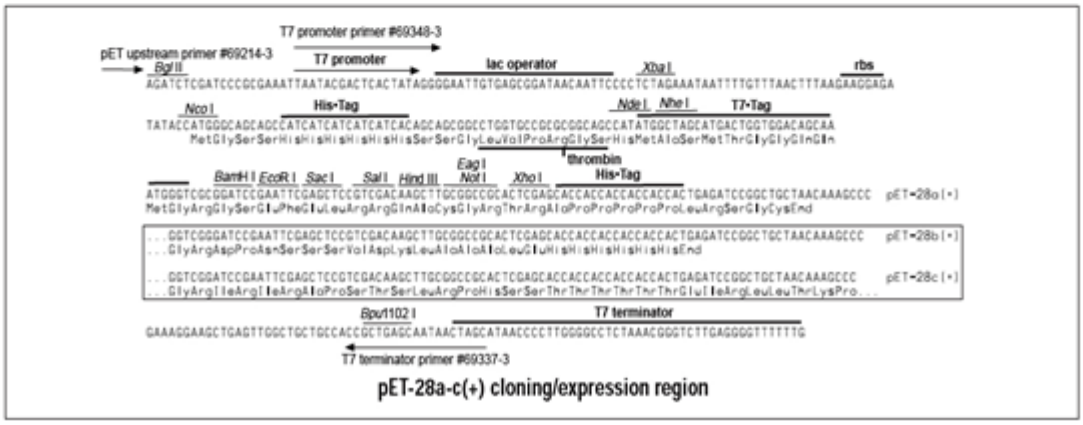

Appendix 12 All formulations of solutions in this study

Solutions for Western Blot

1. Total proteins extracting buffer from *Arabidopsis thaliana* and *Nicotiana benthamiana*: 25 mM Tris-HCl pH 7.5, 1 mM EDTA, 150 mM NaCl, 10% glycerol, adding 1%（V/V）protease inhibitor and 5 mM DTT before use.
2. 9.5 mL 5×Loading Buffer: 1.2 ml 0.5 M Tris/HCl, pH6.8, 5 ml 50% glycerol, 2 ml, 10% SDS, 1 ml 10 mg/ml bromophenol blue, 0.3 ml dd H_2O, store at 4°C in aliquots (950 µl/tube), add 50 µl β-mercaptoethanol (v/v) into each tubes before use.
3. 30% Acr-Bis: 29 g Acrylamide, 1 g N'-methylene-bis acrylamide, dissolve at 37°C in 100 ml dd H_2O, store in dark at 4°C.
4. 12% SDS-PAGE resolving gels：30% Acrylamide 4 ml, 1.5 mol/L Tris-HCl (pH8.8) 2.5 ml, 10% SDS 0.1 ml, 10% APS 0.1 ml, TEMED 10 µl, add ddH_2O to 10 ml.
5. 5% SDS-PAGE stacking gels：30% Acrylamide 1.34 ml, 1.0 mol/L Tris-HCl (pH6.8) 0.5 ml, 10% SDS 80 µl, 10% APS 80 µl, TEMED 8 µl, add ddH_2O to 8 ml.
6. 10×Tris-Glycine electrophoresis buffer: 15.1 g Tris, 94 g, Glycine, 10% SDS 50 ml, add ddH_2O to dissolve and to 1000 ml, adjust to pH 8.3.
7. 1×Transfer Buffer: 100 ml 10×Running buffer, 200 ml Methyl Alcohol, aad ddH_2O to 1000 ml.
8. 10×Running Buffer: 144 g Glycine, 30 g Tris-Base, aad ddH_2O to 1000 ml.
9. 10×TBS: 80 g NaCl, 24.2 g Tris-Base, adjust to pH 7.6, aad ddH_2O to 1000 ml.
10. 1×T-TBS: 100 ml 10×TBS, 500-1000 µl Tween-20, aad ddH_2O to 1000 ml.
11. 5% Blocking Buffer: 5 g skimmed milk, add 1×T-TBS to a final volumn 100 ml.
12. Commassie Blue Staining Solution: 45 ml Methyl Alcohol, 45 ml ddH_2O, 10 ml Acetic Acid, 0.25 g Commassie Blue G250 or R250.
13. Commassie Blue destaining Solution: 45 ml Methyl Alcohol, 45 ml ddH_2O, 10 mlAcetic Acid.
14. IPTG (1 M/L): 1 g IPTG dissolve in 4.2 ml ddH_2O, autoclaved by biofilter, then store at -20°C in aliquots.

Solutions for Polysome Extraction

1. Polysome Extraction Buffer (PEB buffer): 0.2M Tris-HCl, pH 9.0, 0.2 M KCl, 25 mM EGTA, 35 mM $MgCl_2$, 1% Detergent mix [1% (w/v) polyoxyethylene(23) lauryl ether (Brij-35), 1% (v/v) Triton X-100, 1% (v/v) octylphenyl-polyethylene glycol (Igepal CA630), 1% (v/v) polyoxyethylene sorbitan monolaurate 20], 1% deoxycholic acid sodium salt, 1% Polyoxyethlene (10) tridecyl ether, 5 mM DTT, 1×protease inhibitors, 50 μg/ml Cycloheximide, 50 μg/ml Chloramphenicol.
2. 1.6 M sucrose cushion solution: 0.4 M Tris-HCl, pH 9.0, 0.2 M KCl, 5mM EGTA, 35 mM $MgCl_2$, 1.7 M sucrose, 5 mM DDT, 50 μg/ml, Cycloheximide, 50 μg/ml Chloramphenicol.
3. Resuspension Buffer: 0.2 M Tris-HCl, pH 9.0, 0.2M KCl, 25 mM EGTA, 35 mM $MgCl_2$, 5 mM DDT, 50 μg/mL Cycloheximide, 50 μg/ml Chloramphenicol.
4. Sucrose gradients: 15%–60% sucrose [w/v], 10 mM Tris-HCl, pH 7.5, 140 mM KCl, 1.5 mM MgCl2, 100 μg/mL Chloramphenicol, 100 μg/mL Cycloheximide.

Solutions for Northern Blot

1. 10 ml 5× RNA loading buffer: 16 μl saturated aqueous bromophenol blue solution , 80 μl 500 mM EDTA, pH 8.0, 720 μl 37% formaldehyde, 2 ml 100% glycerol, 3084 μl Formamide, 4 ml 10×MOPS buffer , add RNase-free water to 10 ml.
2. 20×SSC: 175.3 g NaCl, 88.2 g, 88.2 g Sodium citrate, adjust to pH 7.0.
3. 10×MOPS: 41.9 g 3-Morpholinopropanesulfonic Acid, 8.2 g Sodium acetate.$3H_2O$, 3.72 g EDTA, adjust to pH 7.0.
4. 1L 1×MOPS: 100 ml 10×MOPS, 20 ml 37% formaldehyde, 880 ml ddH_2O.
5. 2×SSC, 0.1% SDS: 100 ml 20×SSC, 10 ml 10% SDS.
6. 0.1×SSC, 0.1% SDS: 50 ml 2×SSC, 10 ml 10% SDS.
7. 0.2×SSC，1% SDS: 100 ml 2×SSC, 10 g 10% SDS.

Solutions for ELISA

1. PBST buffer: NaCl 8.0 g, $Na_2HPO_4.12H_2O$ 2.9 g, K_2HPO_4 0.2 g, 0.5 ml Tween-20, aad ddH_2O to 1000 ml.
2. Sodium citrate buffer: Citric Acid 10.5 g, Sodium Acetate 6.8 g, aad ddH2O to 1000 ml, adjust to PH 5.0, store in dark at 4°C, add TMB and H_2O_2 before use.
3. TMB stock solution: 0.2 g TMB dissolved in 100 ml ethanol, store in dark at 4°C.
4. 0.05 mol/L Carbonate buffer: Sodium Carbonate 1.59 g, Sodium Hydrogen Carbonate

2.93 g, aad ddH_2O to 1000 ml, adjust to PH9.6.

5. Blocking buffer: 5 g skimmed milk, add 1×PBST to a final volumn 100 ml.

Solutions used in our study

1. 0.5 mol/L EDTA (PH8.0): 186.1 g EDTA dissolved in 800ml ddH_2O, adjust to pH 8.0 with NaOH, aad ddH_2O to 1000 ml, Autolave.
2. 3 M/L NaAc (100 ml): 40.8 g NaAc.3H_2O dissolved in 40 ml ddH_2O, adjust to pH 7.2 with NaOH, aad ddH_2O to 1000 ml, Autolave.
3. CTAB RNA extracting buffer: 1.5% CTAB (W/V), 1.4 M/L NaCl, 20 mM/L EDTA, 100mM/L Tris-HCl, add 2% PVP-40 (W/V) after autoclave, add 0.2% β-Mercaptoethanol (V/V) before use.

Appendix 13 Papers published during PhD study

1. **Xiaofang Ma**, Marie-Claude N., Louis-Valentin Meteignier, Ni Hong, Guoping Wang and Peter Moffett. (2014) Different roles for RNA silencing and RNA processing components in virus recovery and virus-induced gene silencing in plants. J Experimental Botany.
2. **Xiaofang Ma**, Ni Hong, Guoping Wang. (2015) Genetic diversity and evolution of Apple stem pitting virus isolates from pear in China. *Submitted to Canadian Journal of Plant Pathology.*
3. **Xiaofang Ma**, Ni Hong, Guoping Wang. (2015). Coat protein of Apple stem pitting virus possessed viral RNA silencing suppressor activity. *Manuscript preparing.*
4. Bingyu Yao, Guoping Wang, **Xiaofang Ma**, Wenbing Liu, Huihui Tang, Hui Zhu and Ni Hong. (2014) Simultaneous detection and differentiation of three viruses in pear plants by a multiplex RT-PCR. J Virol Methods, 196, 113-119.
5. Ni Hong, **Xiaofang Ma**, Guojun Hu, Hui Zhu, Bingyu Yao, Yangsu Song, Xiaoyan Wu. (2012) Indidence of viral disease on pear plants and the molecular characteristics of three pear virues in china.22nd international conference on virus and other trandmissble diseases of fruit crops (ICVF). 22(3), 123-458.
6. **Xiaofang Ma**, Marie-Claude Nicole, Ni Hong, Guoping Wang, Peter Moffett. (2014) Investigation of the role of Argonaute proteins in Virus-induced gene silencing and recovery in Arabidopsis. XVIth International Congress of Virology (Abstract).
7. 马小方, 胡国君, 唐敏, 王利平, 洪霓, 王国平. （2011）来源于我国梨的苹果茎痘病毒分子变异初步研究 中国植物保护学会 2011 年学术年会会议论文;
8. 马小方, 洪霓, 王国平.（2011）苹果茎痘病毒不同分离物 CP 基因原核表达和抗血清的制备 中国植物病理学会 2011 年学术年会会议论文摘要。

References

Adams M.J., Lefkowitz E.J., King A.M., and Carstens E.B. Ratification vote on taxonomic proposals to the International Committee on Taxonomy of Viruses (2014). *Arch Virol*. **2014**, *159*, 2831-2841.

Adenot X., Elmayan T., Lauressergues D., Boutet S., Bouche N., Gasciolli V., and Vaucheret H. DRB4-dependent TAS3 trans-acting siRNAs control leaf morphology through AGO7. *Curr Biol*. **2006**, *16*, 927-932.

Aglayan K., Sere I.U., Gazel M., and Jelkmann W. Detection of four apple viruses by ELISA and RT-PCR assays in Turkey. *Turk J Agric for*. **2006**, *4*, 241-246.

Agorio A. ARGONAUTE4 is required for resistance to *Pseudomonas syringae* in *Arabidopsis*. *Plant Cell*. **2007**, *11*, 3778-3790.

Alabi O.J., Martin R.R., and Naidu R.A. Sequence diversity, population genetics and potential recombination events in *Grapevine rupestris stem pitting-associated virus* in Pacific North-West vineyards. *J Gen Virol*. **2010**, *91*, 265-276.

Alvarez J.P., Pekker I., Goldshmidt A., Blum E., Amsellem Z., and Eshed Y. Endogenous and synthetic microRNAs stimulate simultaneous, efficient, and localized regulation of multiple targets in diverse species. *Plant Cell*. **2006**, *18*, 1134-1151.

Anandalakshmi R., Pruss G.J., Ge X., Marathe R., Mallory A.C., Smith T.H., and Vance V.B. A viral suppressor of gene silencing in plants. *Proc Natl Acad Sci USA*. **1998**, *95*, 13079-13084.

Axtell M.J. Classification and Comparison of Small RNAs from Plants. *Annu Rev Plant Biol*. **2013**, *64*, 137-159.

Azevedo J., Garcia D., Pontier D., Ohnesorge S., Yu A., Garcia S., Braun L., Bergdoll M., Hakimi M.A., Lagrange T., and Voinnet O. Argonaute quenching and global changes in Dicer homeostasis caused by a pathogen-encoded GW repeat protein. *Genes Dev*. **2010**, *24*, 904-915.

Balagopal V., and Parker R. Polysomes, P bodies and stress granules: states and fates of eukaryotic mRNAs. *Curr Opin Cell Biol*. **2009**, *21*, 403-408.

Bandín I., and Dopazo C.P. Host range, host specificity and hypothesized host shift events among viruses of lower vertebrates. *Vet Res*. **2011**, *42*, 544.

Baulcombe D. RNA silencing in plants. *Nature*. **2004**, *431*, 356-363.

Baumberger N., Tsai C.H., Lie M., Havecker E., and Baulcombe D.C. The Polerovirus silencing suppressor P0 targets ARGONAUTE proteins for degradation. *Curr Biol*. **2007**, *17*, 1609-1614.

Bhattacharjee S., Zamora A., Azhar M.T., Sacco M.A., Lambert L.H., and Moffett P. Virus resistance induced by NB-LRR proteins involves Argonaute4-dependent translational control. *Plant J*. **2009**, *58*, 940-951.

Bohmert K., Camus I., Bellini C., Bouchez D., Caboche M., and Benning C. AGO1 defines a novel locus of *Arabidopsis* controlling leaf development. *Embo J*. **1998**, *17*, 170-180.

Bologna N.G., and Voinnet O. The diversity, biogenesis, and activities of endogenous silencing small RNAs in *Arabidopsis*. *Annu Rev Plant Biol*. **2014**, *65*, 473-503.

Boni M.F., Posada D., and Feldman M.W. An exact nonparametric method for inferring mosaic structure in sequence triplets. *Genetics*. **2007**, *176*, 1035-1047.

Bouche N., Lauressergues D., Gasciolli V., and Vaucheret H. An antagonistic function for Arabidopsis DCL2 in development and a new function for DCL4 in generating viral siRNAs. *Embo J*. **2006**, *25*, 3347-3356.

Boulila M. Putative recombination events and evolutionary history of five economically important viruses of fruit trees based on coat protein-encoding gene sequence analysis. *Biochem Genet*. **2010**, *48*, 357-375.

Brigneti G., Voinnet O., Li W.X., Ji L.H., Ding S.W., and Baulcombe D.C. Viral pathogenicity determinants are suppressors of transgene silencing in *Nicotiana benthamiana*. *Embo J*. **1998**, *17*, 6739-6946.

Brodersen P., Sakvarelidze-Achard L., Bruun-Rasmussen M., Dunoyer P., Yamamoto Y.Y., Sieburth L., and Voinnet O. Widespread translational inhibition by plant miRNAs and siRNAs. *Science*. **2008**, *320*, 1185-1190.

Brodersen P., and Voinnet O. The diversity of RNA silencing pathways in plants. *Trends Genetic*. **2006**, *22*, 268-280.

Burch-Smith T.M., Anderson J.C., Martin G.B., and Dinesh-Kumar S.P. Applications and advantages of virus-induced gene silencing for gene function studies in plants. *Plant J*. **2004**, *39*, 734-746.

Burgyán J., and Havelda Z. Viral suppressors of RNA silencing. *Trends Plant Sci*. **2011**, *16*, 265-272.

Carbonell A., Fahlgren N., Garcia-Ruiz H., Gilbert K.B., Montgomery T.A., Nguyen T., Cuperus J.T., and Carrington J.C. Functional analysis of three *Arabidopsis* ARGONAUTES using slicer-defective mutants. *Plant Cell*. **2012**, *24*, 3613-3629.

Carlsbecker A., Lee J.Y., Roberts C.J., Dettmer J., Lehesranta S., Zhou J., Lindgren O., Moreno-Risueno M.A., Vaten A., Thitamadee S., Campilho A., Sebastian J., Bowman J.L., Helariutta Y., and Benfey P.N. Cell signalling by microRNA165/6 directs gene dose-dependent root cell fate. *Nature*. **2010**, *465*, 316-321.

Carstens E.B. Ratification vote on taxonomic proposals to the International Committee on Taxonomy of Viruses (2009). *Arch Virol*. **2009**, *155*, 133-146.

Chapman E.J., and Carrington J.C. Specialization and evolution of endogenous small RNA pathways. *Nat Rev Genet*. **2007**, *8*, 884-896.

Chiu M.H., Chen I.H., Baulcombe D.C., and Tsai C.H. The silencing suppressor P25 of Potato virus X interacts with Argonaute1 and mediates its degradation through the proteasome pathway. *Mol Plant Pathol*. **2010**, *11*, 641-649.

Covey S.N. Plants combat infection by gene silencing. *Nature*. **1997**, 781-782.

Collier S., Pendle A., Boudonck K.Van R.T., Dolan L., and Shaw P. A distant coilin homologue is required for the formation of cajal bodies in *Arabidopsis*. *Mol Biol Cell*. **2006**, *17*, 2942-2951.

Csorba T., Lozsa R., Hutvagner G., and Burgyan J. Polerovirus protein P0 prevents the assembly of small RNA-containing RISC complexes and leads to degradation of ARGONAUTE1. *Plant J*. **2010**, *62*, 463-472.

Dalmay T., Hamilton A., Rudd S., Angell S., and Baulcombe D.C. An RNA-dependent RNA polymerase gene in *Arabidopsis* is required for posttranscriptional gene silencing mediated by a transgene but not by a virus. *Cell*. **2000**, *101*, 543-553.

Deleris A., Gallego-Bartolome J., Bao J., Kasschau K.D., Carrington J.C., and Voinnet O. Hierarchical action and inhibition of plant Dicer-like proteins in antiviral defense. *Science*. **2006**, *313*, 68-71.

Deng X., Kelloniemi J., Haikonen T., Vuorinen A.L., Elomaa P., Teeri T.H., and Valkonen J.P. Modification of *Tobacco rattle virus* RNA1 to serve as a VIGS vector reveals that the 29K movement protein is an RNA silencing suppressor of the virus. *Mol Plant Microbe Interact*. **2013**, *26*, 503-514.

Dhir S., Tomar M., Thakur P.D., Ram R., Hallan V., and Zaidi A.A. Molecular evidence for *Apple stem pitting virus* infection in India. *Plant Pathol*. **2010**, *59*, 393.

Ding S.W., Li W.X., and Symons R.H. A novel naturally occurring hybrid gene encoded by a plant RNA virus facilitates long distance virus movement. *Embo J*. **1995**, *14*, 5762-5772.

Ding S.W., and Voinnet O. Antiviral immunity directed by small RNAs. *Cell*. **2007**, *130*, 413-426.

Dunoyer P., Himber C., Ruiz-Ferrer V., Alioua A., and Voinnet O. Intra- and intercellular RNA interference in Arabidopsis thaliana requires components of the microRNA and heterochromatic silencing pathways. *Nat Genet*. **2007**, *39*, 848-856.

Dunoyer P., Himber C., and Voinnet O. DICER-LIKE 4 is required for RNA interference and produces the 21-nucleotide small interfering RNA component of the plant cell-to-cell silencing signal. *Nat Genet*. **2005**, *37*, 1356-1360.

Dunoyer P., Melnyk C., Molnar A., and Slotkin R.K. Plant mobile small RNAs. *Cold Spring Harb Perspect Biol*. **2013**, *5*,

Dunoyer P., Schott G., Himber C., Meyer D., Takeda A., Carrington J.C., and Voinnet O. Small RNA duplexes function as mobile silencing signals between plant cells. *Science*. **2010**, *328*, 912-926.

Ender C., and Meister G. Argonaute proteins at a glance. *J Cell Sci*. **2010**, *123*, 1819-1823.

Estevan J., Marena A., Callot C., Lacombe S., Moretti A., Caranta C., and Gallois J.L. Specific requirement for translation initiation factor 4E or its isoform drives plant host susceptibility to *Tobacco etch virus*. *Bmc Plant Biol*. **2014**, *14*, 67.

Farooq A.B., Ma Y.X., Wang Z.Q., Zhuo N., Xu W., Wang G.P., and Hong N. Genetic diversity analyses reveal novel recombination events in *Grapevine leafroll-associated virus 3* in China. *Virus Res*. **2013**, *171*, 15-21.

Feng L., Duan C.G., and Guo H.S. Inhibition of in vivo Slicer activity of Argonaute protein 1 by the viral 2b protein independent of its dsRNA-binding function. *Mol Plant Pathol*. **2013**, *14*, 617-622.

Folimonova S.Y. Developing an understanding of cross-protection by *Citrus tristeza virus*. *Front Microbiol*. **2013**, *4*, 76.

Foster T.M., Lough T.J., Emerson S.J., Lee R.H., Bowman J.L., Forster R.L., and Lucas W.J. A surveillance system regulates selective entry of RNA into the shoot apex. *Plant*

Cell. **2002**, *14*, 1497-1508.

Franks T.M., and Lykke-Andersen J. The control of mRNA decapping and P-body formation. *Mol Cell*. **2008**, *32*, 605-615.

Garcia-Ruiz H., Takeda A., Chapman E.J., Sullivan C.M., Fahlgren N., Brempelis K.J., and Carrington J.C. *Arabidopsis* RNA-dependent RNA polymerases and dicer-like proteins in antiviral defense and small interfering RNA biogenesis during *Turnip Mosaic Virus* infection. *Plant Cell*. **2010**, *22*, 481-496.

Gasciolli V., Mallory A.C., Bartel D.P., and Vaucheret H. Partially redundant functions of Arabidopsis DICER-like enzymes and a role for DCL4 in producing trans-acting siRNAs. *Curr Biol*. **2005**, *15*, 1494-1500.

Gentit P., Foissac X., Svanella-Dumas L., Peypelut M., and Candresse T. Characterization of two different *Apricot latent virus* variants associated with peach asteroid spot and peach sooty ringspot diseases. *Arch Virol*. **2001**, *146*, 1453-1464.

Ghazala W., Waltermann A., Pilot R., Winter S., and Varrelmann M. Functional characterization and subcellular localization of the 16K cysteine-rich suppressor of gene silencing protein of *Tobacco rattle virus*. *J Gen Virol*. **2008**, *89*, 1748-1758.

Ghoshal B., and Sanfaçon H. Temperature-dependent symptom recovery in *Nicotiana benthamiana* plants infected with *Tomato ringspot virus* is associated with reduced translation of viral RNA2 and requires ARGONAUTE 1. *Virology*. **2014**, *456*, 188-197.

Ghoshal B., and Sanfaçon H. Symptom recovery in virus-infected plants: revisiting the role of RNA silencing mechanisms. *Virology*. **2015**, *479-480*, 167-179.

Glasa M., Palkovics L., Komínek P., Labonne G., Pittnerová S., Kúdela O., Candresse T., and Subr Z. Geographically and temporally distant natural recombinant isolates of *Plum pox virus* (PPV) are genetically very similar and form a unique PPV subgroup. *J Gen Virol*. **2004**, *85*, 2671-2681.

Godge M.R., Purkayastha A., Dasgupta I., and Kumar P.P. Virus-induced gene silencing for functional analysis of selected genes. *Plant Cell Rep*. **2008**, *27*, 209-219.

Gy I., Gasciolli V., Lauressergues D., Morel J.B., Gombert J., Proux F., Proux C., Vaucheret H., and Mallory A.C. *Arabidopsis* FIERY1, XRN2, and XRN3 are endogenous RNA silencing suppressors. *Plant Cell*. **2007**, *19*, 3451-3461.

Hamera S., Song X., Su L., Chen X., and Fang R. *Cucumber mosaic virus* suppressor 2b binds to AGO4-related small RNAs and impairs AGO4 activities. *Plant J*. **2012**, *69*, 104-115.

Harvey J.J., Lewsey M.G., Patel K., Westwood J., Heimstadt S., Carr J.P., and Baulcombe D.C. An antiviral defense role of AGO2 in plants. *Plos One*. **2011**, *6*, e14639.

Havecker E.R., Wallbridge L.M., Hardcastle T.J., Bush M.S., Kelly K.A., Dunn R.M., Schwach F., Doonan J.H., and Baulcombe D.C. The *Arabidopsis* RNA-directed DNA methylation argonautes functionally diverge based on their expression and interaction with target loci. *Plant Cell*. **2010**, *22*, 321-334.

Heath L., Van der Walt E., Varsani A., and Martin D.P. Recombination patterns in aphthoviruses mirror those found in other picornaviruses. *J Virol*. **2006**, *80*,

11827-11832.

Hernandez C., Carette J.E., Brown D.J., and Bol J.F. Serial passage of tobacco rattle virus under different selection conditions results in deletion of structural and nonstructural genes in RNA2. *J Virol*. **1996**, *70*, 4933-4940.

Hernandez C., Visser P.B., Brown D.J., and Bol J.F. Transmission of tobacco rattle virus isolate PpK20 by its nematode vector requires one of the two non-structural genes in the viral RNA2. *J Gen Virol*. **1997**, *78*, 465-467.

Hewezi T., Alibert G., and Kallerhoff J. Local infiltration of high- and low-molecular-weight RNA from silenced sunflower (*Helianthus annuus* L.) plants triggers post-transcriptional gene silencing in non-silenced plants. *Plant Biotechnol J*. **2005**, *3*, 81-89.

Himber C., Dunoyer P., Moissiard G., Ritzenthaler C., and Voinnet O. Transitivity-dependent and -independent cell-to-cell movement of RNA silencing. *Embo J*. **2003**, *22*, 4523-4533.

Hiraguri A., Itoh R., Kondo N., Nomura Y., Aizawa D., Murai Y., Koiwa H., Seki M., Shinozaki K., and Fukuhara T. Specific interactions between Dicer-like proteins and HYL1/DRB-family dsRNA-binding proteins in *Arabidopsis thaliana*. *Plant Mol Biol*. **2005**, *57*, 173-188.

Holmes E.C., The evolution and emergence of RNA viruses. Oxford University Press, New York, 2010.

Hutvagner G., and Simard M.J. Argonaute proteins: key players in RNA silencing. *Nat Rev Mol Cell Biol*. **2008**, *9*, 22-32.

Igarashi A., Yamagata K., Sugai T., Takahashi Y., Sugawara E., Tamura A., Yaegashi H., Yamagishi N., Takahashi T., Isogai M., Takahashi H., and Yoshikawa N. *Apple latent spherical virus vectors* for reliable and effective virus-induced gene silencing among a broad range of plants including tobacco, tomato, *Arabidopsis thaliana*, cucurbits, and legumes. *Virology*. **2009**, *386*, 407-416.

Incarbone M., and Dunoyer P. RNA silencing and its suppression: novel insights from in planta analyses. *Trends Plant Sci*. **2013**, *18*, 382-392.

Irvine D.V., Zaratiegui M., Tolia N.H., Goto D.B., Chitwood D.H., Vaughn M.W., Joshua-Tor L., and Martienssen R.A. Argonaute slicing is required for heterochromatic silencing and spreading. *Science*. **2006**, *313*, 1134-1137.

Iwasaki S., Takeda A., Motose H., and Watanabe Y. Characterization of *Arabidopsis* decapping proteins AtDCP1 and AtDCP2, which are essential for post-embryonic development. *Febs Lett*. **2007**, *581*, 2455-2459.

Jaubert M., Bhattacharjee S., Mello A.F., Perry K.L., and Moffett P. ARGONAUTE2 mediates RNA-silencing antiviral defenses against *Potato virus X* in *Arabidopsis*. *Plant Physiol*. **2011**, *156*, 1556-1564.

Jelkmann W. Nucleotide sequences of *Apple stem pitting virus* and of the coat protein gene of a similar virus from pear associated with vein yellows disease and their relationship with potex- and carlaviruses. *J Gen Virol*. **1994**, *75*, 1535-1542.

Jelkmann W., and Keim Konrad R. Immuno-capture polymerase chain reaction and plate-trapped ELISA for the detection of *Apple stem pitting virus*. *J Phytopathol*. **1997**,

11-12, 499-503.

Jones T.R., Kang I.H., Wheeler D.B., Lindquist R.A., Papallo A., Sabatini D.M., Golland P., and Carpenter A.E. CellProfiler Analyst: data exploration and analysis software for complex image-based screens. *Bmc Bioinformatics*. **2008**, *9*, 482.

Jouannet V., Moreno A.B., Elmayan T., Vaucheret H., Crespi M.D., and Maizel A. Cytoplasmic Arabidopsis AGO7 accumulates in membrane-associated siRNA bodies and is required for ta-siRNA biogenesis. *Embo J*. **2012**, *31*, 1704-1713.

Jovel J., Walker M., and Sanfacon H. Recovery of *Nicotiana benthamiana* plants from a necrotic response induced by a nepovirus is associated with RNA silencing but not with reduced virus titer. *J Virol*. **2007**, *81*, 12285-12297.

Karran R.A., and Sanfacon H. *Tomato ringspot virus* coat protein binds to ARGONAUTE 1 and suppresses the translation repression of a reporter gene. *Mol Plant Microbe Interact*. **2014**, *27*, 933-943.

Kasschau K.D., and Carrington J.C. A counterdefensive strategy of plant viruses: suppression of posttranscriptional gene silencing. *Cell*. **1998**, *95*, 461-470.

Katiyar-Agarwal S., Gao S., Vivian-Smith A., and Jin H. A novel class of bacteria-induced small RNAs in *Arabidopsis*. *Genes Dev*. **2007**, *21*, 3123-3134.

Kehr J., and Buhtz A. Long distance transport and movement of RNA through the phloem. *J Exp Bot*. **2008**, *59*, 85-92.

Kim K.W., Eames A.L., and Waterhouse P.M. RNA Processing Activities of the *Arabidopsis* Argonaute Protein Family. *RNA Processing*. **2011**,

Kjemtrup S., Sampson K.S., Peele C.G., Nguyen L.V., Conkling M.A., Thompson W.F., and Robertson D. Gene silencing from plant DNA carried by a Geminivirus. *Plant J*. **1998**, *14*, 91-100.

Klahre U., Crete P., Leuenberger S.A., Iglesias V.A., and Meins F.J. High molecular weight RNAs and small interfering RNAs induce systemic posttranscriptional gene silencing in plants. *Proc Natl Acad Sci USA*. **2002**, *99*, 11981-11986.

Klerks M.M., Leone G., Lindner J.L., Schoen C.D., and Van den Heuvel J.F. Rapid and sensitive detection of *Apple stem pitting virus* in apple trees through RNA amplification and probing with fluorescent molecular beacons. *Phytopathology*. **2001**, *91*, 1085-1091.

Komorowska B., Malinowski T., and Michalczuk L. Evaluation of several RT-PCR primer pairs for the detection of *Apple stem pitting virus*. *J Virol Methods*. **2010**, *168*, 242-247.

Komorowska B., Siedlecki P., Kaczanowski S., Hasiów-Jaroszewska B., and Malinowski T. Sequence diversity and potential recombination events in the coat protein gene of *Apple stem pitting virus*. *Virus Res*. **2011**, *158*, 263-267.

Krishnamurthy K., Heppler M., Mitra R., Blancaflor E., Payton M., Nelson R.S., and Verchot-Lubicz J. The *Potato virus X* TGBp3 protein associates with the ER network for virus cell-to-cell movement. *Virology*. **2003**, *309*, 135-151.

Kumagai M.H., Donson J., Della-Cioppa G., Harvey D., Hanley K., and Grill L.K. Cytoplasmic inhibition of carotenoid biosynthesis with virus-derived RNA. *Proc Natl Acad Sci USA*. **1995**, *92*, 1679-1683.

Kundu J.K. The occurrence of *Apple stem pitting virus* and *Apple stem grooving virus* within field-grown apple cultivars evaluated by RT-PCR. *Plant Protection Science*. **2003**, 88-92.

Lanet E., Delannoy E., Sormani R., Floris M., Brodersen P., Crete P., Voinnet O., and Robaglia C. Biochemical evidence for translational repression by *Arabidopsis* microRNAs. *Plant Cell*. **2009**, *21*, 1762-1768.

Lara J., Purdy M.A., and Khudyakov Y.E. Genetic host specificity of *Hepatitis E virus*. *Infection, Genetics and Evolution*. **2014**, *24*, 127-139.

Leone G., Lindner J.L., Van der Meer F.A., Schoen C.D., and Jongedijk G. Symptoms on apple and pear indicators after back transmition from Nicotiana occidentalis confirm the identy of *Apple stem pitting virus* and *Pear vein yellow virus*. *Acta Horticulturae*. **1997**,

Li C.F., Henderson I.R., Song L., Fedoroff N., Lagrange T., and Jacobsen S.E. Dynamic regulation of ARGONAUTE4 within multiple nuclear bodies in *Arabidopsis thaliana*. *Plos Genet*. **2008**, *4*, e27.

Li C.F., Pontes O., El-Shami M., Henderson I.R., Bernatavichute Y.V., Chan S.W., Lagrange T., Pikaard C.S., and Jacobsen S.E. An ARGONAUTE4-containing nuclear processing center colocalized with Cajal bodies in *Arabidopsis thaliana*. *Cell*. **2006**, *126*, 93-106.

Li F., Pignatta D., Bendix C., Brunkard J.O., Cohn M.M., Tung J., Sun H., Kumar P., and Baker B. MicroRNA regulation of plant innate immune receptors. *Proc Natl Acad Sci USA*. **2012**, *109*, 1790-1795.

Li R., Mock R., Huang Q., Abad J., Hartung J., and Kinard G. A reliable and inexpensive method of nucleic acid extraction for the PCR-based detection of diverse plant pathogens. *J Virol Methods*. **2008**, *154*, 48-55.

Li Y., Zhang Q., Zhang J., Wu L., Qi Y., and Zhou J.M. Identification of microRNAs involved in pathogen-associated molecular pattern-triggered plant innate immunity. *Plant Physiol*. **2010**, *152*, 2222-2231.

Librado P., and Rozas J. DnaSP v5: a software for comprehensive analysis of DNA polymorphism data. *Bioinformatics*. **2009**, *25*, 1451-1452.

Lima M.F., Alkowni R., Uyemoto J.K., Golino D., Osman F., and Rowhani A. Molecular analysis of a California strain of *Rupestris stem pitting-associated virus* isolated from declining Syrah grapevines. *Arch Virol*. **2006**, *151*, 1889-1894.

Lin H., and Spradling A.C. A novel group of pumilio mutations affects the asymmetric division of germline stem cells in the Drosophila ovary. *Development*. **1997**, *124*, 63-76.

Lin S.S., Wu H.W., Jan F.J., Hou R.F., and Yeh S.D. Modifications of the helper component-protease of *Zucchini yellow mosaic virus* for generation of attenuated mutants for cross protection against severe infection. *Phytopathology*. **2007**, *97*, 287-296.

Liu N., Niu J., and Zhao Y. Complete genomic sequence analyses of *Apple Stem Pitting Virus* isolates from China. *Virus Genes*. **2012**, *44*, 124-130.

Liu Q., Feng Y., and Zhu Z. Dicer-like (DCL) proteins in plants. *Funct Integr Genomics*.

2009, *9*, 277-286.

Liu Q., Yao X., Pi L., Wang H., Cui X., and Huang H. The ARGONAUTE10 gene modulates shoot apical meristem maintenance and establishment of leaf polarity by repressing miR165/166 in *Arabidopsis*. *Plant J*. **2009**, *58*, 27-40.

Liu Y., Schiff M., Marathe R., and Dinesh-Kumar S.P. Tobacco Rar1, EDS1 and NPR1/NIM1 like genes are required for N-mediated resistance to *Tobacco mosaic virus*. *Plant J*. **2002**, *30*, 415-429.

Lunden S., Meng B.Z., Jr. Avery J., and Qiu W.P. Association of *Grapevine fanleaf virus*, *Tomato ringspot virus* and *Grapevine rupestris stem pitting-associated virus* with a grapevine vein-clearing complex on *var. Chardonnay*. *Eur J Plant Pathol*. **2010**, *126*, 135-144.

MacDiarmid R. RNA silencing in productive virus infections. *Annu Rev Phytopathol*. **2005**, *43*, 523-544.

MacFarlane S.A. Molecular biology of the tobraviruses. *J Gen Virol*. **1999**, *80*, 2780-2799.

Macfarlane S.A. Tobraviruses-plant pathogens and tools for biotechnology. *Mol Plant Pathol*. **2010**, *11*, 577-583.

MacFarlane S.A., and Popovich A.H. Efficient expression of foreign proteins in roots from tobravirus vectors. *Virology*. **2000**, *267*, 29-35.

Maldonado-Bonilla L.D. Composition and function of P-bodies in *Arabidopsis thaliana*. *Front Plant Sci*. **2014**, 5.

Mallory A., and Vaucheret H. Form, function, and regulation of ARGONAUTE proteins. *Plant Cell*. **2010**, *22*, 3879-3889.

Mallory A.C., and Vaucheret H. ARGONAUTE 1 homeostasis invokes the coordinate action of the microRNA and siRNA pathways. *Embo Rep*. **2009**, *10*, 521-526.

Mandadi K.K., and Scholthof K.B. Plant immune responses against viruses: how does a virus cause disease? *Plant Cell*. **2013**, *25*, 1489-1505.

Margis R., Fusaro A.F., Smith N.A., and Curtin S.J. The evolution and diversification of Dicers in plants. *Febs Lett*. **2006**, *580*, 2442-2450.

Martelli G.P., Adams M.J., Kreuze J.F., and Dolja V.V. Family Flexiviridae: a case study in virion and genome plasticity. *Annu Rev Phytopathol*. **2007**, *45*, 73-100.

Martelli G.P., and Jelkmann W. *Foveavirus*, a new plant virus genus. *Arch Virol*. **1998**, *143*, 1245-1249.

Martin D.P., Posada D., Crandall K.A., and Williamson C. A modified bootscan algorithm for automated identification of recombinant sequences and recombination breakpoints. *Aids Res Hum Retrov*. **2005**, *21*, 98-102.

Martín S., Sambade A., Rubio L., Vives M.C., Moya P., Guerri J., Elena S.F., and Moreno P. Contribution of recombination and selection to molecular evolution of *Citrus tristeza virus*. *J Gen Virol*. **2009**, *90*, 1527-1538.

Martin-Hernandez A.M., and Baulcombe D.C. *Tobacco rattle virus* 16-kilodalton protein encodes a suppressor of RNA silencing that allows transient viral entry in meristems. *J Virol*. **2008**, *82*, 4064-4071.

Mathioudakis M.M., Maliogka V.I., Dovas C.I., Paunović S., and Katis N.I. Reliable RT-PCR detection of *Apple stem pitting virus* in pome fruits and its association with quince fruit deformation disease. *Plant Pathol*. **2009**, *58*, 228-236.

Mathioudakis M.M., Maliogka V.I., Katsiani A.T., and Katis N.I. Incidence and molecular variability of *Apple stem pitting* and *Apple chlorotic leaf spot viruses* in apple and pear orchards in Greece. *J Plant Pathol*. **2010**, *92*, 139-147.

Mathioudakis M.M., and Katis N.I. First record of the *Apple stem pitting virus* (ASPV) in quince in Greece. *J Plant Pathol*. **2006**, *88*, 221.

Melnyk C.W., Molnar A., and Baulcombe D.C. Intercellular and systemic movement of RNA silencing signals. *Embo J*. **2011**, *30*, 3553-3563.

Meng B., Pang S.Z., Forsline P.L., McFerson J.R., and Gonsalves D. Nucleotide sequence and genome structure of *Grapevine rupestris stem pitting associated virus-1* reveal similarities to *Apple stem pitting virus*. *J Gen Virol*. **1998**, *79*, 2059-2069.

Meng B., Rebelo A.R., and Fisher H. Genetic diversity analyses of grapevine *Rupestris stem pitting-associated virus* reveal distinct population structures in scion versus rootstock varieties. *J Gen Virol*. **2006**, *87*, 1725-1733.

Menzel W., Jelkmann W., and Maiss E. Detection of four apple viruses by multiplex RT-PCR assays with coamplification of plant mRNA as internal control. *J Virol Methods*. **2002**, *99*, 81-92.

Merret R., Descombin J., Juan Y.T., Favory J.J., Carpentier M.C., Chaparro C., Charng Y.Y., Deragon J.M., and Bousquet-Antonelli C. XRN4 and LARP1 are required for a heat-triggered mRNA decay pathway involved in plant acclimation and survival during thermal stress. *Cell Rep*. **2013**, *5*, 1279-1293.

Mi S., Cai T., Hu Y., Chen Y., Hodges E., Ni F., Wu L., Li S., Zhou H., Long C., Chen S., Hannon G.J., and Qi Y. Sorting of small RNAs into *Arabidopsis* Argonaute complexes is directed by the 5' terminal nucleotide. *Cell*. **2008**, *133*, 116-127.

Mlotshwa S., Voinnet O., Mette M.F., Matzke M., Vaucheret H., Ding S.W., Pruss G., and Vance V.B. RNA silencing and the mobile silencing signal. *Plant Cell*. **2002**, *14*, 289-301.

Moissiard G., Parizotto E.A., Himber C., and Voinnet O. Transitivity in Arabidopsis can be primed, requires the redundant action of the antiviral Dicer-like 4 and Dicer-like 2, and is compromised by viral-encoded suppressor proteins. *Rna*. **2007**, *13*, 1268-1278.

Moissiard G., and Voinnet O. RNA silencing of host transcripts by cauliflower mosaic virus requires coordinated action of the four Arabidopsis Dicer-like proteins. *Proc Natl Acad Sci USA*. **2006**, *103*, 19593-19598.

Molnar A., Melnyk C.W., Bassett A., Hardcastle T.J., Dunn R., and Baulcombe D.C. Small silencing RNAs in plants are mobile and direct epigenetic modification in recipient cells. *Science*. **2010**, *328*, 872-875.

Morel J.B., Godon C., Mourrain P., Beclin C., Boutet S., Feuerbach F., Proux F., and Vaucheret H. Fertile hypomorphic ARGONAUTE (ago1) mutants impaired in post-transcriptional gene silencing and virus resistance. *Plant Cell*. **2002**, *14*, 629-639.

Moreno A.B., Martinez D.A.A., Bardou F., Crespi M.D., Vaucheret H., Maizel A., and Mallory A.C. Cytoplasmic and nuclear quality control and turnover of single-stranded

RNA modulate post-transcriptional gene silencing in plants. *Nucleic Acids Res*. **2013**, *41*, 4699-4708.

Morozov S.Y., and Solovyev A.G. Triple gene block: modular design of a multifunctional machine for plant virus movement. *J Gen Virol*. **2003**, *84*, 1351-1366.

Mourrain P., Beclin C., Elmayan T., Feuerbach F., Godon C., Morel J.B., Jouette D., Lacombe A.M., Nikic S., Picault N., Remoue K., Sanial M., Vo T.A., and Vaucheret H. Arabidopsis SGS2 and SGS3 genes are required for posttranscriptional gene silencing and natural virus resistance. *Cell*. **2000**, *101*, 533-542.

Moussian B., Schoof H., Haecker A., Jurgens G., and Laux T. Role of the ZWILLE gene in the regulation of central shoot meristem cell fate during Arabidopsis embryogenesis. *Embo J*. **1998**, *17*, 1799-1809.

Moya A., Holmes E.C., and González-Candelas F. The population genetics and evolutionary epidemiology of RNA viruses. *Nat Rev Microbiol*. **2004**, *2*, 279-288.

Mustroph A., Juntawong P., and Bailey-Serres J. Isolation of plant polysomal mRNA by differential centrifugation and ribosome immunopurification methods. *Methods Mol Biol*. **2009**, *553*, 109-126.

Nemchinov L.G., Shamloul A.M., Zemtchik E.Z., Verderevskaya T.D., and Hadidi A. *Apricot latent virus*: a new species in the genus Foveavirus. *Arch Virol*. **2000**, *145*, 1801-1813.

Nolasco G., Santos C., Petrovic N., Teixeira Santos M., Cortez I., Fonseca F., Boben J., Nazaré Pereira A.M., and Sequeira O. *Rupestris stem pitting associated virus* isolates are composed by mixtures of genomic variants which share a highly conserved coat protein. *Arch Virol*. **2006**, *151*, 83-96.

Padidam M., Sawyer S., and Fauquet C.M. Possible emergence of new geminiviruses by frequent recombination. *Virology*. **1999**, *265*, 218-225.

Palauqui J.C., Elmayan T., De Borne F.D., Crete P., Charles C., and Vaucheret H. Frequencies, timing, and spatial patterns of co-suppression of nitrate reductase and nitrite reductase in transgenic tobacco plants. *Plant Physiol*. **1996**, *112*, 1447-1456.

Palauqui J.C., Elmayan T., Pollien J.M., and Vaucheret H. Systemic acquired silencing: transgene-specific post-transcriptional silencing is transmitted by grafting from silenced stocks to non-silenced scions. *Embo J*. **1997**, *16*, 4738-4745.

Parizotto E.A., Dunoyer P., Rahm N., Himber C., and Voinnet O. In vivo investigation of the transcription, processing, endonucleolytic activity and functional relevance of the spatial distribution of a plant miRNA. *Genes Dev*. **2004**, *18*, 2237-2242.

Parker R., and Sheth U. P-bodies and the control of mRNA translation and degradation. *Mol Cell*. **2007**, *25*, 635-646.

Peragine A., Yoshikawa M., Wu G., Albrecht H.L., and Poethig R.S. SGS3 and SGS2/SDE1/RDR6 are required for juvenile development and the production of trans-acting siRNAs in *Arabidopsis*. *Genes Dev*. **2004**, *18*, 2368-2379.

Perea-Resa C., Hernandez-Verdeja T., Lopez-Cobollo R., Del M.C.M., and Salinas J. LSM proteins provide accurate splicing and decay of selected transcripts to ensure normal *Arabidopsis* development. *Plant Cell*. **2012**, *24*, 4930-4947.

Pieterse C.M., Leon-Reyes A., Van der Ent S., and Van Wees S.C. Networking by

small-molecule hormones in plant immunity. *Nat Chem Biol*. **2009**, *5*, 308-316.

Posada D., and Crandall K.A. Evaluation of methods for detecting recombination from DNA sequences: computer simulations. *Proc Natl Acad Sci USA*. **2001**, *98*, 13757-13762.

Pruss G., Ge X., Shi X.M., Carrington J.C., and Bowman V.V. Plant viral synergism: the potyviral genome encodes a broad-range pathogenicity enhancer that transactivates replication of heterologous viruses. *Plant Cell*. **1997**, *9*, 859-868.

Pumplin N., and Voinnet O. RNA silencing suppression by plant pathogens: defence, counter-defence and counter-counter-defence. *Nat Rev Microbiol*. **2013**, *11*, 745-760.

Qu F., Ren T., and Morris T.J. The coat protein of *Turnip crinkle virus* suppresses posttranscriptional gene silencing at an early initiation step. *J Virol*. **2003**, *77*, 511-522.

Qu F., Ye X., Hou G., Sato S., Clemente T.E., and Morris T.J. RDR6 has a broad-spectrum but temperature-dependent antiviral defense role in *Nicotiana benthamiana*. *J Virol*. **2005**, *79*, 15209-15217.

Qu F., Ye X., and Morris T.J. Arabidopsis DRB4, AGO1, AGO7, and RDR6 participate in a DCL4-initiated antiviral RNA silencing pathway negatively regulated by DCL1. *Proc Natl Acad Sci USA*. **2008**, *105*, 14732-14737.

Qu F., and Morris T.J. Suppressors of RNA silencing encoded by plant viruses and their role in viral infections. *Febs Lett*. **2005**, *579*, 5958-5964.

Rand T.A., Petersen S., Du F., and Wang X. Argonaute2 cleaves the anti-guide strand of siRNA during RISC activation. *Cell*. **2005**, *123*, 621-629.

Ratcliff F., Harrison B.D., and Baulcombe D.C. A similarity between viral defense and gene silencing in plants. *Science*. **1997**, *276*, 1558-1560.

Ratcliff F., Martin-Hernandez A.M., and Baulcombe D.C. Technical Advance. *Tobacco rattle virus* as a vector for analysis of gene function by silencing. *Plant J*. **2001**, *25*, 237-245.

Ratcliff F.G., MacFarlane S.A., and Baulcombe D.C. Gene silencing without DNA RNA-mediated cross-protection between viruses. *Plant Cell*. **1999**, *11*, 1207-1216.

Rozas J., Sánchez-DelBarrio J.C., Messeguer X., and Rozas R. DnaSP, DNA polymorphism analyses by the coalescent and other methods. *Bioinformatics*. **2004**, *19*, 2496-2497.

Ruiz M.T., Voinnet O., and Baulcombe D.C. Initiation and maintenance of virus-induced gene silencing. *Plant Cell*. **1998**, *10*, 937-946.

Schmid M., Davison T.S., Henz S.R., Pape U.J., Demar M., Vingron M., Scholkopf B., Weigel D., and Lohmann J.U. A gene expression map of *Arabidopsis thaliana* development. *Nat Genet*. **2005**, *37*, 501-506.

Scholthof H.B. The Tombusvirus-encoded P19: from irrelevance to elegance. *Nat Rev Microbiol*. **2006**, *4*, 405-411.

Scholthof H.B., Alvarado V.Y., Vega-Arreguin J.C., Ciomperlik J., Odokonyero D., Brosseau C., Jaubert M., Zamora A., and Moffett P. Identification of an ARGONAUTE for antiviral RNA silencing in *Nicotiana benthamiana*. *Plant Physiol*. **2011**, *156*, 1548-1555.

Schott G., Mari-Ordonez A., Himber C., Alioua A., Voinnet O., and Dunoyer P. Differential effects of viral silencing suppressors on siRNA and miRNA loading support the existence of two distinct cellular pools of ARGONAUTE1. *Embo J*. **2012**, *31*, 2553-2565.

Schuck J., Gursinsky T., Pantaleo V., Burgyan J., and Behrens S.E. AGO/RISC-mediated antiviral RNA silencing in a plant in vitro system. *Nucleic Acids Res*. **2013**, *41*, 5090-5103.

Schwach F., Vaistij F.E., Jones L., and Baulcombe D.C. An RNA-dependent RNA polymerase prevents meristem invasion by *potato virus X* and is required for the activity but not the production of a systemic silencing signal. *Plant Physiol*. **2005**, *138*, 1842-1852.

Senshu H., Ozeki J., Komatsu K., Hashimoto M., Hatada K., Aoyama M., Kagiwada S., Yamaji Y., and Namba S. Variability in the level of RNA silencing suppression caused by triple gene block protein 1 (TGBp1) from various potexviruses during infection. *J Gen Virol*. **2009**, *90*, 1014-1024.

Seo J.K., Ohshima K., Lee H.G., Son M., and Choi H.S. Molecular variability and genetic structure of the population of *Soybean mosaic virus* based on the analysis of complete genome sequences. *Virology*. **2009**, *393*, 91-103.

Shivaprasad P.V., Chen H.M., Patel K., Bond D.M., Santos B.A., and Baulcombe D.C. A microRNA superfamily regulates nucleotide binding site-leucine-rich repeats and other mRNAs. *Plant Cell*. **2012**, *24*, 859-874.

Shaw J., Love A. J., Makarova S. S., Kalinina N. O., Harrison B. D., and Taliansky, M. E. Coilin, the signature protein of cajal bodies, differentially modulates the interactions of plants with viruses in widely different taxa. *Nucleus*. **2014**, *5*, 85-94.

Smith H.A., Swaney S.L., Parks T.D., Wernsman E.A., and Dougherty W.G. Transgenic plant virus resistance mediated by untranslatable sense RNAs: expression, regulation, and fate of nonessential RNAs. *Plant Cell*. **1994**, *6*, 1441-1453.

Smith J. Analyzing the mosaic structure of genes. *J Mol Evol*. **1992**, *34*, 126-129.

Solovyev A.G., Kalinina N.O., and Morozov S.Y. Recent advances in research of plant virus movement mediated by triple gene block. *Front Plant Sci*. **2012**, *3*, 276.

Solovyev A.G., Stroganova T.A., Zamyatnin Jr A.A., Fedorkin O.N., Schiemann J., and Morozov S.Y. Subcellular sorting of small membrane-associated triple gene block proteins: TGBp3-assisted targeting of TGBp2. *Virology*. **2000**, *269*, 113-127.

Song L., Gao S., Jiang W., Chen S., Liu Y., Zhou L., and Huang W. Silencing suppressors: viral weapons for countering host cell defenses. *Protein Cell*. **2011**, *2*, 273-281.

Song Y., Hong N., Wang L., Hu H., Tian R., Xu W., Ding F., and Wang G. Molecular and serological diversity in *Apple chlorotic leaf spot virus* from sand pear (*Pyrus pyrifolia*) in China. *Eur J Plant Pathol*. **2011**, *130*, 183-196.

Soosaar J.L.M., Burch-Smith T.M., and Dinesh-Kumar S.P. Mechanisms of plant resistance to viruses. *Nat Rev Microbiol*. **2005**, *3*, 789-798.

Souret F.F., Kastenmayer J.P., and Green P.J. AtXRN4 degrades mRNA in *Arabidopsis* and its substrates include selected miRNA targets. *Mol Cell*. **2004**, *15*, 173-183.

Syrgianidis G.D. Problems of virus diseases of deciduous fruit trees in Greece. *Acta Horticulturae*. **1989**, 21-25.

Szittya G., Molnár A., Silhavy D., Hornyik C., and Burgyán J. Short defective interfering RNAs of tombusviruses are not targeted but trigger post-transcriptional gene silencing against their helper virus. *Plant Cell*. **2002**, *14*, 359-372.

Szittya G., Silhavy D., Molnar A., Havelda Z., Lovas A., Lakatos L., Banfalvi Z., and Burgyan J. Low temperature inhibits RNA silencing-mediated defence by the control of siRNA generation. *Embo J*. **2003**, *22*, 633-640.

Takeda A., Iwasaki S., Watanabe T., Utsumi M., and Watanabe Y. The mechanism selecting the guide strand from small RNA duplexes is different among argonaute proteins. *Plant Cell Physiol*. **2008**, *4*, 493-500.

Tamura K., Stecher G., Peterson D., Filipski A., and Kumar S. MEGA6: molecular evolutionary genetics analysis version 6.0. *Mol Biol Evol*. **2013**, *30*, 2725-2729.

Taylor C.E., and Brown D.J.F. Nematode vectors of plant viruses. *NATO Advanced Study Institutes Series. Series A: Life Sciences*. **1997**, *2*,

Teixeira D., Sheth U., Valencia-Sanchez M.A., Brengues M., and Parker R. Processing bodies require RNA for assembly and contain nontranslating mRNAs. *Rna*. **2005**, *11*, 371-382.

Thompson J.D., Gibson T.J., Plewniak F., Jeanmougin F., and Higgins D.G. The CLUSTAL_X windows interface: flexible strategies for multiple sequence alignment aided by quality analysis tools. *Nucleic Acids Res*. **1997**, *25*, 4876-4882.

Thran M., Link K., and Sonnewald U. The *Arabidopsis* DCP2 gene is required for proper mRNA turnover and prevents transgene silencing in *Arabidopsis*. *Plant J*. **2012**, *72*, 368-377.

Tijsterman M., and Plasterk R.H. Dicers at RISC; the mechanism of RNAi. *Cell*. **2004**, *117*, 1-3.

Tuttle J.R., Idris A.M., Brown J.K., Haigler C.H., and Robertson D. Geminivirus-mediated gene silencing from *Cotton leaf crumple virus* is enhanced by low temperature in cotton. *Plant Physiol*. **2008**, *148*, 41-50.

Valentine T., Shaw J., Blok V.C., Phillips M.S., Oparka K.J., and Lacomme C. Efficient virus-induced gene silencing in roots using a modified *Tobacco rattle virus* vector. *Plant Physiol*. **2004**, *136*, 3999-4009.

Valli A., López-Moya J.J., and García J.A. Recombination and gene duplication in the evolutionary diversification of P1 proteins in the family Potyviridae. *J Gen Virol*. **2007**, *88*, 1016-1028.

Varallyay E., and Havelda Z. Unrelated viral suppressors of RNA silencing mediate the control of ARGONAUTE1 level. *Mol Plant Pathol*. **2013**, *14*, 567-575.

Vaucheret H. Plant ARGONAUTES. *Trends Plant Sci*. **2008**, *13*, 350-358.

Vaucheret H., Mallory A.C., and Bartel D.P. AGO1 homeostasis entails coexpression of MIR168 and AGO1 and preferential stabilization of miR168 by AGO1. *Mol Cell*. **2006**, *22*, 129-136.

Vaucheret H., Vazquez F., Crete P., and Bartel D.P. The action of ARGONAUTE1 in the

miRNA pathway and its regulation by the miRNA pathway are crucial for plant development. *Genes Dev*. **2004**, *18*, 1187-1197.

Vazquez F., Gasciolli V., Crete P., and Vaucheret H. The nuclear dsRNA binding protein HYL1 is required for microRNA accumulation and plant development, but not posttranscriptional transgene silencing. *Curr Biol*. **2004**, *14*, 346-351.

Vazquez F., Vaucheret H., Rajagopalan R., Lepers C., Gasciolli V., Mallory A.C., Hilbert J.L., Bartel D.P., and Crete P. Endogenous trans-acting siRNAs regulate the accumulation of *Arabidopsis* mRNAs. *Mol Cell*. **2004**, *16*, 69-79.

Velázquez K., Renovell A., Comellas M., Serra P., García M.L., Pina J.A., Navarro L., Moreno P., and Guerri J. Effect of temperature on RNA silencing of a negative-stranded RNA plant virus: *Citrus psorosis virus*. *Plant Pathol*. **2010**, *59*, 982-990.

Verchot-Lubicz J. A new cell-to-cell transport model for Potexviruses. *Mol Plant Microbe in*. **2005**, *18*, 283-290.

Voinnet O. RNA silencing as a plant immune system against viruses. *Trends Genetic*. **2001**, *17*, 449-459.

Voinnet O. Non-cell autonomous RNA silencing. *Febs Lett*. **2005**, *579*, 5858-5871.

Voinnet O. Induction and suppression of RNA silencing: insights from viral infections. *Nat Rev Genet*. **2005**, *6*, 206-220.

Voinnet O., Cederer C., and Baulcombe D.C. A viral movement protein prevents spread of the gene silencing signal in *Nicotiana benthamiana*. *Cell*. **2000**, *103*, 157-167.

Voinnet O., Pinto Y.M., and Baulcombe D.C. Suppression of gene silencing: a general strategy used by diverse DNA and RNA viruses of plants. *Proc Natl Acad Sci USA*. **1999**, *96*, 14147-14152.

Voinnet O., and Baulcombe D.C. Systemic signalling in gene silencing. *Nature*. **1997**, *389*, 553.

Wang X.B., Jovel J., Udomporn P., Wang Y., Wu Q., Li W.X., Gasciolli V., Vaucheret H., and Ding S.W. The 21-nucleotide, but not 22-nucleotide, viral secondary small interfering RNAs direct potent antiviral defense by two cooperative argonautes in *Arabidopsis thaliana*. *Plant Cell*. **2011**, *23*, 1625-1638.

Weber C., Nover L., and Fauth M. Plant stress granules and mRNA processing bodies are distinct from heat stress granules. *Plant J*. **2008**, *56*, 517-530.

Wong S.M., Lee K.C., Yu H.H., and Leong W.F. Phylogenetic analysis of triple gene block viruses based on the TGB1 homolog gene indicates a convergent evolution. *Virus Genes*. **1998**, *16*, 295-302.

Wu J., Wang Z.W., Shi Z.B., Zhang S., Ming R., Zhu S.L., Zhang S.L. The genome of the pear (*Pyrus bretschneideri* Rehd.). *Genome Research.* **2013**, *23*, 396-408.

Wu Z.B., Ku H.M., Su C.C., Chen I.Z., and Jan F.J. Molecular and biological characterization of an isolate of *Apple stem pitting virus* causing pear vein yellows disease in Taiwan. *J Plant Pathol*. **2010**, *92*, 721-728.

Xie Z., Allen E., Wilken A., and Carrington J.C. DICER-LIKE 4 functions in trans-acting small interfering RNA biogenesis and vegetative phase change in *Arabidopsis thaliana*.

Proc Natl Acad Sci USA. **2005**, *102*, 12984-12989.

Xie Z., Johansen L.K., Gustafson A.M., Kasschau K.D., Lellis A.D., Zilberman D., Jacobsen S.E., and Carrington J.C. Genetic and functional diversification of small RNA pathways in plants. *Plos Biol*. **2004**, *2*, e104.

Xin H.W., and Ding S.W. Identification and molecular characterization of a naturally occurring RNA virus mutant defective in the initiation of host recovery. *Virology*. **2003**, *317*, 253-362.

Xu J., Yang J.Y., Niu Q.W., and Chua N.H. Arabidopsis DCP2, DCP1, and VARICOSE form a decapping complex required for postembryonic development. *Plant Cell*. **2006**, *18*, 3386-3398.

Xu J., and Chua N.H. Arabidopsis decapping 5 is required for mRNA decapping, P-body formation, and translational repression during postembryonic development. *Plant Cell*. **2009**, *21*, 3270-3279.

Yang S., Wang K., Valladares O., Hannenhalli S., and Bucan M. Genome-wide expression profiling and bioinformatics analysis of diurnally regulated genes in the mouse prefrontal cortex. *Genome Biol*. **2007**, *8*, 247.

Ye R., Wang W., Iki T., Liu C., Wu Y., Ishikawa M., Zhou X., and Qi Y. Cytoplasmic assembly and selective nuclear import of *Arabidopsis* Argonaute4/siRNA complexes. *Mol Cell*. **2012**, *46*, 859-870.

Yi H., and Richards E.J. A cluster of disease resistance genes in Arabidopsis is coordinately regulated by transcriptional activation and RNA silencing. *Plant Cell*. **2007**, *19*, 2929-2939.

Yoo B.C., Kragler F., Varkonyi-Gasic E., Haywood V., Archer-Evans S., Lee Y.M., Lough T.J., and Lucas W.J. A systemic small RNA signaling system in plants. *Plant Cell*. **2004**, *16*, 1979-2000.

Yoon J.Y., Joa J.H., Choi K.S., Do K.S., Lim H.C., and Chung B.N. Genetic Diversity of a Natural Population of *Apple stem pitting virus* isolated from apple in Korea. *Plant Pathology J*. **2014**, *30*, 195-199.

Youssef S.A., Moawad S.M., Nosseir F.M., and Shalaby A.A. Detection and identification of *Apple stem pitting virus* and *Apple stem grooving virus* affecting apple and pear trees in Egypt. *Julius-Kühn-Archiv*. **2010**,

Yu D.Q., Fan B.F., MacFarlane S.A., and Chen Z.X. Analysis of the involvement of an inducible *Arabidopsis* RNA-dependent RNA polymerase in antiviral defense. *Mol Plant Microbe Interact*. **2003**, *3*, 206-216.

Zemtchik E.Z., Verderevskaya T.D., and Kalashian Y.A. *Apricot latent virus*: transmission, purification and serology. **1997**, 153-158.

Zhang C.L., Gao R., Wang J., Zhang G.M., Li X.D., and Liu H.T. Molecular variability of *Tobacco vein banding mosaic virus* populations. *Virus Res*. **2011**, *158*, 188-198.

Zhang X., Yuan Y.R., Pei Y., Lin S.S., Tuschl T., Patel D.J., and Chua N.H. *Cucumber mosaic virus*-encoded 2b suppressor inhibits *Arabidopsis* Argonaute1 cleavage activity to counter plant defense. *Genes Dev*. **2006**, *20*, 3255-3268.

Zhang X., Zhang X., Singh J., Li D., and Qu F. Temperature-dependent survival of *Turnip crinkle virus*-infected *Arabidopsis* plants relies on an RNA silencing-based

defense that requires DCL2, AGO2 and HEN1. *J Virol*. **2012**, *86*, 6847-6854.

Zilberman D., Cao X., Johansen L.K., Xie Z., Carrington J.C., and Jacobsen S.E. Role of *Arabidopsis* ARGONAUTE4 in RNA-directed DNA methylation triggered by inverted repeats. *Curr Biol*. **2004**, *14*, 1214-1220.

Zilberman D., Cao X., and Jacobsen S.E. ARGONAUTE4 control of locus-specific siRNA accumulation and DNA histone methylation. *Science*. **2003**, *299*, 716-719.